

*Investigation of suitable microencapsulation
techniques in the preformulation of selected
antiretroviral drugs*



By NNAMDI IKEMEFUNA OKAFOR

*UNIVERSITY of the
WESTERN CAPE*
*A thesis submitted in fulfilment of
the requirements for the degree of*

DOCTOR OF PHILOSOPHY

*School of Pharmacy, Faculty of Natural Sciences,
University of the Western Cape, South Africa.*

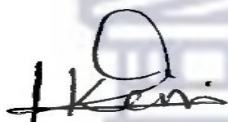
December 2022

Supervisor: Prof Marique Aucamp

DECLARATION

I, the undersigned, hereby declare that the thesis titled ‘Investigation of suitable microencapsulation techniques in the preformulation of selected antiretroviral drugs’ and the entirety of the work contained herein is my own and that I am the sole author of the work and can confirm that this work has not been previously in its entirety or in parts been submitted to any other University for any qualification or degree.

Signed...



Full Name : Nnamdi Ikemefuna Okafor

Date... 23/12/2022



DEDICATION

This thesis is dedicated to God Almighty, Maker of the Heaven and the Earth, my eternal rock of ages, for bringing me this far in life and in my career and to my lovely mother, Mrs Ojiefi Helen Akpunku Okafor and her entire family for their immense support and prayers throughout this journey.



ACKNOWLEDGEMENTS

I would wish to sincerely express my joy and profound gratitude towards my supervisor, Professor Marique Aucamp for her thorough and immense supervision, for her guidance throughout my program, and for giving me the privilege and platform to work with her as well as mentoring and grooming me into one of the finest researchers today. In the same vein, I want to appreciate the School of Pharmacy, Department of Pharmaceutical Sciences, Faculty of Natural Sciences, University of the Western Cape, South Africa for the provision of an enabling and a conducive environment which allowed me to conduct my research without fear and for their partial financial assistance in accomplishing this novel research. I further acknowledge the Agricultural Research Council, Nietvoorbij, Helshoogte, Stellenbosch, South Africa, for giving me access to their laboratory to use of their spray drying equipment for the spray drying of one of our drugs. I am thankful to the Future Leaders African-Independence Research Fellowship (FLAIR) for their partial financial help which enabled the completion of this work.

I want to wholeheartedly appreciate my brother and his family Mr and Mrs Okeke Christian, who were my major backbone throughout this journey including their financial support, encouragement, and prayers. I deeply want to also thank Dr Nnaemeka Joshua Nnaji for his immense support and for also bringing in his expertise into this work.

I wish to extend my appreciation to my spiritual mentors and councillors, Reverend Dr Canon Onyeka Egwuonwu, Reverend Onyekachi Obiekwe, my in-law, Pastor Monday Ugwoke and his family for their enormous prayers throughout my research and to my uncle Chief Mr Samuel Obiora (Ebubedike), I say a big thank you to you all for your support during this journey. I hope to thank all my colleagues especially Candidah Nephawe, Yves Mustafari Ngabo,

Geoffrey Okello, Omobolanle Omotoso, and all my friends including Chibuzor Johnpaul Igwemezie, Nhlamulo Ndlovu, Samson Oselusi, Anderson Longwe, Amanda Mheshe, Awah Felix, Ijeoma Juliet Okafor, and Ijeoma Stella Aririguzo for their roles in one way or the other in the successful completion of this work.

Finally, I would love to still thank my mom and the entire family of Mrs Ojiefi Helen Akpunku Okafor for their love, prayers, and support in the course of this work, I remain indebted to you all and say that this is for you all.

Nnamdi Ikemefuna Okafor

*School of Pharmacy, Department of Pharmaceutical Sciences,
University of the Western Cape, South Africa.*

December 2022

UNIVERSITY *of the*
WESTERN CAPE

ABSTRACT

Introduction: The use of antiretroviral drugs (ARVDs) in the treatment of HIV/AIDS have been promising and effective especially amongst adults as it suppresses the viral load, thereby improving the life expectancy of HIV patients. However, the adoption of the treatment amongst children living with HIV have proved to be challenging. This is because of the poor drug adherence or non-compliance resulting from the lack of child-friendly formulations. The dosage forms are typically large tablets which have led to difficulty in swallowing or needs breaking of the tablets to obtain the correct dose and potentially some sort of dosage form manipulation by mixing it with milk or juice. The limited paediatric formulations that are available are mostly unpalatable, despite being formulated in a syrup or liquid, it still presents with a bitter taste. Therefore, all these factors combined have emphasised the need for child-friendly dosage forms for children suffering from this debilitating disease. Hence, this study focussed on drug microencapsulation techniques such as spray drying, and encapsulation into liposomes as preformulation strategies to formulate spray dried microparticles or liposomes microparticles which could potentially lead to ARV dose reduction having specifically the paediatric population in mind. For this purpose, the natural excipients which are readily available and affordable, including pea protein isolate (PPI), inulin (IN), lecithin (LEC) and cholesterol (CHO) were utilized in the encapsulation of the selected drugs.

Aim: This study was aimed at investigating the microencapsulation of two well-known ARVs, abacavir sulfate (ABC) and zidovudine (AZT) utilising natural occurring excipients and processing methods such as spray drying and liposomal encapsulation.

Methods: To have an understanding of the characteristics of the natural occurring excipients, PPI and IN, used in this study, the first phase was to complete a thorough physicochemical characterization of these excipients using analytical techniques such as the hot-stage microscopy (HSM), thermogravimetric analysis (TGA), differential scanning calorimetry (DSC), powder X-ray diffractometer (PXRD), Fourier infrared spectroscopy (FTIR) as well as functional property determination including the foaming capacity and stability (FC, FS), water holding capacity (WHC), oil absorption capacity (OAC), emulsion activity and stability index, gelling property and film forming ability (FFA). ABC- and AZT-loaded liposomes were formulated using the well-known thin-film hydration method with soy LEC and CHO as excipients. A second microencapsulation method involved the spray drying of ABC and AZT with PPI and IN as microparticles wall formers. This was considered a novel approach since a

literature search did not reveal the microencapsulation of either ARV in combination with the two mentioned natural excipients (PPI and IN). Further to this, the combination of PPI and IN in microencapsulation process has not been documented previously. ABC (SD-ABC) and, AZT (SD-AZT) microparticles as well as ABC (AL) and AZT-loaded liposomes (AZT-L) were subsequently characterised using analytical techniques including HSM, DSC, TGA, FTIR, PXRD, scanning electron microscopy (SEM), transmission electron microscopy (TEM), dynamic light scattering (DLS). The encapsulation efficiency (%EE) of the drug-loaded liposomes and the drug content uniformity in the spray dried microparticles were determined. The drug dissolution studies were performed at pH 1.2 and pH 6.8 and for all drug concentration determinations validated high performance liquid chromatography (HPLC) methods were utilised.

Results: The obtained results from the physicochemical characterization of the pure excipients showed that the excipients are amorphous except CHO which was found to be crystalline. The functional property analyses exhibited promising functional properties for PPI and IN in terms of good WHC, interesting FC and FS, good emulsify ability and gelling strength implying a successful application of these excipients in the spray drying process.

Microencapsulation of ABC *via* spray drying using PPI and IN and the formulation of (AL) was successfully carried out. The results AL revealed a formation of an ABC amorphous dispersion which was confirmed with DSC and PXRD analytical techniques with a uniform and reduced particle size within microparticles range while demonstrating a high percentage drug loading and encapsulation efficiency (%EE) of more than 70% and 90% for the both formulations respectively with over 60% percentage yield for the SD-ABC. For both SD-ABC and AL spherical shapes and morphology have been confirmed using SEM analysis. The equilibrium solubility study (maximum solubility obtained over a 24-hour period) of the pure drug with the excipients (PPI, IN, LEC, CHO) and the drug-loaded microparticles including the spray dried ABC (SD-ABC) and ABC liposomes (AL) carried out in different pH-buffered media revealed an enhanced ABC solubility in the prepared microparticles when compared to the equilibrium solubility of the pure drug and the physical mixture of the drug with the excipients. The release profile of the drug from the microparticles and liposomes demonstrated a rapid and faster rate of drug release releasing over 80% of the drug, thereby further supporting the equilibrium solubility data of an improved SD-ABC microparticles and AL solubility and formation of an ABC amorphous dispersion although the liposomes have shown the potential

to delay the release of the drug after the period of 30 minutes hence should be investigated further for an extended release in future.

The encapsulation of AZT using spray drying and entrapment in liposomes was also prepared and the physicochemical properties of the microparticles was investigated. The result showed a formation of a uniform AZT microparticles and AZT-L formulation with a smaller particle size, good percentage yield and drug loading of 76.1% and 67.2% for the SD-AZT microparticles, and interesting entrapment efficiency and highly surface charge for AZT-L. The physicochemical evaluation of the AZT microparticles and AZT-L confirmed a formation of an amorphous dispersion for both the SD-AZT, and AZT-L as depicted by both the DSC and the PXRD results. The encapsulation of AZT via spray drying using PPI and IN as the coating agents to obtain AZT microparticles and entrapping of AZT-L delivery system has shown that the release of the drug from the respective formulations was not affected by the excipients. The release profiles illustrated a rapid and fast dissolution rate within the first minutes especially for the SD-AZT microparticles however, AZT-L demonstrated the potential of an extended drug release due to a slower dissolution rate observed hence it can further be explored for a surface modification in future towards extended release and targeted delivery that would promote a dose reduction in the treatment of HIV in children.

Keywords: Microencapsulation, HIV/AIDS, paediatric, amorphous dispersions, liposomes, microparticles, delivery systems

UNIVERSITY *of the*
WESTERN CAPE

PUBLICATIONS AND CONFERENCES

Conferences attended

- I. Preparation of an amorphous dispersion of abacavir using spray drying (2021), Okafor NI., Aucamp ME. At the *6th Annual Research Symposium of School of Pharmacy, University of the Western Cape*, South Africa.
- II. Physico-chemical and functional characterization of pea protein and rice protein isolates as pharmaceutical excipients (2020), Okafor NI., Aucamp ME. At the *International Conference of American Association of Pharmaceutical Sciences, United States of America*.
- III. Delegate at the National Conference of the *National Academy of Pharmaceutical Sciences* of South Africa 2019.



TABLE OF CONTENTS

Table of contents

Declaration	II
Dedication	III
Acknowledgements	IV
Abstract	VI
Publications and conferences	IX
Table of contents	X
List of abbreviations	XIX

Chapter One

General introduction

1.1. Background study and problem statement	1
1.2. Aims of the study	3
1.3. Specific objectives of the study	3
1.4. Thesis outline	4
1.5. Conclusion	5
1.6. References	6

Chapter Two

Acquire immunodeficiency syndrome

2.1. Introduction	9
2.2. HIV description/historical background	10
2.3. Pathogenesis and replication of HIV	12
2.4. Symptoms of HIV	13
2.5. Therapeutic treatment	15
2.6. Conclusion	20
2.7. References	21

Figures and Tables

Figure 2.1. Structure of HIV virus (Shyamala, 2017).	11
Figure 2.2. HIV-1 replication cycle in two distinct phases: the early phase (upper portion of diagram) up to integration of the proviral DNA and the late phase, involving every events from transcription to virus budding and maturation adapted from (Souza and Summers, 2005).	13
Figure 2.3. HIV major symptoms with numerous variants at different stages, adapted from (Hägström, 2014).	15
Figure 2.4. Illustration of HIV life cycle and targets for antiretroviral therapy adapted from (Michaud <i>et al.</i> , 2012).	16
Table 2.1. Structures and names of some FDA approved antiretroviral drugs (Michaud <i>et al.</i> , 2012).	18

Chapter Three

Microencapsulation of pharmaceutical compounds

3.1.	Introduction	26
3.2.	Applications of microencapsulation	27
3.2.1.	Application in food industry	27
3.2.2.	Application in agricultural sector	28
3.2.3.	Application in pharmaceutical industry	28
3.3.	Materials for microencapsulation	30
3.3.1.	Wall material	30
3.3.1.1.	Pea protein	32
3.3.1.2.	Inulin	32
3.3.1.3.	Lecithin	35
3.3.1.4.	Cholesterol	37
3.3.2.	Core materials	38
3.3.2.1.	Profile of core the core materials	38
3.3.2.2.	Drug: Abacavir	38
3.3.2.3.	Drug: Zidovudine	41
3.4.	Solid dispersions	44
3.4.1.	Advantages of solid dispersions	45
3.4.2.	Classification of solid dispersions	46
3.5.	Microencapsulation techniques	50
3.5.1.	Spray drying	50
3.5.2.	Spray chilling	52
3.5.3.	Extrusion	53
3.5.4.	Fluidized bed coating	55
3.5.5.	Liposomal entrapment	55
3.5.6.	Freeze drying	57
3.5.7.	Coacervation	58
3.5.8.	<i>In situ</i> polymerization	59
3.5.9.	Solvent evaporation	60
3.5.10.	Pan coating	61
3.5.11.	Electro-spraying	62
3.6.	Empirical studies	64
3.7.	Conclusion	68
3.8.	References	69

Figures and Tables

Figure 3.1.	A simplified schematic depicting the microencapsulation process as adapted from (Timilsena, Haque and Adhikari, 2020)	26
Figure 3.2.	Classification of and various forms of microcapsule (Singh <i>et al.</i> , 2016).	27
Figure 3.3.	Chemical structure of inulin $n = 2 - 60$, adapted from (Kalyani Nair, Kharb and Thompkinson, 2010).	33
Figure 3.4.	Chemical structure of lecithin from (Olisa, 2009).	36
Figure 3.5.	Chemical structure of three major phosphatides (Baeza Jiminez, Lopez Martinez and Garcia, 2014).	36
Figure 3.6.	Chemical structure of cholesterol (Peng <i>et al.</i> , 2008).	37
Figure 3.7.	Chemical structure of ABC (Michaud <i>et al.</i> , 2012).	38
Figure 3.8.	Chemical structure of AZT (Michaud <i>et al.</i> , 2012).	41

Figure 3.9.	Classification of solid dispersions based on distribution of solute compound within the carrier (Teja <i>et al.</i> , 2014).	47
Figure 3.10.	Classification of solid dispersions based on the physical state of the carrier adapted from (Jadav and Paradkar, 2020).	49
Figure 3.11.	Schematic illustration of microencapsulation by spray-drying process (Bakry <i>et al.</i> , 2015).	51
Figure 3.12.	Graphical depiction of spray chilling encapsulation technique from (Oxley, 2012).	52
Figure 3.13.	Schematic depiction of extrusion method adapted from (Liliana and Vladimir, 2013).	53
Figure 3.14.	Schematic diagram of top, bottom, and tangential-spray fluidized-bed coating (Bakry <i>et al.</i> , 2015).	55
Figure 3.15.	Structure of Liposomes (Swaminathan and Ehrhardt, 2011).	56
Figure 3.16.	Schematic illustration of a freeze-dryer (Bakry <i>et al.</i> , 2015).	57
Figure 3.17.	Illustration of microencapsulation by coacervation (Kashif <i>et al.</i> , 2019).	59
Figure 3.18.	Illustration of in-situ polymerization technique in the microencapsulation of essential oils (Bakry <i>et al.</i> , 2015).	60
Figure 3.19.	Schematic diagram of evaporation for preparation of microparticles (Wang <i>et al.</i> , 2016).	61
Figure 3.20.	Schematic representation of pan coating (Bansode <i>et al.</i> , 2010).	62
Figure 3.21.	A schematic representation of electro-spraying process through a single nozzle system (Kashif <i>et al.</i> , 2016).	63
Table 3.1.	List of some marketed microencapsulated drugs and therapeutic use as adapted (Jeffrey Ting <i>et al.</i> , 2018).	29
Table 3.2.	Examples of some natural and synthetic walling materials (Timilsena, Haque and Adhikari, 2020).	31
Table 3.3.	Inulin content in some plants (Singh and Singh, 2010)	34
Table 3.4.	BSC classification adapted from (Bhaskar, OLA and Ghongade, 2018).	44

Chapter Four

Materials and methods

4.1.	Introduction	79
4.2.	Materials used in this study	79
4.3.	Physicochemical characterization of individual compounds and encapsulated ARVs	79
4.3.1.	Hot-stage microscopy (HSM)	80
4.3.2.	Differential Scanning Calorimetry (DSC)	80
4.3.3.	Thermogravimetric analysis (TGA)	80
4.3.4.	Fourier-Transform infrared spectroscopy (FTIR)	81
4.3.5.	Powder X-ray diffraction (PXRD)	81
4.3.6.	Scanning electron microscopy (SEM)	81
4.3.7.	Equilibrium solubility determination	81
4.3.8.	<i>In vitro</i> dissolution testing	82
4.3.9.	High-performance Liquid Chromatography (HPLC)	82
4.4.	Determination of the functional properties of PPI and IN	83
4.4.1.	Foaming capacity and stability	83
4.4.2.	Effect of concentration of PPI and IN on foaming capacity and stabilization	83
4.4.3.	Effect of pH on foaming capacity and stability of PPI and IN	84
4.4.4.	Water holding capacity (WHC)	84
4.4.5.	Oil absorption capacity (OAC)	84
4.4.6.	Emulsification properties	85
4.4.7.	Gelling Property	85
4.4.8.	Film forming ability (FFA)	86
4.5.	Liposomes formulation, optimization, and ABC encapsulation	86
4.6.	Liposomes formulation, optimization, and AZT encapsulation	93
4.7.	Liposomes techniques	95
4.7.1.	Particle size, zeta potential, and polydispersity index	95
4.7.2.	Transmission electron microscopy (TEM)	95
4.7.3.	Encapsulation efficiency (%EE) for drug-loaded liposomes	95
4.8.	Microencapsulation of ABC and AZT through spray drying	96
4.9.	Conclusion	97
4.10.	References	98

Figures and Tables

Table 4.1.	Levels and range of independent variables tested in Central Composite design (CCD)	88
Table 4.2.	Design Matrix of CCD of experiments and response results	90
Table 4.3.	Experimental design for the encapsulation of ABC	92
Table 4.4.	Design matrix and liposomes-loaded formulations (BBD)	93

Table 4.5.	Levels and range of independent variables tested in 2 ³ Box Behnken design (BBD)	94
Table 4.6.	Box Behnken design with observed responses	94

Chapter Five

The physicochemical and functional characterization of pea protein isolate and inulin

5.1.	Introduction	100
5.2.	Results and discussions	101
5.2.1.	Thermal analyses	101
5.2.2.	FTIR	104
5.2.3.	Powder X-ray diffraction	105
5.3.	Determination of the functional properties of PPI and IN	106
5.3.1.	Foaming capacity and stability	106
5.3.2.	Effect of concentration on FC and FS	107
5.3.3.	Effect of pH on FC and FS	108
5.3.4.	Water holding capacity	109
5.3.5.	Oil absorption capacity (OAC)	110
5.3.6.	Emulsifying property	110
5.3.7.	Gelling properties	111
5.3.8.	Film forming ability	112
5.4.	Conclusion	113
5.5.	References	114

Figures and Tables

Figure 5.1.	The TGA trace obtained during the heating of PPI from 25 – 600 °C with (i) depicting the HSM micrograph of PPI collected at 25 °C and (ii) a micrograph collected at approximately 590 °C, exhibiting the charring of PPI.	102
Figure 5.2.	The TGA trace obtained during the heating of IN from 25 – 600 °C with (i) depicting the HSM micrograph of IN collected at approximately 100 °C and (ii) a micrograph collected at approximately 225 °C, exhibiting the degradation of IN.	103
Figure 5.3.	The DSC thermograms obtained with (a) PPI and (b) IN powders.	104
Figure 5.4.	An overlay of the FTIR spectra obtained for (a) PPI and (b) IN.	105
Figure 5.5.	PXRD pattern of PPI obtained at ambient temperature.	105
Figure 5.6.	PXRD pattern of IN obtained at ambient temperature.	106
Figure 5.7.	Effect of concentration on the FC and FS of (a) PPI and (b) IN.	108
Figure 5.8.	Effect of pH on (a) PPI and, (b) IN FC and FS.	109
Figure 5.9.	Picture representing strong gelling strength of (a) PPI, (b) IN.	112

Table 5.1.	Foaming capacity and stability of protein isolates and inulin.	107
Table 5.2.	Water holding, oil absorption capacity and emulsification property of pea protein, rice protein isolates and Inulin.	111

Chapter Six

The microencapsulation of ABC

6.1.	Introduction	116
6.2.	Physicochemical and morphological evaluation of the empty liposomes	117
6.2.1.	Statistical analysis	120
6.2.2.	Response surface plots	123
6.2.3.	TEM analysis	124
6.3.	Physicochemical and morphological evaluation of ABC-loaded liposomes	124
6.3.1.	Determination of the influence of formulation variable on PS, ZP, PDI and %EE	124
6.3.2.	TEM analysis	132
6.3.3.	Thermal analyses	132
6.3.4.	Spectroscopic and morphological analyses	134
6.3.5.	Equilibrium solubility	138
6.3.6.	Drug release studies	138
6.3.7.	Discussion on ABC-loaded liposomes	140
6.4.	Microencapsulation of ABC <i>via</i> spray drying	140
6.4.1.	Thermal analyses	141
6.4.2.	Morphology and habit of SD-ABC	145
6.4.3.	Equilibrium solubility studies	147
6.4.4.	Drug release studies	148
6.4.5.	Discussion of the microencapsulation of ABC <i>via</i> spray drying	150
6.5.	Conclusion	151
6.6.	References	152

Figures and Tables

Figure 6.1.	Surfaces of interactive effects between stirring time and sonication time at (a) PS and (b) surface charge.	123
Figure 6.2.	Unstained TEM images of optimized empty liposomes collected at a magnification of 200 nm and 0.5 μ m.	124
Figure 6.3.	Surface plots showing the effect of lipid ratio and amount of drug variables on the ABC-loaded liposomes.	127
Figure 6.4.	Surface plots showing the effect of lipid ratio and amount of drug variables on ZP.	129

Figure 6.5.	Surface plots showing the effect of lipid ratio and amount of drug variables on %EE of ABC in the liposomes formulations.	131
Figure 6.6.	Unstained TEM micrographs of AL captured at different magnifications.	132
Figure 6.7.	DSC thermograms obtained with ABC, AL, LEC, CHO, and the control.	133
Figure 6.8.	TGA curves for pure compounds (ABC, LEC, CHO), AL, and the control sample.	134
Figure 6.9.	Overlay of the FTIR spectra obtained for pure ABC, AL, LEC, CHO, and the control.	136
Figure 6.10.	Overlay of the PXRD patterns obtained for ABC, AL, LEC, CHO, and the control.	137
Figure 6.11.	SEM micrographs obtained for (a) ABC, (b) CHO, (c) LEC, and (d) freeze-dried AL.	137
Figure 6.12.	Equilibrium solubility of pure ABC, AL, and ABC physical mixture with excipients.	138
Figure 6.13.	ABC release rate of pure ABC, in comparison with the release rate of ABC from the formulated liposomes in aqueous buffered pH 1.2 and 6.8 media.	139
Figure 6.14.	ABC release rate of pure ABC, in comparison with the release rate of ABC from the formulated liposomes in aqueous buffered pH 1.2 and 6.8 media in the dissolution time frame of 10 seconds to 1 minute.	139
Figure 6.15.	DSC thermogram of pure ABC, SD-ABC, PPI, IN, and control	142
Figure 6.16.	TGA curves for (A)SD-ABC, (B) control, (C) pure ABC, (D) PPI, (E) IN.	143
Figure 6.17.	FTIR spectra of pure ABC, SD-ABC, PPI, IN and control	144
Figure 6.18.	SEM images of (A) Pure ABC (B) SD-ABC (C) PPI, (D) IN, (F) control.	146
Figure 6.19.	PXRD pattern of pure ABC, PPI, IN, SD-ABC, and control	147
Figure 6.20.	Equilibrium solubility profiles of Pure ABC, ABC physical mixture and SD-ABC.	148
Figure 6.21.	Drug release profiles of ABC encapsulated in PPI:IN in pH 1.2 and 6.8 buffered aqueous media at $37\text{ }^{\circ}\text{C} \pm 0.5\text{ }^{\circ}\text{C}$.	149
Figure 6.22.	Drug release rate of ABC encapsulated in PPI:IN in pH 1.2 and 6.8 buffered aqueous media at $37\text{ }^{\circ}\text{C} \pm 0.5\text{ }^{\circ}\text{C}$, focusing only on the first minute of dissolution.	149
Table 6.1.	Design Matrix of CCD of experiments and response results.	118
Table 6.2.	Analysis of variance for the Response Surface Quadratic model for the PS of the empty liposomes.	121
Table 6.3.	Analysis of variance for the Response Surface Quadratic model for the surface charge of the empty liposomes.	122
Table 6.4.	Outline of the BBD and subsequent results for the response factors of ABC-loaded liposomes (AL).	125
Table 6.5.	ANOVA results for the Response Surface linear model of the PS of the ABC-loaded liposomes.	128
Table 6.6.	ANOVA for the surface response 2FI model for ZP.	128
Table 6.7.	ANOVA for response surface 2FI model for EE.	130

Chapter Seven

The encapsulation of AZT into liposomes and *via* spray drying

7.1.	Introduction	155
7.2.	Formulation of AZT-loaded liposomes	156
7.2.1.	Optimization – Response surface methodology	156
7.2.2.	Physicochemical characterization of AZT-loaded liposomes	158
7.2.2.1.	PS, ZP, PDI and %EE	158
7.2.2.2.	Transmission electron microscopy (TEM)	167
7.2.2.3.	Thermal analyses	167
7.2.2.4.	Spectroscopic analyses	169
7.2.2.5.	Powder X-ray diffraction (PXRD)	171
7.2.2.6.	Equilibrium solubility	171
7.2.2.7.	<i>In vitro</i> drug release studies	172
7.3.	The microencapsulation of AZT via spray drying using PPI and IN as wall formers	173
7.3.1.	Physicochemical characterization of the SD-AT in comparison with the raw materials and a physical mixture	174
7.3.1.1.	Thermal analyses	174
7.3.1.2.	Spectroscopic analysis of SD-AZT	175
7.3.1.3.	Powder X-ray diffraction of SD-AZT	177
7.3.1.4.	Equilibrium solubility studies	178
7.3.1.5.	<i>In vitro</i> dissolution studies	179
7.4.	Conclusion	180
7.5.	References	181

Figures and Tables

Figure 7.1.	Different dispersed particle sizes of AZT-L.	159
Figure 7.2.	Obtained surface charges of AZT-L.	160
Figure 7.3.	Plots of predicted versus actual data (a) PS, (b) PDI, (c) ZP and (d) %EE.	165
Figure 7.4.	Surface of interactive effects for (a) PS, (b) PDI, (c) ZP and (e) EE with. the left sideshowing the 2D (contour) plots while the 3D plots are on the right side.	166
Figure 7.5.	Unstained TEM images of AZT-L at different capturing magnifications.	167
Figure 7.6.	An overlay of DSC thermograms obtained with pure AZT, LEC, CHO, AZT-L and the control.	168
Figure 7.7.	TGA curves of pure AZT, LEC, CHO, AZT-L, and the control.	169
Figure 7.8.	FTIR spectra of pure AZT, LEC, CHO, AZT-L, and the control.	170
Figure 7.9.	PXRD diffractograms obtained for AZT, LEC, CHO, Control and AZT-L.	171

Figure 7.10.	Solubility profiles of pure AZT, the physical mixture and AZT-L.	172
Figure 7.11.	<i>In vitro</i> dissolution profiles of AZT in comparison with AZT-L.	173
Figure 7.12.	DSC thermographs of pure AZT, PPI, IN, SD-AZT, and the control.	174
Figure 7.13.	TGA curves for pure AZT, PPI, IN, SD-AZT, and the control	175
Figure 7.14.	An overlay of the FTIR spectra of pure AZT, PPI, IN, SD-AZT, and the control.	177
Figure 7.15.	PXRD diffractograms obtained for AZT, PPI, IN and SD-AZT.	178
Figure 7.16.	Equilibrium solubility of pure AZT, AZT: PPI: INU and SD-AZT.	179
Figure 7.17.	<i>In vitro</i> dissolution profiles obtained for AZT and SD-AZT over a 30-minute period in pH 1.2.	179
Table 7.1.	Levels and range of independent variables tested in 2 ³ Box Behnken design (BBD)	157
Table 7.2.	Liposomes encapsulation of AZT using varying lipid ratios (LEC: CHO)	157
Table 7.3.	PS, ZP, PDI and %EE obtained during the RSM experiments	158
Table 7.4.	ANOVA for Quadratic model from BBD for PS	162
Table 7.5.	ANOVA for Quadratic model from BBD for PDI	163
Table 7.6.	ANOVA for Quadratic model from BBD for ZP	163
Table 7.7.	ANOVA for Quadratic model from BBD for EE	164
Table 7.8.	FTIR data of pure AZT, LEC, CHO and AZT in liposomes	170
Table 7.9.	FTIR absorption peaks and functional groups of pure AZT, PPI, IN, SD-AZT, and the control	176

Chapter Eight

General conclusions and recommendations

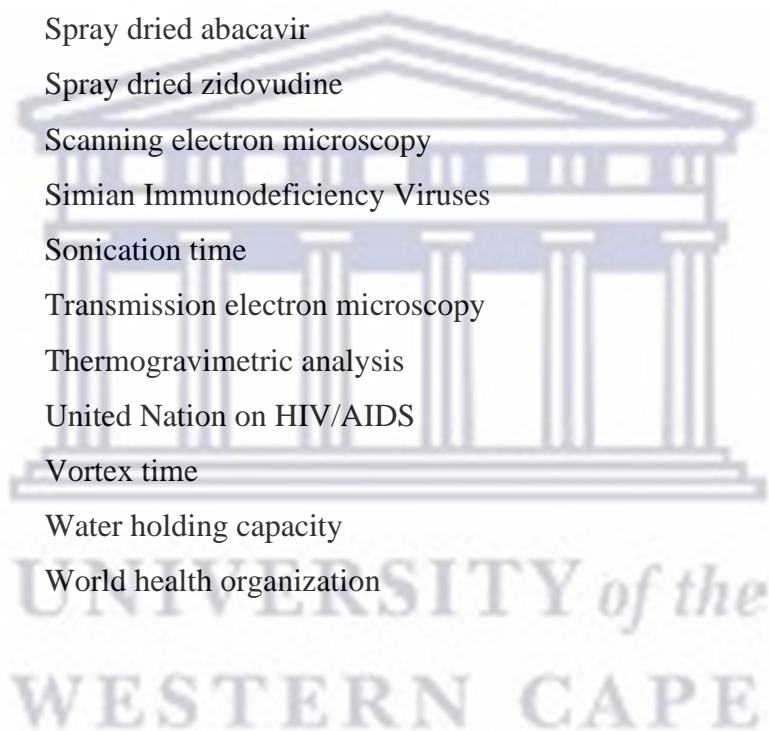
8.1.	Summary and conclusion	186
8.2.	Recommendations	188
8.3.	References	189

LIST OF ABBREVIATIONS

ABC	Abacavir
AIDS	Acquired immunodeficiency syndrome
AL	Abacavir liposomes
ALC-PM	Abacavir lecithin cholesterol physical mixture
API	Active pharmaceutical ingredient
ART	Antiretroviral therapy
Antiretrovirals	ARVs
ARVD	Antiretroviral drug
AZT	Zidovudine
AZT-L	Zidovudine liposomes
BSA	Bovine serum albumin
BSC	Biopharmaceutical classification
CCD	Central composite design
CCR	Chemokine receptor
CHO	Cholesterol
CXCR	Chemokine receptor
CYP	Cytochrome
DDS	Drug delivery system
DFT	Density functional theory
dGTP	Deoxyguanosine-5- triphosphate
DLS	Dynamic light scattering
DMF	Dimethyl Formamide
DMSO	Dimethyl Sulfoxide
DNA	Deoxyribonucleic acid
DSC	Differential scanning calorimetry
DTG	Derivative
EAI	Emulsifying activity index
EDS	Energy dispersive spectroscopy
EE	Encapsulation efficiency
EIs	Entry inhibitors
ESI	Emulsifying stability index
FC	Foaming capacity

FDA	Food and drug administration
FFA	Film forming ability
FIs	Fusion Inhibitors
FS	Foaming stability
FTIR	Fourier Infrared Spectroscopy
GIT	Gastrointestinal tract
GP	Glycoprotein
HAART	Highly active antiretroviral therapy
HCL	Hydrochloric acid
HIV	Human immunodeficiency virus
HPC	Hydroxyl propyl cellulose
HPLC	High performance liquid chromatography
HPMC	Hydroxyl propyl methyl cellulose
HPMCAS	Hydroxyl propyl methyl cellulose acetate succinate
HSM	Hot stage microscopy
HT	Hydration time
IIs	Integrase inhibitors
IN	Inulin
LAS	Lymphadenopathy syndrome
LDS	Liposomes delivery system
LEC	Lecithin
LOD	Limit of detection
LOQ	Limit of quantification
MP	Mass of powder recovered
mSFP	Mass of solid in the feed preparation
NaOH	Sodium hydroxide
NNRTIs	Non-nucleoside reverse transcriptase inhibitors
NRTIs	Nucleoside reverse transcriptase inhibitors
OAC	Oil absorption capacity
PC	Phosphatidylcholine
PCP	Pneumocystis Carinii Pneumonia
PDI	Poly dispersity index
PE	Phosphatidyl ethanolamine

PEG	Polyethylene glycol
PI	Phosphatidyl Inositol
PIs	Protease Inhibitors
PPI	Pea protein isolate
PS	Particle size
PVP	Polyvinyl pyrrolidone
PVPVA	Polyvinyl pyrrolidone vinyl acetate
PXRD	Powdered X-ray diffraction
RNase	Ribonuclease
RPM	Rotation per minute
SD-ABC	Spray dried abacavir
SD-AZT	Spray dried zidovudine
SEM	Scanning electron microscopy
SIVs	Simian Immunodeficiency Viruses
ST	Sonication time
TEM	Transmission electron microscopy
TGA	Thermogravimetric analysis
UNAIDS	United Nation on HIV/AIDS
VT	Vortex time
WHC	Water holding capacity
WHO	World health organization



Chapter One

1. General Introduction

1.1. Background study and problem statement

Since the emergence of acquired immunodeficiency syndrome (AIDS) infection in 1981, and the identification of the human immunodeficiency virus (HIV) in 1983 as the causative agent, over 65 million people have been affected by this virus and more than 25 million people have lost their lives to this devastating infectious disease majorly in the developing countries and more particularly in the Sub-Saharan African region (Shahiwala and Amiji, 2007; UNAIDS, 2021). In this 21st century, HIV still pose a public health threat globally with approximately 37.9 million people currently living with the disease. This includes more than 1.8 million children aged less than 15 years majorly in the Sub-Saharan African setting where 91% of the HIV children were discovered in 2012 (Alebel *et al.*, 2020). Today, AIDS remains the leading cause of deaths among children in the entire globe which had led to over 190,000 deaths in children in 2013 and now children account for 18% of HIV related deaths. Majority of these children tend to lose their lives if they are not placed on antiretroviral treatment (ART) especially in the income deprived countries where HIV among children has become rampant and at the same time they are unable to access the treatment (Pontali *et al.*, 2001; Committee on Paediatric Aids, 2007; Ryan Phelps and Rakhmanina, 2011). The use of the antiretroviral drugs in the treatment of HIV is the only available clinical standard or means of managing this devastating infectious disease for both adults and children. The treatment includes the combination of three or more highly active antiretroviral therapy (HAART) which are classified into; nucleoside reverse transcriptase inhibitors (NRTs), non-nucleoside reverse transcriptase inhibitors (NNRT), protease inhibitors (PIs), and fusion inhibitors (FIs), hence there are over 20 approved antiretroviral agents (ARVs) available today (Shahiwala and Amiji, 2007). Since the introduction of HAART in the treatment of HIV, there has been tremendous success in the expectancy and lives of the infected persons, especially in the developed nations and particularly amongst adults through suppression and depletion of the viral burden thereby hindering replication of the virus in the cells (Shahiwala and Amiji, 2007; Tewodros *et al.*, 2010).

Despite the significant advances in the treatment of HIV using HAART generally, the treatment in children is hindered by poor drug adherence, drug resistance which has culminated to therapeutic and virological failure amongst HIV-positive children (Rosenbloom *et al.*, 2012).

This is because of the complexity associated with HAART as it is required daily for a lifetime hence causing severe side effects. Many of the prescribed ARVs possess low oral bioavailability due to poor aqueous solubility, short half-life thereby requiring higher dose administration and most often increased dose frequency. Overall, children find taking ARVs on a daily basis difficult due to limited ARV-specific, paediatric formulations and specifically the palatability or the bitter taste of most of these formulations (Cram *et al.*, 2009; Chiappetta *et al.*, 2010; Lisziewicz and Toke, 2013; Owen and Rannard, 2016; Chakravarty and Vora, 2021). Although there are currently some oral liquid paediatric formulations such as the ritonavir-boosted lopinavir paediatric formulation which consists of an oral solution of ethanol and propylene glycol, hence the use in treating HIV children have been derailed by the undesirable taste, and the administration of high volumes of the liquid formulation dose (Giardiello *et al.*, 2016; Dubrocq, Rakhmanina and Phelps, 2017). Therefore, exploring other formulation techniques is paramount in the treatment of this debilitating disease. Microencapsulation of drugs to prepare multi-particulates are a strategy that could be employed to potentially eradicate most of the mentioned challenges associated with ARV delivery to paediatric patients (Shahiwala, 2011; Lopez *et al.*, 2015; Giardiello *et al.*, 2016).

Microencapsulation has been defined as the science or technique of encapsulation of active ingredients either liquid or solid into a coating material to form microcapsules of varying sizes ranging from nanometer to micrometer while fostering protection of the encapsulated material from environmental degradation, volatilization or deterioration (Fei *et al.*, 2015; Yang *et al.*, 2020). The advantages of spray drying includes the effectiveness in protecting the core materials, ease of operation in the formulation, production of microcapsules of low water content or activity, production of fine powder of high quality and stability, it is scalable and, cost-effective (Maria Ré, 2006; Poshadri and Kuna, 2010). Liposomal drug delivery systems are known for its biocompatibility, biodegradability, low toxicity, ability to encapsulate both hydrophilic and hydrophobic drugs, it can be made to target a particular site of action, and have been used in further enhancing the poor solubility of drugs (Sahoo and Labhasetwar, 2003; Poshadri and Kuna, 2010; Mansoori *et al.*, 2012; Akbarzadeh *et al.*, 2013). Therefore, the spray drying, and liposomes microencapsulation techniques have been adopted in this research for solubility enhancement, encapsulation, improving the short half-life and potential taste masking of abacavir (ABC) and zidovudine (AZT). Furthermore, clinics and hospitals, especially in rural areas, do not necessarily stock and dispense liquid formulations due to storage requirements and the difficulty of transporting several bottles of the formulations from

the clinic to home. This leads to caregivers of children suffering from HIV to manipulate adult dosage forms such as tablets and capsules into a more palatable form. Usually, this is done through crushing of the tablet or breaking of the capsule shell and mixing it with water or milk. The rationale of this study was therefore to microencapsulate either ABC or AZT using natural and cost-effective excipients such as pea protein isolate, inulin, lecithin, or cholesterol as potential microencapsulation materials. For this study, focus was placed on natural occurring excipients, not only to manufacture microparticles that are cost-effective but also to provide, although minimal, some nutritional benefit to children who will be taking such formulations. Furthermore, since little is known in terms of the use of the natural polysaccharide, inulin and pea protein isolate as pharmaceutical excipients, some part of this study was explorative of nature.

1.2. Aims of the study

This work is aimed at investigating the microencapsulation of ABC and AZT drugs to either improve the solubility and as well increasing the short half-life of the ARVs even more, which could then facilitate dose volume reduction in children or to render the two ARVs into more palatable powder dosage forms and potentially cause delayed or sustained release and possible taste masking. To achieve these aims, specific objectives were investigated.

1.3. Specific objectives of this work were:

- I. To investigate and establish the functional properties of pea protein isolate (PPI) and inulin (IN) to ascertain their microencapsulation ability alone and in combination with one another.
- II. Complete physicochemical characterization of all pure compounds (ABC, AZT, PPI, IN, LEC, and CHO) to facilitate a thorough drug-excipient compatibility study. To achieve this objective several analytical techniques including the hot-stage microscopy (HSM), differential scanning calorimetry (DSC), thermogravimetric analysis (TGA) and Fourier-transform infrared spectroscopy (FTIR) were all utilized.
- III. Investigation and optimization of spray-drying of ABC and AZT using pea protein isolate and inulin as microencapsulation materials.
- IV. Investigation and optimization of liposomal encapsulation of ABC and AZT using soy lecithin and cholesterol as microencapsulation materials.

- V. Physicochemical characterization of the most optimal microencapsulated ABC and AZT preparations.

1.4. Thesis Outline

This thesis is organized into nine chapters and is designated as follows:

Chapter 1: This chapter briefly introduced the background of the study and disseminated the aims and objectives of this research study.

Chapter 2: This chapter is a review of relevant literature on HIV/AIDS, emphasizing the challenges associated with the treatment of this disease in neonates and children.

Chapter 3: A literature review on microencapsulation, focusing on materials typically used in microencapsulation, various types of microencapsulation processes and characteristics of microparticles obtained through this technique.

Chapter 4: This chapter describes the materials and methods used in the entire study.

Chapter 5: Describes the investigated functional properties of inulin and pea protein isolate as micro-encapsulants followed by the compatibility testing of ABC and AZT with all the excipients used in this study.

Chapter 6: Investigated the microencapsulation of ABC using spray dry and liposomes processes and the physicochemical characterization of the obtained ABC microparticles and drug-loaded liposomes.

Chapter 7: This chapter studied the encapsulation and physicochemical characterization of AZT into liposomes and *via* spray drying.

Chapter 8: Summarized all the findings emanating from this study and as well provided recommendations for future studies.

1.5. Conclusion

This chapter has carefully laid the background study on HIV and the related problems and challenges with the use of HIV drugs in the treatment, especially in children and has equally highlighted how these problems could be addressed in the sections of the aims and objectives of the study. The chapter has further shown the outline and organization of this study from chapters 1 to 8.



1.6. References

- Akbarzadeh, A. *et al.* (2013) ‘Liposomes: Classification, preparation, and applications’, *Nanoscale Research Letters*, 8(10), pp. 1–9.
- Alebel, A. *et al.* (2020) ‘Mortality rate among HIV-positive children on ART in Northwest Ethiopia: A historical cohort study’, *BMC Public Health*. *BMC Public Health*, 20(1), pp. 1–11.
- Chakravarty, M. and Vora, A. (2021) ‘Nanotechnology-based antiviral therapeutics’, *Drug Delivery and Translational Research*. *Drug Delivery and Translational Research*, 11(3), pp. 748–787.
- Chiappetta, D. A. *et al.* (2010) ‘Efavirenz-loaded polymeric micelles for paediatric anti-HIV pharmacotherapy with significantly higher oral bioavailability’, *Nanomedicine*, 5(1), pp. 11–23.
- Committee on Paediatric Aids, (2007) ‘Increasing Antiretroviral Drug Access for Children With HIV Infection’, *American Academy of Pediatrics*, 119(14), pp. 338–45.
- Cram, A. *et al.* (2009) ‘Challenges of developing palatable oral paediatric formulations’, *International Journal of Pharmaceutics*, 365(2), pp. 1–3.
- Dubrocq, G., Rakhmanina, N. and Phelps, B. R. (2017) ‘Challenges and Opportunities in the Development of HIV Medications in Paediatric Patients’, *Pediatric Drugs*. Springer International Publishing, 19(2), pp. 1–98.
- Fei, X. *et al.* (2015) ‘Microencapsulation mechanism and size control of fragrance microcapsules with melamine resin shell’, *Colloids and Surfaces A: Physicochemical and Engineering Aspects*, (469), pp. 300–306.
- Giardiello, M. *et al.* (2016) ‘Accelerated oral nanomedicine discovery from miniaturized screening to clinical production exemplified by paediatric HIV nanotherapies’, *Nature Communications*; *Nature Publishing Group*, (7), pp. 1–10.
- Liszewicz, J. and Toke, E. R. (2013) ‘Nanomedicine applications towards the cure of HIV’,

Nanomedicine: Nanotechnology, Biology, and Medicine, 9(1), pp. 28–38.

Lopez, F. L. *et al.* (2015) ‘Formulation approaches to pediatric oral drug delivery : benefits and limitations of current platforms Formulation approaches to pediatric oral drug delivery : benefits and limitations of current platforms’, *Expert opinioin on Drug Delivery*, 12(11), pp. 1727–1740.

Mansoori, M. *et al.* (2012) ‘A Review on Liposomes’, *International Journal of Advanced Research in Pharmaceutics and Bio Sciences*, 2(4), pp. 453–464.

Owen, A. and Rannard, S. (2016) ‘Strengths, weaknesses, opportunities and challenges for long acting injectable therapies: Insights for applications in HIV therapy’, *Advanced Drug Delivery Reviews*, 103, pp. 144–156.

Pontali, E. *et al.* (2001) ‘Adherence to combination antiretroviral treatment in children’, *HIV Clinical Trials*, 2(6), pp. 466–473.

Poshadri, A. and Kuna, A. (2010) ‘Microencapsulation technology: a review’, *Journal of Research Angrau*, 38(6), 86–102.

Ré, M. I. (2006) ‘Formulating drug delivery systems by spray drying’, *Drying Technology*, 24(4), pp. 433–446.

Rosenbloom, D. I. S. *et al.* (2012) ‘Antiretroviral dynamics determines HIV evolution and predicts therapy outcome’, *Nature Medicine*. Nature Publishing Group, 18(9), pp. 1378–1385.

Ryan Phelps and Rakhmanina, N. (2011) ‘Antiretroviral Drugs in Pediatric HIV-Infected Patients’, *Pediatric Drugs*, 13(3), 175–192.

Sahoo, S. K. and Labhasetwar, V. (2003) ‘Nanotech approaches to drug delivery and imaging’, *Drug Discovery Today*, 8(24), pp. 1112–1120.

Shahiwala, A. (2011) ‘Formulation approaches in enhancement of patient compliance to oral drug therapy’, *Expert Opinion on Drug Delivery*, 8(11), pp. 1521–1529.

Shahiwala, A. and Amiji, M. M. (2007) ‘Nanotechnology-based delivery systems in HIV/AIDS

therapy', *Future HIV Therapy*, 1(1), pp. 49–59.

Tewodros, M. *et al.* (2010) 'Emerging nanotechnology approaches for HIV/AIDS treatment and prevention R eview', *Nanomedicine*, 5(2), pp. 269–285.

UNAIDS (2021) 'Global HIV Statistics; Fact Sheet 2021, Ending the AIDS epidemic'. (Accessed 7 March 2021).

Yang, M. *et al.* (2020) 'Microencapsulation Delivery System in Food Industry - Challenge and the Way Forward', *Advances in Polymer Technology*.



Chapter Two

2. ACQUIRED IMMUNODEFFICIENCY SYNDROME (AIDS)

2.1. Introduction

The acquired immunodeficiency syndrome (AIDS) caused by the human immunodeficiency virus (HIV), is a lentivirus (type of retrovirus) reported to be affecting the human white blood cells (Becken *et al.*, 2019). Since the emergence and the discovery of this virus, globally, more than 50 million people have been infected while killing over 16 million people. Annually there occur approximately 6 million new HIV infections, posing a global threat to human health (Merson *et al.*, 2008). There are two major types of HIV namely, HIV-1 and HIV-2 with HIV-1 being the main cause of the HIV pandemic. (Jacobs 2005). Highly active antiretroviral therapy (HAART), a combination of two or more antiretroviral drugs (ARVs), from different drug classes remains the only means of managing HIV and has afforded millions of people clinical relief however, due to the challenges associated with HAART such as, toxicities of the treatment, high treatment costs, frequent dose administration, to mention but just a few while HIV-1 infection still remain a significant global health and socio-economic burden (Hahn *et al.*, 2000; Phelps *et al.*, 2010; Sharp and Hahn, 2010; Ryan Phelps and Rakhmanina, 2011).

UNIVERSITY of the
WESTERN CAPE

2.2. HIV description/historical background

HIV is a roughly, spherical shaped virus (Figure 2.1) with its outer envelope bearing various spikes that are made up of four glycol-proteins (gp20), with the same number of gp41 attached to the membrane and the capsid embedded beneath the proteins envelop. The capsid, is made up of a hollow and cone shape consisting of another gp24 with a generic HIV material, a two strand RNA which is made up of close to 9200 nucleotide bases, integrase, a protease, ribonuclease, with other two proteins, (p6, p7) attached inside the viral core (Hutchinson, 2001). HIV/AIDS was first reported in 1981 in the United States of America which was found between homosexuals having a complicated and rare disease named *Pneumocystis carinii* pneumonia with some of these men having contacted and lived with Kaposi sarcoma at the same time currently named jirovecii (Gottlieb *et al.*, 2004; Jacobs, 2005). Later, the symptoms of AIDS were then seen in other population groups like female sex workers, heterosexuals, and blood transfusion recipients, and among the heterosexual population of Zaire or Belgian Congo now the Republic of Congo in Africa where the earliest known positive HIV-1 infection was identified (Jacobs, 2005; Nikolopoulos, Kostaki and Paraskevis, 2016). HIV was identified as a reverse transcriptase containing the virus (retrovirus) in 1983 and was tagged the causative agent of AIDS by Barré-Sinoussi and co-workers who isolated the virus from a homosexual man with a persistent lymphadenopathy syndrome (LAS) (Barre-Sinoussi *et al.*, 1983). This was further supported by Levy and co-workers who identified a similar virus and named it AIDS-associated retrovirus (ARV) (Levy *et al.*, 1984). This led to the hypothesis suggesting that LAS was heavily linked with the HIV infection (AIDS), however, no conclusion was drawn nor provided (Barre-Sinoussi *et al.*, 1983). Later, in 1984, further investigation from Gallo supported the findings of Barre-Sinoussi from the Pasteur Institute that the isolated virus was from a member of the retrovirus family. During this time, several physicians still argued that LAS rather emerged from the Epstein-Barr virus (EBV) due to the discovery of enlarged lymph nodes in most of the viral infections (Vahlne, 2009). As time went by, HIV-1 previously referred as retrovirus was identified the main causative agent of HIV, and was renamed the AIDS related virus HIV by the International Committee on the Taxonomy and since then, HIV has become a known high-risk disease in recent history affecting individuals including the children (Kallings, 2008).

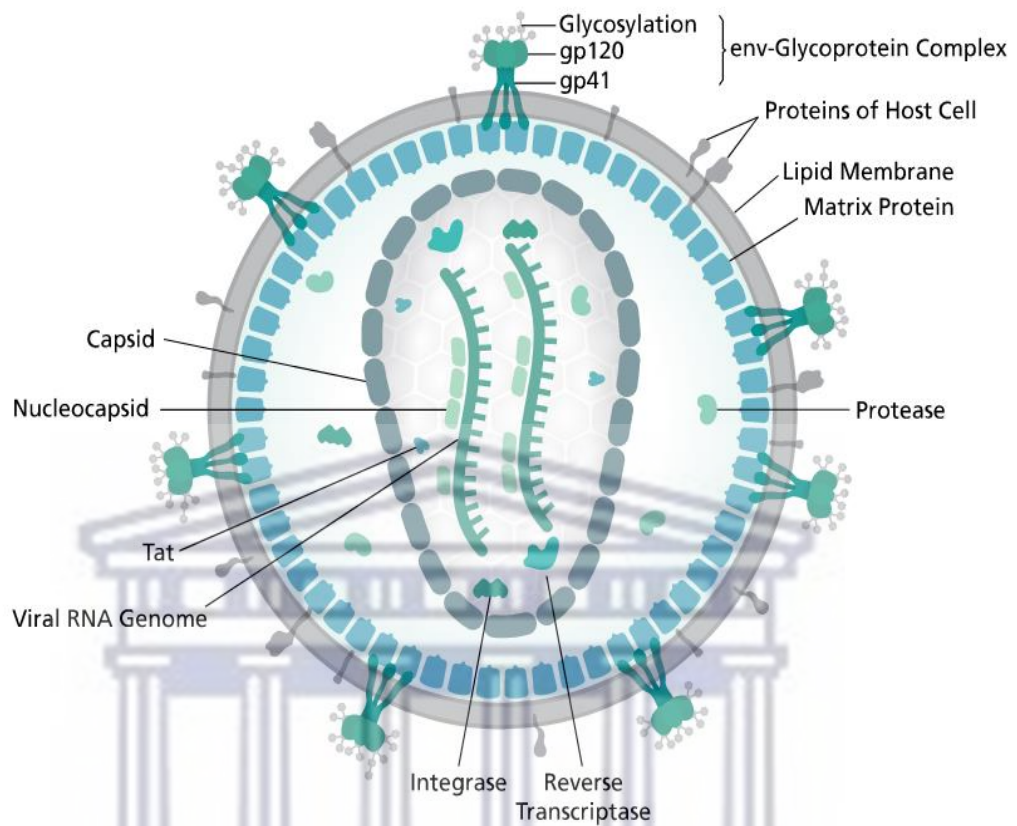


Figure 2.1. Structure of HIV virus (Shyamala, 2017).

UNIVERSITY of the
WESTERN CAPE

2.3. Pathogenesis and replication of HIV

HIV is genetically a member of the retroviridae family and have been affecting diverse species or groups of animals (Brown *et al.*, 2012). The occurrence and clustering of the virus (AIDS) in diverse group of animals is best interpreted by mean of the virus (HIV) transmission in a similar manner to that of hepatitis B virus through sexual contact, by blood inoculation or blood products and through mother to new born infant (perinatal transmission) (Hutchinson, 2001; Sharp and Hahn, 2011). The major target of HIV is by activated CD4 T-lymphocytes. The entry of the virus is by interactions with CD4T with some of the chemokine co-receptors (CCR5 or CXCR4). In the process of replication, cells like monocytes, macrophages and dendritic cells and chemokine receptors are also infected. Several hosts of proteins interact with HIV proteins or the DNA to either restrict or promote replication of the virus in some specific types of cells (Maartens *et al.*, 2014). This receptor molecules (CD4 cells), which are the primary target for the virus as demonstrated in Figure 2.2 undergoes conformational interactions thereby promoting mediation of the glycoprotein 41 (gp41) to mediate fusion of the viral envelope with the host cell membrane hence the viral core gets released in the cytoplasm. The gp41 subgroup is made of essential fusogenic hydrophobic peptides through the amino terminus, fusion of the viral and cellular membrane is activated (Lawn, 2004).

HIV entry pathway into cells are divided into three major events starting with the virus attachment to the cell, activation and fusion with the viral envelope trimeric complex, made of the glycoproteins (gp120, gp41) that identifies the virus entry in the target cells (Eckert and Kim, 2001; Simon *et al.*, 2006; Fanales-Belasio *et al.*, 2011). The host proteins interact with the virus protein or the DNA in a manner that the virus replication in the specific cells is either restricted or replicated. The first replication which takes place at the lymph organ region (the draining lymph node) which consist of slight viral variant leading to primary amplification or enlargement. As the infected T lymphocyte cells or the virions enters the bloodstream, secondary amplification or replication in the gastrointestinal tract (GIT), spleen and bone marrow take place, hence susceptible cells become more infected (Maartens *et al.*, 2014).

Although individuals may look healthy enough within the primary stage of the infection, at that period, there is an active multiplication and replication of the virus in the blood stream and lymph nodes, causing some sort of damage to the immune system due to the viral load burst. Children are known to differ from adults, hence the viral replication among them is high while having high HIV-1 viral load, high rate of CD4+ cells destruction or damage, viral mutation

and faster disease progression rate but with better immunologic antiretroviral response (Mothi *et al.*, 2015). At the point when the plasma HIV load is depleted and the CD4+ cell count is low, the infected person is regarded to have developed AIDS (Moir *et al.*, 2010 Hassan M. Naif, 2013).

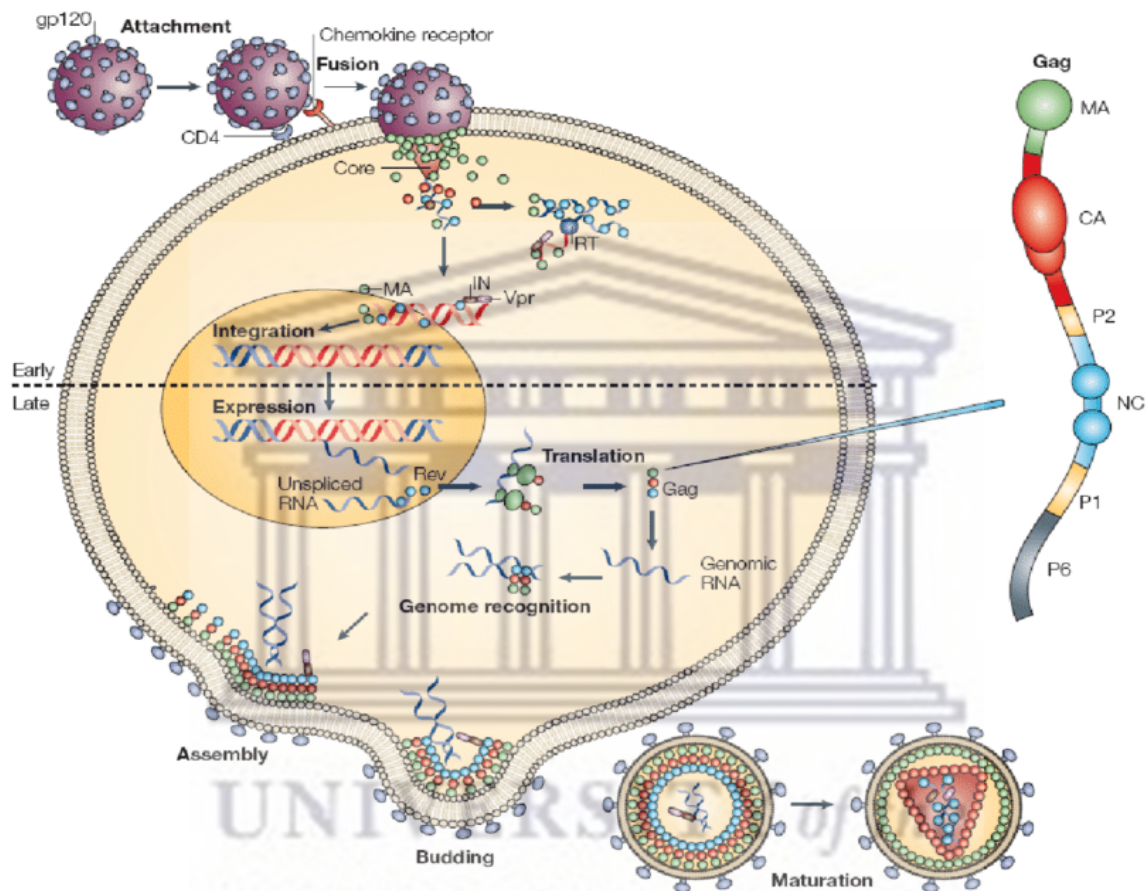


Figure 2.2. HIV-1 replication cycle in two distinct phases: the early phase (upper portion of diagram) up to integration of the proviral DNA and the late phase, involving every events from transcription to virus budding and maturation adapted from (Souza and Summers, 2005).

2.4. Symptoms of HIV

Ranging from few days to few weeks since exposure to HIV, the majority of the infected persons exhibits symptoms (Figure 2.3) resembling flu-like or mononucleosis-like illness, such as fever, maculopapular rash, oral ulcers, lymphadenopathy, arthralgia, pharyngitis, malaise, weight loss and myalgia (Fanales-Belasio *et al.*, 2011). Other signs such as oral candidiasis in the oesophagus, with disorder in the central nervous system, diarrhoea, pneumonia and some other gastrointestinal complaints have been reported in acutely infected patients (Mohamed,

Lu and Mounmin, 2019). These clinical features are quite heterogeneous, and it has been reported that individuals who display more severe and durable symptoms in the course of acute infection tend to progress more rapidly to AIDS (Moir, Chun and Fauci, 2011; Martin and Carrington, 2013; Naif, 2013). Acute symptomatic stage of HIV-1 infection lasts between 7 and 10 days, and rarely longer than 14 days. During the acute HIV-1 infection stage, dramatic decrease in the number of CD4+ T-cells is recorded with increase in viremia levels before the onset of antiviral immune response (Fanales-Belasio *et al.*, 2011). The CD4+ T cells start to increase once more as the immune response is evoked with a drop in the viremia level. At the same time, there is detection of qualitative functional deficiency or damage of the immune system to the virus and some other antigens. This is due to the virus inducing, very early after infection, a dysfunction of CD4+ T cells and other cells of the immune system. Majority of these symptoms tend to exist for 1 - 3 weeks, except lymphadenopathy, lethargy, and malaise, which can persist for several months which then requires a long course of combined drugs treatment. HIV symptoms vary among infants, children, and adolescents (Sharland and Bryant, 2009). Many of them are highly asymptomatic from birth with no trace of abnormal findings. However, diagnosis of acute HIV is made among infants when they present with a positive HIV antibody test or when they exhibit symptoms such as oral thrush, severe pneumonia or sepsis (Mothi *et al.*, 2015).



Main symptoms of Acute HIV infection

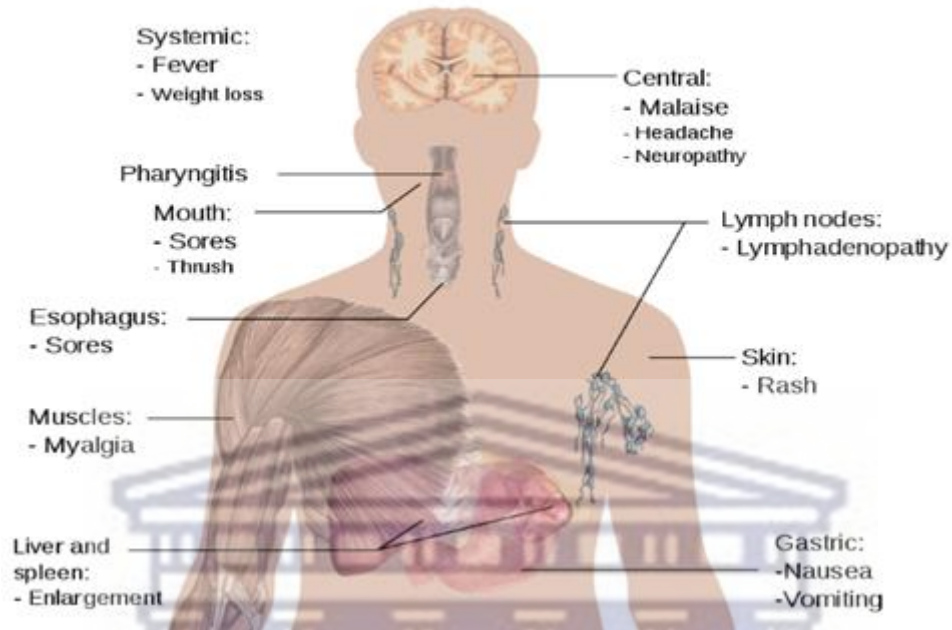


Figure 2.3. HIV major symptoms with numerous variants at different stages, adapted from (Häggström, 2014).

2.5. Therapeutic treatment of HIV

Antiretroviral therapy (ART) was developed for the management of the viral infection, and controlling of the disease progression, thereby improving the quality of life of the patient (Ramana *et al.*, 2012). ART is seen as the best option due to the long-lasting viral suppression and, subsequently, for reduction of morbidity and mortality. There are over 23 US Food and Drug Administration (FDA) recommended ARVs for the treatment of HIV and some of these drugs are presented in Table 2.1. Standard ART regimens in both adults and children involve the combination of two nucleoside reverse transcriptase inhibitors (NRTIs), the backbone treatment, with any other third ARV such as a non-nucleoside reverse transcriptase inhibitor (NNRTI), protease inhibitor (PI), or integrase inhibitor (II). Although, current drugs do not eradicate HIV-1 infection initiation of the ART results in the suppression of the plasma viral load, with increased CD4 counts usually within 3 – 6 months with enhanced clinical staging as ART targets the viral transcriptase or the protease as have been shown in Figure 2.4 (Simon *et al.*, 2006; Sharland and Bryant, 2009; Gupta and Jain, 2010; Maartens *et al.*, 2014).

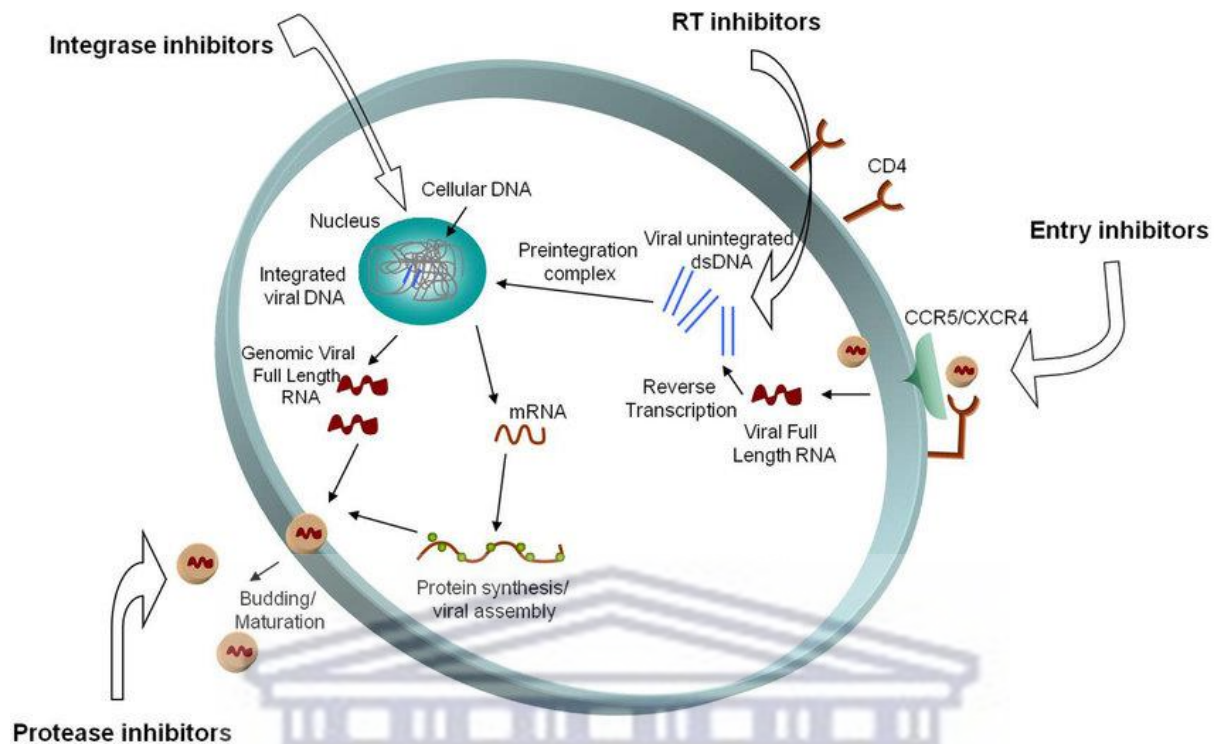


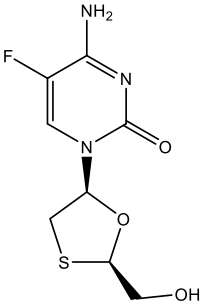
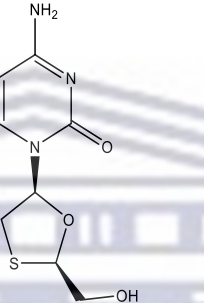
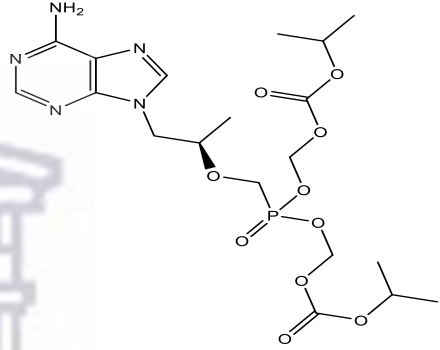
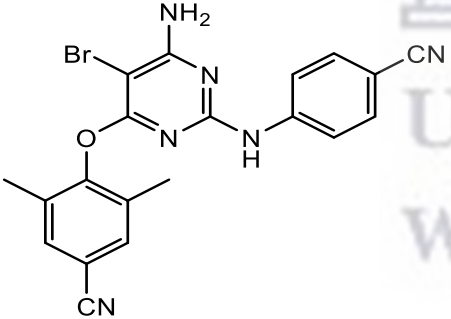
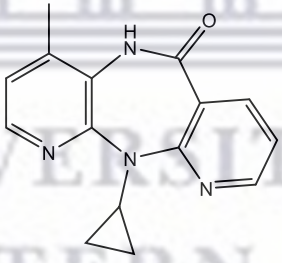
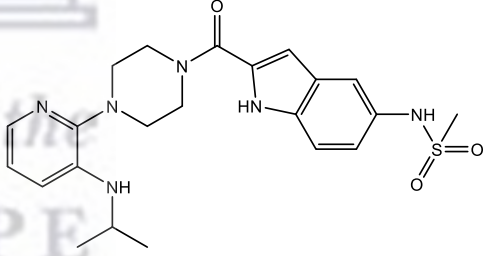
Figure 2.4. Illustration of HIV life cycle and targets for antiretroviral therapy adapted from (Michaud *et al.*, 2012)

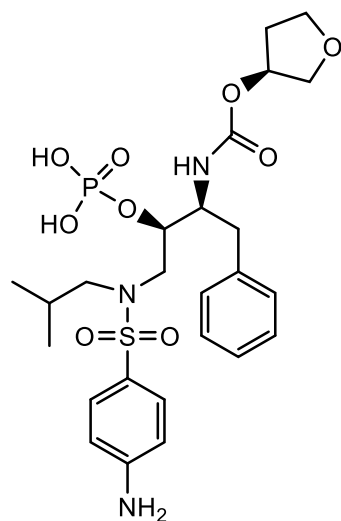
Despite the significant increase in the number of HIV patients receiving ART, from 3% in 2000 to 46% in 2015, and increased access to less expensive ART, approximately only half of the children who need ART could access or afford them. These children account for 4.9% of the global HIV population but it is sad to note that only 6% of (35 of 583) clinical antiretroviral drugs were paediatric formulation with only 5% of all subjects, hence they (children) are not being prioritized enough unlike in adults in the appropriate antiretroviral drug development (Dubrocq *et al.*, 2017). Currently, out of 2.1 million children living with HIV, only 58% were found to receive treatment with most children from developing countries being unable to access ART. Use of ART has shown to achieve high therapeutic efficacy in the treatment of HIV disease especially amongst adults in both low- and high-income countries by improving the prognosis of HIV-related individuals, reducing HIV-related mortality and morbidity while minimizing other opportunistic infections (Ryan Phelps and Rakhmanina, 2011; Arage *et al.*, 2014). However, there are numerous challenges that exist which prevents children with HIV/AIDS from maintaining treatment adherence which includes: stigma associated with HIV, cost of medicine, difficult swallowing and dose adjustment, dispensability, short half-life and regimen complexity, the challenge of bitter taste, and drug resistance due to long term therapy in children living with HIV. These drawbacks have further contributed to several severe side

effects among children such as hypersensitivity reaction, lactic acidosis, hyperlipidaemia, bone demineralization which are contrary to adults receiving ART (Sharland and Bryant, 2009; Dubrocq *et al.*, 2017). In this regard, there is an urgent need to improve current ARV dosage forms and to make it more child friendly.

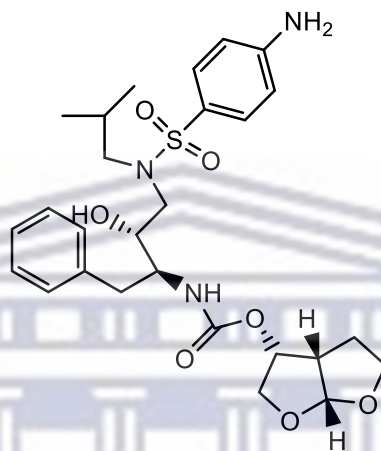


Table 2.1. Structures and names of some FDA approved antiretroviral drugs (Michaud *et al.*, 2012)

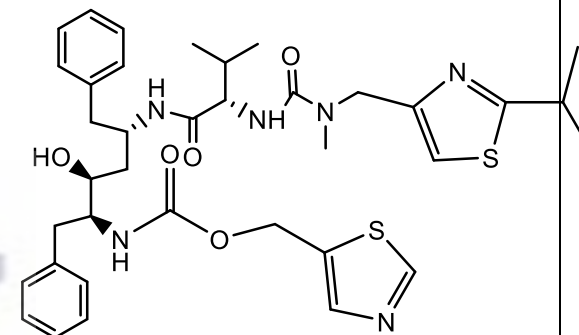
NRTIs		
 <p>4-amino-5-fluoro-1-((2R,5S)-2-(hydroxymethyl)-1,3-oxathiolan-5-yl)pyrimidin-2(1H)-one (Emtricitabine)</p>	 <p>4-amino-1-((2R,5S)-2-(hydroxymethyl)-1,3-oxathiolan-5-yl)pyrimidin-2(1H)-one (Lamivudine)</p>	 <p>(R)-((((1-(6-amino-9H-purin-9-yl)propan-2-yl)oxy)methyl)phosphoryl)bis(oxy))bis(methylene) diisopropyl bis(carbonate) (Tenofovir disoproxil)</p>
NRTIs		
 <p>4-((6-amino-5-bromo-2-((4-cyanophenyl)amino)pyrimidin-4-yl)oxy)-3,5-dimethylbenzotrile (Etravirine)</p>	 <p>11-cyclopropyl-4-methyl-5,11-dihydro-6H-dipyrido[3,2-b:2',3'-e][1,4]diazepin-6-one (Nevirapine)</p>	 <p>N-(2-(4-(3-(isopropylamino)pyridin-2-yl)piperazine-1-carbonyl)-1H-indol-5-yl)methanesulfonamide (Rescriptor)</p>
PIs		



(S)-tetrahydrofuran-3-yl ((2S,3R)-4-((4-amino-N-isobutylphenyl)sulfonamido)-1-phenyl-3-(phosphonoxy)butan-2-yl)carbamate
(Fosamprenavir)

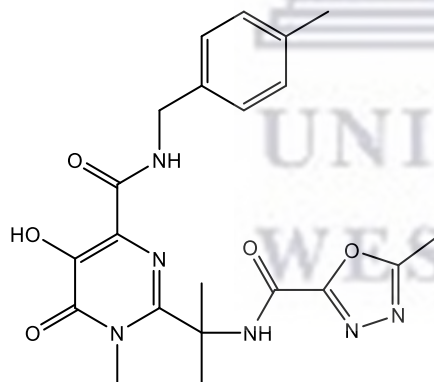


(3R,3aS,6aR)-hexahydrofuro[2,3-b]furan-3-yl ((2S,3R)-4-((4-amino-N-isobutylphenyl)sulfonamido)-3-hydroxy-1-phenylbutan-2-yl)carbamate
(Darunavir)

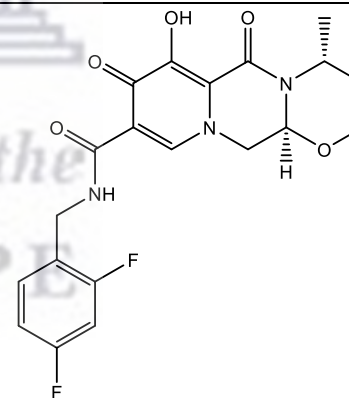


thiazol-5-ylmethyl ((2S,3S,5S)-3-hydroxy-5-((S)-2-(3-((2-isopropylthiazol-4-yl)methyl)-3-methylureido)-3-methylbutanamido)-1,6-diphenylhexan-2-yl)carbamate
(Ritonavir)

IIs



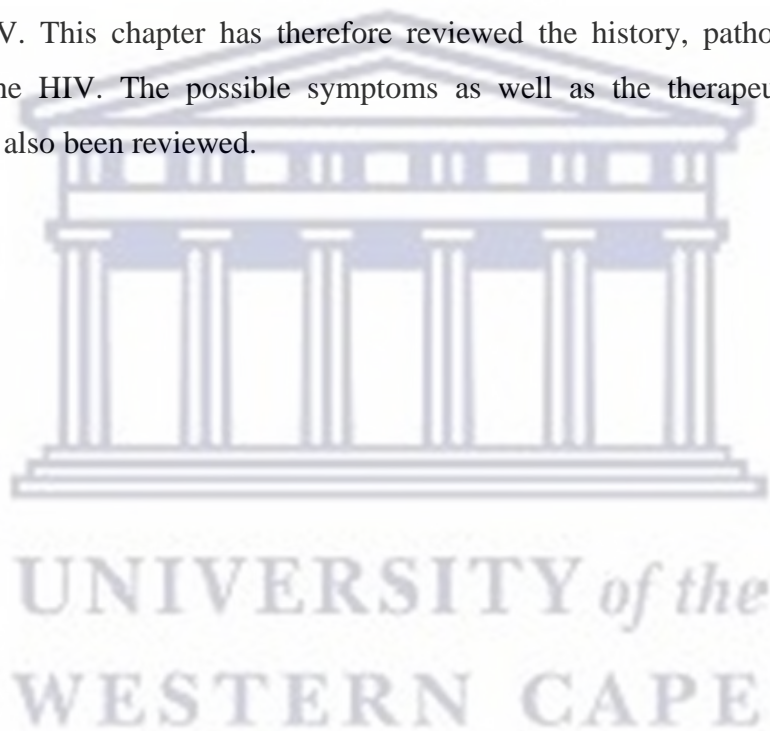
N-(2-(5-hydroxy-1-methyl-4-((4-methylbenzyl)carbamoyl)-6-oxo-1,6-dihydropyrimidin-2-yl)propan-2-yl)-5-methyl-1,3,4-oxadiazole-2-carboxamide
(Raltegravir)



(4R,12aS)-N-(2,4-difluorobenzyl)-7-hydroxy-4-methyl-6,8-dioxo-3,4,6,8,12,12a-hexahydro-2H-pyrido[1',2':4,5]pyrazino[2,1-b][1,3]oxazine-9-carboxamide
(Dolutegravir)

2.6. Conclusion

Since the emergence and the discovery of this virus, globally, more than 50 million people have been infected while killing over 16 million people with an annual rate of 6 million new HIV infections being detected hence posing a global threat to human health. Two major types of the virus have been identified namely, HIV-1 and HIV-2 with HIV-1 the primary cause of the pandemic today globally. Earliest identification of HIV-1 reported that HIV-1 originated from Congo around 1959 to 1960 and was transmitted to human from the two common captive chimpanzee, *Pan troglodytes*. Since the origin and identification of this virus in humans, it has continuously caused severe threat to public health of people. Although HAART have been adopted in the treatment to improve the health of HIV people, however there is not a permanent cure yet for HIV. This chapter has therefore reviewed the history, pathogenesis, and the replication of the HIV. The possible symptoms as well as the therapeutic treatment of HIV/AIDS have also been reviewed.



2.7. Reference

- Apetrei, C., Robertson, D.L. and Marx, P.A. (2004) 'The history of SIVs and AIDS: Epidemiology, phylogeny and biology of isolates from naturally SIV infected non-human primates (NHP) in Africa', *Frontiers in Bioscience*, (9), pp. 225–254.
- Arage, G., Tessema, G.A. and Kassa, H. (2014) 'Adherence to antiretroviral therapy and its associated factors among children at South Wollo Zone Hospitals, Northeast Ethiopia : a cross-sectional study', *BioMedical Central Public Health*, 14(365), pp. 1–7.
- Barre-Sinoussi, F. *et al.* (1983) 'Isolation of a T-lymphotropic retrovirus from a patient at risk for acquired immune deficiency syndrome (AIDS)', *Science*, 220(4599), pp. 868–871.
- Becken, B. *et al.* (2019) 'Human Immunodeficiency Virus 1: History, Epidemiology, Transmission, and Pathogenesis', *In: Domachowske J. (1st edn) Introduction to Clinical Infectious Disease*, pp. 417–423.
- Brown, S.P., Cornforth, D.M. and Mideo, N. (2012) 'Evolution of virulence in opportunistic pathogens: Generalism, plasticity, and control', *Trends in Microbiology*, 20(7), pp. 336–342.
- Chesney, M.A. (2000) 'Factors Affecting Adherence to Antiretroviral Therapy', *Clinical Infectious Diseases*, 30(2), pp. 171–176.
- Cock, K.M., Mbori-ngacha, D. and Marum, E. (2002) 'Shadow on the continent: public health and HIV/AIDS in Africa in the 21st century', *The Lancet*, (360), pp. 67–72.
- Dubrocq, G., Rakhmanina, N. and Phelps, B.R. (2017) 'Challenges and Opportunities in the Development of HIV Medications in Pediatric Patients', *Pediatric Drugs*, 19(2), pp. 91–98.
- Eckert, D.M. and Kim, P.S. (2001) 'Mechanisms of Viral Membrane Fusion and ITs inhibition', *Annual Review of Biochemistry*, 70(1), pp. 777–810.
- Fanales-Belasio, E. *et al.* (2011) 'HIV virology and pathogenic mechanisms of infection: a brief overview', *Ann Ist Super Sanità*, 47(4), pp. 363–372.
- Fettig, J. *et al.* (2014) 'Global epidemiology of HIV', *Infectious Disease Clinics of North America*. Elsevier Inc, 28(3), pp. 323–337.
- Gottlieb, G. *et al.* (2004) 'Dual HIV-1 infection associated with rapid disease progression', *Infectious Diseases in Clinical Practice*, 12(4), pp. 250–268.

- Greene, W.C. (2007) 'A history of AIDS: Looking back to see ahead', *European Journal of Immunology*, (37), pp. 94–102.
- Gupta, U. and Jain, N.K. (2010) 'Non-polymeric nano-carriers in HIV/AIDS drug delivery and targeting', *Advanced Drug Delivery Reviews*. Elsevier B.V., 62(4–5), pp. 478–490.
- Hägström, M. (2014) 'Medical gallery of Mikael Häggström 2014', *Wiki Journal of Medicine*, 1(2), pp. 1–53.
- Hahn, B.H. *et al.* (2000) 'AIDS as a zoonosis: Scientific and public health implications', *Science*, 287(5453), pp. 607–61.
- Hirsch, V.M. *et al.* (1989) 'An African primate lentivirus (SIVsmclosely related to HIV-2', *Nature*, 339(6223), pp. 389–392.
- Hutchinson, J.F. (2001) 'The Biology and Evolution of HIV', *Annual Review Anthropol*, (30), pp. 85–108.
- Jacobs, G.B. (2005) 'Investigation of the molecular epidemiology of HIV-1 in Khayelitsha , Cape Town , using serotyping and genotyping techniques Co-promoter', *Stellenbosch University, South Africa*.
- Kallings, L.O. (2008) 'The first postmodern pandemic: 25 years of HIV/AIDS', *Journal of Internal Medicine*, (263), pp. 218–243.
- Kharsany, A.B.M. and Karim, Q.A. (2016) 'HIV Infection and AIDS in Sub-Saharan Africa: Current Status, Challenges and Opportunities', *The Open AIDS Journal*, 10(1), pp. 34–48.
- Kilmarx, P.H. (2009) 'Global epidemiology of HIV', *Current Opinion in HIV and AIDS*, 4(4), pp. 240–246.
- Korber, B. *et al.* (2000) 'Timing the ancestor of the HIV-1 pandemic strains', *Science*, 288(5472), pp. 1789–1796.
- Lawn, S.D. (2004) 'AIDS in Africa: The impact of coinfections on the pathogenesis of HIV-1 infection', *Journal of Infection*, 48(1), pp. 1–12
- Levy, J.A. *et al.* (1984) 'Isolation of lymphocytopathic retroviruses from San Francisco patients with AIDS', *Science*, 225(4664), pp. 840–842.
- Levy, J.A. (1993) 'The transmission of HIV and factors influencing progression to AIDS', *The American Journal of Medicine*, 95(1), pp. 86–100.

- Lindegren, M.L, Steinberg, S. and Byers, R.H. (2000) 'Epidemiology of HIV / AIDS in Children', *Pediatric Clinic of North America*, 47(1), pp. 21–39.
- Maartens, G., Celum, C. and Lewin, S.R. (2014) 'HIV infection: Epidemiology, pathogenesis, treatment, and prevention', *The Lancet*, 384(9939), pp. 258–271.
- Martin, M.P. and Carrington, M. (2013) 'Immunogenetics of HIV disease', *Immunological Reviews*, 254(1), pp. 245–264.
- Merson, M.H. *et al.* (2008) 'The history and Challenge of HIV prevention', *The Lancet* 372(9637), pp. 475 – 488.
- Michaud, V. *et al.* (2012) 'The dual role of pharmacogenetics in HIV treatment: Mutations and polymorphisms regulating antiretroviral drug resistance and disposition', *Pharmacological Reviews*, 64(3), pp. 803–833.
- Mohamed, A.A., Lu, X.L. and Mounmin, F.A. (2019) 'Diagnosis and treatment of esophageal candidiasis: current updates', *Canadian Journal of Gastroenterology and Hepatology*.
- MMWR (2011) 'Centre for disease control: HIV Surveillance-United States:1981-2008'.
- Moir, S. *et al.* (2010) 'B cells in early and chronic HIV infection: Evidence for preservation of immune function associated with early initiation of antiretroviral therapy', *Blood*, 116(25), pp. 5571–5579.
- Moir, S., Chun, T.W. and Fauci, A.S. (2011) 'Pathogenic Mechanisms of HIV Disease', *Annual Review of Pathology: Mechanisms of Disease*, 6(1), pp. 223–248.
- Morison, L. (2001) 'The global epidemiology of HIV/AIDS', *British Medical Bulletin*, (58), pp. 7–18.
- Mothi, S.N. *et al.* (2015) 'Paediatric HIV - trends & challenges', *Indian Journal of Medical Research*, (134), pp. 912–919.
- Naif, H.M. (2013) 'Pathogenesis of HIV infection', *Infectious Disease Reports*, 5(SUPPL.1), pp. 26–30.
- Nikolopoulos, G.K., Kostaki, E.G. and Paraskevis, D. (2016) 'Overview of HIV molecular epidemiology among people who inject drugs in Europe and Asia', *Infection, Genetics and Evolution; Elsevier B.V.*, (46), pp. 256–268.
- Phelps, B.R. *et al.* (2010) 'Experiencing antiretroviral adherence : helping healthcare staff

better understand adherence to paediatric antiretrovirals', *Journal of the International AIDS Society*, 13(48), pp. 2–5.

Quinn, T.C. (2008) 'HIV epidemiology and the effects of antiviral therapy on long-term consequences', *Aids*, 22(3), pp. 1–11.

Ramana, L.N. *et al.* (2012) 'Investigation on the stability of saquinavir loaded liposomes: Implication on stealth, release characteristics and cytotoxicity', *International Journal of Pharmaceutics*. Elsevier B.V., 431(1–2), pp. 120–129.

Ryan Phelps and Rakhmanina, N. (2011) 'Antiretroviral Drugs in Pediatric HIV-Infected Patients', *Pediatric Drugs*, 13(3), pp. 175–192.

Santiago, M.L. *et al.* (2002) 'SIVcpz in wild chimpanzees', *Science*, 295(5554), pp. 465–487.

Sharland, M. and Bryant, P.A. (2009) 'Paediatric HIV infection', *Medicine*, 37(7), pp. 371–373.

Sharp P.M. and Hahn B.H. (2011) 'Origins of HIV and the AIDS pandemic', *Cold Spring Harbor Perspectives in Medicine* 1:a006841.

Sharland, M. and Bryant, P.A. (2009) 'Paediatric HIV infection', *Medicine*, 37(7), pp. 371–373.

Shyamala, J. (2017) *Formulation design, development and in vitro evaluation of abacavir sulphate gastroretentive microspheres*. JKKN College of Pharmacy.

Silvestri, G. *et al.* (2003) 'Nonpathogenic SIV infection of sooty mangabeys is characterized by limited bystander immunopathology despite chronic high-level viremia', *Immunity*, 18(3), pp. 441–452.

Simon, V., Ho, D. and Karim, Q.A. (2006) 'HIV/AIDS epidemiology, pathogenesis, prevention, and treatment', *Lancet*, 368(5), pp. 489–504.

Souza, V.D. and Summers, M.F. (2005) 'How retroviruses select their genomes', *Nature Reviews microbiology*, 3, 643–655.

UNAIDS (2018) 'Global HIV Statistics- Fact sheet'. Available at: http://www.unaids.org/sites/default/files/media_asset/UNAIDS_FactSheet_en.pdf%0. (Accessed 4 April 2020).

UNAIDS (2019) 'Global HIV and AIDS statistics-Fact sheet, World AIDS day, 2019 Fact

Sheet'. (Accessed 12 June 2020).

Vahlne, A. (2009) 'A historical reflection on the discovery of human retroviruses', *Retrovirology* 6(40). doi10.1186/1742-4690-6-40.



Chapter Three

3. Microencapsulation of pharmaceutical compounds

3.1. Introduction

Microencapsulation is the science or technique primarily adopted in the encapsulation of a core material in the solid or liquid state by entrapment of this material by a wall former or carrier. Typically this process produces small solid particles of varying sizes within the nanometre to micrometre range (Figure 3.1) (Poshadri and Kuna, 2010; Dubey AK and Dey BK, 2012). The concept of microencapsulation technology was first engineered and patented by Schleicher and Green in the 1950s for the formulation of dye encapsulated capsules which was specifically developed for the purpose of paper copying (Agnihotri *et al.*, 2012; Paulo and Santos, 2017).

Since then, the application of microencapsulation have been employed and explored in several fields and industries such as in the agricultural, pharmaceutical, food, cosmetics, biomedical, and electronic industries for various purposes (Estevinho *et al.*, 2013). The numerous benefits of microencapsulation, especially in the agricultural and pharmaceutical industries, include the encapsulation of adhesives, dyes, live cells, active enzymes, flavours, fragrances, controlled or delayed release of the active ingredients, masking of unpleasant taste and improved solubility (Gouin, 2004; Desai and Park, 2005).

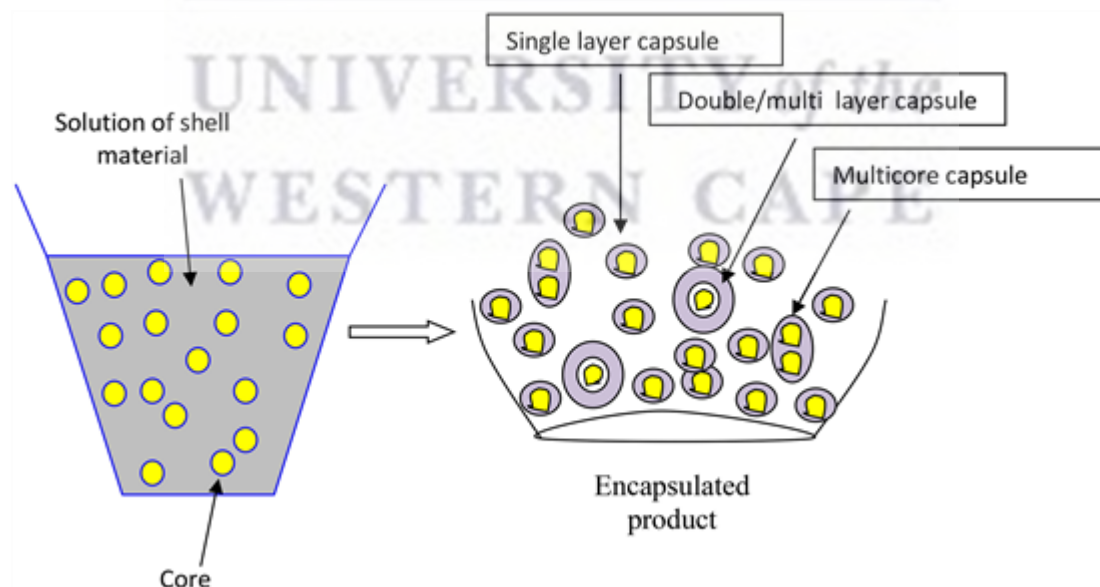


Figure 3.1. A simplified schematic depicting the microencapsulation process as adapted from (Timilsena, Haque and Adhikari, 2020).

The obtained products from a microencapsulation process are regarded as microparticles which can further be classified as microspheres or microcapsules. Microcapsules vary in size (1 – 100 μm) and shape and are dependent on the method and materials adopted. Most of the microspheres and microcapsules are formed through the application of a wide range of polymers or monomers involving different techniques hence the sizes and morphology tends to differ (Agnihotri *et al.*, 2012). These microcapsules are classified into various categories as depicted in Figure 3.2 namely: mononuclear microcapsule (core being surrounded by the shell), polynuclear microcapsule (having many core materials entrapped within the shell), matrix (the cores are evenly or homogeneously dispersed within the shell).

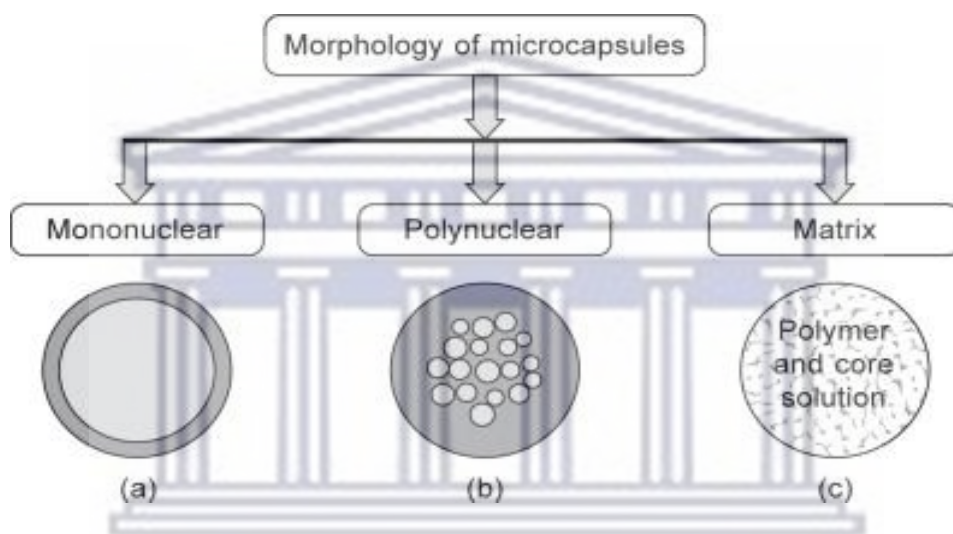


Figure 3.2. Classification of and various forms of microcapsule (Singh *et al.*, 2016).

3.2. Applications of microencapsulation

The application of microencapsulation has gathered momentum across various sectors, it has attracted mentionable interests from researchers and product developers hence it has been adopted in several sectors. Although the application of the microencapsulation in other sectors have been highlighted, however, the primary focus of microencapsulation in this work is on the pharmaceutical applications.

3.2.1. Application in food industry

Microencapsulation in food industry has obtained significant interest due to ever increasing demand by consumers towards healthy food supply (Dubey, Shami and Rao, 2009; França *et al.*, 2019; Arenas-Jal, Suñé-Negre and García-Montoya, 2020). Some food active compounds are highly unstable upon exposure to oxygen, light, some pH levels, and food processing conditions (Kouam, Songmene, Balazinski and Hendrick, 2013). Therefore,

microencapsulation in the food industry aims to minimize the reactivity of the food ingredients to environmental and processing conditions (Paulo and Santos, 2017). Several active compounds are volatile in nature hence this technology is required to decrease the growing concern of waste and evaporation of the volatile ingredients to the processing medium and masking of unpleasant tastes from active ingredients and allowing homogeneous distribution of food ingredients (Kouam, Songmene, Balazinski and Hendrick, 2013). This technique has aided application of microencapsulation in food industries and has considerably promoted the addition of functional ingredients in industrial formulated foods, thereby improving food texture, colour, flavour, and stability due to the presence of preservatives (Paulo and Santos, 2017).

3.2.2. Application in the agricultural sector

The attack of agricultural produce by insects has drawn attention towards effective measures in avoiding produce loss. Adopting the application of synthetic pheromones have become a potential alternative over the conventional means of managing pests in agriculture. Sex-pheromone is seen as a measure for mass trapping of insects, monitoring of the population and disrupting the mating process between the male and female insects (Dubey, Shami and Rao, 2009). In this regard, microencapsulation, have been adopted by formulation of encapsulated insect attractant pheromones using various polymers such as polyurea, Arabic gum and gelatin as micro-encapsulants (Chen, Fang and Zhang, 2007; Dubey, Shami and Rao, 2009). Microencapsulation in agricultural sector have also been applied towards minimizing the chemical impact of fertilizers on the quality of crop production. Earlier work on encapsulated fertilizer in a polymeric micro-structure of urea investigated the biological activity on maize and sunflower as target plants (Tolescu *et al.*, 2014). This work found a significant nutrient recovery and low chemical soil pollution with similar productivity to the pure fertilizer.

3.2.3. Application in the pharmaceutical industry

The common purpose of microencapsulation in the pharmaceutical industry is geared towards the discovery of the most effective drug delivery system (DDS), that would be widely accepted for the treatment of a particular disease hence reducing the side effects and reaction from the drugs, targeting the specific site of action, promoting a sustained or prolonged release of the compound, increasing shelf-lives and improving patient compliance (Obeidat, 2009; Paulo and Santos, 2017). Many of the APIs are known to have short half-lives, something that might be addressed through microparticles which could exhibit sustained drug release. Many drugs show

inadequate chemical stability and can easily degrade via hydrolysis or oxidation. More also, many of the APIs are known for their metallic, salty, or bitter taste hence are aversive to both children and adults thereby resulting to low or poor patient compliance, especially in cases of frequent administration (Walsh *et al.*, 2018; Penazzato *et al.*, 2019). Microencapsulation of APIs is therefore a strategy aimed at addressing some or all the mentioned challenges. This pharmaceutical pre-formulation technique is not something new to the pharmaceutical industry, as can be seen from the list of some of the approved and marketed microencapsulated products (Table 3.1).

Table 3.1. List of some marketed microencapsulated drugs and therapeutic use as adapted (Jeffrey Ting *et al.*, 2018)

Trade name	Treatment	Drugs	Excipients
Isoptin-SRE	Anti-hypertensive	Verapamil	HPC/HPMC
Sporanox	Antifungal	Itraconazole	HPMC
Nivadil	Anti-hypertensive, cerebral artery occlusion	Nivaldipine	HPMC
Rezulin	Anti-diabetic	Troglitazone	PVP
Intelence	HIV	Etravirine	HPMC
Norvir	HIV	Ritonavir	PVP-VA
Afeditab	Anti-hypertensive	Nifedipine	Poloxamer
Fenoglide	Anti-cholesterol	Fenofibrate	PEG
Onmel	Antifungal	Itraconazole	PVP-VA/HPMC
Kaletra	HIV	Lopinavir/Ritonavir	PVA-VA
Kalydeco	Cystic fibrosis	Ivacaftor	HPMCAS
Zelboraf	Melanoma skin cancer	Vemurafenib	HPMCAS
Incivek	Antiviral: hepatitis C	Telaprevir	HPMCAS
Certican and Zortress	Immunosuppressant	Everolimus	HPMC

3.3. Materials for microencapsulation

The two main materials involved in microencapsulation are namely the wall or shell material and the core material or the active ingredient.

3.3.1. Wall material

Wall material is commonly designated as the protector of the main active ingredient in microencapsulation. From literature, it is evident that a good number of wall or shell materials have been extensively used and studied already. During microencapsulation, selection of the wall materials is a crucial step because selection of the right coating material(s) determines both the physical and chemical characteristics of the generated microcapsules. The coating materials are required to demonstrate a high level of microencapsulating agent features such as: the film forming capacity, enough cohesiveness with the core material without compromising physical and chemical compatibility and not reacting with the active ingredient (Agnihotri *et al.*, 2012). An ideal walling or coating material according to Suganya and Anuradha (2017) should possess the following characteristics before they are considered for microencapsulation. This includes:

- ✚ Non-toxicity
- ✚ Chemically inert to the core material
- ✚ Good stabilization of the core material
- ✚ Low viscosity
- ✚ Non-hygroscopic
- ✚ Tasteless
- ✚ Cost-effective
- ✚ Film forming, flexible, brittle, and pliable

Several natural and synthetic materials exist that have been studied extensively as walling agents using microencapsulation techniques. They are either natural or synthetic polymers, proteins, or carbohydrates. Some of these walling agents are listed in Table 3.2.

Table 3.2. Examples of some natural and synthetic walling materials (Timilsena, Haque and Adhikari, 2020)

Types of walling agents	Examples
Natural polymers	Pea protein, rice protein, whey protein, albumin, collagen, gelatin, lipids, wax, paraffin, beeswax, oil, and fats
Synthetic polymers	Polymethyl methacrylate, methyl cellulose, carboxyl methyl cellulose, acrolein, glycidyl methacrylate, lactides, glycolides, polyalkyl cyanoacrylate
Carbohydrates / Polysaccharides	Agrose, starch, chitosan, maltodextrin, inulin, corn syrup
Modified starch	Poly dextran, poly starch, acacia gum, sodium alginate, carrageenan

For this study, walling agents such as pea protein isolate, inulin, lecithin, and cholesterol were selected. This is because these coating materials have shown potential in pharmaceutical application due to their nutritive values and characteristic functional features of good walling agents therefore, they are discussed below. These excipients are cost-effective and readily available hence scintillated the researcher's interest for uses in microencapsulation, solubility enhancement and taste masking of antiretroviral drugs.

3.3.1.1. Pea protein isolate

Pea is commonly regarded as *Pisum sativum*, a leguminous plant family of *Fabaccae* and a hexameric form of protein consisting of 150-170 kDa molecular mass and 7s (S as the Svedberg unit) sedimentation coefficient, indicating the sedimentation of the pea protein particles during centrifugation (Lam *et al.*, 2018). Pea protein is one of the most cultivated crop in almost 84 countries for either human or livestock consumption because of its high protein and carbohydrate contents (Lu *et al.*, 2019). Globally, peas are considered a staple food (Duranti and Gius, 1997). The demand for pea protein has caused a steady rise in production over the past 30 years and is regarded as the most produced legume after soybean, peanuts, and dry beans (Vidal-Valverde *et al.*, 2003; Lu *et al.*, 2019). Pea protein is prepared in three main forms namely; flour, concentrate or isolate via methods such as dry milling of dehulled peas, acid leaching or wet processing respectively (Owusu-Ansah and Mc curdy, 1991).

Pea proteins are made up of two major storage fractions called the IIS (*legumin*) and 7s (*vicilin*) (Lam *et al.*, 2018). Vicilin are trimeric protein of 150 – 170kDa with a molar mass subunit ~47kDa, ~50kDa, ~34kDa and ~30kDa and α , β , and γ 9s subunits with high level of protein (35 – 40%) and carbohydrate (24 – 49%). Also contained is fat (1.5 – 2.0%), essential vitamins and minerals, 10 -15% insoluble and 2.9% soluble dietary fibre, non-carbohydrate starch enriched with lysine but less methionine and tryptophan (Owusu-Ansah and Mccurdy, 1991, Barac *et al.*, 2015). Pea protein has been extensively used in the food industry due to its nutritional and health value, availability, cost effectiveness, the high digestibility, low allergenicity and negative health controversies (Lu *et al.*, 2019). Pea protein possesses some interesting functional properties including good emulsifying ability, foaming capacity, stability and encapsulating and shielding features which favoured its use as food additive. Hence these necessitated the selection of pea protein isolate in this work as an encapsulating agent for ARVs aimed to be subsequently formulated into paediatric dosage forms.

3.3.1.2. Inulin

Inulin is regarded as a non-structural and naturally occurring plant derived carbohydrate with the chemical structure depicted in Figure 3.3 (Drabińska, Zieliński and Krupa-Kozak, 2016; Ahmed and Rashid, 2019). Primarily, inulin consists of the fructosyl (β C2 – 1) linkage of each molecule (Kalyani Nair, Kharb and Thompkinson, 2010). Inulin is known as a poly-dispersed mixture of molecules having similar chemical structure represented as *Gfn* with “G” standing

for methyl of glucosyl, “f” moiety of fructosyl and “n” number of fructosyl moiety linked by β (1,2) linkages (Singh and Singh, 2010; Mensink *et al.*, 2015).

Chemical formular of inulin: $C_6nH_{10n+2}O_{5n+1}$

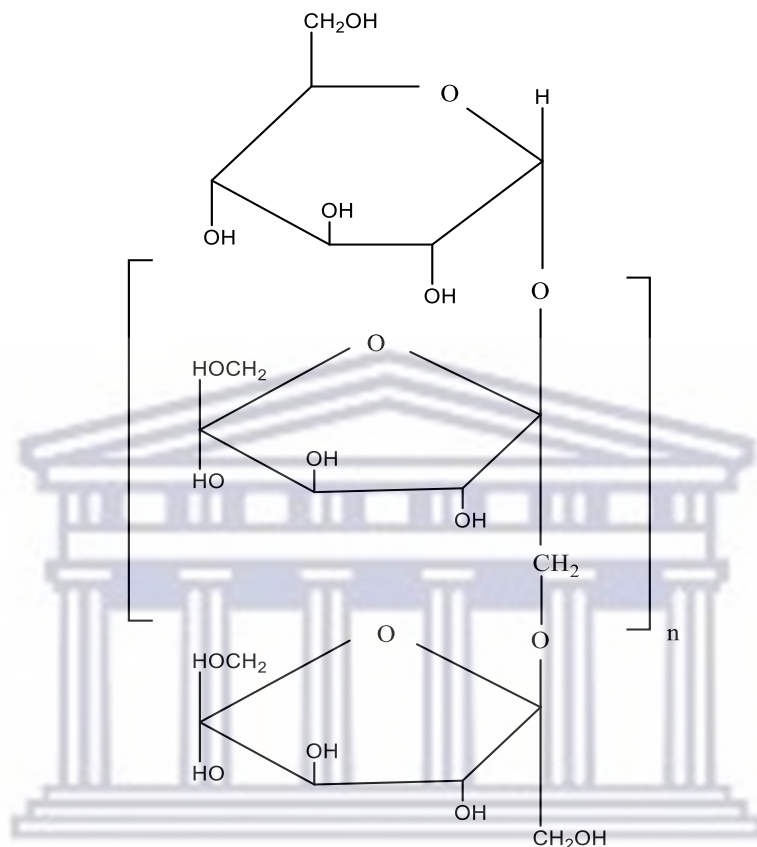


Figure 3.3. Chemical structure of inulin $n = 2 - 60$, adapted from (Kalyani Nair, Kharb and Thompkinson, 2010).

Several dicotyledonous species store inulin in form of fructans with the linear β (2 – 1) fructo furanosyl unit and the branched or complex fructans commonly found in the monocots (Kaur and Gupta, 2002; Mensink *et al.*, 2015). Inulin is mainly found in plants such as leeks, onions, wheat, asparagus (*Asparagus officianalis*), garlic, Jerusalem artichoke (*Hellanthus tuberlusus*), and chicory (*Cichorium intybus*) (Roberfroid, 2002; Kalyani Nair, Kharb and Thompkinson, 2010). Table 3.3 highlights several sources of inulin as well as the percentage content of inulin present.

Table 3.3. Inulin content in some plants (Singh and Singh, 2010)

Common name	Plant part	Inulin content (%)
Garlic	bulb	9 – 16
Salify	roots	10 – 15
Jerusalem artichoke	tubers	14 – 19
Dahila	tubers	15 – 20
Chicory	roots	15 – 20
Agave	lobes	17 – 10
Kuth	roots	18 – 20
Camas	bulb	12 – 22
Leek	bulb	3 – 10
Barley	grains	0.5 – 1.5
Dandelion	leaves	12 – 15
Yacon	roots	3 – 19
Murnong	roots	8 – 13

In the pharmaceutical industries, the health benefits of inulin include the use as a dietary fibre, adds good caloric value, the non-digestibility of the monosaccharide moiety aides in formations of bacterial fuel and gases, lactation that boost the energy metabolism of the body cell, use as a stabilizing agent in the membrane, a solubilizer for enhancing poorly soluble compounds, and can serve as a sweetener or flavouring agent (Vereyken *et al.*, 2003; Saavedra-Leos *et al.*, 2014). It has been used in local drug delivery for targeting of the colon since it cannot be hydrolysed by the digestive enzymes in the gastrointestinal tract but can only be hydrolysed by inulinase present in the colon due to the presence of the batido bacteria. These characteristic features of inulin therefore aided the selection as a potential co-former in the development of amorphous solid dispersions.

3.3.1.3. Lecithin

Lecithin (Figure 3.4) is one of the major components of liposomes. A name derived from the Greek word "Lekithos" because around 1847, lecithin was used in describing nitrogen and phosphorus materials of sticky and orange-coloured forms mainly isolated from egg yolk and later materials from blood, brain, bile and even some organic materials (Wendel, 2000). Later, it was discovered that the nitrogen component of lecithin is made of choline, a known organic base found in the brain of the living organism. Currently, lecithin is generally used in describing not only the phosphatidylcholine, but also used to denote the crude phospholipid mixture composed of the phosphatidylcholine (PC), phosphatidylethanolamine (PE), phosphatidylinositol (PI) and some other fatty acid compounds like the sterols, triglycerides, carbohydrates, and glycolipids (Figure 3.5) (Wendel, 2000; Wu and Wang, 2003; Adriana *et al.*, 2014). Lecithin has been extensively used in various fields including agricultural, food, cosmetic as well as in the pharmaceutical field. In agriculture, lecithin has been used in animal feeds as an essential ingredient for providing the necessary phospholipid to aquatic organisms and as an antioxidant in the feed. Lecithin in fertilizers act as condition and spreading agent, used in pesticides as adhesives, emulsifier, stabilizer, dispersing agent and even viscosity modifier (Wendel, 2000).

In pharmaceutical application, lecithin has been explored as an excipient or as an active agent, as lipid lowering agent or as liver protector due to the emulsifying property. It is used as a primary source for the dietetic phosphatidylcholine highly required in the lipid metabolism (Palacios and Wang, 2005; Rossi, 2007; Olisa, 2009). Lecithin as excipient has been adopted in formulation of drug delivery systems or carriers for various active pharmaceutical ingredients (APIs) such as in the formulation of liposomes, micelles, and emulsions in oral, buccal, and topical applications. For these reasons they target specific sites of action with sustained release as enhancement and solubilizing agent, and for reduction of toxicity. Some of these delivery systems such as liposomes are capable of entrapping both the hydrophilic and the hydrophobic drugs within the lipid or aqueous layer thereby improving their solubility, stability and protecting the drugs while delivering the drugs to specific cells or organs over time. Other therapeutic uses of lecithin are as emulsifying agents for injectables and as dispersants for vitamins (Rossi, 2007; Van Nieuwenhuyzen and Tomás, 2008).

Lecithin is mainly found in egg yolk, in oil seeds of soybeans, corn germ, cotton, flax and sunflower. Soybean lecithin is widely used because of its availability and good emulsifying

feature, taste and appearance, solubility enhancement of poorly soluble drugs and formation of solid dispersions hence it was chosen for this work (Nieuwenhuyzen and Tomás, 2008).

Chemical formula of lecithin: $C_{35}H_{66}NO_7P$



Figure 3.4. Chemical structure of lecithin from (Olisa, 2009)

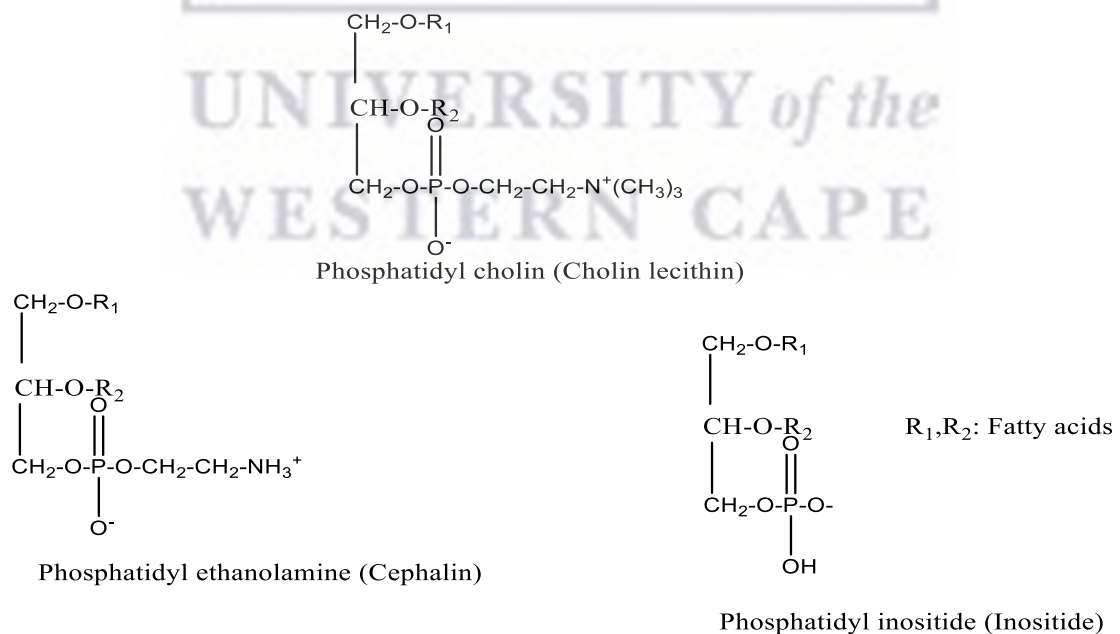


Figure 3.5. Chemical structure of three major phosphatides (Baeza-Jimenez; Lopez Martinez and Garcia, 2013).

3.3.1.4. Cholesterol

Cholesterol (Figure 3.6) is a known four ring and a complex structural molecule found in the mammalian cell membrane and an essential precursor for many physiological processes. Cholesterol not only serves as a molecule of regulation itself, but also forms the backbone of all steroid hormones, bile acid and vitamin D analogues. Cholesterol molecule forms part of the major growth and development through all the life stages (Narwal *et al.*, 2019; Schade, Shey and Eaton, 2020). This molecule is one of the major constituents of liposomes along with lecithin hence it helps in stabilizing the lipid bilayer, regulating the permeability of the membrane, and giving rigidity to the membrane as well as providing stability to the plasma which are the major reasons in selecting cholesterol in the formulation of liposomes in this study. The major sources of cholesterol are poultry, eggs, dairy, meat and even sea food (Haeri *et al.*, 2014; Albuquerque *et al.*, 2016). Cholesterol is moderately soluble in organic solvents such as chloroform, acetone, methanol, ethanol, benzene, ether, hexane but practically insoluble in water, with a molecular mass of 386.65 g/mol, melting point between the temperature 148.5 – 150 °C, boiling point of 360 °C and density of 1.052 g/cm³.

Chemical formula: C₂₇H₄₆O

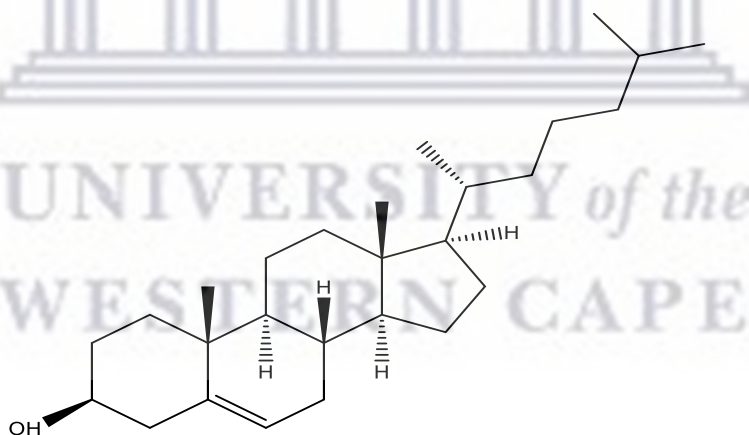


Figure 3.6. Chemical structure of cholesterol (Peng *et al.*, 2008).

3.3.2. Core material of microencapsulation

Core materials are the active compounds or active ingredients to be coated. They are either liquid or solid in nature and may vary in their composition since the core material can be dispersed or dissolved (Agnihotri *et al.*, 2012). Many pharmaceuticals, even cosmetics, agricultural and food materials have been encapsulated using different microencapsulation techniques, hence abacavir (ABC) and zidovudine (AZT) antiretroviral as the active pharmaceutical ingredients were chosen as the major core materials in this study due to their importance, recommendation, and prescription in HIV paediatric treatment hence the profile of these drugs is discussed below.

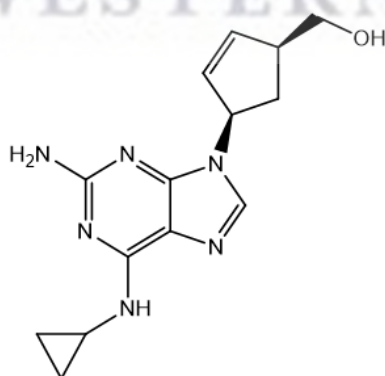
3.3.2.1. Profile of the core materials

3.3.2.2. Drug: Abacavir

Description

Abacavir (ABC) is a potent member of the nucleoside reverse transcriptase inhibitors (NTRIs) and a synthetic analogue carboxylic nucleoside of guanosine. It is primarily administered in adults and children older than 3 months orally in combination with other antiretroviral regimens in the treatment of HIV-1 and HIV-2. It functions by slowing down the viral loads and replication through blocking the reverse transcriptase enzyme hence improving the life of HIV patients (Kennewell, 2006; Eckhardt and Gulick, 2017). However, the use of the drug in children for an effective treatment has been made difficult due the limitations including the large size of the drug, unpalatable taste, severe side effects due to the frequent administration.

Molecular structure



Systemic IUPAC name

((1S,4R)-4-(2-amino-6-(cyclopropylamino)9-H-purin-9-yl)cyclopent-2-en-1-yl)methanol

Figure 3.7. Chemical structure of ABC (Michaud *et al.*, 2012)

Chemical properties

Formula:	C ₁₄ H ₁₈ N ₆ O
Synonyms:	Ziagen, Abacavir sulfate
Molecular weight:	286.339 g/mol.
CAS Registry number:	136470-78-5
Melting point:	165 °C
Water Solubility:	1.21 mg/mL or 77 mg/mL (sulfate salt)

Physical state of ABC

A white to white off powder in a solid form.

Solubility

ABC is soluble in water (77 mg/ml), in an organic solvent such as dimethyl sulfoxide (DMSO) (<1 mg/ml at 25 °C), ethanol (< 1 mg/ml at 25 °C) and in methanol.

Mechanism of action

ABC is a synthetic analogue of the carboxylic nucleoside. It is intracellularly converted by the cellular enzymes to form the active metabolites of carbovir triphosphate, an analogue of deoxyguanosine-5'-triphosphate (dGTP). Cabovir by inhibiting the activity of HIV-1 reverse transcriptase, interacts and competes with the natural substrate dGTP and by its incorporation into viral DNA. Due to the absence of a 3'-OH group in the incorporated analogue, the formation of the 5 to 3 phosphodiester linkages responsible for the DNA chain elongation therefore terminating the viral DNA growth (Shyamala, 2017).

Pharmacokinetics

Absorption

The absorption of ABC is through the oral administration with rapid and extensive tablet bioavailability of 83%.

Binding:

Binding of ABC to plasma proteins is approximately 50%.

Elimination:

The elimination half-life ($T_{1/2}$) of ABC is approximately 1.5 hours.

Metabolism

ABC is not metabolized by the P-450 Cytochrome enzymes. The elimination of ABC is by the hepatic metabolism by the alcohol dehydrogenase and glucuronosyltransferase to produce a 5'-

carboxylic acid metabolite and 5'-glucuronide metabolites, respectively but have no antiviral activity.

Excretion

ABC parent compound is mainly excreted through urine (1%) and as metabolites (81%) while 61% is excreted through faeces.

Indication and usage

ABC is indicated in the treatment of HIV-1 in combination with other antiretroviral.

Drug category

It is an antiretroviral agent.

Route of Administration and Dosage

ABC is orally administered and available as 300 mg tablets and oral solution (20 mg/ml). The dose recommendation for adults is 600 mg daily or 300 mg twice taken with or without food. The standard paediatric dose of ABC in children aged 3 months to 16 years is based on weight. A dose adjustment of 200 mg daily is required with patients with mild hepatic insufficiency but contradicted in patients with renal insufficiency and patients with severe hepatic insufficiency (Eckhardt and Gulick, 2017).

Paediatric and infant Dose

3 months or older

Oral solution: 8 mg/kg orally twice a day or 16 mg/kg orally once a day.

Maximum dose: 600 mg/day.

Tablets

14 to less than 20 kg: 150 mg orally twice a day or 300 mg orally once a day.

20 to less than 25 kg: 150 mg orally in the morning and 300 mg in the evening, or 450 mg orally once a day.

25 kg or more: 300 mg orally twice a day or 600 mg orally once a day.

Precautions

A dose adjustment of 200 mg daily is required with patients having mild hepatic insufficiency but contradicted in patients suffering from renal insufficiency and patients with severe hepatic insufficiency. Administration of ABC in patients with the generic marker HLA-B*5701 should be reduced or completely avoided as it is associated with the hypersensitivity reaction in such patients. ABC increases clearance of methadone, hence, increase in methadone dose is recommended (Eckhardt and Gulick, 2017).

Adverse Reaction and Drug Interactions

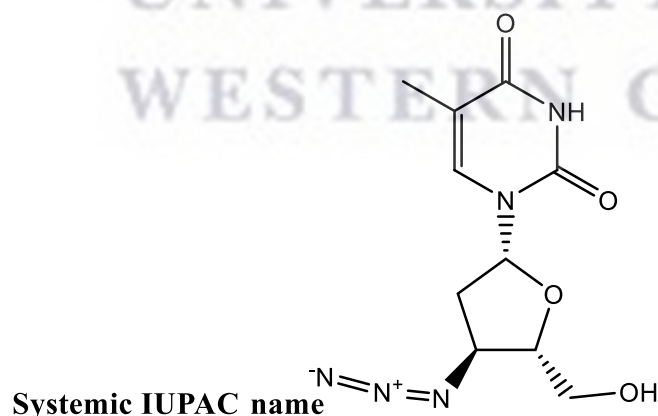
ABC is associated with severe and significant side effects or reactions including hypersensitivity reaction associated with high fever, rash, and constitutional, gastrointestinal, and a pulmonary symptom. Some other attributed side effects attributed to ABC are headache, malaise and fatigue, chills, nausea and vomiting, dreams, or sleep disorders, and even cardiovascular events (Eckhardt and Gulick, 2017; Shyamala, 2017). All these highlights the need for the encapsulation of the drug in a delivery to minimize these challenges and severe side effects.

3.3.2.3. Drug: Zidovudine (AZT)

Description

Zidovudine (AZT) is a class of the nucleoside reverse transcriptase inhibitors (NRTIs) and a synthetic analogue of thymidine that has been licenced for use in combination with other antiretroviral drugs against HIV-1 even in children with HIV. After phosphorylation to the active metabolite, it inhibits the DNA polymerase to reduce the replication in the cell hence resulting in the suppression of the virus and improvement of the life expectancy in HIV patients (Aliyu, 2012). The effective use of AZT in children is marred by its poor aqueous solubility, the frequent and daily administration, short half-life, and poor palatable taste hence a nanotechnology will be a way out in eradicating these challenges.

Molecular structure



Systemic IUPAC name 1-((2*R*,4*S*,5*S*)-4-azido-5-(hydroxymethyl)tetrahydrofuran-2-yl)-5-methylpyrimidine-2,4(1*H*,3*H*)-dione

Figure 3.8. Chemical structure of AZT (Michaud *et al.*, 2012)

Chemical Properties:

Formula:	C ₁₀ H ₁₃ N ₅ O ₄
Molecular weight:	267.244 g/mol
Monoisotopic:	267.097 g/mol
CAS Registry number:	30516-87-1
Melting point:	113 – 115 °C
Water Solubility:	25.0 mg/mL in water at 25 °C

Physical state

AZT is a white to beige, odourless, and crystalline solid.

Solubility

AZT is soluble in water (25.0 mg/ml), and in some organic solvents like ethanol (10 mg/ml), dimethyl sulfoxide (DMSO) (30 mg/ml), dimethyl formamide (DMF) (30 mg/ml).

Mechanism of action

AZT is a thymidine synthetic analogue of the nucleoside and an antiviral agent. In the mechanism of action AZT, the drug is phosphorylated or converted to form the active triphosphate which then actively inhibits the incorporation of the thymidine into the viral DNA by reverse transcriptase thereby decreasing the synthesis of the viral DNA. Through the incorporation and the conversion into the DNA, triphosphate interferes with the HIV-1 life cycle and stops the replication of the viral DNA chains and as well stopping the extra linkages of phosphodiester to the inactive or unreactive 3' -azido group causing a formation of the incomplete DNA. The conversion of AZT into monophosphate can also limit the viral replication through the inhibition of the essential part of the reverse transcriptase called the ribonuclease (RNase) (Wilde and Langtry, 1993; Sperling, 1998).

Pharmacokinetics

Absorption

AZT is extensively absorbed after oral administration (64% bioavailability, tablet) and gets the peak serum concentration within 0.5 – 1.5 hours.

Binding

Binding of AZT to the plasma protein is >38%.

Metabolism

AZT is extensively metabolised in the liver through the enzyme diphospho-glucuronosyltransferase to the inactive hepatic metabolite of the 3' -azido-3' deoxy-5-O-β-D-glucopyranuronosyl

thymidine. It is neither the substrate nor the inducer of the cytochrome P-450 (CYP450) (Paintsil and Cheng, 2008; Tsibris and Hirsch, 2014).

Elimination:

The elimination half-life ($T_{1/2}$) of AZT is approximately 1 hour but, in some cases, it is extended especially in patients with altered hepatic function.

Excretion

AZT is primarily and predominantly excreted renally. Equivalent of 40% of AZT is lost to the first pass metabolism, while 70 to 90% of AZT and the metabolite are found in the urinary excretion, 60 and 75% of the intravenous and oral AZT have been detected in the urinary excretion of the metabolite with 18 and 14% of AZT are primarily excreted as the main drug with minimal metabolism of AZT with the kidney.

Indication and usage

AZT is employed in the treatment of HIV-1 and administered together with other antiretroviral drugs and have been used in the prevention of maternal-foetal HIV transmission.

Drug category

Antiretroviral agents.

Route of Administration and Dosage

AZT is mainly administered orally and available as tablets (300 mg), capsules (100 mg) or syrup (50 mg/5ml) and available in co-formulations. The common and standard dose for adults is 600 mg/day or in divided doses of 300 mg twice daily in combination with other antiretroviral drugs. For the paediatric dosing, the dosage and administration are based on the weight or the body surface area (Mondal, 2007; Eckhardt and Gulick, 2017).

Doses in children and infant based on weight

Body weight 8 – 13 kg: 100 mg twice daily.

Body weight 14 – 20 kg: 100 mg in the morning and 200 mg in the evening.

Body weight 21 – 27 kg: 200 mg twice daily.

Body weight 28 – 29 kg: 200 – 250 mg twice daily.

Body weight 30 and above: 300 mg twice daily.

Precautions

An adjusted dose of 100 mg every 8 hours is recommended for patients suffering from renal impairment which could cause peritoneal haemodialysis or continuous Ven-venous hemofiltration.

Adverse Reaction and Drug Interactions

The use of AZT is commonly associated with several severe reactions among adults or children. Major toxicity reported in the use of AZT includes headache, high nausea, anorexia, myalgias, vomiting and malaise, lipoatrophy. Other hematologic toxicity like neutropenia and chronic anaemia have been reported. Symptomatic myopathy and myositis have also been reported with a prolonged use of AZT (E.g. > 1 year) (Sperling, 1998; Eckhardt and Gulick, 2017).

3.4. Solid dispersions

Solid dispersions are one of the interesting and promising strategies adopted in enhancing the oral bioavailability of poorly water soluble drugs (Gurunath *et al.*, 2013). In 1961, Obi and Sekiguchi were the first to discover a promising method capable of enhancing the dissolution and oral absorption of poorly soluble drugs which was later experimented by Mayersohn and Gibaldi in 1966 (Gurunath *et al.*, 2013). This strategy was later defined by Chiou and Reigelman as the entrapment of one or more active compound into an inert matrix carrier or delivery system at solid state developed either by fusion, solvent evaporation or melting (Gurunath *et al.*, 2013; Huang and Dai, 2014; Bhaskar, OLA and Ghongade, 2018). The matrix can be either crystalline or amorphous. According to the biopharmaceutical classification system (BCS), based on the solubility and permeability (Table 3.4), over 40% of drug compounds are regarded as poorly soluble thereby requiring larger doses to produce therapeutic effect and in turn result to toxic effects. Therefore, the use of solid dispersions is reported to significantly improve the drug wettability, bioavailability, and dissolution rate of poorly soluble drugs (Bhaskar, OLA and Ghongade, 2018).

Table 3.4. BSC classification adapted from (Bhaskar, OLA and Ghongade, 2018)

BSC class	Solubility in aqueous environment	Permeation over (intestinal) membrane
Class I	High solubility	High permeability
Class II	Low solubility	High permeability
Class III	High solubility	Low permeability
Class IV	Low solubility	Low permeability

Since the discovery of the solid dispersions, the strategy has been heavily explored in the pharmaceutical industry due to the several benefit it offers (Mishra *et al.*, 2015; Bhaskar, OLA and Ghongade, 2018) .

3.4.1. Advantages of solid dispersions

- ✦ Formation of particles with reduced size which in turn result to high surface area thereby causing increased rate of dissolution.
- ✦ Formation of particles with enhanced wettability which aids the solubility of the drug.
- ✦ The particles obtained from the solid dispersions are highly porous depending on the nature of the carrier hence solid dispersions can be developed using the linear and reticular polymers known for higher porosity.
- ✦ The drug in the amorphous form requires little or no energy to break up the crystal lattice in the dissolution process. This indicates a higher degree of solubility of the amorphous drug than the crystalline state of the drug.
- ✦ The faster dissolution and absorption of the amorphous form of drug may lead to quick onset of action: Solubility of drug candidate in aqueous media imparts faster dissolution profiles and absorption of drug results in immediate inception of action.
- ✦ Masking of unpleasant taste, smell of drugs is highly achievable.
- ✦ Solid dispersions offer more accurate and adequate dose than liquid or gaseous systems as they give rise to solid oral dosage forms instead of liquid because solubilization products convert into solid powder state.
- ✦ The risk of the drug particle agglomeration in the dissolution media could be minimized by using the surfactants or emulsifiers which enhances the dissolution rate of the drug.

Despite the intriguing advantages of the solid dispersions strategy, the approach is also limited in a manner that its application has not been completely utilized in the large-scale industries hence very few marketed products based solid dispersions are available. Some of these limitations of the solid dispersions includes:

- ✦ The possibility of recrystallization of the amorphous drug which exist as thermodynamically unstable hence they are likely to transform into a more likely stable form through recrystallization.
- ✦ There is a problem of stability hence the stability of the amorphous particles depends on the type of the solvent used as different approaches requires individual set of conditions like carriers and solvent system, product results from such methods imparts specific storage conditions failing to which leads to stability issues.

- ✚ It is so expensive at the commercial level due to the technical requirement and the methodology to produce amorphous solid dispersions.
- ✚ The reproducibility of the physico-chemical features varies with the different methods of solid dispersions formation.

3.4.2. Classification of solid dispersions

Solid dispersions can be classified based on the dissemination or distribution of solute compound within the carrier matrix as:

- ❖ Eutectic mixture
- ❖ Solid solution
- ❖ Microfine crystalline dispersions

Eutectic mixture: The eutectic mixture is composed of two major components (the drug and the polymer) which are miscible in their molten or liquid form but have limited miscibility in their solid state and can be formed by the rapid cooling of the co-melt of the two components. When these two components are mixed in a particular proportion, they tend to form a single melting point less than the individual melting point (Kumar *et al.*, 2014; Teja *et al.*, 2014; Siraj *et al.*, 2019).

Solid solution: The solid solution as the name implies is made of the solid solute dissolved in the solvent hence particle size relatively reduced to the molecular state (Kumar Das *et al.*, 2013). Solid solution is further divided into three namely based on their miscibility into continuous versus discontinuous solid solution: substitutional crystalline solid, interstitial solid and amorphous solid solution as demonstrated in Figure 3.7. The difference between these three solid solutions is that in the substitutional crystalline solid solution, a solute molecule can replace a solute carrier in the crystal lattice but only when the size of the solute molecule is approximately equal to the size of the solute carrier, the interstitial solid solution is rather made of the two melted or dissolved solutes within the interstices of the carrier matrix hence the size of the solute should not exceed 0.59 times the diameter of the solvent and there is formation of only discontinuous type of dispersion here whereas the amorphous solid solution is composed of the drug molecularly dispersed irregularly within the amorphous carrier (Kumar Das *et al.*, 2013; Teja *et al.*, 2014; Ghule *et al.*, 2018).

Microfine crystalline dispersion: This type of dispersion is composed of the crystalline drug molecularly dispersed in a carrier (Ghule *et al.*, 2018).

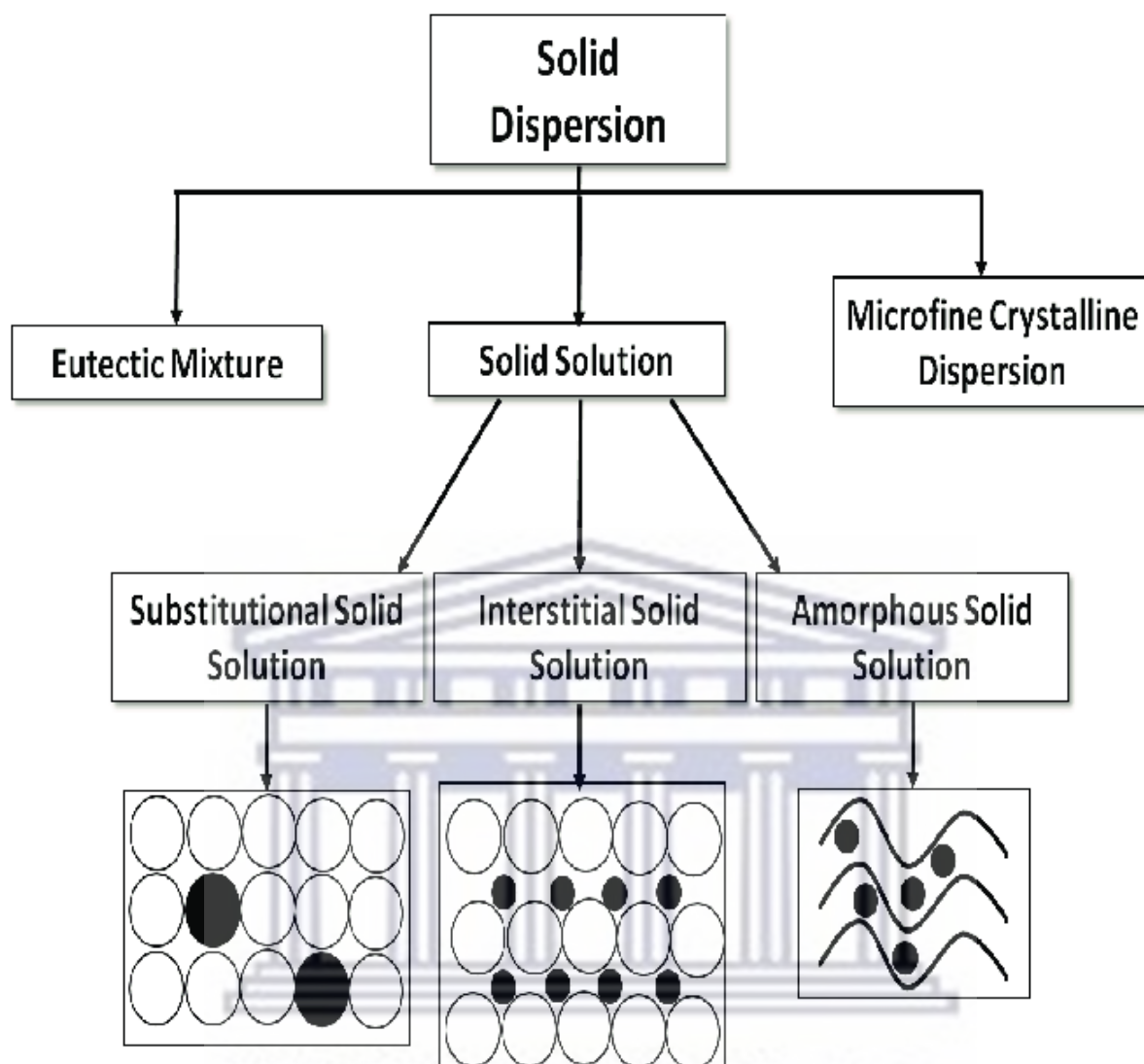


Figure 3.9. Classification of solid dispersions based on distribution of solute compound within the carrier (Teja et al., 2014).

3.4.3. Classification based on the physical state of the carrier

Solid dispersions can further be classified according to the physical state of the carrier as first generation, second generation, third generation, fourth generation, and fifth generation.

First generation: The formation of this form of solid dispersions includes the use of crystalline carriers like sugar, mannitol, urea, sorbitol hence it is regarded as crystalline carriers. Most of its carriers have high melting point therefore preparation of solid dispersions by melting method is not ideal. The first generation has good stability thermodynamically because of the crystalline state of the carrier, produces faster release with increased bioavailability compared to the conventional formulations; however, it has less solubility compared to the amorphous forms (Kim *et al.*, 2011; Singh, Baghel and Yadav, 2011; Mishra *et al.*, 2015; Bhaskar, OLA and Ghongade, 2018; Siraj *et al.*, 2019).

Second generation: This form of solid dispersions is mostly composed of amorphous carriers basically polymers and are made of a single-phase homogeneous system. The drug is molecularly and irregularly dispersed in this form of solid dispersions in a very small size and are regarded to form in a supersaturated state emanating from the forced solubilization. The amorphous solid dispersions are divided into amorphous solid solution (glass solution) and amorphous solid suspensions depending on the physical state of the drug. In the amorphous solid solution, a molecularly homogenous dispersion is formed from a complete mixture of the drug and amorphous carrier which are miscible with each other and are of two separate phases. Due to the presence of the forced solubilization in the second generation, the drug is highly supersaturated in the carrier therefore there is always the possibility of drug particle reduction to a molecular level, wettability and dispersibility of the drug to form amorphous form of the drug and carriers (Kim *et al.*, 2011; Singh, Baghel and Yadav, 2011; Mishra *et al.*, 2015; Bhaskar, OLA and Ghongade, 2018; Siraj *et al.*, 2019).

Third generation: Despite the improvement of dissolution rate and enhancement of the bioavailability of the drug through solid dispersions, the possible supersaturation state of the drug has been reported to result to precipitation of the drug from the solid dispersions and in turn decrease the concentration of the drug both in vitro and in vivo to cause limited bioavailability of the drug. Due to this phenomenon, the surface-active agents, or emulsifiers like inulin, comprisal, inutac, poloxamer are adopted in the third generation as carriers, surfactants, or additives to minimize possible precipitation or recrystallization because of the ability to maintain polymeric purity that improves in vivo bioavailability and drug stability (Singh, Baghel and Yadav, 2011; Mishra *et al.*, 2015; Bhaskar, OLA and Ghongade, 2018; Siraj *et al.*, 2019).

Fourth generation: This form of solid dispersions is designed primarily for the release of poorly water-soluble drugs with a short half-life. It is further regarded as controlled release dispersion. The essence of the formation is to enhance the solubility and prolong the release of the drug through the mechanism of diffusion or erosion. Some of the retarded polymers used in the form of solid dispersions include ethyl cellulose, polyethylene oxide, hydroxyl propyl cellulose, Eudragit (Mishra *et al.*, 2015; Bhaskar, OLA and Ghongade, 2018; Siraj *et al.*, 2019).

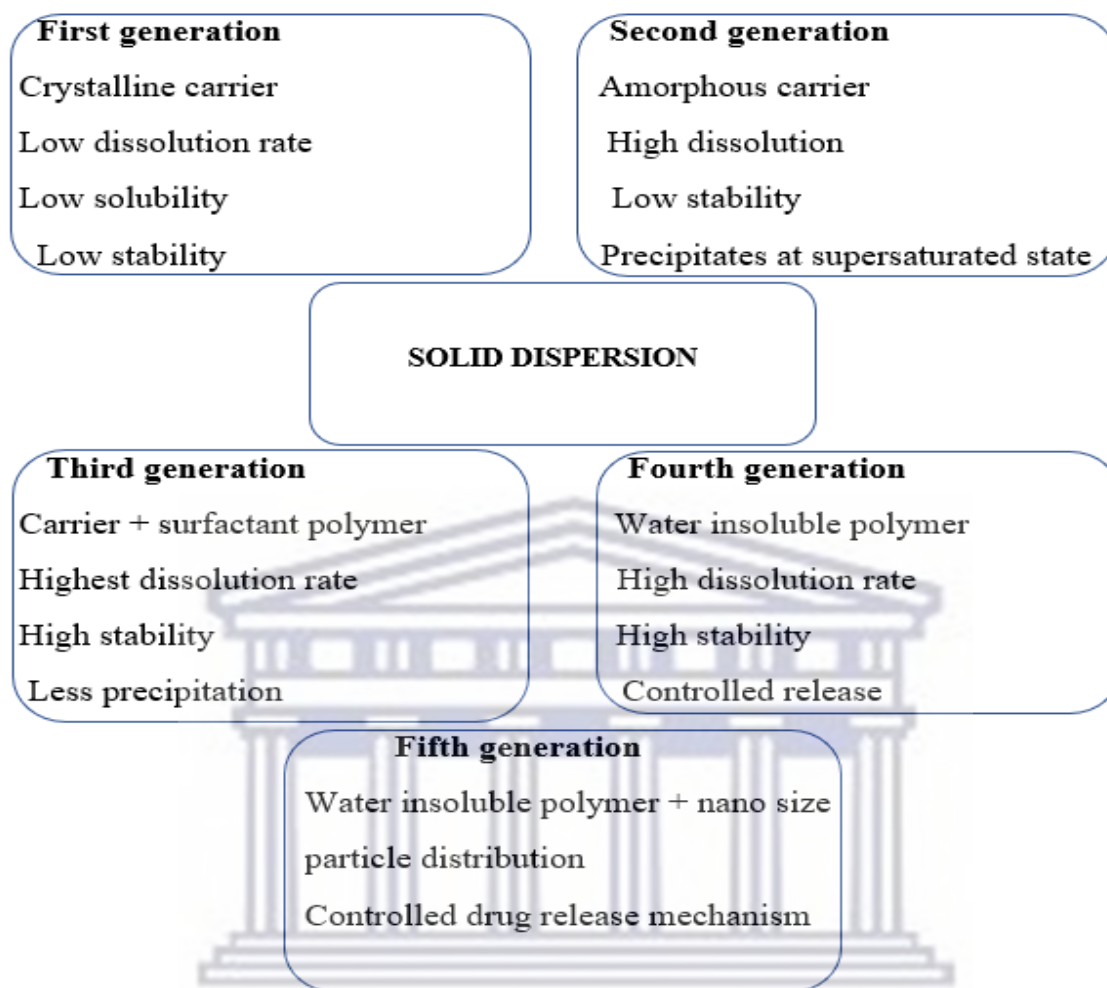


Figure 3.10. Classification of solid dispersions based on the physical state of the carrier adapted from (Jadav and Paradkar, 2020).

Fifth generation: The fifth generation of the solid dispersions was introduced such that the functional performance of the final product could be improved by the formation of nano and micron size structures. This was because of the adoption of multiple multidisciplinary approaches like polymeric science, fluid dynamics, nanoscience, nanotechnology, and even solid dispersions. Due to the report of burst release from the fourth-generation solid dispersions originating from the release of the drug particles on the surface of the solid dispersions, which causes rapid action and leading to immediate availability of the drug before being accompanied by the slow and controlled release of the drug over time, therefore the burst release mechanism affecting the therapeutic effect and efficacy of the developed formulation hence the fifth generation solid dispersions was then introduced. Using several advanced nanotechnology approaches, multiple of nanoparticles even for fifth generation have been developed which are

mainly core shell, Janus, and triple-layered structures that could prohibit the mechanism of the burst release from the fourth generation. The release of the drug in the fifth-generation solid dispersions is mainly by the programmed and controlled functional performance of the drug and the carrier molecule while in the other generations (first – fourth), the release of the drug is primarily based on the drug and the carrier physicochemical properties.

3.5. Microencapsulation Techniques

There are several microencapsulation techniques, with varying features, identifications, adaptation and specifications and they have been explored in the encapsulation of the desired microcapsules considering the size, shape as well as the physicochemical properties of the core material and the encapsulating agents. Some of these techniques are listed and summarized below.

3.5.1. Spray drying

The spray drying (Figure 3.11) is regarded as one of the microencapsulation techniques commonly and widely used in the encapsulation of various active ingredients. In this method, the active ingredient or compound is dissolved in a polymer solution to form a dispersed polymer suspension which is sprayed into a hot chamber. As the evaporation takes place due to the use of solvents, the coating material solidifies onto the active particles causing the formation of microcapsules of polynuclear and matrix form (Poshadri and Kuna, 2010; Agnihotri *et al.*, 2012). This technique is the most widely and commonly used encapsulation technique since its discovery by Boake Roberts in 1937. Since its discovery, spray drying has become efficiently adopted technique over other techniques even in the pharmaceutical studies where the method is mainly used for the drying of the heat sensitive compounds such as enzymes, pharmaceutical proteins with no huge loss of activity, taste masking of the bitter active compounds, enhancement of the poorly soluble drugs, improving the flow properties of the microcapsules, coating of the core materials and formulation microcapsules with a controlled release of the active ingredients (Sollohub and Cal, 2012; Seremeta *et al.*, 2014; Eun *et al.*, 2020). Spray drying offers several advantages which includes the economic value and effectiveness in protecting the core materials, relatively simple to operate, low water activity, and the suitability for transport and storage hence it is the widely employed technique over other many others and the major reason in selecting the technique in our study for the solubility enhancement and taste masking of the antiretroviral drugs (Maria Ré, 2006; Poshadri and Kuna, 2010).

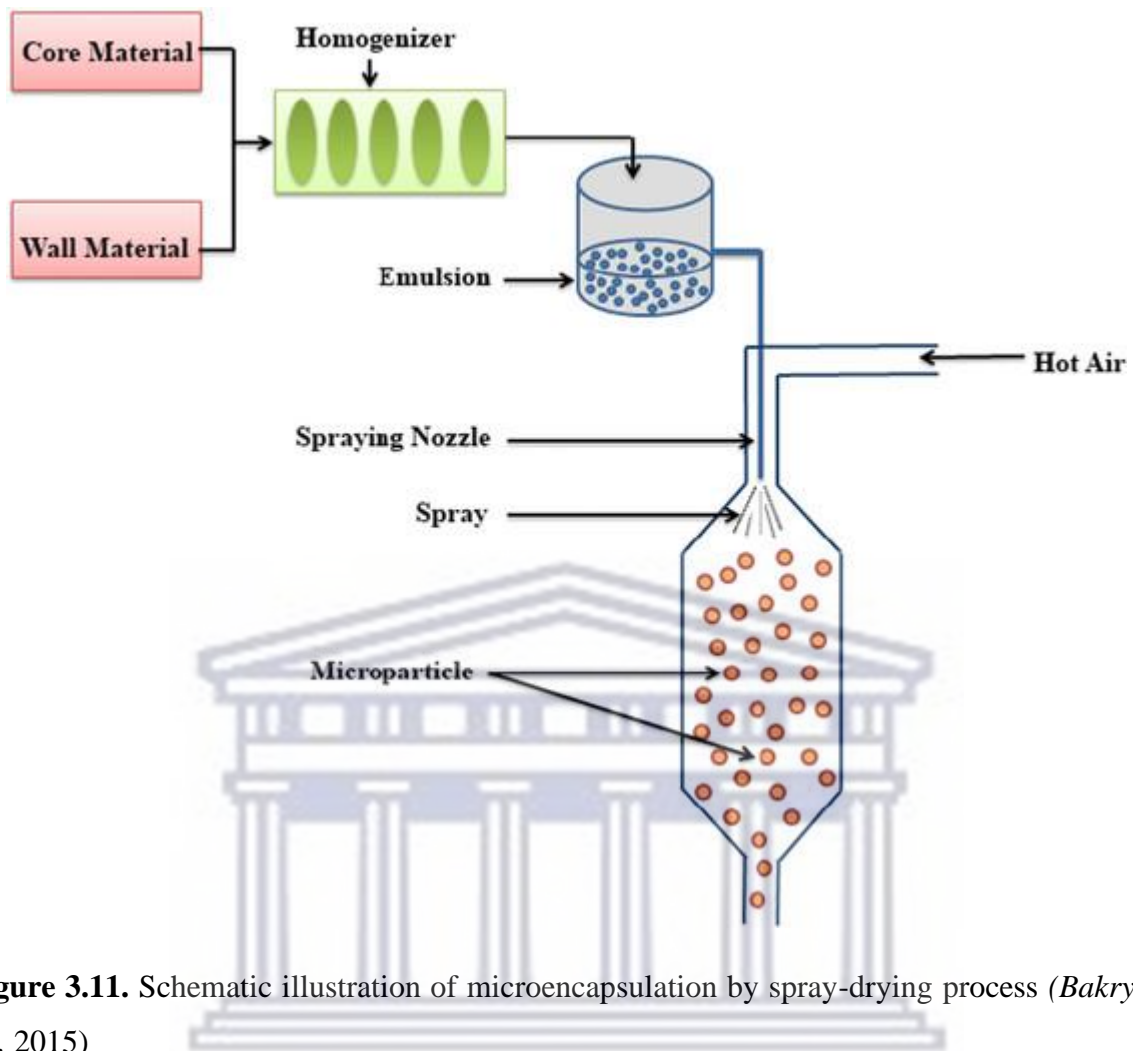


Figure 3.11. Schematic illustration of microencapsulation by spray-drying process (*Bakry et al., 2015*)

UNIVERSITY of the
WESTERN CAPE

3.5.2. Spray Chilling

The spray chilling (Figure 3.12) is also regarded as spray cooling, spray congealing or prilling with many resemblances with the spray drying technique. This process involves the mixing of the core material with the carrier to form a slurry which is atomized with the chilled air and quite different from the heated air being generated from the spray drying method (Risch, 1995; Oxley, 2012). In this process, vegetable oil (32 – 42 °C) is used to for the hydrogenation and fractionation of the outer material leading to the production of the particles through cooling and hardening of the droplets as compared to the evaporation of the solvent in spray drying. The spray chilling method is also used in the encapsulation of non-soluble, frozen liquids, heat-sensitive materials (Gouin, 2004; Poshadri and Kuna, 2010; Oxley, 2012). Spray chilling offers similar advantages like the spray drying technique such as in the masking of the bitter taste or odour, improving of the solubility of the poorly soluble core materials for potential delayed release, improving the stability of low stable ingredients, and ability to reduce hygroscopicity of the individual ingredients. It is simple to operate, relatively cheap, highly scalable and requires no use of organic solvents or high temperature. However, spray chilling technique is disadvantaged with low entrapment efficiency, release of the active material on storage (Okuro, Eustáquio de Matos and Favaro-Trindade, 2013).

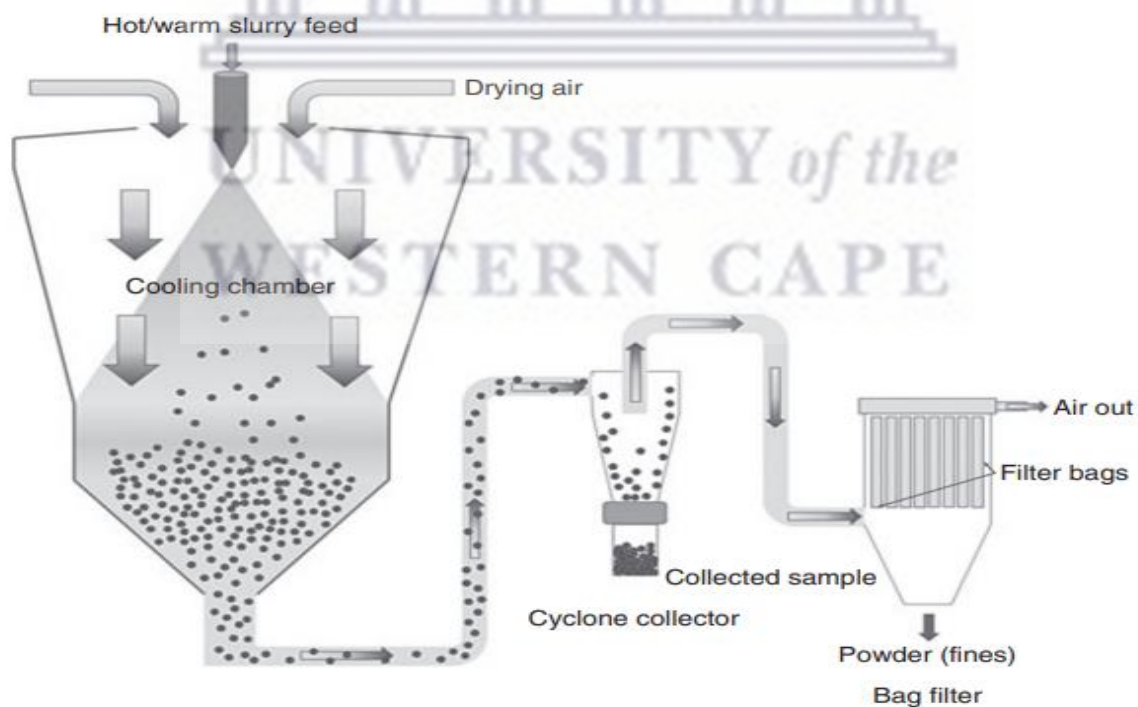


Figure 3.12. Graphical depiction of spray chilling encapsulation technique from (Oxley, 2012)

3.5.3. Extrusion

In the extrusion process (Figure 3.13), sodium alginate is the main encapsulating agent. The active compound is properly mixed with in the sodium alginate solution which is immobilized because of the strong polysaccharide gel formed in the presence of the multivalent ion. The mixture is then subjected to a drop-wise extrusion into a hardening solution such as sodium chloride using a reduced calibre pipette or syringe. This method has been heavily utilized mainly in the encapsulation of nutraceuticals, precarious flavours especially with the use of glassy carbohydrate as the coating agents (Poshadri and Kuna, 2010). The major advantage of this process is the improvement of the half-life of most of the compounds associated with oxidation problems including citrus oils. This is because the atmospheric gases disperse slowly through the hydrophilic glassy matrix and in the process creating an impermeable hurdle against oxygen. Although this method has been in existence, the formation of larger particles (500–1,000 μm) using this method has limited its application especially in the pharmaceutical, and food industries where mouth feel is an important factor (Poshadri and Kuna, 2010; Silva *et al.*, 2014).

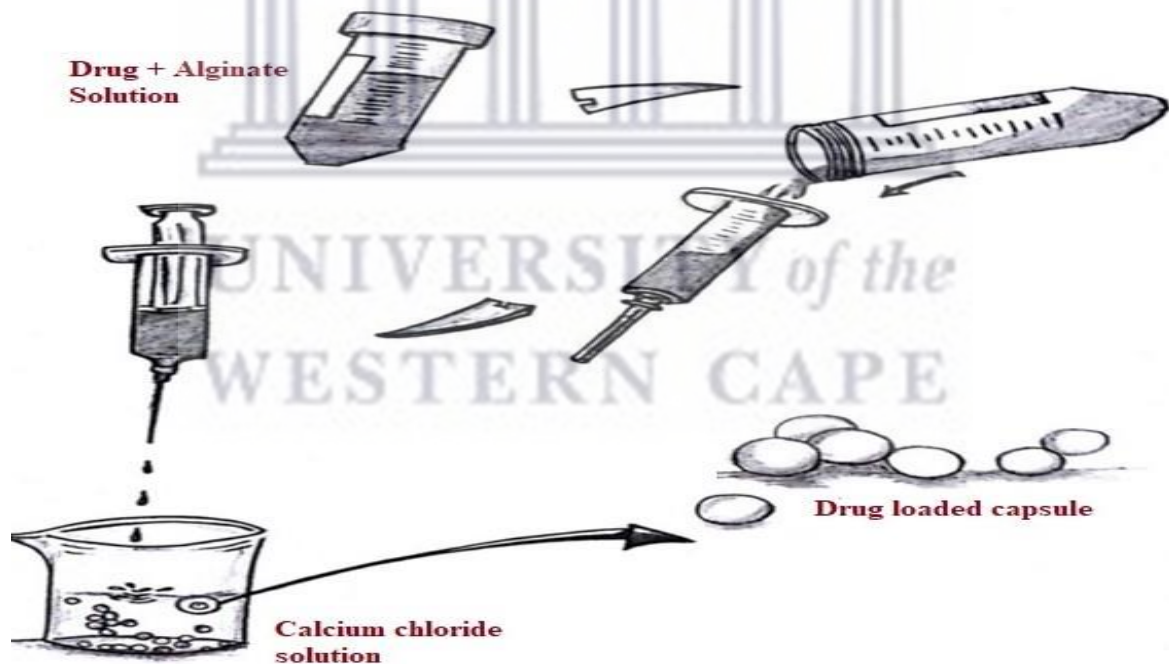


Figure 3.13. Schematic depiction of extrusion method adapted from (Liliana and Vladimir, 2013)

3.5.4. Fluidized Bed Coating

Fluidized bed coating microencapsulation technology typically deals with the suspension of the powder particle in a stream that is air controlled and steadily maintained at a constant and specific temperature and humidity while spraying with a coating material in a continuous manner. There is a formation of thin layer on the surface of the suspended particle by the coating agents as time progresses. And for this reason, the choice of the coating material becomes important as only coating materials with good viscosity property and thermally stable are considered as to enable atomizing and pumping and formation of film over the particle's surface (Dewettinck and Huyghebaert, 1999; Teunou and Poncelet, 2005). The coating of particles involving this technique is determined by the time interval of the particles in the chamber where 5 to 50% of coating is applied. With this method, the formation and production of particle sizes of 50 to 500 microns is achieved while utilizing various forms of coating agents. The advantage of this technique includes the high rate of moisture removal, good thermal efficiency, low cost of maintenance, ability to transport materials inside the dryer easily. However, there are several limitations associated with this process including high consumption of the electrical power, high pressure drops, formation of agglomeration of the fine powder, formation of non-uniform quality product (Law and Mujumdar, 2014). The fluid-bed coating is made of different coaters as depicted in Figure 3.14 including the top spray, bottom spray, and tangential spray (Gouin, 2004; Bakry *et al.*, 2015).

The coating solution is pumped downwards in a counter current manner in the top spray system with the presence of air on the fluid bed which will allow the movement and transfer of the porous or solid particles to the coating region hence become microencapsulated. Due to the opposing flows of the coating material and particles, the encapsulation tends to increase with a minimal agglomeration or cluster formation. This fluid-bed top spray coater is used extensively in microencapsulation to produce microcapsules in the range of 2 and 100 μm with a high yield of the encapsulated particles unlike in the bottom spray and tangential spray. The bottom spray further known as the Wurster system, is used for coating particles as small as 100 μm . Coating using this process includes a coating chamber of a cylindrical stainless-steel nozzle that sprays the coating material and a cribriform bottom plate (Bakry *et al.*, 2015; Kaushik *et al.*, 2015). As the particles move from bottom to top through the cribriform bottom plate and pass through the nozzle zone, particles become microencapsulated by the coating material and continued until a desired thickness and weight is achieved. The microcapsules then solidify through the evaporation of the solvent and hardened by cooling. This method has

the potentials of achieving a controlled release formulations than any other coating technologies and can recoat an already spray dried microparticles for an improved half-life and protection with mostly aqueous solutions such as gums, fats, or waxes, ethanolic solutions of synthetic polymers are used during the fluidized bed coating processes. (Gouin, 2004; Bakry et al., 2015; Kaushik *et al.*, 2015).

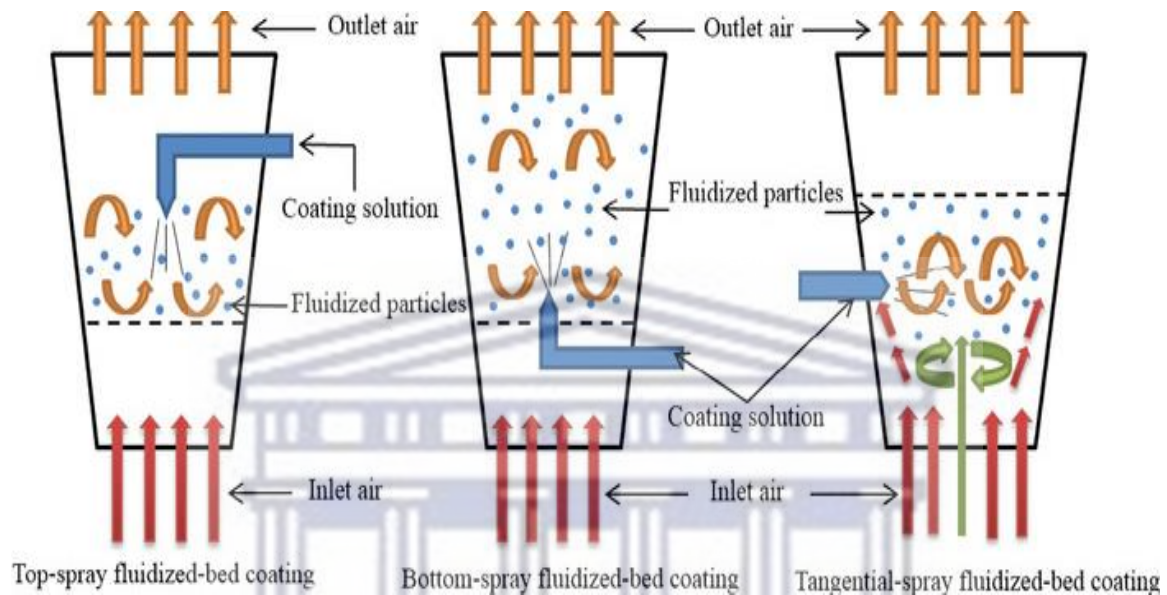


Figure 3.14. Schematic diagram of top, bottom, and tangential-spray fluidized-bed coating (Bakry *et al.*, 2015)

3.5.5. Liposomal Entrapment

Liposomes (Figure 3.15) are regarded as the smallest and spherical artificial vesicles produced from natural or synthetic phospholipids (Akbarzadeh *et al.*, 2013). Liposomes has been hugely studied due to the several and multiple advantages it offers such as the biocompatibility, biodegradability, the low toxicity, the tendency of encapsulating both hydrophilic and hydrophobic drugs, it can be made to target a specific site of action, act as a solubilizing agent and can be modified to control their biological behaviour due to its physicochemical and biophysical features (Sahoo and Labhassetwar, 2003; Poshadri and Kuna, 2010; Mansoori *et al.*, 2012; Akbarzadeh *et al.*, 2013). Liposomes have been applied in every field and in drug delivery including the delivery of vaccines, hormones, enzymes, and vitamins into the body. The manufacturing and the clinical features of liposomes including the batch to batch variability, the simplicity of the formulation, the scalability, and the biocompatibility which have given credence to it as approved formulation technique by the United States Food and

Drug Administration (FDA), and other regulatory bodies. Depending on the size and lipid composition of liposomes, the permeability, stability, surface activity and affinity can be varied. Liposomes can range from 25 nm to several microns in diameter and can be stored by freeze-drying. The commonly used phospholipid in the production of liposomes is the phosphatidylcholine (PC), otherwise referred as lecithin. It is made of the two hydrophobic fatty acid “tails” and a hydrophilic phosphate “head” held together by a glycerol molecule (Mansoori *et al.*, 2012). The hydrophilic head has strong water affinity while the hydrophobic tails comprising of two long fatty acid chains are repelled by water (Sahoo and Labhassetwar, 2003; Mansoori. *et al.*, 2012; Akbarzadeh *et al.*, 2013; Sercombe *et al.*, 2015). Due to these overwhelming advantages and diverse applications of liposomes, it has become the most widely studied delivery system today hence it has been explored in our work for improving the solubility and potential taste masking of the antiretroviral drugs.

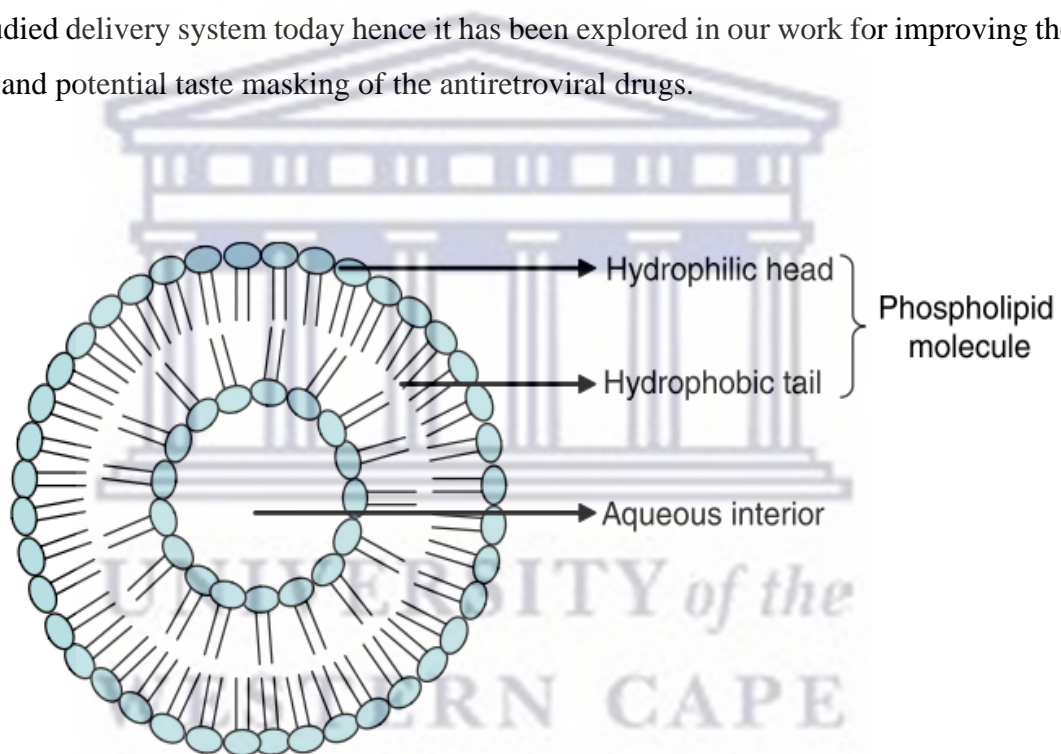


Figure 3.15. Structure of Liposomes (Swaminathan and Ehrhardt, 2011).

3.5.6. Freeze-drying

Freeze-drying, also further regarded as lyophilization or cryodesiccation, is a microencapsulation technique used primarily in the dehydration of the compounds and materials even aromas such as oils which are sensitive to heat. By the use of the drying process using this technique, the oil gets dissolved in the water and frozen between $-90\text{ }^{\circ}\text{C}$ and $-40\text{ }^{\circ}\text{C}$ with a decreased surrounding pressure and sufficient heat as to allow the frozen water in the material to sublime. This technique (Figure 3.16) has been successfully adopted in the encapsulation of some water-soluble essences and aromas (oils) such as fish, flaxseed, walnut, and olive oil. The freeze-dried product particles generated using this technique is poised to have the maximum retention of volatile compounds when compared to that of the spray drying technique (Poshadri and Kuna, 2010; Bakry *et al.*, 2015).

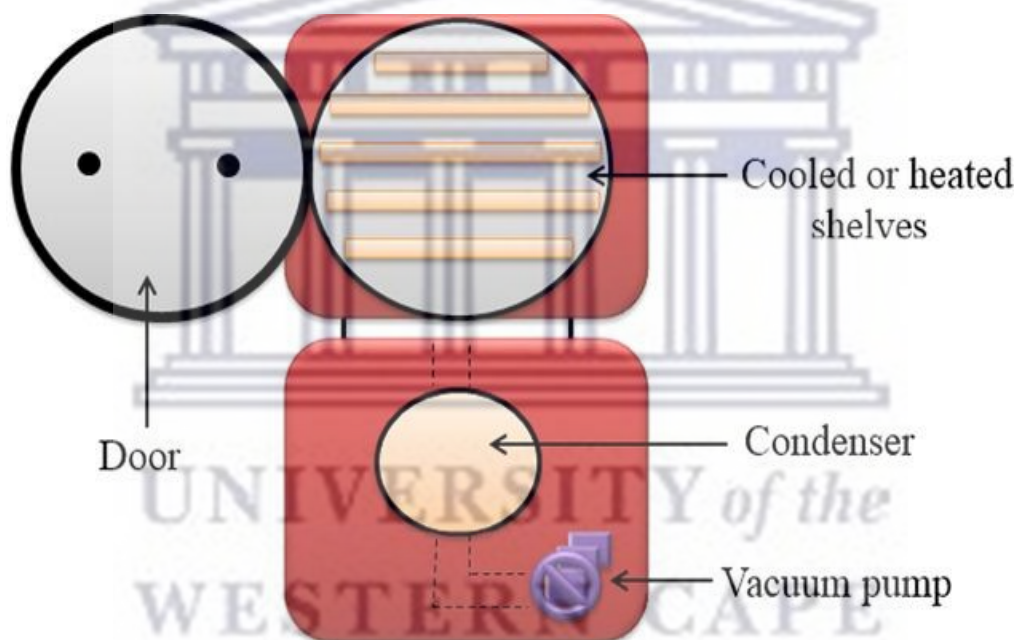


Figure 3.16. Schematic illustration of a freeze-dryer (Bakry *et al.*, 2015).

3.5.7. Coacervation

Coacervation is one of the oldest and most widely used microencapsulation techniques for the encapsulation of various materials. This technique (Figure 3.17) deals with the electrostatic attraction involving two biopolymers having opposite charges in a narrow pH range and at the end of the process, the liquid phase is displaced from the rich phase commonly regarded as the coacervate (Gouin, 2004; Kashif *et al.*, 2019). One of the major benefits of the technique is the tendency to completely entrap the core material within the matrix. This method is made up of two types namely, the simple coacervation and complex coacervation. In general, during simple coacervation process, a single colloidal solute is transferred to the aqueous solution of polymer while two colloids of opposite charges are instead added to a polymeric solution in complex coacervation. Therefore, the formation of microcapsules by the complex coacervation method is through the ionic interactions of oppositely charged polymers such as the positive charges of protein molecules and the anionic macromolecules like gelatin and Arabic gum. However, in the simple coacervation, most of the polymers used are basically non-solvent or water-soluble polymers especially gelatin and gums targeted at forming microcapsules through a hydrophobic interaction with other polymers or proteins (Xiao *et al.*, 2014; Kashif *et al.*, 2019). The complex coacervate is produced when these two opposite charges are neutralized with each other. This method includes the separation of a liquid phase of coating material from a polymeric solution followed by the coating of that phase as a uniform layer around suspended core particles. Coating material usually deposits on the surface of core material and becomes hard by chemical or thermal cross linking resulting in solid capsules when the total free energy of the system is decreased (Gouin, 2004; Bakry *et al.*, 2015; Kashif *et al.*, 2019). This method is highly advantageous over many other techniques in the sense that it is scalable, requires little or no solvents, it has a high payload, cheap and reproducible mainly for the encapsulated oils hence this technique has been adopted on industrial level (Xiao *et al.*, 2014).

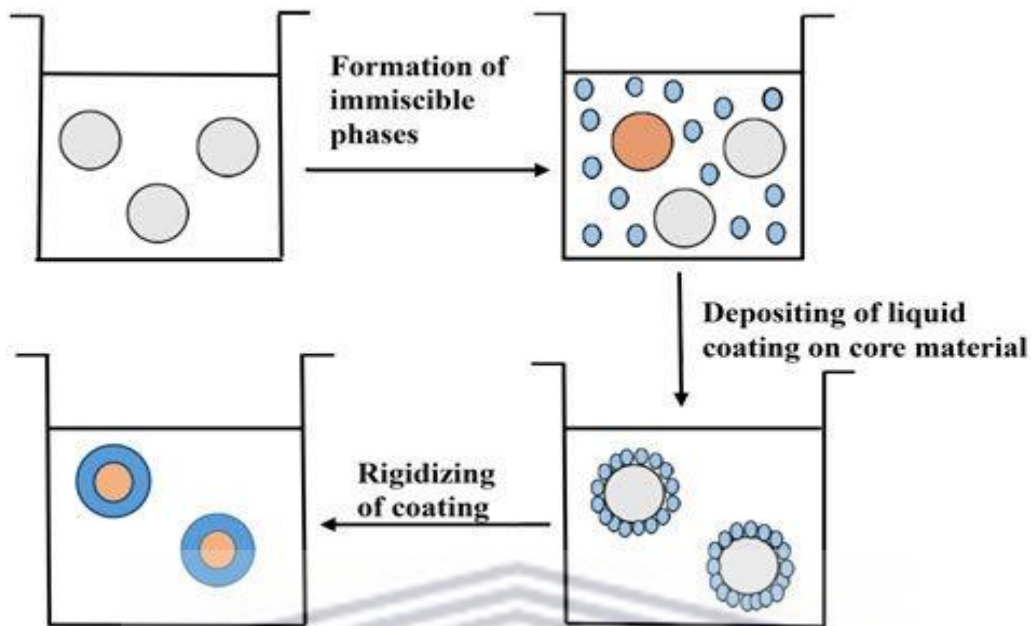


Figure 3.17. Illustration of microencapsulation by coacervation (Kashif *et al.*, 2019).

3.5.8. *In situ* polymerization

The *in-situ* polymerization technique (Figure 3.18) is the most widely used microencapsulation method mainly for the formation and production of functional fibres and microcapsules. The formation of the capsules in this process normally occurs on the surface of the particle by using precipitants, or a change in pH, temperature, or solvent quality (Hwang *et al.*, 2006; Jyothi *et al.*, 2010; Nguon *et al.*, 2018). One of the distinctive characteristics of this method from other polymerization process for encapsulation is that no reactants or reactive agents are included in the core material. Multifunctional monomers including the isocyanates and multifunctional acid chlorides, used individually or in combination are the major coating materials used for the encapsulation using this technique. These multifunctional monomers are usually dissolved in a liquid core material and dispersed in aqueous phase of the dispersing agent, followed by an addition of a reactant multifunctional amine to the mixture thereby resulting to a rapid polymerization at the interface to form capsules. Initially, a low molecular weight prepolymer will be formed, with time, the size of the pre-polymer grows and deposits on the surface of the dispersed core material thereby generating a solid capsule shell (Jyothi *et al.*, 2010). Different forms of shells are formed depending on the polymerization monomer introduced to the reactor. The typical examples include the use of a urea shell formed when isocyanate is reacted with amine, poly-nylon or polyamide shell which are formed when acid chloride reacts with amine,

and polyurethane shell is produced when isocyanate reacts with hydroxyl containing monomer (Jyothi *et al.*, 2010; Poshadri and Kuna, 2010; Agnihotri *et al.*, 2012; Bakry *et al.*, 2015).

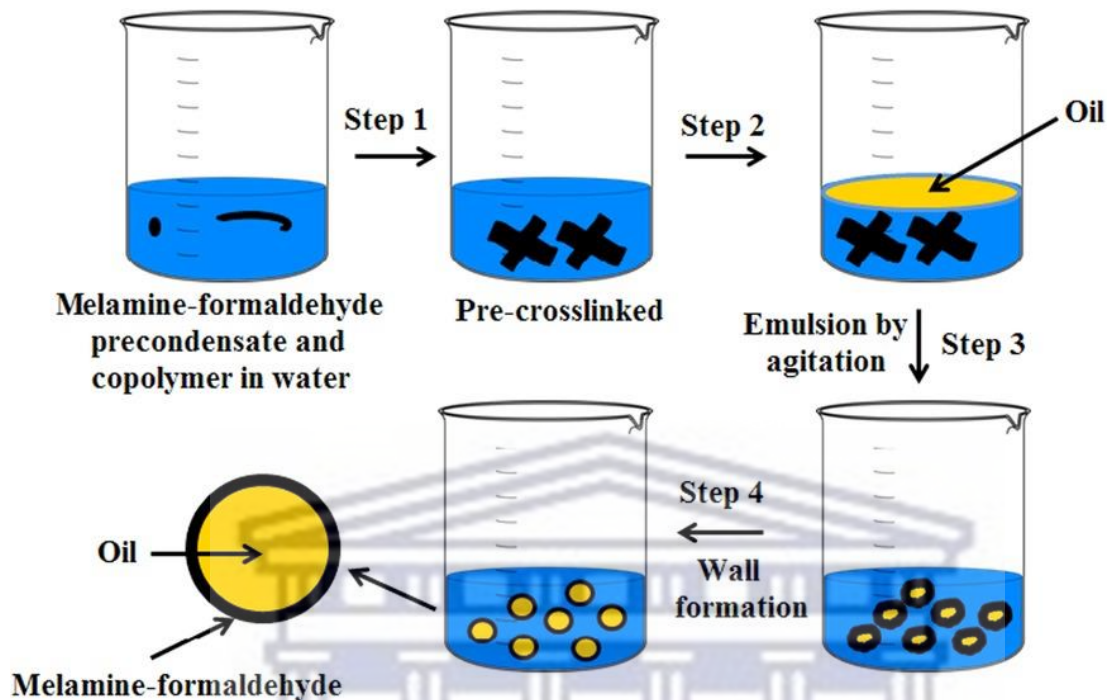


Figure 3.18. Illustration of in-situ polymerization technique in the microencapsulation of essential oils (Bakry *et al.*, 2015).

3.5.9. Solvent Evaporation

The processes of the solvent evaporation are performed in a liquid manufacturing vehicle with dissolution of microcapsules in a volatile solvent which are immiscible with manufacturing liquid phase hence this technique (Figure 3.19) have been used in the formation of different capsules even in the pharmaceutical industry (Freitas, Merkle and Gander, 2005; Gupta AK and Dey BK, 2012; Kashif *et al.*, 2019). This method follows four major steps in the formation of capsules including:

- I. The dissolution or dispersion of the core material into an organic solvent containing the shell forming agent.
- II. Emulsifying the dispersed phase of the step in an aqueous or phase (continuous phase) immiscible with the dispersion phase.
- III. Removal of the solvent from dispersion using the method of solvent evaporation as the droplets of dispersion to solid capsules.

IV. The harvesting, drying and conversion of the solid capsules into powder form using postprocessing.

Chloroform has been the most common solvent used in synthesizing microcapsules using this technique, however, the use of dichloromethane is now also common because of its low toxicity, high volatility, immiscibility in water and low boiling point. The choice and the selection of the right solvent to be used using this process is very highly crucial as solvents play very important role in the synthesis of microcapsules hence solvent to be considered for this method should possess the following characteristics namely: simple dissolution of polymer, high volatility, low boiling point with little or no toxic nature (Freitas, Merkle and Gander, 2005; Gupta AK and Dey BK, 2012; Kashif *et al.*, 2019).

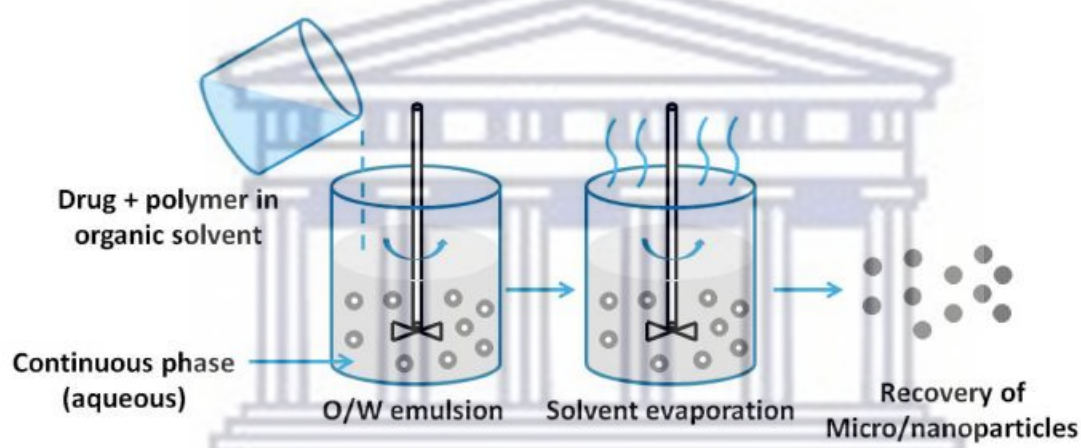


Figure 3.19. Schematic diagram of evaporation for preparation of microparticles (Wang *et al.*, 2016).

3.5.10. Pan-coating

The pan coating (Figure 3.20) which is one of the oldest and widely used method in the pharmaceutical industry in the production of coated particles or tablets of smaller sizes. In using this technique, the particles are constantly tumbled in a pan or other device followed by gentle application of the coating material during the coating process. Solid particle sizes above 600 μm are generally regarded as essential for effective coating (Bansode *et al.*, 2010). This technique has been extensively adopted in the formation of beads with controlled release. In this method, the active ingredients are coated onto the spherical substrates like the nonpareil sugar seeds, and then coated with protective layers of various polymers (Singh *et al.*, 2010). Practically, the coating is applied as a solution, or as an atomized spray, to the desired solid

core material in the coating pan and to remove the coating solvent, warm air is passed over the coated materials as the coatings are being applied in the coating pans and in some cases, final solvent removal is occur in the drying oven (Bansode *et al.*, 2010; Singh *et al.*, 2010; Agnihotri *et al.*, 2012).

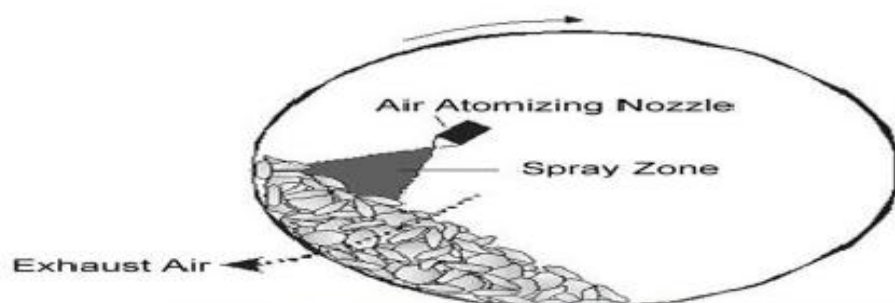


Figure 3.20. Schematic representation of pan coating (Bansode *et al.*, 2010).

3.5.11. Electro-spraying

Electro-spraying (Figure 3.21) or electrohydrodynamic spraying is a method of liquid atomization by the electrical forces. The liquid continuously flows through a capillary nozzle which is maintained at high electric potential and forced by the electric field into a dispersion of fine, highly charged droplets. The basic principles of this process includes the utilization of electrical shear to dominate surface tension force of a pendant droplet of biopolymer solution at capillary nozzle thereby creating electrically charged polymer jets (Augustin and Oliver, 2012; Taheri and Jafari, 2019). The application of the electric field to a droplet then creates an electric charge which competes with the cohesive force of the particle. when it dominates coupled with a demotion in the surface tension and ultimately nanoparticles are obtained (Tapia-hernández and Rodríguez-félix, 2017). Factors such as the concentration of the polymer, shear viscosity, molecular weight of the polymer/solvent and the electro-spraying process including the electric potential, the electric difference, flow rate, distance between the tip of the needle and the collector determines the size and the morphology of the nanoparticles produced (Kashif *et al.*, 2016; Tapia-hernández and Rodríguez-félix, 2017; Taheri and Jafari, 2019). Electro-spraying has shown few advantages over other conventional methods thereby making it attractive to produce cargo carriers for biomedical applications. It is used in the encapsulation of sensitive biomolecules and even living cells since it can be performed at ambient temperature. The encapsulation efficiency using this technique is maximized due to

the possible absence of an external medium that allows the dissolution or migration of water-soluble cargos. This method is capable of reproducibly producing drug-loaded particles of sizes between 5 nm – 100 μm of narrow distribution. This technique could be used in producing hollow particles, porous microparticles, cell-shaped microparticles and even multi-layered microspheres (Raval *et al.*, 2019; Taheri and Jafari, 2019; Wang, Jansen and Yang, 2019).

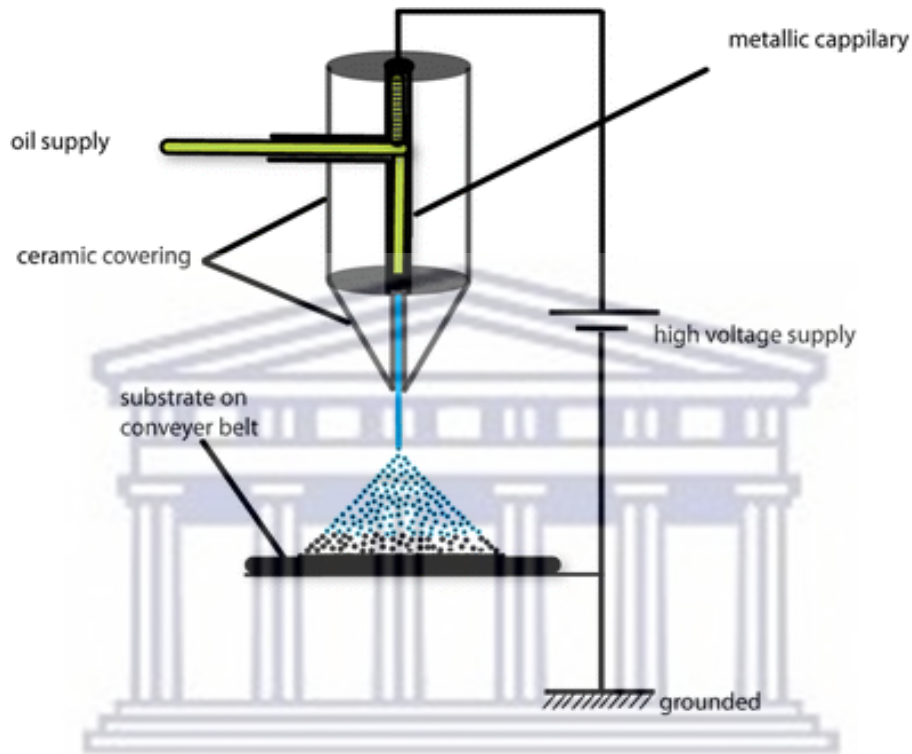


Figure 3.21. A schematic representation of electro-spraying process through a single nozzle system (Kashif *et al.*, 2016).

UNIVERSITY of the
WESTERN CAPE

3.6. Empirical Literature Studies

Costa *et al.*, (2015) investigated the effective stabilization of conjugated linoleic acid using the spray drying technique and at the same time varied different wall systems consisting of a pea protein isolate alone at varied core material ratio or pea protein blended with maltodextrin and carboxymethyl cellulose at a varying ratio. The result from the physical-chemical properties of the microparticles which includes investigation into the parameters (core retention, microencapsulation efficiency, particle size and moisture) at different conjugated linoleic acid with maltodextrin and pea protein isolate (1:1:3) revealed the most promising result. However, the addition of maltodextrin did not influence the oxidative stability of the conjugated linoleic acid, but its presence improved the desired physical-chemical characteristics instead.

Panizzon *et al.*, (2014) developed and characterized a new gelatin matrix for the microencapsulation of daidzein and genistein from soy extract through the process of spray drying, to produce solid dispersions aimed at overcoming the solubility challenges of the core materials and to foster a controlled release. The impact of soy extract ratio to the solid state, yield, morphology, encapsulation efficiency, particle size distribution, release kinetics and cumulative release were evaluated. Analyses showed integral microparticles and high drug content with a yield of 43.6 and 55.9%, respectively for daidzein and genistein with a mean size ($p > 0.05$). X-ray diffraction revealed an amorphous solid state of the microparticles. The *In vitro release* tests showed a drastic increase in the dissolution profile of microparticle. The results concluded that use of the soy extract for microencapsulation might offer a good system for improving drug solubility, bioavailability, and the release of the active compounds.

Chiappetta *et al.*, (2009) studied the microencapsulation and taste masking of an indinavir-loaded pH-sensitive microparticles made from the insoluble polymer (Eudragit E100) using the double emulsion/solvent evaporation method. The taste of the indinavir-loaded microparticles which was investigated through the selection of the randomised sensory experiments of ten healthy volunteers, confirmed a molecularly dispersed formulation of the drug with the microparticle. The sensory taste masking from the volunteers showed that the indinavir microparticle with 15% of the drug exhibited an acceptable taste.

Tafere et al., (2021) studied the formulation, *in vitro* characterization, and optimization of taste-masked orally disintegrating co-trimoxazole tablet by exploring the direct compression technique. The taste masking was performed using the methods of addition of the sweetening agent such as the crospovidone and the solid dispersions using a pH sensitive polymer (Eudragit E100) through solvent evaporation. Results revealed a rapid disintegration of the co-trimoxazole orally disintegrating tablet, with a percentage friability less than 1% and an enhanced dissolution profile. They reported an acceptable bitterness threshold of trimethoprim of 150 µg/ml hence reported a successful taste masking.

Laelorspoen, Wongsasulak and Yoovidhya, (2014) studied the encapsulation of *Lactobacillus acidophilus* while using the zein-alginate core-shell for the production of *Lactobacillus* microcapsule *via* electro-spraying. The survival of the probiotic *Lactobacillus acidophilus* in gastric fluid was investigated and was found to be enhanced by embedding the bacteria cells in alginate microcapsules. The resultant microcapsules were further coated with citric acid concentration as was also electro-sprayed. Results demonstrated that increased citric acid concentration did not affect the microcapsule size, but instead, the survival cell number significantly decreased due to an increase in the zein solution acidity with the size and surface wrinkles of the microcapsules further found to decrease as the applied voltage increased.

Okafor et al., (2019) investigated the encapsulation of efavirenz antiretroviral drug in liposomes through the thin film hydration method of liposomes preparation. Obtained data from the work showed that efavirenz entrapped in liposomes at the ratio 1:1 of lecithin to cholesterol, depicted the highest encapsulation efficiency with high surface charge of -53.5 ± 0.06 mV indicating high stability of efavirenz in the liposomes. A trend of controlled release result of efavirenz from liposomes was observed when compared to the dissolution release profile of un-entrapped efavirenz.

The microencapsulation involving probiotic *Saccharomyces cerevisiae* var. *boulardi* was studied in different wall materials of gelatin, whey protein concentrate, modified starch, maltodextrin, pea protein isolates and gum by **Arslan et al., (2015)** where they adopted the spray drying technique at varying inlet temperatures (80 °C and 125 °C). Their results showed that whey protein concentrates, and gum Arabic gave the highest product yield. The survivability of *Saccharomyces cerevisiae* var. *boulardi* however did not change with the wall materials but instead increased at the lower temperature. The survivability in a stimulated gastric solution test at different pH levels and durations showed that gum Arabic, gelatin, and pea protein were the best wall materials while microcapsules produced at higher drying

temperature (125 °C) showed a higher resistance to the gastric solution than those of the lower drying temperature (80 °C).

Pearnchob and Bodmeier, (2003) developed a novel powder coating technology for extended-release pellets based on the acrylic polymer, Eudragit. The mixture of micronized Eudragit[®] plus talc with a liquid feed (plasticizer plus binder solution) were sprayed separately onto propranolol hydrochloride-loaded pellets in a fluidized bed coater to produce coated pellets which were heat-cured under different conditions (40 to 60 °C). Formation of film by the polymer particles was studied through the determination of the glass transition and the minimum polymer-softening temperatures. The coated pellets were characterized with respect to their morphology, release, and stability properties. Their result showed that a high concentration of plasticizer (40% polymer) and a thermal treatment led to the drug release. Curing the pellets resulted in release profiles, which did not change during storage for 3 years, with the coated pellets showing a smooth, continuous surface and a dense film structure after the curing.

Kumar *et al.*, (2011) studied the formulation of lamivudine microspheres in multiple emulsion form with osmogen and different polymers using solvent evaporation method. They prepared and evaluated the controlled release of lamivudine microspheres using osmogen like sodium chloride, and polymers like ethyl cellulose, cellulose acetate, and polyvinyl alcohol as a continuous phase. The prepared microspheres were characterized for the percentage drug content, encapsulation efficiency, *in vitro* dissolution studies, *in vitro* kinetic studies, and accelerated stability studies. Fourier infrared studies confirmed a stable character of lamivudine in the microspheres. Scanning electron microscopy revealed that the microspheres were smooth and spherical in nature. The release kinetics study revealed that the prepared microspheres were best fitted to the zero order, Higuchi model, Hixson Crowell models and modified cube root equation for the best formulation. The release kinetics data and characterization studies indicated that the drug release from microspheres followed the diffusion-controlled pattern while also confirming a stable microsphere.

Bock *et al.*, (2011) evaluated the use of electro-spraying as a promising technique for generating a reproducible particle of polycaprolactone, a biodegradable polymer. Result established from the study demonstrated narrow size distributions and average particle sizes ranging from 10 to 20 µm were obtained by controlling the electro-spraying flow rate and polymer concentration. The morphology of the particles was shown to be spherical with a

homogeneous embossed texture, determined by the polymer entanglement regime taking place during electro-spraying process. This process revealed no toxic residue based on preliminary cell work using DNA quantification assays, hence validating this method as suitable for further loading of bioactive components.

Shah et al., (2008) designed, optimized, and characterized artemether taste masked microparticles using the coacervation process employing Eudragit E 100 as the coating agent and sodium hydroxide solution as non-solvent for the polymer. Their optimized microparticles batch was characterized using FTIR and DSC. The multiple linear regression analysis revealed a reduced bitterness of artemether from controlling the drug release of microparticles at pH 6.8 and increasing the amount of Eudragit E100. They reported that increase in the amount of polymer caused a reduction in the drug release from microparticles at pH > 5 which was attributed to insolubility and thus the bitterness of artemether was found to reduce. However, an increase in the amount of polymer resulted in an improved dissolution, which in turn could lead to an improved availability of artemether in stomach. Optimized microparticles prepared using 0.04 g of artemether and 15 mL of 1% (m/V) solution of Eudragit E100 showed complete bitter taste masking with improved drug release at pH 1.2.

Xu and Hanna, (2007) evaluated the Bovine serum albumin loaded tripolyphosphate cross-linked chitosan capsules by utilizing the electro-spraying technique. Bovine serum albumin loaded tripolyphosphate cross-linked chitosan was produced as capsules while applying a sufficiently strong electric field to overcome the surface tension of a droplet. An investigation on the parameters including the effects of concentrations of initial chitosan and tripolyphosphate solutions, flow rate and bovine serum albumin/chitosan weight ratio on the physical properties of the mixtures conducted; the morphology, size, and yield of the capsules; Bovine serum albumin encapsulation efficiency and loading capacity, and *in vitro* release were established. The capsules were found to be spherical in shape with capsule size increasing with increase in the flow rate. Increase in the concentrations of chitosan and tripolyphosphate solutions increased the yield with an increase in the flow rate resulting to high encapsulation efficiency and further enhancing the bovine serum albumin release rate.

3.7. Conclusion

Microencapsulation is an advanced technology that have been adopted in entrapping active ingredients (core material) within an encapsulating material, thereby protecting the active ingredient from environmental attacks. This technology has been employed across several sectors for several purposes but have been heavily explored in the pharmaceutical industries for the encapsulation of the active ingredients within a coating agent to produce different morphological micro-particulates, nanoparticles, of varying sizes with an improved pharmacological property required for an effective treatment. There are various forms of microencapsulation techniques with each having striking properties and unique method of producing different forms of microparticles of varying sizes. Most of these technologies have all been explored in the pharmaceutical sector for various purposes such as improving shelf-life of the core material, stability, solubility, release of the active ingredients, handling, taste masking, colour, and odour. Due to these advantages of microencapsulation, this chapter has discussed extensively the various advantages of microencapsulation, the limitations, microencapsulation agents, core materials used in the study, solid dispersion as a strategy for solubility improvement, different microencapsulation techniques and several studies involving different microencapsulation techniques especially with taste masking and solubility enhancement of the core materials.



UNIVERSITY *of the*
WESTERN CAPE

3.8. References

Adriana, R.M. *et al.* (2014) 'Importance of lecithin for encapsulation processes', *African Journal of Food Science*, 8(4), pp. 176–183.

Agnihotri, N. *et al.* (2012) 'Microencapsulation – A Novel Approach in Drug Delivery : A Review', *Indo Global Journal of Pharmaceutical Science*, 2(1), pp. 1–20.

Ahmed, W. and Rashid, S. (2019) 'Functional and therapeutic potential of inulin: A comprehensive review', *Critical Reviews in Food Science and Nutrition*, 59(1), pp. 1–13.

Gupta, A.K, and Dey B.K. (2012) 'Microencapsulation for controlled drug delivery: A comprehensive review', *Sunsari Technical College Journal*, 1(1), pp. 48–54.

Akbarzadeh, A. *et al.* (2013) 'Liposomes: Classification, preparation, and applications', *Nanoscale Research Letters*, 8(10), pp. 1–9.

Albuquerque, T.G. *et al.* (2016) 'Cholesterol determination in foods: Comparison between high performance and ultra-high performance liquid chromatography', *Food Chemistry*, 193, pp. 18–25.

Aliyu, S. (2012) 'Viral, fungal, protozoal and helminthic infections', *Clinical Pharmacology*: (11th edn). doi:10.1016/B978-0-7020-4084-9.00054-9.

Arenas-Jal, M., Suñé-Negre, J.M. and García-Montoya, E. (2020) 'An overview of microencapsulation in the food industry: opportunities, challenges, and innovations', *European Food Research and Technology*, 246(7), pp. 1371–1382.

Arslan, S. *et al.* (2015) 'Microencapsulation of probiotic *Saccharomyces cerevisiae* var . *boulardii* with different wall materials by spray drying', *LWT - Food Science and Technology*, 63(1), pp. 685–690.

Augustin, M.A. and Oliver, C.M. (2012) 'An overview of the development and applications of nanoscale materials in the food industry, Nanotechnology in the Food, Beverage and Nutraceutical Industries'. Wood Publishing Limited, Australia pp 3 – 39.

Baeza Jimenez, R., Lopez-Martinez, L.X. and Garcia, H.S. (2014) 'Biocatalytic modification of food lipids: reactions and applications', *Revista Mexicana de Ingenieria Quimica*, 13(1), pp. 29 – 47.

Bakry, A.M. *et al.* (2015) 'Microencapsulation of Oils : A Comprehensive Review of Benefits

, Techniques , and Applications’, *Comprehensive Reviews in Food Science and Food Safety*, (15), pp. 143–182.

Bansode, S.S. *et al.* (2010) ‘Microencapsulation : A review’, *International Journal of Pharmaceutical Sciences Review and Research*, 1(2), pp. 38–43.

Barac M.B. *et al.* (2015) 'Techno-functional properties of pea (*Pisum sativum*), Protein isolates – A review', *Acta Periodica Technologica*, (46), pp 1 – 269.

Bhaskar, R., OLA, M. and Ghongade, R.M. (2018) ‘Review: Solid Dispersions Technique for Enhancement of Solubility of Poorly Soluble Drug’, *Indian Journal of Pharmaceutical and Biological Research*, 6(02), pp. 43–52.

Bock, N. *et al.* (2011) ‘Electrospraying, a Reproducible Method for Production of Polymeric Microspheres for Biomedical Applications’, *Polymers*, (3), pp. 131–149.

Chen, Z., Fang, Y. and Zhang, Z. (2007) ‘Synthesis and assessment of attractiveness and mating disruption efficacy of sex pheromone microcapsules for the diamondback moth, *Plutella xylostella* (L.)’, *Chinese Science Bulletin*, 52(10), pp. 1365–1371.

Chiappetta, D.A. *et al.* (2009) ‘Indinavir-loaded pH-sensitive microparticles for taste masking: Toward extemporaneous pediatric anti-HIV/AIDS liquid formulations with improved patient compliance’, *AAPS PharmSciTech*, 10(1), pp. 1–6.

Costa, A.M.M. *et al.* (2015) ‘Effective stabilization of CLA by microencapsulation in pea protein’, *Food Chemistry* (168), pp. 157–166.

Das, S.K. *et al.* (2013) ‘Solid Dispersions : An Approach to Enhance the Bioavailability of Poorly Water-Soluble Drugs’, *International Journal of Pharmacology and Pharmaceutical Technology*, pp. 37–46.

Desai, K.G.H. and Park, H.J. (2005) ‘Recent Developments in Microencapsulation of Food Ingredients’, *Drying Technology*, 3937(23), pp. 1361–1394.

Derwetting, K. and Huyghebaert, A. (1999), 'Fluidized bed-coating in food-technology; Trends in Food science technology", *Food science and technology*, (10), pp.163–168.

Drabińska, N., Zieliński, H. and Krupa-Kozak, U. (2016) ‘Technological benefits of inulin-type fructans application in gluten-free products – A review’, *Trends in Food Science and Technology*, 5(6), pp. 149–157.

- Dubey, R., Shami, T. and Rao, K.B. (2009) 'Microencapsulation Technology and Applications', *Defence Science Journal*, 59(1), pp. 82–95.
- Duranti, M. and Gius, C. (1997) 'Legume seeds: Protein content and nutritional value', *Field Crops Research*, 53(13), pp. 31–45.
- Eckhardt, B.J. and Gulick, R.M. (2017) *Drugs for HIV Infection*. (4th edn) Infectious Diseases. doi:10.1016/B978-0-7020-6285-8.00152-0.
- Estevinho, B.N. *et al.* (2013) 'Microencapsulation with chitosan by spray drying for industry applications - A review', *Trends in Food Science and Technology*, 31(31), pp. 138–155.
- Eun, J.B. *et al.* (2020) 'A review of encapsulation of carotenoids using spray drying and freeze drying', *Critical Reviews in Food Science and Nutrition*, 60(21), pp. 3547–3572.
- França, D. *et al.* (2019) 'Nano and Microencapsulated Nutrients for Enhanced Efficiency Fertilizer', in *Polymers for Agri-Food Applications*, pp. 29–44.
- Freitas, S., Merkle, H.P. and Gander, B. (2005) 'Microencapsulation by solvent extraction/evaporation: Reviewing the state of the art of microsphere preparation process technology', *Journal of Controlled Release*, 102(2), pp. 313–332.
- Ghule, P. *et al.* (2018) 'Amorphous solid dispersions: A promising technique for improving oral bioavailability of poorly water-soluble drugs', *South African Pharmaceutical Journal*, 85(1), pp. 50–56.
- Gouin, S. (2004) 'Microencapsulation: industria appraisal of existing technologies and trends', *Trends in Food Science and Technology*, (15), pp. 330–347.
- Gurunath, S. *et al.* (2013) 'Amorphous solid dispersions method for improving oral bioavailability of poorly water-soluble drugs', *Journal of Pharmacy Research*, 6(4), pp. 476–480.
- Haeri, A. *et al.* (2014) 'Preparation and characterization of stable nanoliposomal formulation of fluoxetine as a potential adjuvant therapy for drug-resistant tumors', *Iranian Journal of Pharmaceutical Research*, (13), pp. 3–14.
- Huang, Y. and Dai, W.G. (2014) 'Fundamental aspects of solid dispersions technology for poorly soluble drugs', *Acta Pharmaceutica Sinica B*, 4(1), pp. 18–25.
- Hwang, J.S. *et al.* (2006) 'Preparation and characterizaation of melmine-formaldehyde resin

microcapsules containing fragrant oil', *Biotechnology and Bioprocess Engineering*, (11), pp. 332–336.

Kouam, J., Songmene V., Balazinski M., and Hendrick P. (2013) 'Microencapsulation and its uses on food science and technology: a review', *IntechOpen*. doi: <http://dx.doi.org/10.5772/intechopen.81997>.

Jadav, N.B. and Paradkar, A. (2020) Solid dispersions: Technologies used and future outlook. technologies used and future outlook., *Nanopharmaceuticals: Expectations and Realities of Multifunctional Drug Delivery Systems*. doi:10.1016/B978-0-12-817778-5.00005-1.

Jeffrey Ting, M. *et al.* (2018) 'Advances in Polymer Design for Enhancing Oral Drug Solubility and Delivery', *Bioconjugate Chemistry*, (29), pp. 939–952.

Jyothi, N.V.N. *et al.* (2010) 'Microencapsulation techniques, factors influencing encapsulation efficiency', *Journal of Microencapsulation*, 27(3), pp. 187–197.

Kalyani Nair, K., Kharb, S. and Thompkinson, D.K. (2010) 'Inulin dietary fiber with functional and health attributes - a review', *Food Reviews International*, 26(2), pp. 189–203.

Kashif, I. *et al.* (2019) 'Phase change materials , their synthesis and application in textiles — a review', *The Journal of The Textile Institute*, pp. 1–14.

Kashif, M. *et al.* (2016) 'Electrospraying : a Novel Technique for Efficient Coating of Foods', *Food Engineering Reviews*, (9), pp. 112–11

Kaur, N. and Gupta, A.K. (2002) 'Applications of inulin and oligofructose in health and nutrition', *Journal of Biosciences*, 27(7), pp. 703–714.

Kaushik, P. *et al.* (2015) 'Microencapsulation of omega-3 fatty acids: A review of microencapsulation and characterization methods', *Journal of functional foods*, 19(5), pp. 868–881.

Kennewell, P.D. (2006) 'Major drug introductions', in Elsevier (1st edn) *Comprehensive Medicinal Chemistry II*. Swindon: *Comprehensive Medicinal Chemistry II*, pp. 97–249. doi:10.1016/b0-08-045044-x/00003-1.

Kim, K.T. *et al.* (2011) 'Solid Dispersions as a Drug Delivery System', *Journal of Pharmaceutical Investigation*, 41(3), pp. 125–142.

Kumar, S. *et al.* (2014) 'A review on solid dispersions and its application', *World Journal of*

Pharmaceutical Research, 8(4), 340–354.

Laelorspoen, N., Wongsasulak, S. and Yoovidhya, T. (2014) ‘Microencapsulation of *Lactobacillus acidophilus* in zein – alginate core – shell microcapsules via electrospraying’, *Journal of functional foods*, 7(14), pp. 3–10.

Lam, A.C.Y. *et al.* (2018) ‘Pea protein isolates : Structure , extraction , and functionality’, *Food Reviews International*, 34(2), pp. 126–147.

Law, C. and Mujumdar, A. (2014) ‘Fluidized bed dryers’, in AS, M. (ed.) *Handbook of industrial drying*. (4th edn), Boca Raton, Florida: CRC Press, pp. 161–190.

Liliana, S.C. and Vladimir, V.C. (2013) ‘Probiotic encapsulation’, *African Journal of Microbiology Research*, 7(40), pp. 4743–4753.

List, G.R. (2015) *Soybean Lecithin: Food, Industrial Uses, and Other Applications, Polar Lipids: Biology, Chemistry, and Technology*. AOCS Press. doi:10.1016/B978-1-63067-044-3.50005-4.

Lu, Z.X., He J.F., Zhang Y.C. and Bing D.J. (2019) ‘Composition , physicochemical properties of pea protein and its application in functional foods’, *Critical Review in Food Science and Nutrition*, doi:10.1080/10408398.2019.1651248.

Kumar, M.A.A. *et al.* (2011) ‘Formulation of Lamivudine Microspheres in Multiple Emulsion Form Using Osmogen And Different Polymers - Studying the release profiles’, *International Journal of Drug Development and Research*, 3(3), pp. 277–284.

Mansoori, M. *et al.* (2012) ‘A Review on Liposomes’, *International Journal of Advanced Research in Pharmaceutics and Bio Sciences*, 2(4), pp. 453–464.

Mensink, M.A. *et al.* (2015) ‘Carbohydrate Polymers Inulin , a flexible oligosaccharide . II : Review of its pharmaceutical applications’, *Carbohydrate Polymers*, 134, pp. 418–428.

Michaud, V. *et al.* (2012) ‘The dual role of pharmacogenetics in HIV treatment: Mutations and polymorphisms regulating antiretroviral drug resistance and disposition’, *Pharmacological Reviews*, 64(3), pp. 803–833.

Mishra, D.K. *et al.* (2015) ‘Amorphous solid dispersions technique for improved drug delivery: basics to clinical applications’, *Drug Delivery and Translational Research*, 5(6), pp. 552–565.

Mondal, D. (2007) ‘Zidovudine’, *The Comprehensive Pharmacology*, pp. 1–4.

doi:10.1016/B978-008055232-3.62876-4.

Narwal, V. *et al.* (2019) 'Cholesterol biosensors: A review', *Steroids*, 143, pp. 6–17.
doi:10.1016/j.steroids.2018.12.003.

Nguon, O. *et al.* (2018) 'Microencapsulation by in situ Polymerization of Amino Resins', *Polymer Reviews*, 58(2), pp. 326–375.

Obeidat, W. (2009) 'Recent Patents Review in Microencapsulation of Pharmaceuticals Using the Emulsion Solvent Removal Methods', *Recent Patents on Drug Delivery & Formulation*, 3(3), pp. 178–192.

Okafor, N.I. *et al.* (2019) 'Encapsulation and physicochemical evaluation of efavirenz in liposomes', *Journal of Pharmaceutical Investigation*, (45), pp. 1–8.

Okuro, P.K., Eustáquio de Matos, F. and Favaro-Trindade, C.S. (2013) 'Technological challenges for spray chilling encapsulation of functional food ingredients', *Food Technology and Biotechnology*, 51(2), pp. 171–182.

Olisa, N.M. (2009) Extraction, Characterization and Industrial Uses of Lecithin From Three Varieties of Cucumis melo (Melon) oil.

Onwulata C. (2005) 'Fluid-bed coating', in Press, CRC Press. (1st edn) Encapsulated and powdered foods. <https://doi.org/10.1201/9781420028300>.

Owusu-Ansah, Y.J. and Mc curdy, S.M. (1991) 'Pea proteins: A review of chemistry, technology of production, and utilization', *Food Reviews International*, 7(1), pp. 103–134.

Oxley, J.D. (2012) 'Spray cooling and spray chilling for food ingredient and nutraceutical encapsulation', In SAS Masson (4th edn) *Encapsulation Technologies and Delivery Systems for Food Ingredients and Nutraceuticals.* Woodhead Publishing limited, USA.
doi:10.1533/9780857095909.2.110.

Paintsil, E. and Cheng, Y.C. (2008) 'Antiviral Agents', *Encyclopedia of Virology*, pp. 142–154.

Palacios, L.E. and Wang, T. (2005) 'Egg-yolk lipid fractionation and lecithin characterization', *Journal of the American Oil Chemists' Society*, 82(8), pp. 571–578.

Panizzon, G.P. *et al.* (2014) 'Preparation of Spray-Dried Soy Isoflavone-Loaded Gelatin Microspheres for Enhancement of Dissolution: Formulation, Characterization and in Vitro

Evaluation', *Pharmaceutics*, (6), pp. 599–615.

Paulo, F. and Santos, L. (2017) 'Materials Science and Engineering C Design of experiments for microencapsulation applications : A review', *Materials Science & Engineering*, (77), pp. 1327–1340.

Pearnchob, N. and Bodmeier, R. (2003) 'Dry Powder Coating of Pellets with Micronized Eudragit[®] RS for Extended Drug Release', *Pharmaceutical Research*, 20(12), pp. 1970–1976.

Penazzato, M. *et al.* (2019) 'Prioritising the most needed paediatric antiretroviral formulations: the PADO4 list', *The Lancet HIV*, 6(9), pp. e623–e631.

Peng, L. *et al.* (2008) 'The Interaction Between Cholesterol and Human Serum Albumin', *Protein & Peptide Letters*, 15(4), pp. 360–364.

Poshadri, A. and Kuna, A. (2010) 'Microencapsulation technology: a review', *Journal of Research Angraui*, 38(6), pp. 86–102.

Raval, D. *et al.* (2019) 'A review on electrospraying technique for encapsulation of nutraceuticals', *International Journal of Chemical Studies*, 7(5), pp. 1183–1187.

Ré, M.I. (2006) 'Formulating drug delivery systems by spray drying', *Drying Technology*, 24(4), pp. 433–446.

Risch, S.J. (1995) 'Encapsulation: Overview of Uses and Techniques', in Reineccius, R (ed) *Encapsulation and Controlled Release of Food Ingredients*. G.A. Washington, DC USA: American Chemical Science, pp. 2–7.

Roberfroid, M.B. (2002) 'Functional foods: concepts and application to inulin and oligofructose', *British Journal of Nutrition*, 87(2), pp. 139–143.

Rossi, M. (2007) 'Use of lecithin and lecithin fractions', in *Bioactive Egg Compounds*, pp. 229–239.

Saavedra-Leos, M.Z. *et al.* (2014) 'Physical properties of inulin and inulin-orange juice: Physical characterization and technological application', *Carbohydrate Polymers*, 105(1), pp. 10–19.

Sahoo, S.K. and Labhasetwar, V. (2003) 'Nanotech approaches to drug delivery and imaging', *Drug Discovery Today*, 8(24), pp. 1112–1120.

Schade, D.S., Shey, L. and Eaton, R.P. (2020) 'Cholesterol review: A metabolically important

molecule', *Endocrine Practice*, 26(12), pp. 1514–1523.

Sercombe, L. *et al.* (2015) 'Advances and challenges of liposomes assisted drug delivery', *Frontiers in Pharmacology*, (6), pp. 1–13.

Seremeta, K.P. *et al.* (2014) 'Spray-dried didanosine-loaded polymeric particles for enhanced oral bioavailability', *Colloids and Surfaces B: Biointerfaces*, (123), pp. 515–523.

Shyamala, J. (2017) 'Formulation design, development and in vitro evaluation of abacavir sulphate gastroretentive microspheres'. JKKN College of Pharmacy.

Silva, P. da *et al.* (2014) 'Microencapsulation: concepts, mechanism, methods and some applications in food industry', *Ciencia Rural, Santa Maria*, 44(7), pp. 1304–1311.

Singh, M. *et al.* (2016) 'Microencapsulation and its various aspects: A review', *International Journal of Advanced Research*, 4(6), pp. 2094–2108.

Singh, M.N. *et al.* (2010) 'Microencapsulation: A promising technique for controlled drug delivery', *Research in Pharmaceutical Sciences*, 5(2), pp. 65–77.

Singh, R.S. and Singh, R.P. (2010) 'Production of Fructooligosaccharides from Inulin by Endoinulinases and Their Prebiotic Potential', *Food technology and Biotechnology*, 48(4), pp. 435–450.

Singh, S., Baghel, R. and Yadav, L. (2011) 'A review on solid dispersions', *International Journal of Pharmacy and Life Science*, 2(9), pp. 1078–1095.

Siraj, S. *et al.* (2019) 'Review on solid dispersions of poor water soluble drug by using natural polymers', *The Pharma Innovation Journal*, 8(1), pp. 631–636.

Sollohub, K. and Cal, K. (2012) 'Molecular Nanomedicine Towards Cancer', *Journal of Pharmaceutical sciences*, 101(7), pp. 2271–2280.

Sperling, R. (1998) 'Zidovudine', *Infectious Diseases in Obstetrics and Gynecology*, 6(5), pp. 197–203.

Suganya, V. and Anuradha, V. (2017) 'Microencapsulation and Nanoencapsulation: A Review', *International Journal of Pharmaceutical and Clinical Research*, 9(3), pp. 233–239.

Swaminathan, J. and Ehrhardt, C. (2011) 'Liposomes for Pulmonary Drug Delivery', in Smith, H. and Hickey, A. (5th edn), *Controlled Pulmonary Drug Delivery, Advances in Delivery Science and Technology* Dublin, Ireland, pp. 313–334.

Tafere, C. *et al.* (2021) 'Disintegrating co-trimoxazole tablet by direct compression', *PLoS ONE*, 16(3), pp. 1–35.

Taheri, A. and Jafari, S.M. (2019) 'Nanostructures of gums for encapsulation of food ingredients, Biopolymer Nanostructures for Food Encapsulation Purposes'. doi:10.1016/B978-0-12-815663-6.00018-5.

Tapia-hernández, J.A. and Rodríguez-félix, F. (2017) 'Nanocapsule formation by electrospraying, Nanoencapsulation Technologies for the Food and Nutraceutical Industries.' doi:10.1016/B978-0-12-809436-5/00009-4.

Teja, S.B. *et al.* (2014) 'Drug-excipient behavior in polymeric amorphous solid dispersions', *Journal of Excipients and Food Chemicals*, 4(3), pp. 70–94.

Timilsena, Y.P., Haque, A. and Adhikari, B. (2020) 'Encapsulation in the Food Industry : A Brief Historical Overview to Recent Developments', *Food and Nutrition Sciences*, 11, pp. 481–508.

Tolescu, C. *et al.* (2014) 'Microencapsulated fertilizers for improvement of plant nutrition', *Journal of the Serbian Chemical Society*, 79(6), pp. 659–668.

Tsibris, A.M.N. and Hirsch, M.S. (2014) 'Antiretroviral Therapy for Human Immunodeficiency Virus infectio. In Practice of Infectious Diseases (8th edn). Elsevier Inc. doi:10.1016/B978-1-4557-4801-3.00130-2.

Van Nieuwenhuyzen, W. and Tomás, M.C. (2008) 'Update on vegetable lecithin and phospholipid technologies', *European Journal of Lipid Science and Technology*, 110(5), pp. 472–486.

Vereyken, I.J. *et al.* (2003) 'Structural requirements of the fructan-lipid interaction', *Biophysical Journal*, 84(5), pp. 3147–3154.

Vidal-Valverde, C. *et al.* (2003) 'Assessment of nutritional compounds and antinutritional factors in pea (*Pisum sativum*) seeds', *Journal of the Science of Food and Agriculture*, 83(4), pp. 298–306.

Walsh, J. *et al.* (2018) 'Patient acceptability, safety and access: A balancing act for selecting age-appropriate oral dosage forms for paediatric and geriatric populations', *International Journal of Pharmaceutics*, 536(2), pp. 547–562.

Wang, J., Jansen, J.A. and Yang, F. (2019) 'Electrospraying : Possibilities and Challenges of Engineering Carriers for Biomedical Applications — A Mini Review', *Frontiers in Chemistry*, (7), pp. 1–9.

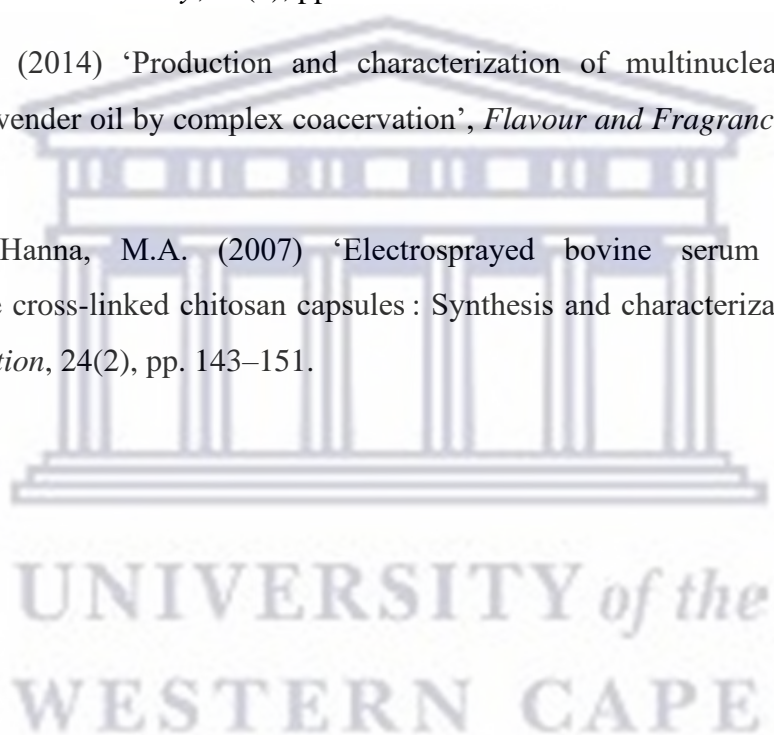
Wang, Y. *et al.* (2016) 'Manufacturing Techniques and Surface Engineering of Polymer Based Nanoparticles for Targeted Drug Delivery to Cancer', *Nanomaterials*, 6(26), pp. 1–18.

Wendel (2000) 'Lecithin: The first 150 year part 11, evolution to the global pharmaceutical industry', *Inform*, (11), pp. 992–997.

Wu, Y. and Wang, T. (2003) 'Soybean lecithin fractionation and functionality', *Journal of the American Oil Chemists' Society*, 80(4), pp. 319–326.

Xiao, Z. *et al.* (2014) 'Production and characterization of multinuclear microcapsules encapsulating lavender oil by complex coacervation', *Flavour and Fragrance Journal*, 29(3), pp. 166–172.

Xu, Y. and Hanna, M.A. (2007) 'Electrosprayed bovine serum albumin-loaded tripolyphosphate cross-linked chitosan capsules : Synthesis and characterization', *Journal of Microencapsulation*, 24(2), pp. 143–151.



Chapter Four

4. Materials and methods

4.1. Introduction

This chapter describes in detail, all the materials and methods adopted in this work starting from the functional analyses of the coating materials to the spray drying and liposomes encapsulation of ABC and AZT drugs. The details of all the analytical techniques used in the physicochemical characterization and analyses of all the pure drugs, the coating materials, the spray dried drugs and the drug-loaded liposomes have been established in this chapter as well.

4.2. Materials used in this study

Abacavir sulfate (ABC), zidovudine (AZT) and pea protein isolate (PPI) was purchased from DB Fine Chemicals (Pty) Ltd (Johannesburg, South Africa). The PPI consisted of 80% protein, 9% extractable fat, 1 & fibre and 7% moisture. Soybean lecithin (LEC) and cholesterol (CHO) were procured from Sigma-Aldrich (Johannesburg, South Africa). Inulin (IN) with a degree of polymerisation > 10 was purchased from Savannah Fine Chemicals (Pty) Ltd. (Milnerton, South Africa). Ammonium acetate, chloroform, hydrochloric acid, glacial acetic acid, and chromatography grade acetonitrile were procured from Merck (Johannesburg, South Africa) and were used with no further purification. Sodium chloride, disodium hydrogen phosphate, citric acid, and Tween[®]80 were supplied by Kimix Chemicals (Cape Town, South Africa).

Distilled water was obtained from a Milli-Q Elix[®] Essential 3 water purification system from Merck[®] (Johannesburg, South Africa) and ultrapure HPLC water with a resistivity of $18.2 \text{ M}\Omega\cdot\text{cm}^{-1}$ was obtained from a Lasec[®] Purite laboratory water system.

4.3. Physicochemical characterization of individual compounds and encapsulated ARVs

Throughout this study various physicochemical characterization techniques were utilised. The study was structured to first and foremost investigate the physicochemical characteristics of ABC, AZT, PPI, IN, LEC and CHO. This was studied to confirm compatibility of the individual compounds with one another, especially since the compounds were planned to be mixed and processed together to obtain encapsulated drug particles. The second phase of the study was to investigate the functional properties associated with PPI and IN only, since this protein and polysaccharide were to be used in the microencapsulation of ABC and AZT through spray drying. The third and fourth stages involved the encapsulation of ABC and AZT

utilising two very different encapsulation techniques and during these stages the same physicochemical characterization techniques were employed. For the purpose of brevity, the physicochemical characterization techniques will not be repeated in each relevant section. The details of these characterization techniques will therefore be described in the following paragraphs and where necessary, reference to the relevant paragraphs shall be made.

4.3.1. Hot-stage microscopy (HSM)

The possibility of denaturation, melting point sublimation or dehydration of the individual compounds, physical mixtures as well as the encapsulated ARVs were determined using HSM. An Olympus SZX7 (Tokyo, Japan) microscope equipped with a Linkam THMS600 heating stage (Surrey, UK) was utilised. A temperature range of 25 - 300 °C set at a rate of 10 °C/ min was used for the HSM analysis. A small amount of the powder (0.5 mg) under investigation was placed on a microscope slide on the heating stage. The microscope was focused so that the individual powder particles were clearly visible. Micrographs were captured at 25 °C intervals, whilst the heating stage heated the sample. Once any thermal event was observed micrographs were taken at shorter temperature intervals. The HSM was carried out twice (once without silicon oil and once with silicon oil), this was to ensure that no thermal event was missed due to submergence or non-submergence in silicon oil. The observations made with the HSM then served as an indication of the temperature range required for subsequent differential scanning calorimetry (DSC) analyses.

4.3.2. Differential Scanning Calorimetry (DSC)

The possibility of protein denaturation, phase transformations or mere melting points were determined using the technique of DSC. A PerkinElmer DSC 8000 (Waltham, USA) was used. Samples of approximately 2 -5 mg were accurately weighed into aluminum sample pans. Subsequently, the pans were sealed. Nitrogen was used as purge gas at a flow rate of 50 ml/min and the heating rate was set to 10 °C/min over a range of 25 – 300 °C.

4.3.3. Thermogravimetric analysis (TGA)

TGA was carried out using a TGA 4000 (PerkinElmer Waltham, USA). The samples, weighing 2 – 5 mg each were placed in a porcelain crucible. Subsequently, a heating program of 10 °C/min from ambient temperature to 300 °C was used. This was done under a nitrogen purge of 40 ml/min. The moisture lost during heating of the samples were documented.

4.3.4. Fourier-Transform infrared spectroscopy (FTIR)

A Perkin Elmer (Waltham, USA) Fourier-Transform infrared spectrometer (FTIR) was used to obtain information on the functional groups present in all the compounds, physical mixtures and the encapsulated ARVs. A small amount of sample was placed upon the scanning crystal surface of the FTIR and forced applied at a pressure gauge of approximately 60% within the scanning range of 400 to 4000 cm^{-1} and IR-spectra captured using Spectrum® software 6.3.5 version and being replotted using origin software and analyzed.

4.3.5. Powder X-ray diffraction (PXRD)

PXRD was used for the determination of the solid-state habit (amorphous or crystalline) of the pure drug, the spray dried, and drug loaded samples as well as the excipients used in this study. A Bruker D8 Advance (Karlsruhe, Germany) diffractometer was used. Scans were obtained at ambient conditions and a scanning range of $4^\circ 2\theta - 40^\circ 2\theta$ was used at a rate of $0.1^\circ/\text{s}$.

4.3.6. Scanning electron microscopy (SEM)

SEM analysis of all the samples was done using an AURIGA Field Emission High-Resolution Scanning Electron Microscope (HRSEM), Zeiss (Germany). Powder samples were mounted onto aluminum stubs using carbon tape. The mounted samples were subsequently coated with a thin layer of gold-palladium. An accelerating voltage of 5 keV and a filament current of 2,359 A were used.

4.3.7. Equilibrium solubility determination

The equilibrium solubility of the pure ARVs were compared with the equilibrium solubility of each ARV when combined into the following physical mixtures: drug:IN, drug:PPI, drug:LEC:CHO and then also post encapsulation. The solubility determinations were carried out using the well-known shake-flask method with some minor modification. An excess amount of sample was added to a test tube (n=6) containing 10 ml of aqueous buffered solution (pH 1.2, 4.5, 6.8) or deionized water to form a supersaturated solution with precipitate at the bottom of the test tube. Subsequently, the test tubes were sealed with Parafilm™ (Bemis Inc., Neenah, USA) and agitated in an ES-80 orbital shaker -incubator (Monitoring and Control Laboratories Pty, Ltd, England) at 150 rpm maintained at $37.0 \pm 0.5^\circ\text{C}$ for 24 hours. Subsequently, the samples were filtered using a syringe filter with $0.22\ \mu\text{m}$ pore size followed by 1 ml of the filtrate diluted to 25 ml using the respective buffer solution or deionized water. The resulting solutions were then analyzed using a suitable HPLC method.

4.3.8. *In vitro* dissolution testing

The dissolution studies for pure ABC, pure AZT and the subsequent encapsulated drugs were carried out using a Vankel 700 dissolution bath apparatus (Varian, Palo Alto, USA). Three different aqueous buffered media (pH 1.2, 4.5, 6.8) at a paddle rotation of 50 rpm and a temperature of 37.0 ± 0.5 °C were used. In each instance, sufficient sample was weighed to allow a single human dose of each of the ARVs to be used during the dissolution testing. To each weighed powder sample, double the weight of acid-washed glass beads (≤ 60 μm), obtained from Sigma-Aldrich, Johannesburg, South Africa, was added. Subsequently, an aliquot (2 ml) of the pre-heated dissolution medium was added to the powder: glass bead mixture and was thoroughly mixed through vortexing using a Janke and Kunkel IKA, Labortechnik (Wasserburg, Germany) vortex and then transferred into the 500 ml dissolution medium. At different time intervals (10 s, 20 s, 30 s, 40 s, 60 s, 10 min, 20 min, and 30 min), 2 ml aliquots were withdrawn with no media replacement. The samples were then filtered using a 0.22 μm membrane syringe filter and subsequently analyzed using a suitable HPLC method.

4.3.9. High-performance Liquid Chromatography (HPLC)

A pharmacopoeial method for the identification and quantification of ABC was utilized (USP-NF, 2020). An Azura (Knauer, Berlin, Germany) HPLC system equipped with a quaternary pump, PDA detector, autosampler, and column thermostat was utilized. A Kinetex[®] (Phenomenex, Torrance, USA) C₁₈ column (150 x 4.6 mm, 5 μm) was used as stationary phase with a mobile phase consisting of ultrapure water: acetonitrile: orthophosphoric acid (80:20:1) along with a flow rate of 2.0 ml.min⁻¹. A detection wavelength of 278 nm was utilized. For ABC identification and quantification purposes, standard solutions were prepared to provide a working concentration of 0.2 mg/ml using ultrapure water as the diluent. The standard solution was subsequently filtered using a 0.45 μm syringe filter. Linearity for the analytical method was established across a concentration range of 5 – 50 $\mu\text{g/ml}$, providing a correlation coefficient (r^2) of 0.999.

The USP Pharmacopeia monograph method for AZT with some minor changes were used for the detection and quantification of AZT throughout this study (USP-NF, 2020). A Kinetex (Phenomenex, Torrance, USA) C₁₈ column (150 x 4.6 mm, 5 μm in particle size) was used as stationary phase and a mobile phase consisting of ultrapure water: methanol (80:20 v/v) with the flow rate of 1.0 ml.min⁻¹ was used to obtain analyte elution at a detection wavelength of 265 nm. For the identification and quantification of the AZT a working standard solution of

0.2 mg/ml was prepared from the standard solution while using ultrapure water as the diluent followed by filtration using a 0.45µm nylon syringe filter. Linearity of the analytical solution was established across the concentration range of 2 – 45 µg/ml with the correlation coefficient of $r^2=0.999$.

4.4. Determination of the functional properties of PPI and IN

4.4.1. Foaming capacity and stability

Foaming property of PPI and IN as well as the combination of PPI with IN were firstly evaluated by adopting a method published by Du *et al* (2016), with little modification. For this experiment, 50 ml of a concentration of 20 g/ml of PPI or IN was respectively prepared in distilled water. Using a 1:1 (weight ratio) PPI:IN mixture, the same concentration (20 g/ml) was prepared in a similar manner for comparison purposes. The suspension was homogenized using a high speed Janke and Kunkel IKA Laborstechnik (Staufen, Germany) mixer at 10, 000 rpm for 2 minutes. The whipped PPI or IN solution was transferred into 100 ml graduated cylinders and the volume before and after homogenization at 0 and 30 minutes were measured. The reaction was done in triplicate and the foaming capacity and stability calculated using the equation below (Du *et al.*, 2016).

$$\text{Foam capacity (\%)} = \frac{V_0 - V}{V} \times 100 \quad (\text{Equation 4.1})$$

$$\text{Foam stability (\%)} = \frac{V_1 - V}{V} \times 100 \quad (\text{Equation 4.2})$$

V – Initial volume

V_0 – Volume after homogenization

V_1 – Volume after 30 minutes of homogenization

4.4.2. Effect of concentration of PPI and IN on foaming capacity and stabilization

The effect of increase in concentration of PPI and IN on their foaming capacity and stability was studied by employing the method used by Timilsena, Haque and Adhikari (2020), with some modification. For this evaluation, (20, 40, 60, 80 and 100 mg/ml) suspensions of either PPI or IN was prepared by dissolving them individually in distilled water to generate 50 ml suspensions. Foam was formed by stirring using a high speed Jankel and Kunkel IKA

Labortechnik homogenizer (Staufen, Germany) at 12, 000 rpm for 2 minutes. Foam volumes were recorded, and foam capacity and stability calculated using the above equations 4.1 and 4.2. This analysis was done in triplicate.

4.4.3. Effect of pH on foaming capacity and stability of PPI and IN

The effect of pH on the foaming capacity and stability of PPI and IN was investigated using a method published by Cordero-De-LosSantos *et al* (2005), with little modification. Protein isolate suspensions 40 mg/ml were prepared in distilled water to form 50 ml protein or and their pH adjusted using either 2 M HCl or 1 M NaOH. The suspensions were stirred using a high speed Janke and Kunkel IKA Labortechnik (Staufen, Germany) at 12, 000 rpm for 2 minutes. The foam volume and stability were recorded and calculated using equation 1 and 2. The study was repeated in triplicate.

4.4.4. Water holding capacity (WHC)

Water holding capacity of PPI and IN were carried out using a method reported by Du *et al.*, (2018). An accurate amount (0.5 g) of either PPI or IN was added to 10 ml of distilled water (V_1) in a 15 ml centrifuge tube. The solution was mixed, kept for 80 minutes, and then centrifuged using a Beckman Coulter 64 Allegra centrifuge (Indianapolis, USA) at 10, 000 rpm for 3 minutes. The free water was transferred into a graduated cylinder and the volume (V_2) measured. The experiment was also evaluated for the protein treated inulin. This was done in triplicate and water holding capacity calculated as:

$$WHC \left(\frac{g}{ml} \right) = (V_1 - V_2) / WX 100 \quad (\text{Equation 4.3})$$

4.4.5. Oil absorption capacity (OAC)

A slightly modified method of Yu *et al* (2017) was used in evaluating the oil absorption capacity of PPI and IN and also for protein treated inulin. Briefly, 0.5 g of PPI, IN or the protein treated IN was dissolved in 6 g Tween[®] 80 and stirred for 30 minutes. The mixture was centrifuged at 10,000 g for 20 minutes using a Beckman Coulter 64 Allegra centrifuge (Indianapolis, USA). The free oil was pipetted out and the volume of the free oil was measured and recorded. OAC was defined as the weight of the oil absorbed per gram of the sample. The analysis was done in triplicate and OAC calculated using the equation:

$$OAC \left(\frac{g}{g \text{ of sample}} \right) = \frac{F_2 - F_1}{F_0} \quad (\text{Equation 4.4})$$

Where F_0 is the weight of the dry sample (g), F_1 is the weight of the tube plus the dry sample (g) and F_2 is the weight of the tube plus the sediment (g).

4.4.6. Emulsification properties

The emulsifying activity index (EAI) and emulsifying stability index (ESI) of PPI and IN were analysed by adopting a method used by Rodsamran and Sothornvit (2018) with minor modification. PPI or IN solutions (10mg/ml) was prepared and adjusted to pH 11. These solutions/suspensions were subsequently stirred at 30 °C for 30 minutes upon which 18 ml was mixed with 2 ml of Tween[®] 80 and homogenized using a high speed Janke and Kunkel IKA Labortechnik (Staufen, Germany) at 10, 000 rpm for 2 minutes to form an emulsion. At two different time intervals (0 and 10 minutes), 50µl of the formed emulsion was pipetted from the bottom of the tube and diluted using 5 ml of 0.1% sodium dodecyl sulfate (SDS). The samples were analysed using a Shimadzu200 UV-visible spectrophotometer (Kyoto, Japan) and absorbance at 0 minutes (A_0) and 10 minutes (A_{10}) at 500 nm was recorded and EAI and ESI calculated using the equations (4.5) and (4.6).

$$EAI \left(\frac{m^2}{g} \right) = \frac{2 \times 2.303 \times A_0}{0.1 \times WE} \quad (\text{Equation 4.5})$$

$$ESI \text{ (min)} = \frac{A_0 \times 10}{A_0 - A_{10}} \quad (\text{Equation 4.6})$$

4.4.7. Gelling Property

In evaluating the gelling property of PPI and IN and the protein treated inulin, a method reported by Bildstein, Lohmann and Hennigs (2008) was adopted and slightly modified. Different amounts of protein and inulin (0.5, 1.0, 2.0 and 3.0 g) were prepared in distilled water to form 10 ml of protein or inulin solution in a 15 ml centrifuge tube. The obtained protein and inulin solutions were homogenized using a Janke and Kunkel IKA Labortechnik VF2 homogenizer (Staufen, Germany). The solutions were stored overnight at 4 °C and then heated to a temperature of 80 °C for 30 minutes. The solutions were further stored overnight at 4 °C. The gelling capacity of the PPI and IN were determined by evaluating the amount of the remaining free water and a stronger gel is formed if the content inside the test tube doesn't slip out. The analysis was conducted in triplicate.

4.4.8. Film forming ability (FFA)

Filming forming strength of PPI, IN and protein treated IN were examined using an adopted and slightly modified method from Salgado *et al* (2010). Films were prepared using a solvent casting method by dispersing an accurate amount (5 g) of PPI, IN or PPI:IN in 100 ml distilled water. The dispersions were mixed by stirring under room temperature for 30 minutes. The resulting admixture was kept overnight for a clear and bubble free dispersion. A particular volume of the dispersion (20 ml) was transferred into polystyrene Petri dishes (64 cm²) and dried in an oven at 60 °C for 7 hours followed by peeling of the film from the casting surface. This analysis was done in triplicate.

4.5. Liposomes formulation optimization and ABC encapsulation

Prior to the encapsulation of ABC in the liposomes, Design Expert 11 (State-Ease, Inc., Minneapolis, MN, USA) software was used for the design of the experiment as well as the regression and graphical analyses of the obtained experimental data. Considering a full factorial design that involves the same number of factors (*k*) and levels (*n*), a significant number of liposomes formulations requiring preparation and subsequent characterization would be inevitable. Although this approach would provide the most comprehensive insight into the behavior of a liposomal system. It is characterized by high costs and time consumption (Jankovic, Chaudhary and Goia, 2021). Response surface methodology (RSM) is concerned with the interaction effects of experimental factors with a limited number of planned experiments (Khannous *et al.*, 2011; Iloamaeke *et al.*, 2021). In this study, several variables typically used in the formulation of liposomes, such as (1) the ratio of CHO to LEC (CHO: LEC), (2) stirring time (min), (3) hydration fluid volume (ml), (4) sonication duration of vesicle suspension (min), (5) vortex time (min) of vesicle suspension were investigated (Table 4.1). The interaction effects of these variables on the particle size distribution (PS), surface charge (zeta potential), and the polydispersity index (PDI) of the prepared liposomes were investigated. This optimization was carried out so as to obtain and establish the optimal parameters suitable for the encapsulation of the drug-loaded liposomes (Okafor *et al.*, 2019). The central composite design (CCD) was used to design the experiments only for the optimization. Fifty experimental runs of the experimental design were used, and each variable at three levels of low (-1), medium (0), and high (+1) were included in the model. The levels and range of independent variables are shown in Table 4.1. The main effects and interactions between factors were determined in the experimental design matrix by the central composite

design (CCD), as shown in Table 4.2. The data in Table 4.2 were evaluated by multiple regression analysis. The second-order polynomial equation fitted better between the responses represented by particle size (Y_1), the surface charge of the prepared liposomes (Y_2), and polydispersity index (Y_3), and the input variables stirring time (A), sonication duration (B), vortex time (C), cholesterol ratio (D) and volume of water (E). The quadratic equation model for predicting the optimal conditions can be expressed according to equation 4.7 (Dutka, Ditaranto and Løvås, 2015).

$$Y = \beta_0 + \sum_{i=1}^k \beta_i X_i + \sum_{i=1}^k \beta_{ii} X_i^2 + \sum_{1 \leq i < j \leq k} \beta_{ij} X_i X_j + \varepsilon \quad (\text{Equation 4.7})$$

where Y is the response variable to be modeled, β_0 is the regression coefficient for the intercept, β_i is the linear coefficient, β_{ii} is the quadratic coefficient, β_{ij} is the regression coefficient for interaction terms, k the number of factors studied and optimized in the experiment and ε the random error while X_i and X_j are the independent variables (A, B, C). The central composite design (CCD) captures extreme factor combinations, unlike the Box Behnken Design (BBD), which does not examine borderline regions. These characteristics can both be of advantage considering the experimental problem because certain cases may require the extreme combinations to be examined. Still, other cases may involve physically impossible combinations (Rakić *et al.*, 2014).

BBD design of experiment was selected for the encapsulation of the drug loaded liposomes. This is because of the efficiency and effectiveness of BBD to CCD and three level factorial designs. Hence the effectiveness of is determined by the number of coefficients in the calculated models divided by the number of the experiments. The BBD stands is regarded more effective when the combinations at their peak of lowest levels under similar conditions are not included (Ferreira *et al.*, 2005; Kumar and Bishnoi 2015). The consequence is that BBD has fewer variables therefore will reduce experimental cost and decrease optimization time significantly. Based on this optimization, suitable parameters were selected for the liposomal encapsulation of ABC and AZT respectively. In agreement, optimization of empty liposomes has been reported earlier by Sedighi and co-workers (2019) before they incorporated hydrophobic do-decanethiol coated gold nanoparticles.

Table 4.1: Levels and range of independent variables tested in Central Composite design (CCD)

Factor	Low level (-1)	Medium level (0)	High level (+1)
Stirring time (min) (A)	30	45	60
Sonication time (min) (B)	10	20	30
Vortex time (min) (C)	2	4	
CHO ratio (weight : weight*) (D)	1	2	3
Water volume (E)	6 ml	8 ml	10 ml

*LEC content was kept constant

The well-known thin-film hydration method was used during the formulation of the empty and drug-loaded liposomes. An appropriate amount of LEC and CHO were accurately weighed and dissolved in 1 ml chloroform using a 25 ml round bottom flask. The organic solvent was removed through rotary evaporation using a Büchi rotary evaporator (Büchi, Switzerland) connected to a KNF Laboport Neuberger vacuum pump (Trenton, USA) with the water bath maintained at 60 °C and flask rotation at 250 rpm for 5 min to form a thin film on the surface of the flask.

The obtained thin film was stored in a desiccator overnight at ambient temperature. For the thin-film hydration, different volumes of water, as shown in Table 4.2, were added to each of the thin films and were hydrated utilizing varying hydration times at 60 °C. For each hydrated thin film, the generated lipid suspension was then transferred into a 50 ml centrifuge tube and centrifuged at 8,000 rpm, at room temperature for 10 min using a high-speed Beckman Coulter

64 Allegra centrifuge (Indianapolis, USA). The supernatant was decanted off and transferred into a 15 ml test tube and subsequently vortexed and sonicated using different times (Tables 4.1 and 4.2) to generate empty liposomes before being analyzed for particle size (PS), zeta-potential (ZP), polydispersity index (PDI), and shape using dynamic light scattering (DLS) and transmission electron microscopy (TEM), respectively.

From the interpretation of the DoE data, the best empty liposomes were chosen for the encapsulation of the drug in a liposomal system. Two variable factors, namely, LEC: CHO mass ratio and amount of drug (mg), were used for the next set of DoE (BBD) to obtain drug-loaded liposomes (Table 4.3). These variables were applied at three levels to generate thirteen possible formulations, as shown in Table 4.4, to ascertain the effect of lipid ratio and the amount of the drug on the encapsulation efficiency (%EE), PS, and ZP of the formulations.

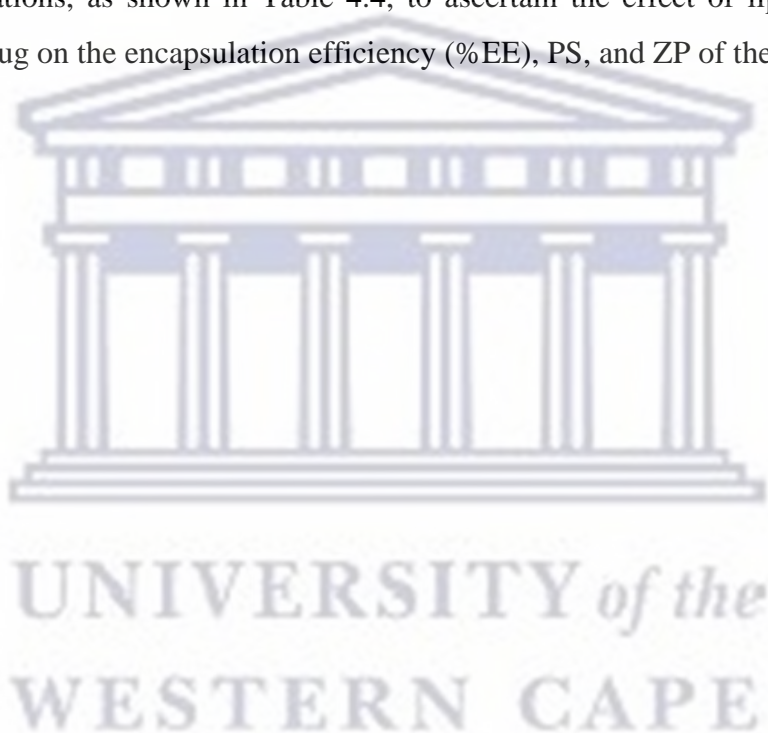


Table 4.2: Design Matrix of CCD of experiments and response results

Run	Factor 1 Stirring time (A) min	Factor 2 Sonication time (B) min	Factor 3 Vortex time (C) min	Factor 4 CHO:LEC (D) Ratio to LEC	Factor 5 Hydration fluid volume (E) ml	Y ₁ Particle size nm	Y ₂ Surface charge mV	Y ₃ PDI
F1	45	20	4	2	8	751.65	-38.34	0.366
F2	60	30	6	3	10	1004.4	-36.61	0.794
F3	45	20	4	2	10	1080.7	-43.22	0.332
F4	30	10	6	3	10	1530.43	-42.33	0.058
F5	60	30	6	1	10	1022.3	-30.46	0.125
F6	45	20	4	2	6	890.85	-28.46	0.191
F7	45	20	4	2	8	1262.45	-35.18	0.560
F8	60	10	6	3	10	1248.32	-46.35	0.142
F9	30	30	2	3	10	992.85	-45.45	0.707
F10	60	30	6	3	6	750.95	-39.05	0.243
F11	30	30	2	1	6	1016.55	-32.22	0.572
F12	60	30	6	1	6	1468.28	-24.95	0.582
F13	30	30	2	1	10	1378.5	-30.14	0.466
F14	30	30	6	3	6	728.35	-43.25	0.322
F15	60	30	2	1	6	626.45	-27.55	0.773
F16	60	30	2	1	10	689.75	-352.9	0.223
F17	60	20	4	2	8	886.43	-32.33	0.649
F18	30	20	4	2	8	845.25	-51.25	0.281
F19	45	20	4	2	8	989.32	-34.43	0.256
F20	30	30	6	3	10	1656.24	-32.53	0.121
F21	30	10	2	1	6	645.55	-35.45	0.126
F22	30	30	6	1	10	699.75	-29.75	0.254
F23	45	20	4	2	8	969.21	-31.35	0.337
F24	60	10	2	1	6	706.05	-29.55	0.406
F25	60	10	6	1	10	763.95	-31.43	0.993

Run	Factor 1 Stirring time (A) min	Factor 2 Sonication time (B) min	Factor 3 Vortex time (C) min	Factor 4 CHO:LEC (D) Ratio to LEC	Factor 5 Hydration fluid volume (E) ml	Y ₁ Particle size nm	Y ₂ Surface charge mV	Y ₃ PDI
F26	45	20	2	2	8	969.21	-40.18	0.631
F27	30	10	6	1	6	660.77	-36.21	0.494
F28	60	10	2	1	10	685.25	-35.35	0.734
F29	45	20	4	3	8	1214.14	-49.22	0.399
F30	60	10	6	1	6	607.43	-34.23	0.126
F31	45	20	4	2	8	883.75	-37.25	0.814
F32	30	10	6	1	10	517.25	-43.85	0.565
F33	30	30	2	3	6	945.55	-27.85	0.763
F34	30	10	2	3	6	906.45	-26.55	0.825
F35	60	10	2	3	6	1096.35	-25.02	0.669
F36	30	10	2	1	10	585.55	-27.65	0.223
F37	60	10	6	3	6	1659.57	-26.35	0.753
F38	60	30	2	3	6	1393.52	-37.25	0.775
F39	45	30	4	2	8	869.43	-54.05	0.109
F40	60	10	2	3	10	380.74	-44.32	0.228
F41	30	10	6	3	6	1392.31	-38.84	0.396
F42	45	20	4	2	8	743.85	-40.81	0.298
F43	30	30	6	1	6	590.04	-25.46	0.346
F44	45	20	6	2	8	892.05	-51.15	0.182
F45	45	20	4	2	8	885.15	-41.95	0.242
F46	45	10	4	2	8	812.65	-45.85	0.378
F47	60	30	2	3	10	948.25	-41.75	0.202
F48	45	20	4	2	8	810.35	-33.05	0.759
F49	45	20	4	1	8	612.34	-34.25	0.516
F50	30	10	2	3	10	1487.25	-42.16	0.224

Table 4.3: Experimental design for the encapsulation of ABC

LEC: CHO mass ratio	ABC weight (mg)
2:1	50
1:1	75
1:2	100

In order to obtain drug loading of the liposomes, the thin-film hydration involved either 50, 75, or 100 mg ABC dissolved in 10 ml distilled water, which was subsequently added to the thin film, continuously stirring at 400 rpm for 1 hr at 60 °C. Subsequently, the generated lipid suspension was transferred to a 50 ml centrifuge tube and centrifuged at 8,000 rpm using a Beckman Coulter 64 Allegra centrifuge (Indianapolis, USA) for 10 min to remove the non-encapsulated ABC particles. The isolated pellets (non-encapsulated ABC) were further investigated to determine the encapsulation efficiency (%EE), paragraph 2.3.3. The supernatant was transferred into a 15 ml centrifuge tube, vortexed for 2 min using a Janke and Kunkel IKA Labortechnik (Wasserburg, Germany) vortex, and homogenized utilizing an ultrasonic bath (Branson 3210 Danbury USA) at 60 °C for 10 min. The drug-loaded liposomes were then freeze-dried using a Freezone 6 Labconco freeze dryer connected to a vacuum pump at 0.120 mBar. The freeze-dried sample was subsequently stored for further analyses, while the physical mixture of ABC and the excipients was prepared as the control for comparative purposes. Investigation of the optimal conditions for liposomes encapsulation performed agrees with the work of Ducat *et al.*, (2010) in which they optimized and developed a formulation of peptide-loaded liposomes.

Table 4.4: Design matrix and liposomes loaded formulations (BBD)

Formulation code	LEC: CHO mass ratio	Amount of drug (mg)
L1	1:1	75
L2	1:1	75
L3	1:2	100
L4	1:2	75
L5	1:1	75
L6	1:2	50
L7	1:1	75
L8	2:1	75
L9	1:1	50
L10	2:1	50
L11	1:1	100
L12	2:1	75
L13	2:1	100

4.6. Liposomes formulation, optimization, and AZT encapsulation

As described in paragraph 4.4 for the liposomes formulation of AZT, Design Expert 11 (State-Ease, Inc., Minneapolis, MN, USA) software was used for design of the experiment, regression and graphical analyses of the data obtained. Herein, the central Box-Behnken (BBD) was further used to design the experiment and data obtained was modelled with it. The experimental design consisted of two variables with three levels i.e., low (-1), medium (0) and high (+1) giving 13 experimental runs. The levels and range of independent variables are shown in Table 4.5. The main effects and interactions between factors were determined as shown in the experimental design matrix by the BBD in Table 4.6. For liposomes formulation, the same method as described as part of paragraph 4.5 was used.

Table 4.5: Levels and range of independent variables tested in 2³ Box Behnken design (BBD)

Factor	Low level (-1)	Medium level (0)	High level (+1)
Lipid ratio (LR)	1:1	1:2	1:3
Amount of drug (DA)	50 mg	75 mg	100 mg
Response	Unit		
Particle size	nm		
Polydispersity index			
Zeta potential	-mV		
Encapsulation efficiency	%		

Table 4.6: Box Behnken design with observed responses

Run	Factor 1 Lipid ratio	Factor 2 Amount of drug (mg)	Response 1 PS (nm)	Response 2 PDI	Response 3 ZP (-mV)	Response 4 EE (%)
1	2	75	483.23	0.192	-40.92	95.28
2	2	75	470.16	0.125	-40.93	95.05
3	3	100	575.14	0.254	-62.66	93.71
4	3	75	435.12	0.195	-58.41	93.86
5	2	75	464.74	0.167	-58.33	95.07
6	3	50	243.47	0.179	-55.24	94.02
7	2	75	476.16	0.162	-59.35	95.57
8	1	75	483.26	0.164	-54.42	90.23
9	2	50	302.67	0.127	-60.13	96.91
10	1	50	304.21	0.124	-49.84	91.61
11	2	100	562.72	0.291	-48.44	96.14
12	2	75	474.24	0.148	-40.24	95.62
13	1	100	516.7	0.284	52.36	90.04

4.7. Liposomes characterization techniques

Empty liposomes, as part of the optimization process, were analyzed in terms of particle size (PS), zeta potential (ZP), polydispersity index (PDI), transmission electron microscopy (TEM). Drug-loaded liposomes were analyzed in terms of PS, ZP, PDI, TEM, percentage encapsulation efficiency (%EE), dried vesicle morphology determined by scanning electron microscopy (SEM) and powder X-ray diffraction (PXRD), physicochemical properties of dried liposomes and individual compound compatibility utilizing differential scanning calorimetry (DSC), thermogravimetric analysis (TGA), Fourier-transform infrared spectroscopy (FTIR), equilibrium solubility testing and drug release rate.

4.7.1. Particle size, zeta potential, and polydispersity index

PS, ZP, and PDI of the empty liposomes formulations obtained during the optimization process were analyzed using a Malvern Nano ZS 90 Zetasizer (Malvern Instruments, UK). These analyses were conducted in duplicate, and the best formulations with the least variation in PS and PDI and those that resulted in the most acceptable ZP were selected for shape analysis. Only the best formulations were furthered to drug encapsulation studies.

4.7.2. Transmission electron microscopy (TEM)

The empty and drug-loaded liposomes formulations with the least PDI from the optimization process were selected and further analysed for shape to confirm the presence of liposomes within the formulations using TEM equipment (Carl Zeiss Libra120 kV, Oberkochen, Germany). Prior to the microscopic evaluation, the liquid sample of both the empty and drug loaded liposomes were spotted on a copper grid and kept under room temperature for 24 hours for proper drying before checking the microscopic analysis.

4.7.3. Encapsulation efficiency (%EE) for drug-loaded liposomes

For determination of the percentage encapsulation efficiency (%EE), the isolated pellets (non-encapsulated drug) were dissolved in 30 ml of the mobile phase (paragraph 4.3.9). The resulting solution was analyzed using the HPLC methods, as described in paragraph 4.3.9. Furthermore, a control of either ABC or AZT, without the lipid components was prepared by following the liposomes preparation method (paragraph 4.5) but excluding the addition of the lipid components. This was performed to allow the theoretical evaluation and determination of the total drug concentration used during the formulation. Upon estimating the entrapped drug in the liposomes (AL), samples were diluted 1/100 using the mobile phase. The resulting

solutions were filtered using 0.45µm filters into HPLC vials and were subsequently analyzed using the HPLC method. The %EE was evaluated using equation (4.8).

$$\%EE = \frac{\text{Total amount of free drug} - \text{Amount of drug in pellet}}{\text{Total amount of free drug}} \times 100 \quad (\text{Equation 4.8})$$

4.8. Microencapsulation of ABC and AZT through spray drying

A Büchi B-290 Mini spray-dryer (Büchi Labortechnik AG, Flawil, Switzerland) was used to carry out the spray-drying of the various feed preparations. For both ABC and AZT, the feed preparation consisted of 16 g PPI, 16 g IN and 8 g ARV homogenised in distilled water. Throughout the spray-drying process the feed preparation was homogenised in the distilled water and maintained at the target temperature (60 °C) using a heated magnetic stirrer. Pressurised and dehumidified air was generated using a Haug SO45-E2-ASY oil-free air compressor (Haug Kompressoren AG, St. Gallen, Switzerland) and a Büchi B-296 dehumidifier, was used as the drying medium. The dehumidifier standardises (the drying air by removing moisture with a cold trap (<5 °C). An inlet air temperature of 220 °C was maintained and the outlet air temperature was continuously measured by the in-line temperature gauge. For comparison purposes a control was also spray dried, of which the feed preparation consisted of 16 g PPI and 16 g IN homogenised in distilled water.

After spray drying, three major responses were obtained, namely: the production yield, the moisture content of the spray dried product and drug loading. The moisture content of the spray dried powders was measured using the Mettler-Toledo HR73 Halogen moisture analyser (Greifensee, Switzerland) by placing approximately 2 g of the sample in an aluminum dish at 100 °C and desiccated for 60 min and subsequently the percentage moisture content was recorded. The percentage yield and drug loading of the spray dried drug was calculated using the following equations (Seremeta *et al.*, 2014; Tshweu *et al.*, 2014):

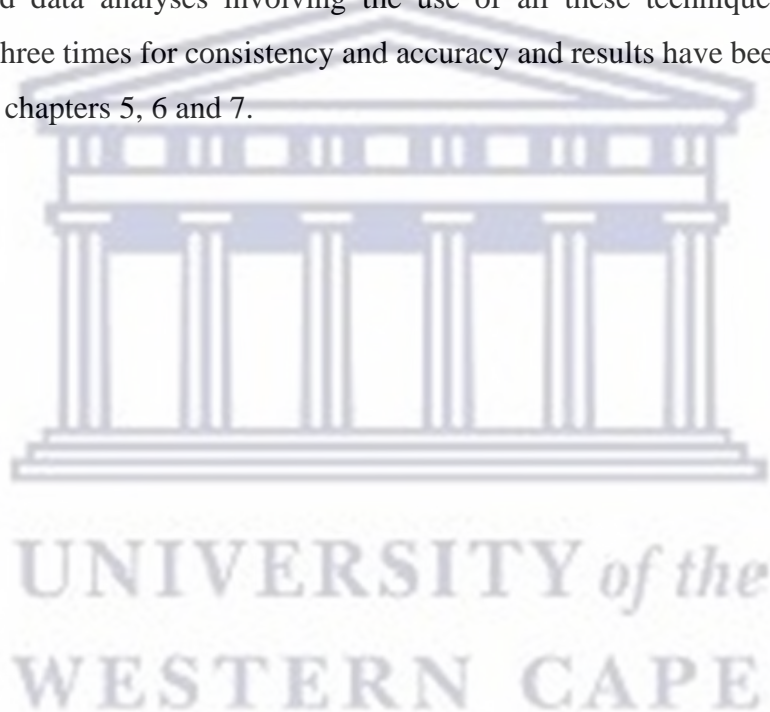
$$\% \text{ Yield} = \frac{\text{Total weight of the recovered spray dried product}}{\text{Total weight of solid in the feed solution}} \times 100 \quad (\text{Equation 4.9})$$

$$\% \text{ Drug loading} = \frac{\text{Weight of drug in the spray dried product}}{\text{Weight of the recovered spray dried product}} \times 100 \quad (\text{Equation 4.10})$$

After these parameters were recorded the spray dried samples were stored in tightly sealed glass containers in a desiccator until all other physicochemical characterization analyses were done, as described in paragraphs 4.3.1 – 4.3.6.

4.9. Conclusion

The chapter has carefully presented the details of all the materials and methods which was employed in this study. It has further given a clear descriptions and details of all the analytical techniques and equipments used in the functional analyses of the coating materials, preparation of the microcapsules and in the physicochemical characterization of the respective pure drugs, coating materials, the sprayed dried microparticles, and the drug-loaded liposomes. The experimental and data analyses involving the use of all these techniques were carefully repeated two to three times for consistency and accuracy and results have been fully presented and discussed in chapters 5, 6 and 7.



4.10. References

Bildstein, M., Lohmann, M. and Hennigs, C. (2008) ‘An enzyme-based extraction process for the purification and enrichment of vegetable proteins to be applied in bakery products’, *European Food Research Technology*, (228), pp. 177–186.

Ducat, E, *et al.* (2019) ‘The experimental approach as a practical approach to develop and optimize a formulation of peptide loaded liposomes’ *APPS Pharm Sci.Tech*, 11(2). doi10.1208/s12249-010-9463-3.

Dutka, M., Ditaranto, M. and Løvås, T. (2015) ‘Application of a central composite design for the study of NO_x emission performance of a low NO_x burner’, *Energies*, 8(5), pp. 3606–3627.

Ferreira, S.L.C. *et al.* (2007) ‘Box-Behnken design: An alternative for analytical method’, *Analytica Chimica Acta* (597), pp. 179–189.

Iloamaeke, I.M. *et al.* (2021) ‘Mercenaria mercenaria shell: Coagulation-flocculation studies on colour removal by response surface methodology and nephelometric kinetics of an industrial effluent’, *Journal of Environmental Chemical Engineering*, 9(4), pp. 105715.

Jankovic, A., Chaudhary, G. and Goia, F. (2021) ‘Designing the design of experiments (DOE) – An investigation on the influence of different factorial designs on the characterization of complex systems’, *Energy and Buildings*, (250), pp. 111298.

Kumar, S.S., and Bishnoi N.R. (2015) ‘Coagulation of landfill leachates by FeCl₃; Process optimization using Box-Behnken design (RSM)’, *Applied water science*, (7), pp. 1943–1953.

Khannous, L. *et al.* (2011) ‘Optimization of coagulation-flocculation process for pastas industry effluent using response surface methodology’, *African Journal of Biotechnology*, 10(63), pp. 13823–13834.

Okafor, N.I. *et al.* (2019) ‘Encapsulation and physicochemical evaluation of efavirenz in liposomes’, *Journal of Pharmaceutical Investigation*, (45), pp. 1–8.

Rakić, T. *et al.* (2014) ‘Comparison of Full Factorial Design, Central Composite Design, and Box-Behnken Design in Chromatographic Method Development for the Determination of Fluconazole and its Impurities’, *Analytical Letters*, 47(8), pp. 1334–1347.

Rodsamran, P. and Sothornvit, R. (2018) ‘Physicochemical and functional properties of protein concentrate from by-product of coconut processing’, *Food Chemistry*, (241), pp. 364–371.

Salgado, P.R. *et al.* (2010) 'Food Hydrocolloids Biodegradable sunflower protein films naturally activated with antioxidant compounds', *Food hydrocolloids*, 24(5), pp. 525–533.

Santos, M.Y.C. *et al.* (2005) 'Physicochemical and Functional Characterization of Amaranth (*Amaranthus hypochondriacus*) Protein Isolates Obtained by Isoelectric Precipitation and Micellisation', *Food Science Technology International*, 11(4), pp. 269–280.

Sedighi M. *et al.* (2019) 'Rapid optimization of liposomes characteristics using a combined microfluidics and design of experiment of experiment approach', *Drug delivery and Translational Research* (9), pp. 404–413.

Seremeta, K.P. *et al.* (2014) 'Spray-dried didanosine-loaded polymeric particles for enhanced oral bioavailability', *Colloids and Surfaces B: Biointerfaces*, (123), pp. 515–523.

Timilsena, Y.P., Haque, A. and Adhikari, B. (2020) 'Encapsulation in the Food Industry: A Brief Historical Overview to Recent Developments', *Food and Nutrition Sciences*, (11), pp. 481–508.

Tshweu, L. *et al.* (2014) 'Enhanced oral bioavailability of the antiretroviral efavirenz encapsulated in poly(epsilon-caprolactone) nanoparticles by a spray-drying method', *Nanomedicine*, 9(12), pp. 1821–1833.

United States Pharmacopeia USP-NF. (2020) Abacavir Sulfate. doi:10.1016/S1055-3290(06)60358-0. (Accessed 20 June 2020).

United States Pharmacopeia USP-NF. (2020) 'Zidovudine', Available at https://online.uspnf.com/uspnf/document/1_guid-932118B3-6D73-4497-A816-46DC73307D0B_3_en-US. (Accessed 20 September 2020).

Yu, M. *et al.* (2017) 'Food Chemistry Physicochemical and functional properties of protein extracts from *Torreyia grandis* seeds', *Food Chemistry*, (227), pp. 453–460.

Chapter Five

5. The physicochemical and functional characterization of pea protein isolate and inulin

5.1. Introduction

Pharmaceutical excipients are natural or synthetic materials or additives used along with the active pharmaceutical ingredient (API) in designing the dosage forms either as functional or non-functional agents. The majority of solid dosage forms on the market, today, contain excipients to almost 90% weight of each product and further forms 0.5% of the pharmaceutical market (Narang and Boddu, 2015). Pharmaceutical excipients are considered as inert additives which can serve several purposes in the pharmaceutical formulation such as imparting on the stability of the API, enhance the flowability of a powder blend, control the release of the API, to mention just a few. The selection of excipients to be used in a pharmaceutical formulation is a crucial step. Therefore it is considered paramount to characterise excipients in combination with a specific API well, especially when a decision is to be made between natural and/or synthetic excipients (Yochana *et al.*, 2018).

The global “greener” trends in basically all consumer sectors also sparked renewed interest in the use of natural excipients in dosage form development. Natural excipients could in some instances be the best choice because of their biocompatibility, affordability, low toxicity, and environmental friendliness. Many reports show natural excipients to have diverse pharmaceutical applications such as diluents, binders, flavouring agents, disintegrants, thickeners in oral liquids, protective colloids in suspensions, gelling agents and also as carriers in formulation for immediate or sustained release dosage forms (Choudhary and Pawar, 2014; Goswami and Naik, 2014).

As already described in Chapter 3, pea protein (*Pisum sativum*) accounts for 20-25% protein, 40-50% starch and 10-20% fibre. It is classified into four main groups namely: globulin, albumin and glutelin. It has a grounded amino acid profile which contains lysine, leucine and phenylamine and could be considered a strong candidate as a natural excipient to be used in pharmaceutical formulations owing to exhibited biodegradability and good functional properties (Taherian *et al.*, 2011; Lu *et al.*, 2019).

Inulin (IN) belongs to the subgroup of fructan carbohydrate composed of the β -D fructosyl subgroups linked by (2 \rightarrow 1) glycosidic bond but usually ends with (1 \leftrightarrow 2) bonded α - D glucosyl group and varies in chain lengths (Mensink *et al.*, 2015). IN has been used in

pharmaceutical formulations as a substitute for fat or sugar having a low caloric value, as an orally delivered drug for colon targeting, for delaying drug release in the stomach, used as a sweetener and the longer chain shows significance as a potential fat replacer and texture modifier, hence highly recommended in pharmaceutical products intended for oral drug delivery (Conceic *et al.*, 2014). IN have further been used as cryoprotectant in protecting molecules and compounds from damage during freeze drying, as a stabilizing excipient mainly for molecules like protein, enzymes with low stability in aqueous medium and in several relevant pharmaceutical delivery systems such as pEGylated liposomes, virosomes with and without plasmid DNA, lipoplexes and therefore, have been chosen over oligofructose in our ongoing research as a potential micro-encapsulant, in combination with PPI (Mensink *et al.*, 2015). Therefore, the main aim of this work was to evaluate the physicochemical and functional properties of PPI and IN also establish how these two natural excipients could potentially influence one another in terms of their functional properties.

5.2. Results and Discussions

5.2.1. Thermal analyses

HSM in combination with TGA analysis was used to investigate the thermal behaviour of PPI and IN. During heating of PPI, onset of degradation was observed at ≈ 225.5 °C. As depicted in Figure 5.1, this was observed as a slight yellowish colouration. Further heating showed complete degradation when it charred to a pitch-black colour at 296.3 °C. The obtained TGA trace of PPI showed a small initial weight loss of 2.86% which occurred at approximately 96.31 °C. This is close to the boiling point of water, thereby suggesting that it can be attributed to a small amount of surface adsorbed water. Most of the weight loss amounting to 73.90% at an onset temperature of 290.49 °C up until the analysis was stopped at 600.00 °C. This significant amount of weight loss correlated with the complete degradation of PPI as observed using HSM.

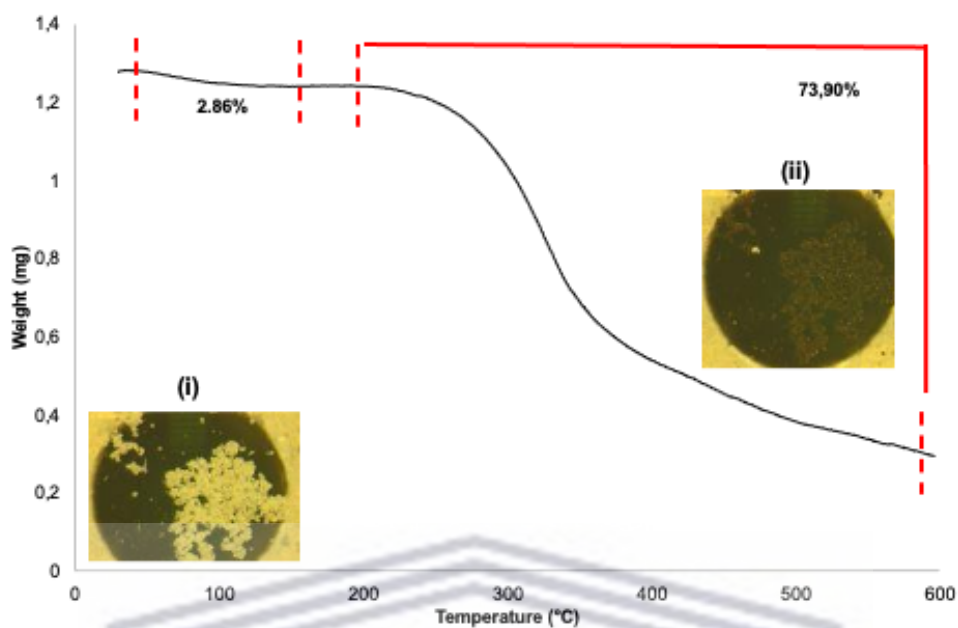


Figure 5.1. The TGA trace obtained during the heating of PPI from 25 – 600 °C with (i) depicting the HSM micrograph of PPI collected at 25 °C and (ii) a micrograph collected at approximately 590 °C, exhibiting the charring of PPI.

Figure 5.2 depicts the TGA thermogram obtained for IN during heating from 25 – 600 °C. An initial weight loss of 4.80% was observed from about 30 – 110 °C and upon comparison with HSM data it was confirmed to be moisture loss due to clear bubble evolution (Figure 5.2(i)) observed. Upon further heating a sudden weight loss at approximately 210 °C was observed followed by a more gradual weight loss from 300 °C. HSM data revealed that this weight loss is linked to the degradation of IN which turned from a white to a caramel-brown appearance. A total weight loss of 86.97% was quantified for IN during heating from ambient to 600 °C.

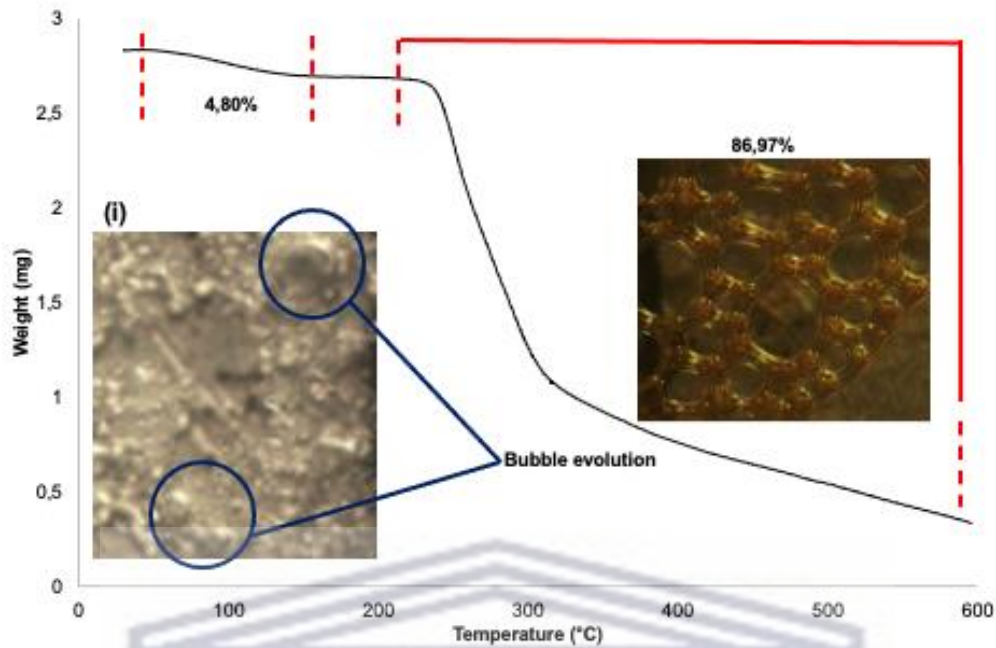


Figure 5.2: The TGA trace obtained during the heating of IN from 25 – 600 °C with (i) depicting the HSM micrograph of IN collected at approximately 100 °C and (ii) a micrograph collected at approximately 225 °C, exhibiting the degradation of IN.

The thermograms obtained for both PPI and IN during DSC analysis are depicted in Figure 5.3. The results show that both PPI and IN exhibited no melting during heating. The absence of a clearly defined melting endotherm correlates well with the HSM data, which showed no melting but rather just degradation. The lack of a clearly defined melting point also indicates that both PPI and IN possess amorphous habits, which is expected given their complex protein and polysaccharide structures.

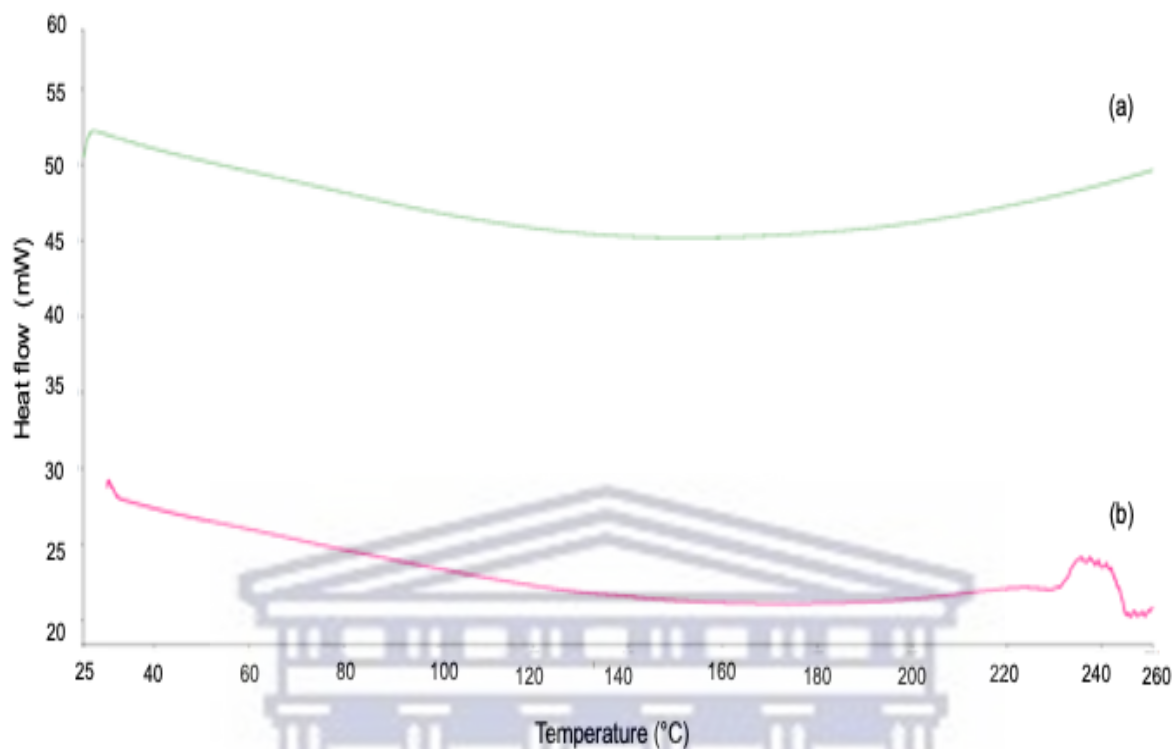


Figure 5.3. The DSC thermograms obtained with (a) PPI and (b) IN powders.

5.2.2. FTIR analysis

FTIR result of PPI and IN is shown in Figure 5.4. PPI demonstrated an absorption band at 3274.93 cm^{-1} due to O-H stretching, 2925.36 cm^{-1} from a C-H absorption band, 1630.01 cm^{-1} attributed to a C=O amide group I stretching band, 1528.89 cm^{-1} due to N-H and C-N stretching of an amide group II, at 1393.23 cm^{-1} from N-H and C-N vibration bending from amide III, 1234.94 cm^{-1} due to C-O-C symmetric stretching and 1099 cm^{-1} ascribed to the C-O strong vibration. IN showed the presence of stretching bands at 3286.16 cm^{-1} due to -OH stretching, at 2931.16 cm^{-1} attributed to the aliphatic CH_2 , 1641.18 cm^{-1} ascribed to the C=C stretching vibration, 1417.11 cm^{-1} due to the -OH vibration band, at 1018.72 being attributed to C-O-C bending and at 930.55 as result of the $\beta 2 \rightarrow 1$ glycosidic bond.

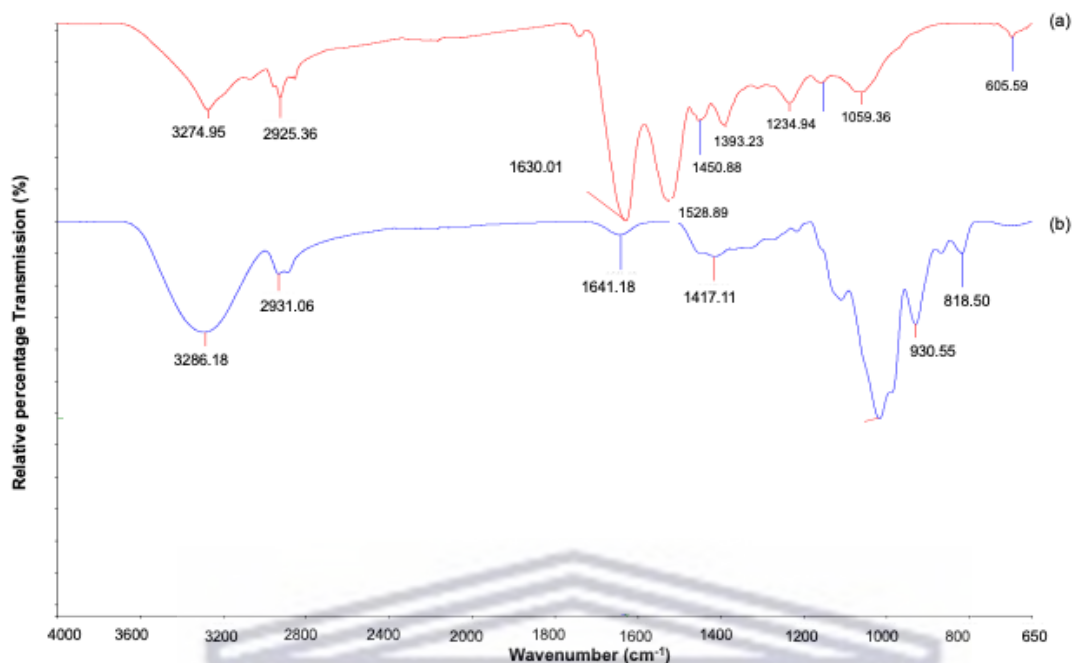


Figure 5.4. An overlay of the FTIR spectra obtained for (a) PPI and (b) IN.

This data was considered baseline data at this point in time of the study, to be used during the comparison of FTIR data obtained for the encapsulated ARVs.

5.2.3. Powder X-ray diffraction

The obtained PXRD patterns further confirmed the amorphous state of PPI and IN (Figures 5.5 and 5.6) as was preliminary concluded from HSM and DSC data. The patterns showed a typical halo diffraction pattern, which is indicative of amorphous materials.

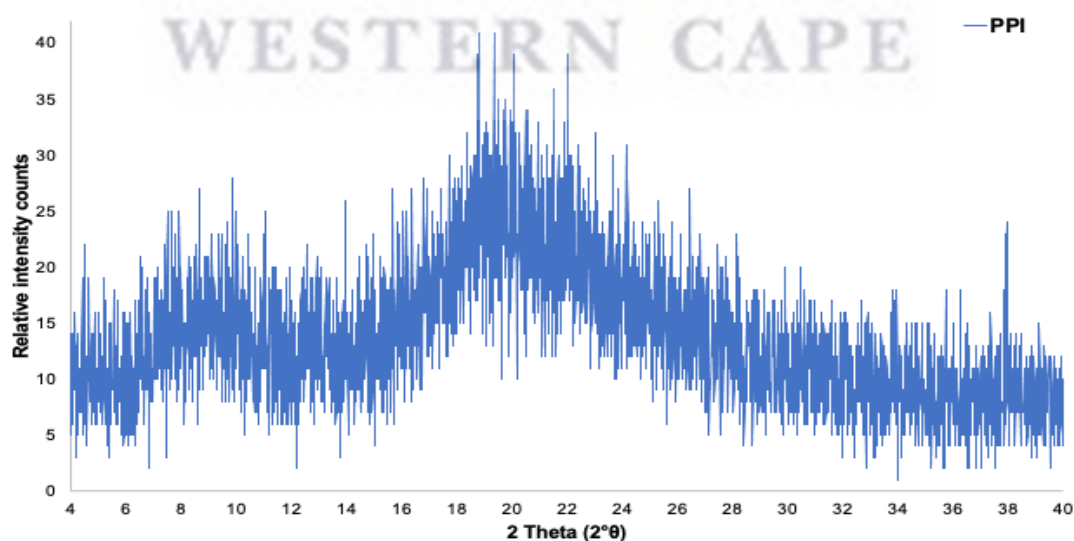


Figure 5.5. PXRD pattern of PPI obtained at ambient temperature.

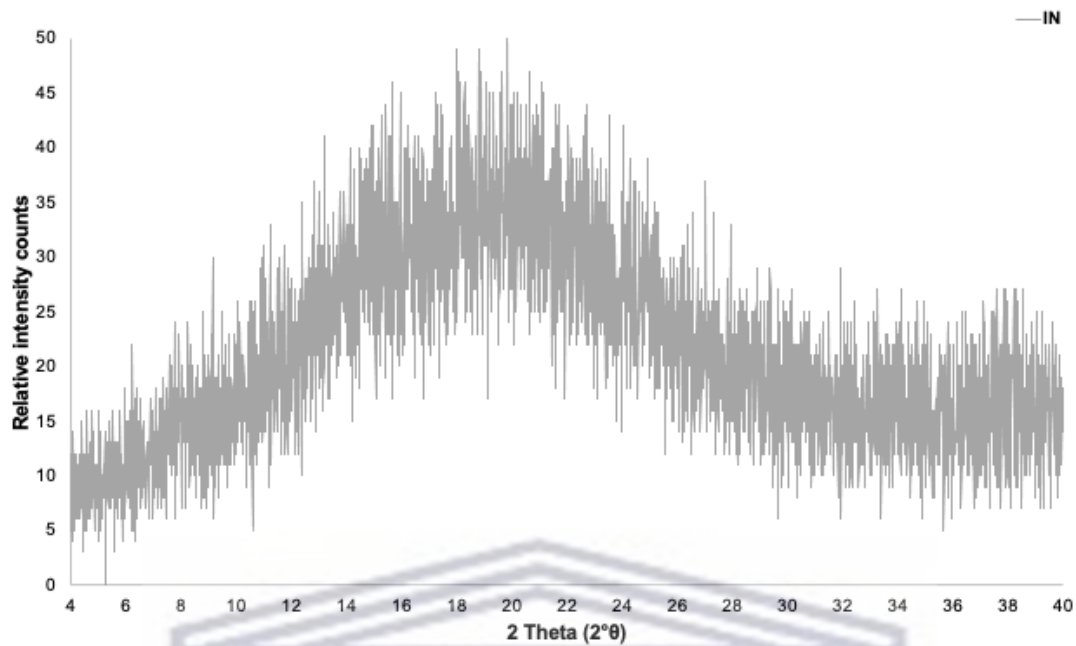


Figure 5.6. PXRD pattern of IN obtained at ambient temperature.

5.3. Determination of the functional properties of PPI and IN

5.3.1. Foaming capacity and stability

The experimentally determined foaming capacity (FC) of PPI and IN is presented in Table 5.1 along with the FC of the PPI:IN combination. FC is referred to as the interfacial area formed as a result of gas (bubble) dispersion within a liquid or solid continuous phase, mainly in water, while foam stability (FS) is the ability of a material to stabilize foams against mechanical or gravitational stresses. The obtained results showed that PPI and IN demonstrated high foaming capacity individually of above 50% which is considered good FC value compared to low established FC of 10% (Lam *et al.*, 2018). FS values showed to decrease greatly after 30 minutes in both PPI and IN. The combination of PPI:IN exhibited higher FC and more FS. The higher foaming ability of the PPI:IN combination could be attributed to the strong hydrogen interaction between PPI and IN thereby unfolding more interfacial spaces for air bubbling thereby leading to increased FC and supports the argument that higher hydrophobicity gives rise to higher foaming ability. Hence, more stable protein-based films are formed with cohesive interfacial films as a result of the increased hydrogen bonding, hydrophobic and electrostatic interactions (Barac *et al.*, 2015; Lam *et al.*, 2018).

Table 5.1: Foaming capacity and stability of protein isolates and inulin

Protein type	% Foam Capacity	% Foam stability (n=3)
Pea protein isolate	58.69 ± 1.96	28.43 ± 2.95
Inulin	58.33 ± 2.61	28.80 ± 4.40
Pea: Inulin mixture	83.20 ± 3.14	51.03 ± 3.07

5.3.2. Effect of concentration on FC and FS

The result obtained from the increase in concentration of PPI and IN is depicted in Figure 5.7. The FC and FS of PPI and IN increased as the concentration increased. The increase in the FC of PPI:IN could be because of increased air bubbles trapped within the interfacial protein or IN film formed. It could also be described that at increased concentration of the proteins, high polypeptide chains are produced to form more interfacial film and could have prompted increase in FC and FS. But FS is also dependent on net protein charge, which can reduce interactions between entrapped air particles. This is similar and in agreement with the findings from (Chao and Aluko, 2018; Timilsena, Haque and Adhikari, 2020) , who reported increase in protein FC and FS as the concentration increases which in turn created strong interfacial films as the foam capacity and stability increased accordingly.



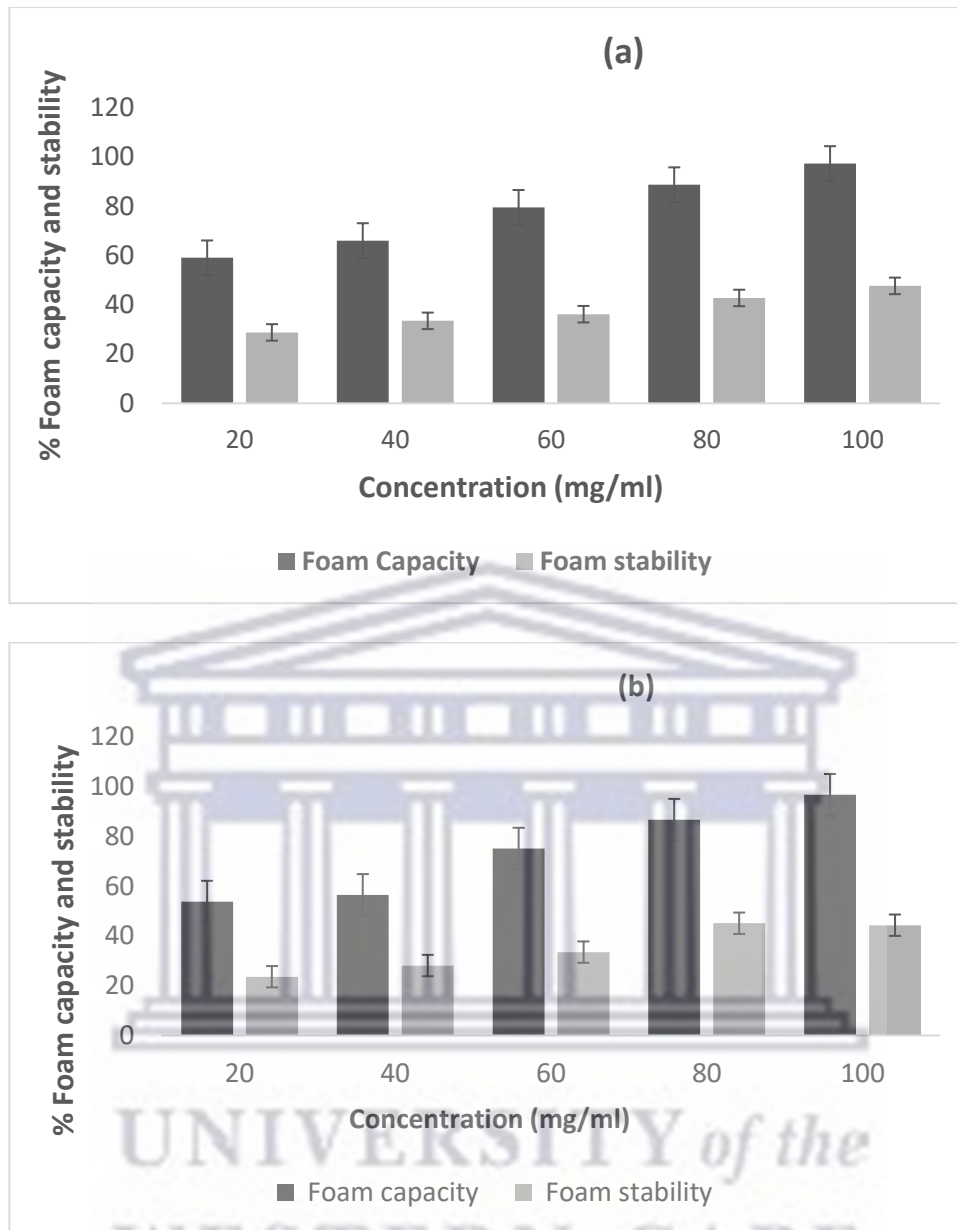


Figure 5.7. Effect of concentration on the FC and FS of (a) PPI and (b) IN.

5.3.3. Effect of pH on FC and FS

The effect of pH on FC and FS is depicted in Figure 5.8. The obtained result showed that PPI at pH 3, 7 and 11 recorded higher FC and FC than at pH 5 and 9, however, FC was more pronounced at pH 3 and 7. It could be deduced that at these pH-values, a higher concentration of the proteins was solubilised and adsorbed at the gas – water interface as a result of higher net charge of protein or surface hydrophobicity hence leading to more protein unfolding within the air and water interface with improved protein flexibility (Taherian *et al.*, 2011; Chao and Aluko, 2018). The FC and FS of IN was discovered to be more pronounced at both the acidic

and alkaline pH with lower FC and FS observed at pH 7. This is an indication that both acidic and alkaline pH media favours solubility of inulin.

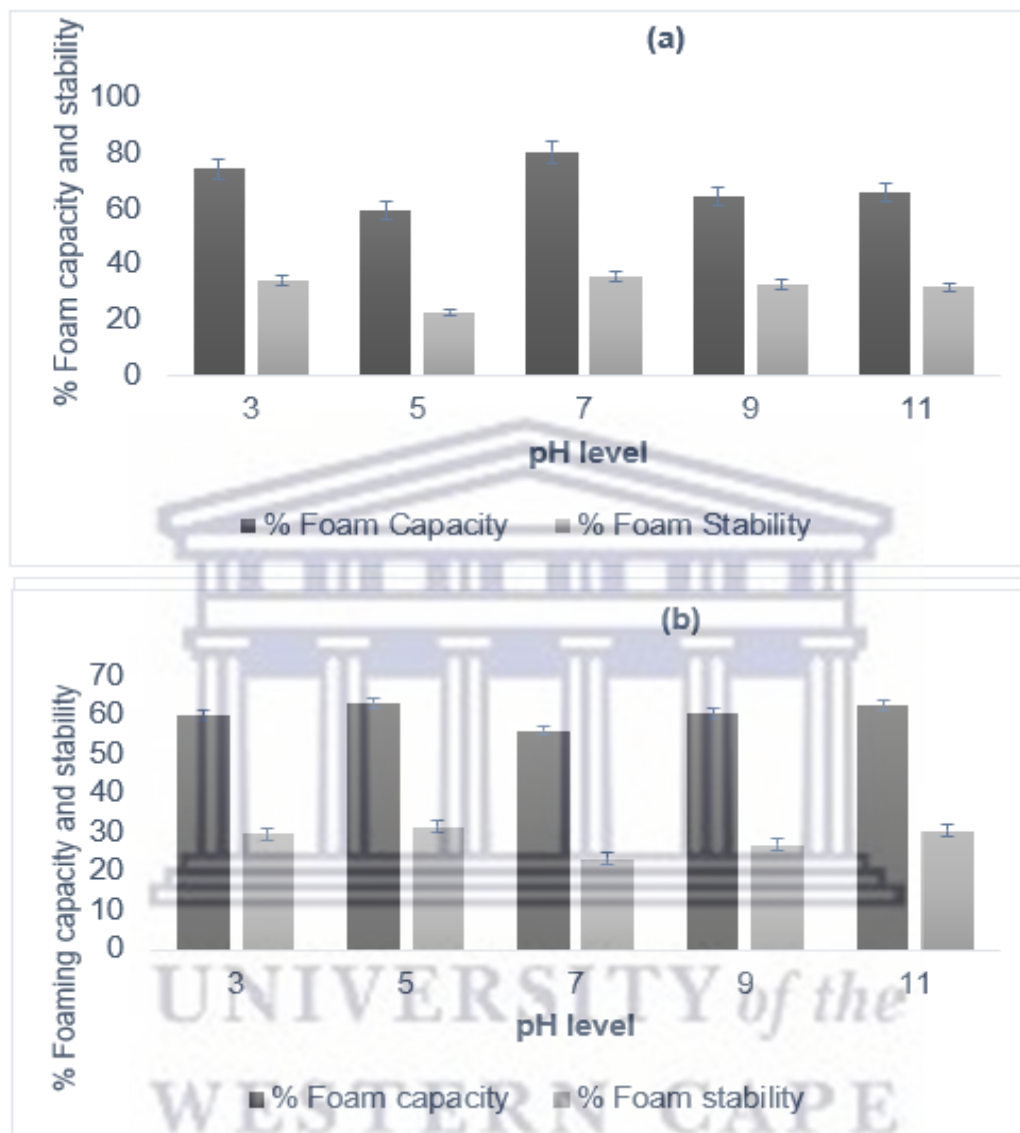


Figure 5.8. Effect of pH on (a) PPI and, (b) IN FC and FS.

5.3.4. Water holding capacity

Water holding capacity (WHC) of protein which is defined as the ability to trap or absorb water is regarded as a crucial factor especially in food industry in packed bakery food for maintenance of mouthfeel and freshness of baked food while providing food systems with an optimal texture (Amagliani *et al.*, 2017). In this work, however, water holding capacity will be detrimental. Water might trigger stability issues, especially during long term storage of the microencapsulated ARVs. Additional adsorbed water might lead to microencapsulated

particles to aggregate – ‘stick’ together, thus negatively affecting the behaviour and processability of the powder. Aspects such as flowability might be influenced detrimentally. In the pharmaceutical field WHC might be an indication of how a spray dried or electro sprayed powder will behave during exposure to high relative humidity. From the obtained WHC (Table 5.2), PPI revealed a WHC of 4.3 ml.g⁻¹ while IN showed little or no WHC. The combination of PPI and IN, displayed no significant increase in the WHC (4.6 ml.g⁻¹). The inability of IN to absorb water in this regard confirms its complete dissolution in water however, several factors like protein conformation, amino acid composition, concentration, and ratio of the surface polarity to hydrophobicity have been touted to affect WHC (Barac *et al.*, 2015).

5.3.5. Oil absorption capacity (OAC)

Oil absorption capacity (OAC) is regarded as the binding strength of fat by the nonpolar ends of the protein chains (Du *et al.*, 2018). The OAC promotes suitable enhancement of the excipients in the mouth. The obtained result of the OAC as outlined in Table 5.2 revealed an OAC value of 2.4 g/g for PPI, 1.6 g/g for IN and 2.8 g/g for PPI: IN. This is an indication that PPI in combination with IN accumulates more oil because of increased hydrophobicity and increased hydroxyl group interaction between the protein and IN, thereby creating more voids or space to entrap more oil (Twinomuhwezi, Awuchi and Rachael, 2020). The generated result shows a good OAC for PPI, IN and their mixture and possibly when used in the encapsulation, will facilitate and enhance a swift and smooth drug transportation orally.

5.3.6. Emulsifying property

The emulsion activity index (EAI) and emulsifying stability index (ESI) are two major parameters which determines the measure of the emulsion capacity formation of a material and ability of the emulsion to be stable for a given period of time. The EAI and ESI values of PPI, IN and PPI:IN ranged from 35.01 – 40.12 m²/g and 7.66 to 12 .44 min, respectively. There was no significant increase when the protein was combined with IN. The obtained EAI and ESI values may be an indication of the exposure of denatured protein isolate to the hydrophobic group dissociation and partial opening of globular proteins hence causing high surface activity and adsorption at the water and oil interface (Rodsamran and Sothornvit, 2018). Similar EAI and ESI value have also been reported for peanut and Indiana black gram protein by Zhang *et al.*, (Zhang *et al.*, 2014) hence supports the obtained results.

Table 5.2. Water holding, oil absorption capacity and emulsification property of pea protein, rice protein isolates and Inulin

Protein type	WHC (mL/g)	OAC (g/g)	EAI (m²/g)	ESI (min) (n=3)
Pea protein isolate	4.3 ± 0.22	2.4 ± 0.11	35.01 ± 1.22	7.66 ± 0.12
Inulin	Soluble	1.6 ± 0.12	38.23 ± 1.16	9.93 ± 0.24
Pea: Inulin mixture	4.6 ± 0.14	2.8 ± 0.12	38.12 ± 1.26	12.44 ± 0.16

5.3.7. Gelling properties

Gelation of materials is regarded as the ability to form a three dimensional network within an aqueous solvent which is capable of withstanding pressure, hence the interaction could be affected by some factors like pH, ionic strength, concentration, endogenous and exogenous enzymes temperature, and additives (Boye *et al.*, 2010; Tomé, Pires and Batista, 2014; Lu *et al.*, 2019). From the gelling analysis, PPI exhibited good gelling strength at 1 and 2 g with a smaller amount of water (4.6 and 2.2 ml) recorded respectively, however a stronger gelling capacity at of 3 g was obtained as no water was seen or recorded. The obtained gelling property of PPI from this work is quite different to the result of Bildstein, Lohmann and Hennigs, (2008) who reported no gelling strength of PPI. However, the result of good gelling capacity of PPI supports Messian, Chihi and Sok (2015) claim who reported a higher gelling strength of PPI as a result of high content of globulins and vicilin. IN revealed a strong gelling property at 2 g and 3 g quantity. PPI:IN at lower quantity (0.5 g and 1 g) showed weak gelling capacity but at 2 g and 3 g quantity, showed better gelling strength with little volume of water (3.2 ml and 2.8 ml) recorded. Gel formation by inulin have been reported to be proportional to its concentration thereby leading to formation of gelation as a result of precipitation and the interaction between the dissolved inulin chains (Ahmed and Rashid, 2019). It was however concluded that the combination of PPI and IN did not alter the gelling capability of the combination.

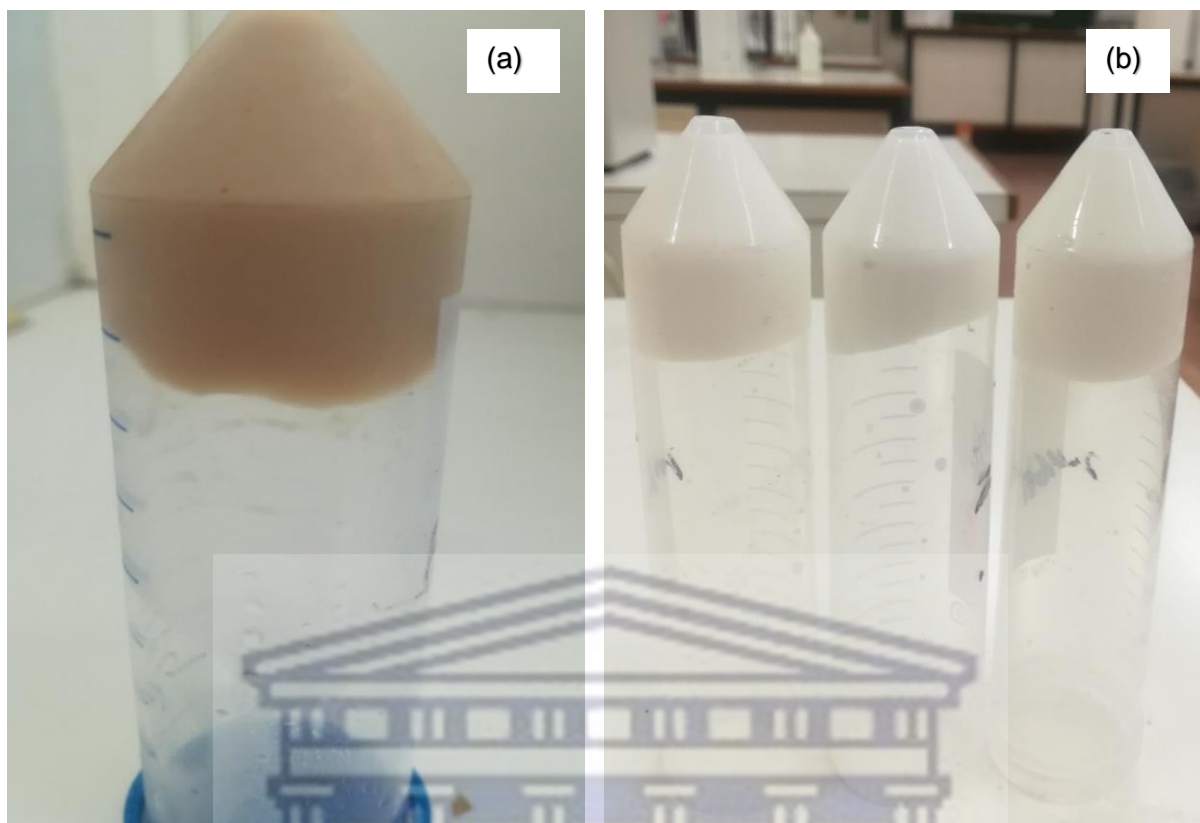


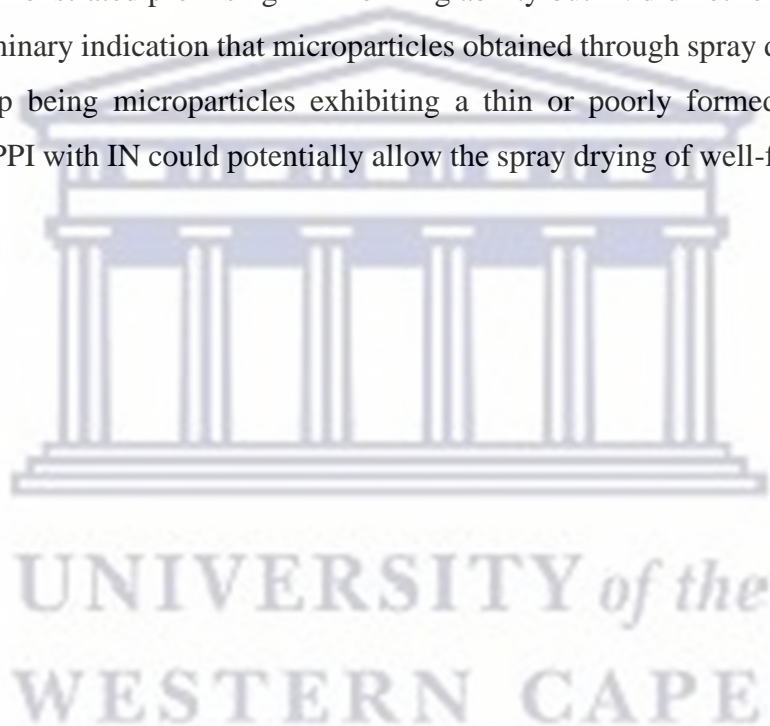
Figure 5.9. Picture representing strong gelling strength of (a) PPI, (b) IN.

5.3.8. Film forming ability

The film forming ability of PPI and the polysaccharide IN, and their combination revealed that PPI was able to form a film, however the obtained film was weak and brittle thereby lacking necessary features of a good, strong, or elastic film. Upon hydration, this film tends to easily break and lack swelling capacity. There was no film obtained with IN as well as the combination of IN and PPI. The lack of film forming ability of IN in this work is contrary to reports of good film forming property of IN and could have been because of factors such as concentration, degree of polymerization or methodology applied in the film formation (Mensik *et al.*, 2015).

5.4. Conclusion

This was a preliminary study which probed the possibility of using PPI and IN as excipients, especially for the formulation of microparticles. The essential goal of this study was to determine the physicochemical and functional properties of PPI, IN and PPI:IN to eventually conclude on their applicability in the pharmaceutical manufacturing environment. The result showed that both excipients exist in an amorphous nature but with high thermal stability. The functional properties evaluation of PPI, IN and PPI:IN revealed that the FC and FS was positively affected when PPI and IN were combined. Increase in the concentration and evaluation of pH, revealed that FC and FS of PPI and IN are dependent on concentration and pH level. PPI demonstrated promising film forming ability but IN did not form any film. This could be a preliminary indication that microparticles obtained through spray drying containing IN could end up being microparticles exhibiting a thin or poorly formed wall/shell. The combination of PPI with IN could potentially allow the spray drying of well-formed and intact walls/shells.



5.5. References

- Ahmed, W. and Rashid, S. (2019) 'Functional and therapeutic potential of inulin: A comprehensive review', *Critical Reviews in Food Science and Nutrition*, 59(1), pp. 1–13.
- Amagliani, L. *et al.* (2017) 'The composition, extraction, functionality and application of rice proteins: A review', *Trends in Food Science & Technology*, (64), pp. 1–12.
- Barac, M.B. *et al.* (2015) 'Techno-functional properties of pea (*Pisum sativum*) Protein Isolates- A review', *Acta periodica technologica*, (46), pp. 1–18.
- Bildstein, M., Lohmann, M. and Hennigs, C. (2008) 'An enzyme-based extraction process for the purification and enrichment of vegetable proteins to be applied in bakery products', *European Food Research Technology*, (228), pp. 177–186.
- Boye, J.I. *et al.* (2010) 'Comparison of the functional properties of pea, chickpea and lentil protein concentrates processed using ultrafiltration and isoelectric precipitation techniques', *Food Research International*, 43(2), pp. 537–546.
- Chao, D. and Aluko, R. (2018) 'Foaming properties of an isolated pea protein by thermal pretreatment', *CyTA - Journal of Food*, 16(1), pp. 357–366.
- Choudhary, P.D. and Pawar, H.A. (2014) 'Recently Investigated Natural Gums and Mucilages as Pharmaceutical Excipients: An Overview', *Journal of Pharmaceutics*, pp. 1–9.
- Conceic, A. *et al.* (2014) 'Carbohydrate Polymers Inulin-type fructans: A review on different aspects of biochemical and pharmaceutical technology', *Carbohydrate Polymers*, (101), pp. 368–378.
- Du, M. *et al.* (2018) 'Food Hydrocolloids of Mung bean protein', *Food hydrocolloids*, (76), pp. 131–140.
- Goswami, S. and Naik, S. (2014) 'Natural gums and its pharmaceutical application', *Journal of Scientific and Innovative Research*, 3(1), pp. 112–121.
- Lam, A.C.Y. *et al.* (2018) 'Pea protein isolates: Structure, extraction, and functionality', *Food Reviews International*, 34(2), pp. 126–147.
- Lu, Z.X. *et al.* (2019) 'Composition, physicochemical properties of pea protein and its application in functional foods', *Critical Review in Food Science and Nutrition*, 8(398), pp. 1–14.

- Mensink, M.A. *et al.* (2015) 'Carbohydrate Polymers Inulin , a flexible oligosaccharide: Review of its pharmaceutical applications', *Carbohydrate Polymers*, (134), pp. 418–428.
- Mession, J., Chihi, M.L. and Sok, N. (2015) 'Effect of globular pea proteins fractionation on their heat-induced aggregation and acid cold-set gelation', *Food hydrocolloids*, (46), pp. 233–243.
- Narang, A.S. and Boddu, S.H.S. (2015) 'Excipient Applications in Formulation Design and Drug Delivery', in *Design and Drug Delivery*, pp. 1–10.
- Rodsamran, P. and Sothornvit, R. (2018) 'Physicochemical and functional properties of protein concentrate from by-product of coconut processing', *Food Chemistry*, (241), pp. 364–371.
- Taherian, A.R. *et al.* (2011) 'Comparative study of functional properties of commercial and membrane processed yellow pea protein isolates', *Food Research International*, 44(8), pp. 2505–2514.
- Timilsena, Y.P., Haque, A. and Adhikari, B. (2020) 'Encapsulation in the Food Industry : A Brief Historical Overview to Recent Developments', *Food and Nutrition Sciences*, (11), pp. 481–508.
- Tomé, A.S., Pires, C. and Batista, I. (2014) 'Protein gels and emulsions from mixtures of Cape hake and pea proteins', *Journal of Science Food Agriculture*, (95), pp. 289–298. doi:10.
- Twinomuhwezi, H., Awuchi C.G., and Rachael M. (2020) 'Comparative study of the proximate composition and functional properties of composite flours of Amaranth, Rice, Millet, and soybean', *American Journal of Food Society and Nutrition*, 6(1), 6–19.
- Yochana, S. *et al.* (2018) 'Pharmaceutical excipients and pediatric formulations', *Chimica Oggi/Chemistry Today*, 30(5), pp. 14–18.
- Zhang, Q.T. *et al.* (2014) 'Influence of ultrasonic treatment on the structure and emulsifying properties of peanut protein isolate', *Food and Bioproducts Processing*, 92(1), pp. 30–37.

Chapter Six

6. The microencapsulation of ABC

6.1. Introduction

As already discussed in Chapter 2, the primary cause of AIDS, still poses a severe health threat associated with severe stigma to both adults and children of all ages (Dirajlal-Fargo, Koay and Rakhmanina, 2020). Although several strategies are employed to prevent the transmission of this virus from mother to child, more than ≈ 2.1 million children younger than 15 years are still suffering from this virus on a global level (Shah, 2007; Sosnik, Chiappetta and Carcaboso, 2009; Schlatter, Deathe and Vreeman, 2016). Numerous strategies have proven effective treatment for HIV-infected patients; however, HIV treatment in children has not been without some significant difficulties. HIV treatment in children is mainly hampered by poor patient compliance (Pontali *et al.*, 2001; Pontali, 2005; Hoang Thi *et al.*, 2012; Walsh *et al.*, 2018). Proper or complete compliance to treatment regimens is crucial in HIV treatment. It has been reported to decrease viral loads, minimize severe symptoms, reduce viral resistance, and ultimately allow patients to lead longer, healthier lives. Therefore, addressing the causes of poor drug compliance among children is paramount (Chiappetta *et al.*, 2010). The lack of treatment adherence in paediatric patients is mainly attributed to inadequate paediatric-specific dosage forms. The physical size of tablets or even the volume of a liquid formulation remains difficult for small children to swallow. Even if an ARV is formulated as a syrup or suspension, the extremely bitter taste associated with most ARVs still leads to the unpalatability of such dosage forms. These factors heavily hamper the attainment of total treatment adherence among HIV-infected children and thus limit their survival (Ryan Phelps and Rakhmanina, 2011; Ivanovska *et al.*, 2014). ABC and AZT are two ARVs that still form part of the first-line treatment regimen for HIV-infected children. Although solution formulations exist for these drugs, it remains challenging to administer it to neonates, infants, and children (Penazzato *et al.*, 2019). Therefore, designing a delivery system that contains liposomes could offer the ability to mask the unpleasant taste of ABC and, secondly, provide the ability to reduce the daily dose due to increased drug solubility and dissolution.

As discussed in Chapter 3, liposomes are spherical and self-assembled colloidal structures composed of natural or synthetic phospholipids and cholesterol ranging from nanometer to microns to form an aqueous core and lipid bilayers (Bozzuto and Molinari, 2015; Kim, 2016).

Liposomes are regarded as the most studied drug delivery system due to several advantages, such as acceptable biocompatibility, biodegradability, the ability to offer site-targeted drug release, and entrapment of both hydrophilic and hydrophobic drugs, improved drug solubility and low toxicity (Ramana *et al.*, 2010; Pattni, Chupin and Torchilin, 2015).

Therefore, the primary aim of this study was to investigate the potential of entrapping ABC and AZT drugs in liposomes delivery system and as well establish the effect of the particle size reduction and the drug delivery system on the *in vitro* behaviour of the ARV drugs hence offering fundamental evidence to further develop ABC- or AZT-loaded liposomes into pleasant tasting, highly effective dosage forms aimed toward HIV-infected children.

6.2. Physicochemical and morphological evaluation of the empty liposomes

For ease of reference, Table 4.2 is duplicated here as Table 6.1. From the obtained results, the effect that formulation parameters have on liposomes characteristics was assessed. It was observed that F40 (Table 6.1), which was prepared using the longest hydration time (60 min), vortex time of 2 min, and 10 min sonication time with 10 ml of distilled water used as hydration fluid, gave rise to the smallest particle size (PS), a high zeta potential (ZP) and a well-accepted polydispersity index (PDI) value and based on this, the parameters for F4 was selected in the drug loaded liposome preparation. This indicates that the duration of the hydration period plays a significant role in achieving a desired liposomes particle size. Furthermore, it became apparent that a higher volume of the hydration fluid also affected the PS since the highest volume of hydration medium also gave rise to the smallest liposomes. In terms of the surface charges, F39 prepared utilising 45 min hydration time, 4 min vortex time, 30 min of sonication with 8 ml of water resulted in the highest ZP. This suggested the significant role of a well-hydrated thin-film and highly sonicated formulation on the surface charge; therefore, at the higher sonication time a highly charged liposomes were produced. The PDI depicts distribution of the liposomes size within a formulation. PDI-values less than 0.5 signify a monodispersed system, while PDI-values above 0.70 indicate a broad size distribution. In this regard, F20 prepared using a hydration time of 30 min, sonication time of 30 min, vortex time of 6 min, and a water volume of 10 ml produced the lowest PDI value. Therefore, a monodispersed liposomes system can be produced by utilizing increased stirring, sonication, and vortex time.

Table 6.1: Design Matrix of CCD of experiments and response results

Run	Factor 1 Stirring time (A) min	Factor 2 Sonication time (B) min	Factor 3 Vortex time I min	Factor 4 CHO:LEC (D) Ratio to LEC	Factor 5 Hydration fluid volume I ml	Y ₁ Particle size nm	Y ₂ Surface charge Mv	Y ₃ PDI
F1	45	20	4	2	8	751.65	-38.34	0.366
F2	60	30	6	3	10	1004.4	-36.61	0.794
F3	45	20	4	2	10	1080.7	-43.22	0.332
F4	30	10	6	3	10	1530.43	-42.33	0.058
F5	60	30	6	1	10	1022.3	-30.46	0.125
F6	45	20	4	2	6	890.85	-28.46	0.191
F7	45	20	4	2	8	1262.45	-35.18	0.560
F8	60	10	6	3	10	1248.32	-46.35	0.142
F9	30	30	2	3	10	992.85	-45.45	0.707
F10	60	30	6	3	6	750.95	-39.05	0.243
F11	30	30	2	1	6	1016.55	-32.22	0.572
F12	60	30	6	1	6	1468.28	-24.95	0.582
F13	30	30	2	1	10	1378.5	-30.14	0.466
F14	30	30	6	3	6	728.35	-43.25	0.322
F15	60	30	2	1	6	626.45	-27.55	0.773
F16	60	30	2	1	10	689.75	-352.9	0.223
F17	60	20	4	2	8	886.43	-32.33	0.649
F18	30	20	4	2	8	845.25	-51.25	0.281
F19	45	20	4	2	8	989.32	-34.43	0.256
F20	30	30	6	3	10	1656.24	-32.53	0.121
F21	30	10	2	1	6	645.55	-35.45	0.126
F22	30	30	6	1	10	699.75	-29.75	0.254
F23	45	20	4	2	8	969.21	-31.35	0.337
F24	60	10	2	1	6	706.05	-29.55	0.406
F25	60	10	6	1	10	763.95	-31.43	0.993

Run	Factor 1 Stirring time (A) min	Factor 2 Sonication time (B) min	Factor 3 Vortex time I min	Factor 4 CHO:LEC (D) Ratio to LEC	Factor 5 Hydration fluid volume I ml	Y ₁ Particle size nm	Y ₂ Surface charge Mv	Y ₃ PDI
F26	45	20	2	2	8	969.21	-40.18	0.631
F27	30	10	6	1	6	660.77	-36.21	0.494
F28	60	10	2	1	10	685.25	-35.35	0.734
F29	45	20	4	3	8	1214.14	-49.22	0.399
F30	60	10	6	1	6	607.43	-34.23	0.126
F31	45	20	4	2	8	883.75	-37.25	0.814
F32	30	10	6	1	10	517.25	-43.85	0.565
F33	30	30	2	3	6	945.55	-27.85	0.763
F34	30	10	2	3	6	906.45	-26.55	0.825
F35	60	10	2	3	6	1096.35	-25.02	0.669
F36	30	10	2	1	10	585.55	-27.65	0.223
F37	60	10	6	3	6	1659.57	-26.35	0.753
F38	60	30	2	3	6	1393.52	-37.25	0.775
F39	45	30	4	2	8	869.43	-54.05	0.109
F40	60	10	2	3	10	380.74	-44.32	0.228
F41	30	10	6	3	6	1392.31	-38.84	0.396
F42	45	20	4	2	8	743.85	-40.81	0.298
F43	30	30	6	1	6	590.04	-25.46	0.346
F44	45	20	6	2	8	892.05	-51.15	0.182
F45	45	20	4	2	8	885.15	-41.95	0.242
F46	45	10	4	2	8	812.65	-45.85	0.378
F47	60	30	2	3	10	948.25	-41.75	0.202
F48	45	20	4	2	8	810.35	-33.05	0.759
F49	45	20	4	1	8	612.34	-34.25	0.516
F50	30	10	2	3	10	1487.25	-42.16	0.224

6.2.1. Statistical analysis

Using Design Expert 11, the experimental responses were used to analyse the data statistically. The obtained data were evaluated by multiple regression analysis. The second-order polynomial equation fitted better between the responses represented by particle size (Y_1), the surface charge of the prepared liposomes (Y_2), and polydispersity index (Y_3), and the input variables stirring time (A), sonication duration (B), vortex time (C), ratio (D) and volume of water (E). The statistical significance of the quadratic model was evaluated by the analysis of variance (ANOVA). The quadratic equations obtained from the ANOVA are given in equations 6.1 (PS) and 6.2 (surface charge):

$$Y_1 = +945.76 - 14.84A + 28.21B + 47.04C + 182.25D + 21.28E + 10.54AB + 63.91AC - 46.74AD - 105.96AE - 56.87BC - 116.79BD + 37.85BE + 52.70CD + 19.90CE + 15.29DE \quad (\text{Equation 6.1})$$

$$Y_2 = -33.04 + 3.56A - 3.74B - 1.15C - 2.56D - 5.33E - 3.56AB + 2.40AC - 1.68AD - 1.57AE + 2.00BC - 1.93BD + 3.68BE - 4.92CD + 3.62CE - 3.93DE \quad (\text{Equation 6.2})$$

However, equation 6.3 is a linear equation obtained from the ANOVA for the Y_3 (polydispersity index) response:

$$Y_3 = +0.43 + 0.049A + (4.853 \times 10^{-4})B - 0.060C + (3.559 \times 10^{-3})D - 0.59E \quad (\text{Equation 6.3})$$

Model terms were evaluated by the p -value, lack of fit, F test, coefficient of determination (R^2), and adequate precision (AP). In Tables 6.2 and 6.3, the F-test values of the empty liposomes show that the quadratic model is significant towards the PS and surface charge responses. However, the linear model is significant for the polydispersity index response, and the quadratic model is insignificant.

Table 6.2: Analysis of variance for the Response Surface Quadratic model for the PS of the empty liposomes

Source	Sum of Squares	df	Mean Square	F Value	p-value Prob > F	
Model	2.513E+006	15	1.675E+005	2.90	0.0049	significant
A-Stirring time	7482.92	1	7482.92	0.13	0.7209	
B-Sonication time	27055.08	1	27055.08	0.47	0.4981	
C-Vortex time	75237.66	1	75237.66	1.30	0.2614	
D-Ratio	1.129E+006	1	1.129E+006	19.58	< 0.0001	
E-Water volume	15395.65	1	15395.65	0.27	0.6088	
AB	3554.30	1	3554.30	0.062	0.8055	
AC	1.307E+005	1	1.307E+005	2.27	0.1415	
AD	69895.93	1	69895.93	1.21	0.2787	
AE	3.593E+005	1	3.593E+005	6.23	0.0176	
BC	1.035E+005	1	1.035E+005	1.79	0.1893	
BD	4.364E+005	1	4.364E+005	7.57	0.0095	
BE	45847.71	1	45847.71	0.79	0.3789	
CD	88857.47	1	88857.47	1.54	0.2231	
CE	12666.35	1	12666.35	0.22	0.6424	
DE	7480.17	1	7480.17	0.13	0.7210	
Residual	1.961E+006	34	57684.98			
Lack of Fit	1.763E+006	27	65313.77	2.31	0.1270	
Pure Error	1.978E+005	7	28259.62			
Cor Total	4.474E+006	49				

Table 6.3: Analysis of variance for the Response Surface Quadratic model for the surface charge of the empty liposomes

Source	Sum of Squares	df	Mean Square	F Value	p-value Prob > F	
Model	5268.29	15	351.22	2.04	0.0418	significant
A-Stirring time	430.26	1	430.26	2.50	0.1229	
B-Sonication time	475.13	1	475.13	2.76	0.1056	
C-Vortex time	45.08	1	45.08	0.26	0.6119	
D-Ratio	222.87	1	222.87	1.30	0.2628	
E-Water volume	966.76	1	966.76	5.62	0.0235	
AB	404.70	1	404.70	2.35	0.1342	
AC	183.84	1	183.84	1.07	0.3084	
AD	90.45	1	90.45	0.53	0.4732	
AE	78.75	1	78.75	0.46	0.5031	
BC	128.00	1	128.00	0.74	0.3942	
BD	118.97	1	118.97	0.69	0.4113	
BE	432.92	1	432.92	2.52	0.1218	
CD	776.18	1	776.18	4.52	0.0409	
CE	419.05	1	419.05	2.44	0.1277	
DE	495.34	1	495.34	2.88	0.0987	
Residual	5844.56	34	171.90			
Lack of Fit	4649.59	27	172.21	1.01	0.5416	not significant
Pure Error	1194.98	7	170.71			
Cor Total	11112.86	49				

6.2.2. Response surface plots

The response surface plots indicate that the optimized condition for empty liposomes preparation is located inside the design boundary. 3D-surface plots of interactive effects between stirring time and sonication time at the following conditions: vortex time of 4 minutes, CHO ratio of 2 and water volume of 8 ml for (a) PS and (b) ZP responses are shown in Figure 6.1(a) and (b).

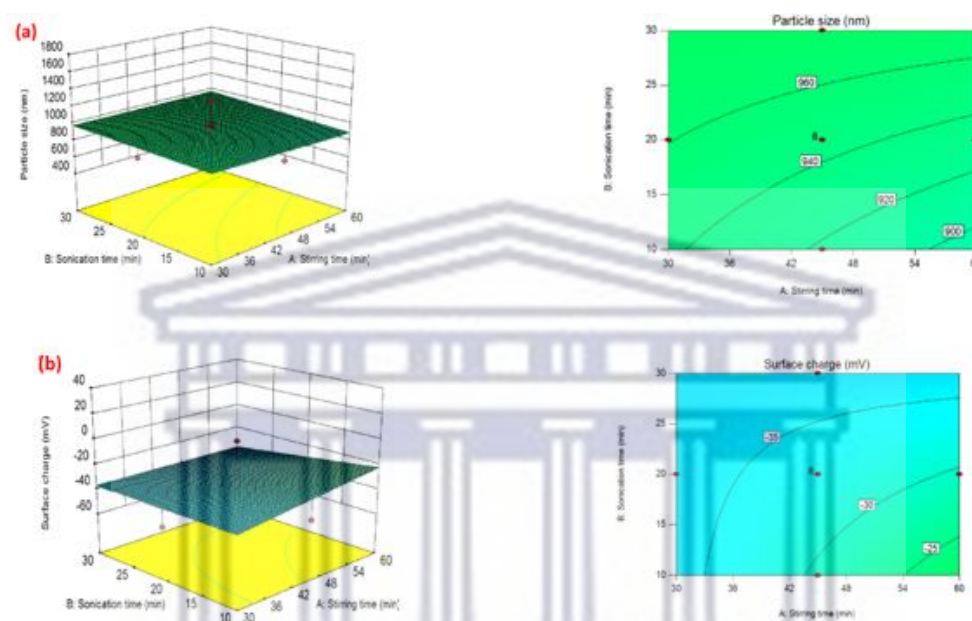


Figure 6.1. Surfaces of interactive effects between stirring time and sonication time at (a) PS and (b) surface charge.

The smallest PS measured for empty liposomes were 517.25 nm and 380.74 nm and were obtained at two conditions:

- 30 min stirring time, 10 min sonication time, 6 min vortex time, cholesterol ratio of 1 and water volume of 10 ml; and
- 60 min stirring time, 10 min sonication time, 2 min vortex time, cholesterol ratio of 3, and water volume of 10 ml.

These conditions gave surface charge and polydispersity index values of -43.85 Mv and 0.2275 for condition (a) and -44 Mv and 0.2275 for condition (b), indicating that the surface charge of these two formulations gave the smallest particle size of prepared empty liposomes. However, increasing the stirring time and cholesterol ratio at decreased vortex time caused smaller PS for the empty liposomes. Similar reports on the significant effects of the stirring time, with increased cholesterol ratio and vortex time on PS of liposomes, have been reported

earlier (Rushmi *et al.*, 2017; Wang *et al.*, 2019; Bapolisi, 2020). Considering these parameters which produced the PS, the parameters for F40 were selected for the encapsulation of the drug.

6.2.3. TEM analysis

The presence of liposomes in the optimized formulation was confirmed using transmission electron microscopy (Figure 6.2). The selected formulations with the lowest PDI were selected for this analysis which confirmed the presence of spherical-shaped particles known to be liposomes as depicted in the TEM images, thereby supporting the obtained result from the DLS analysis. The result further showed a well dispersed formulation hence little, or no aggregation is expected in the drug-loaded liposomes.

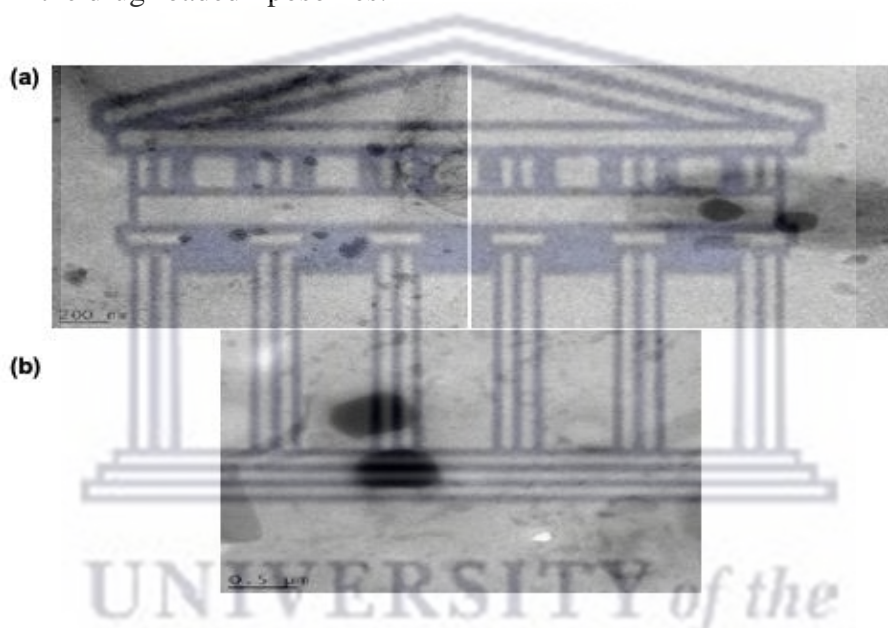


Figure 6.2. Unstained TEM images of optimized empty liposomes collected at a magnification of 200 nm and 0.5 μm .

6.3. Physicochemical and morphological evaluation of ABC-loaded liposomes

6.3.1. Determination of the influence of formulation variables on PS, ZP, PDI, and %EE

The ABC liposomes formulations (AL) were evaluated in terms of PS, ZP, and PDI using the technique of dynamic light scattering. The Design Expert 11 (State-Ease, Inc., Minneapolis, MN, USA) software was used for the design of experiment, regression, and graphical analyses of the data obtained. The Box-Behnken design (BBD) was used to design the experiment, and the data obtained were modelled. The main effects and interactions between the two factors were determined, as shown in Table 6.4. The data were evaluated by multiple regression

analysis and a second-order polynomial equation fitted better between the responses represented by percentage encapsulation efficiency (%EE) (response 1), PS (response 2), and ZP (response 3). These responses are Y in the equations and the input variables of the lipid ratio (A) and the amount of drug (B).

Table 6.4: Outline of the BBD and subsequent results for the response factors of ABC-loaded liposomes (AL)

Run	Factor 1 Lipid ratio (LEC: CHO) (A)	Factor 2 Amount of drug (B)	Response 1 %EE	Response 2 PS	Response 3 ZP
	Min	mg	%	nm	Mv
L1	2	75	92.66	439.34	-45.53
L2	2	75	95.24	459.23	-44.14
L3	3	100	96.94	522.64	-54.24
L4	3	75	97.06	496.43	-44.62
L5	2	75	95.01	419.16	-46.12
L6	3	50	97.33	451.13	-46.93
L7	2	75	94.81	490.18	-42.67
L8	1	75	97.45	472.12	-42.16
L9	2	50	90.95	429.62	-41.06
L10	1	50	94.45	400.66	-43.92
L11	2	100	89.12	445.83	-42.16
L12	2	75	95.51	420.57	-41.67
L13	1	100	96.35	498.11	-38.46

The results obtained with the drug-loaded liposomes are shown in Table 6.4 and Figure 6.3. Results showed the PS within nano range, and well homogenized ABC-loaded liposomes with low PDI values therefore indicating little or no aggregation and hence highly acceptable in liposomes drug delivery and could potentially enhance the oral bioavailability of the encapsulated drug as previously reported (Ming Ong *et al.*, 2016). The entrapment of ABC in the liposomes showed reduced liposomes PSs, in comparison with the empty liposomes (Table 6.1) which could be attributed to the long stirring and sonication time selected during the drug

encapsulation. However, the varying drug lipid ratios has shown not to influence the PS significantly (Figure 6.3). The observed responses of the thirteen formulations were fitted to various models by using the Design Expert software version 11. The quadratic models were the best fit for the studied responses for PS, ZP, and %EE. The generated quadratic equation for PS is given as:

$$PS = 457.31 + 16.55LR + 30.86AD \quad (\text{Equation 6.4})$$

where LR is the lipid ratio, AD denotes the amount of drug while, Figure 6.3 is the plot of equation 6.4. It shows that variations of the amount of drug and lipid ratio gave linear PS response such that statistical *p*-values for the amount of drug and lipid ratio are respectively more than and less than 0.05. Table 6.4 indicates that the amount of drug and lipid ratio respectively had non-significant on PS. The ZP of the drug-loaded liposomes demonstrated strong surface charges due to the strong electrostatic interactions or force of repulsion between the liposome's particles. Equation 6.5 is non-linear and it is plotted in Figure 6.4.

$$ZP = 44.13 - 3.54LR - 0.49AD - 3.19 (LR*AD) \quad (\text{Equation 6.5})$$

where ZP is zeta potential, LR is lipid ratio, and AD denotes the amount of drug. Presented in Table 6.5 are the statistical *p*-values for variation of the amount of drug, lipid ratio, and amount of drug/lipid ratio interaction such that lipid ratio and amount of drug/lipid ratio interaction have significant values and amount of drug showed non-significant *p*-value. This is because the lipid ratio and amount of drug/lipid ratio interaction have *p*-values of more than 0.05, and the *p*-value of the amount of drug is less than 0.05.

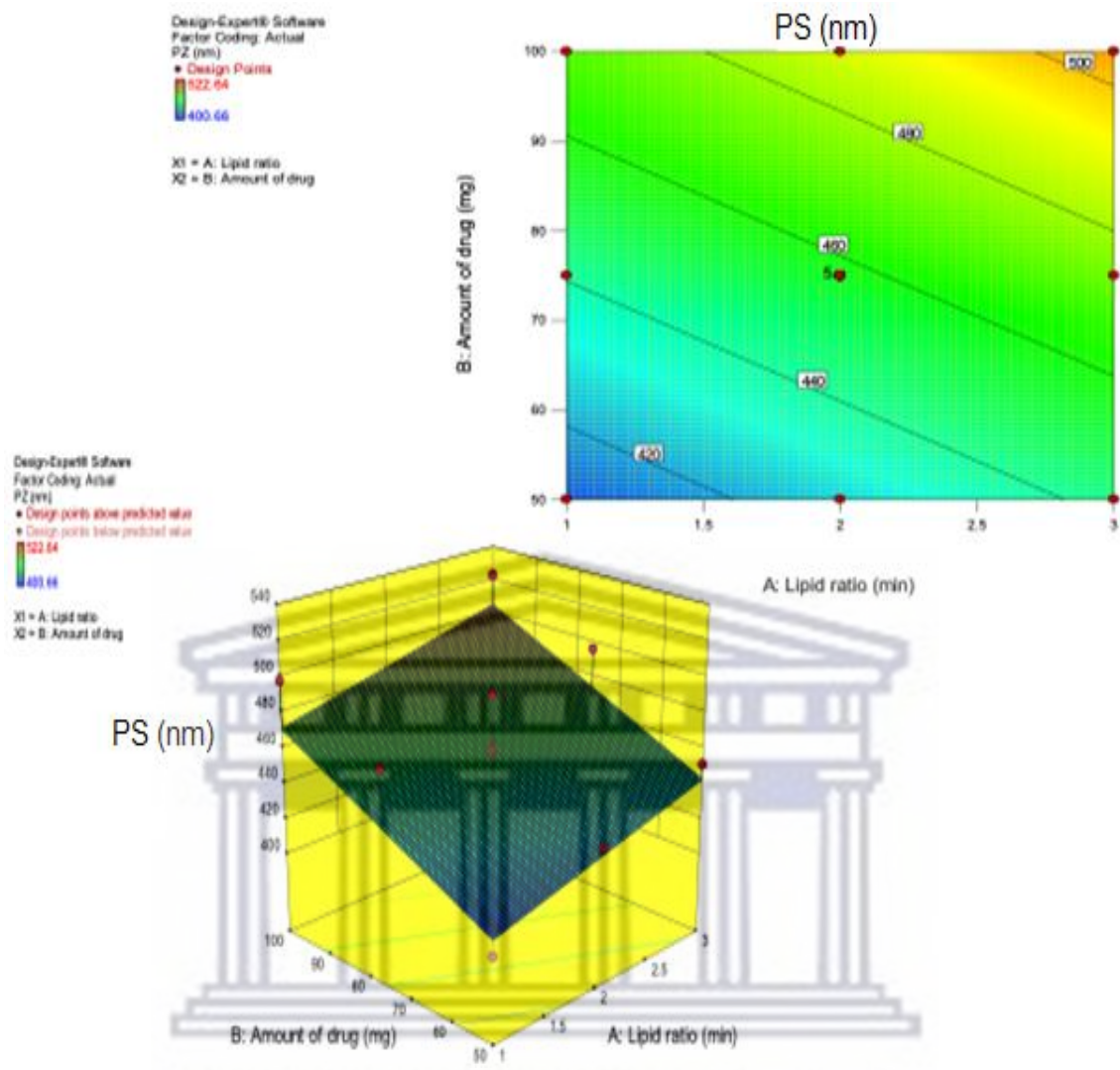


Figure 6.3. Surface plots showing the effect of lipid ratio and amount of drug variables on the ABC-loaded liposomes.

UNIVERSITY of the
WESTERN CAPE

Table 6.5: ANOVA results for the Response Surface linear model of the PS of the ABC-loaded liposomes

ANOVA for Response Surface Linear model						
Analysis of variance table [Partial sum of squares – Type III]						
	Sum of		Mean	F	p-Value	
Source	Squares	df	Square	Value	Prob>F	
Model	7358.40	2	3679.20	4.24	0.0465	<i>Significant</i>
A-Lipid ratio	1643.75	1	1643.75	1.89	0.1989	
B-Amount of drug	57144.65	1	5714.65	6.58	0.0281	
Residual	8682.19	10	868.22			
<i>Lack of Fit</i>	5144.32	6	857.39	0.97	0.5377	<i>Not significant</i>
<i>Pure Error</i>	3537.87	4	884.47			
Cor Total	16040.60	12				

PS	=	
+457.31		
+16.55	* A	
+30.86	* B	
Response	2	PS

Table 6.6: ANOVA for the surface response 2FI model for ZP

ANOVA for Response Surface 2FI model						
Analysis of variance table [Partial sum of squares – Type III]						
	Sum of		Mean	F	p-Value	
Source	Squares	df	Square	Value	Prob>F	
Model	117.48	3	39.16	4.24	0.0139	Significant
A-Lipid ratio	75.26	1	75.26	1.89	0.0071	
B-Amount of drug	1.45	1	1.45	6.58	0.6416	
AB	40.77	1	40.77		0.0310	
Residual	56.30	9	6.26			
Lack of Fit	42.25	5	8.45	2.41	0.2078	Not significant
Pure Error	14.05	4	3.51			
Core Total	173.78	12				

ZP	=	
-44.13		
-3.54	* A	
-0.49	* B	
-3.19	* AB	
Response	3	ZP

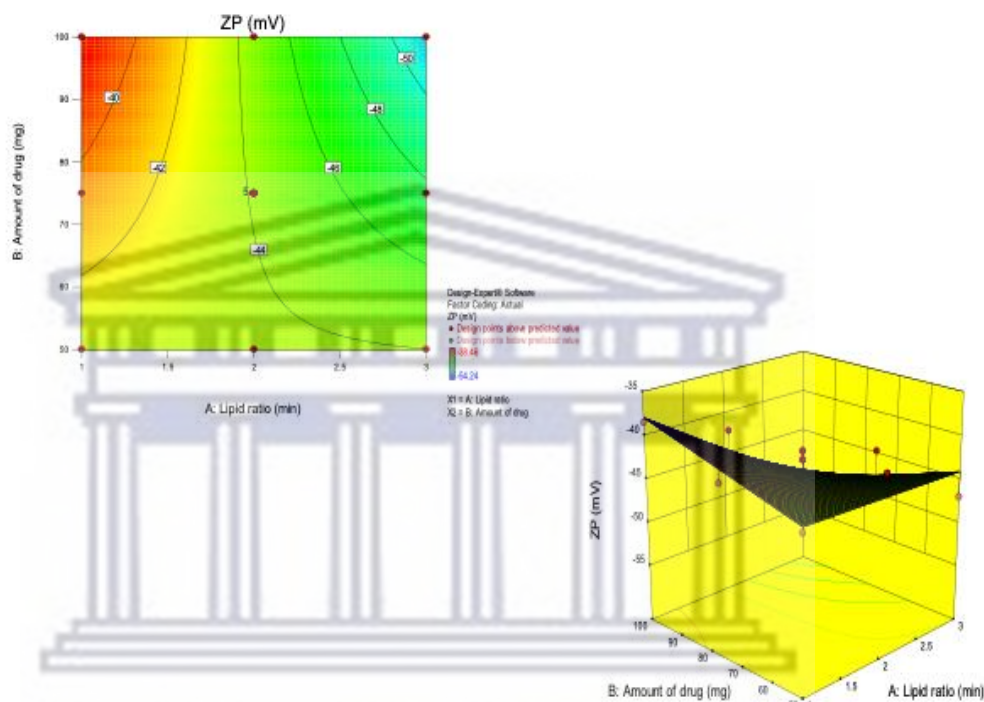


Figure 6.4. Surface plots showing the effect of lipid ratio and amount of drug variables on ZP.

The percentage encapsulation efficiency (%EE) of AL is presented in Table 6.7. The result revealed high %EE in all the liposomes formulations, with F5 consisting of LEC: CHO in the ratio 1:1 with 75 mg of the drug showing a significant increase, therefore, the highest %EE. The varying lipid ratio and amount of the encapsulated ABC, as demonstrated in Figure 6.5, was observed to have significantly influenced the %EE of ABC. However, no negative impact resulting from increased cholesterol was observed. Thus, the increase in CHO ratio did not interfere with the tight packing of lipids in the vesicles but could have acted more as a solubilizing agent for the hydrophilic ABC. The higher %EE of ABC in the liposomes highlights the tendency of the liposomes delivery system to entrap both hydrophilic and hydrophobic compounds. Hence ABC, which is highly water-soluble, was significantly entrapped in the liposomes, which could be attributed to the hydrophilicity or the solubilizing effect of the liposomes.

Furthermore, it was observed that encapsulation of ABC in the liposomes resulted in an increased PS when compared with the empty liposomes. This could have contributed to an enhanced %EE of ABC by the increased particle size creating more voids, thereby entrapping more drug. The effect of increased particle size on %EE has been reported by Ramana *et al.*, (2010), who reported particle size to have a significant impact on the %EE of nevirapine. An increase in the CHO ratio showed no negative impact on %EE. Higher %EE of water-soluble drugs has been reported, such as in the case of *Cordeyceps sinensis* (CS1197), a water-soluble compound (Shashidhar and Manohar, 2018). Formulation L5, which gave the highest %EE, based on the selected parameters with the BBD was further selected and reproduced for further analyses in comparison with the pure drug and the control. Equation 6.6 is non-linear, plotted in Figure 6.5.

$$\%EE = 94.15 + 0.51LR - 0.053AD - 0.57(LR*AD) + 4.36(LR)^2 - 2.86(AD)^2 \quad (\text{Equation 6.6})$$

where %EE is encapsulation efficiency and other acronyms remain the same. Presented in Table 6.7 is the statistical *p*-values for the amount of drug, lipid ratio, and drug/lipid ratio interaction. In all instances the *p*-values are more than 0.05 thus showing to be insignificant variables.

Table 6.7: ANOVA for response surface 2FI model for EE

ANOVA for Response Surface 2FI model						
Analysis of variance table [Partial sum of squares – Type III]						
	Sum of		Mean	F	p-Value	
Source	Squares	df	Square	Value	Prob>F	
Model	60.03	5	12.01	4.24	0.0340	Significant
A-Lipid ratio	1.58	1	1.58	1.89	0.4586	
B-Amount of drug	0.017	1	0.017	6.58	0.9373	
AB	1.31	1	1.31		0.4982	
A ²	52.46	1	52.46		0.0027	
B ²	22.62	1	22.62	2.41	0.0209	
Residual	17.99	7	2.57			
Lack of Fit	12.79	3	4.26	3.28	0.1408	Not significant
Pure Error	5.20	4	1.30			
Cor Total	78.02	12				

EE	=
+94.15	
+0.51	* A
-0.053	* B
-0.57	* AB
+4.36	* A ²
-2.86	* B ²
Response	1 EE

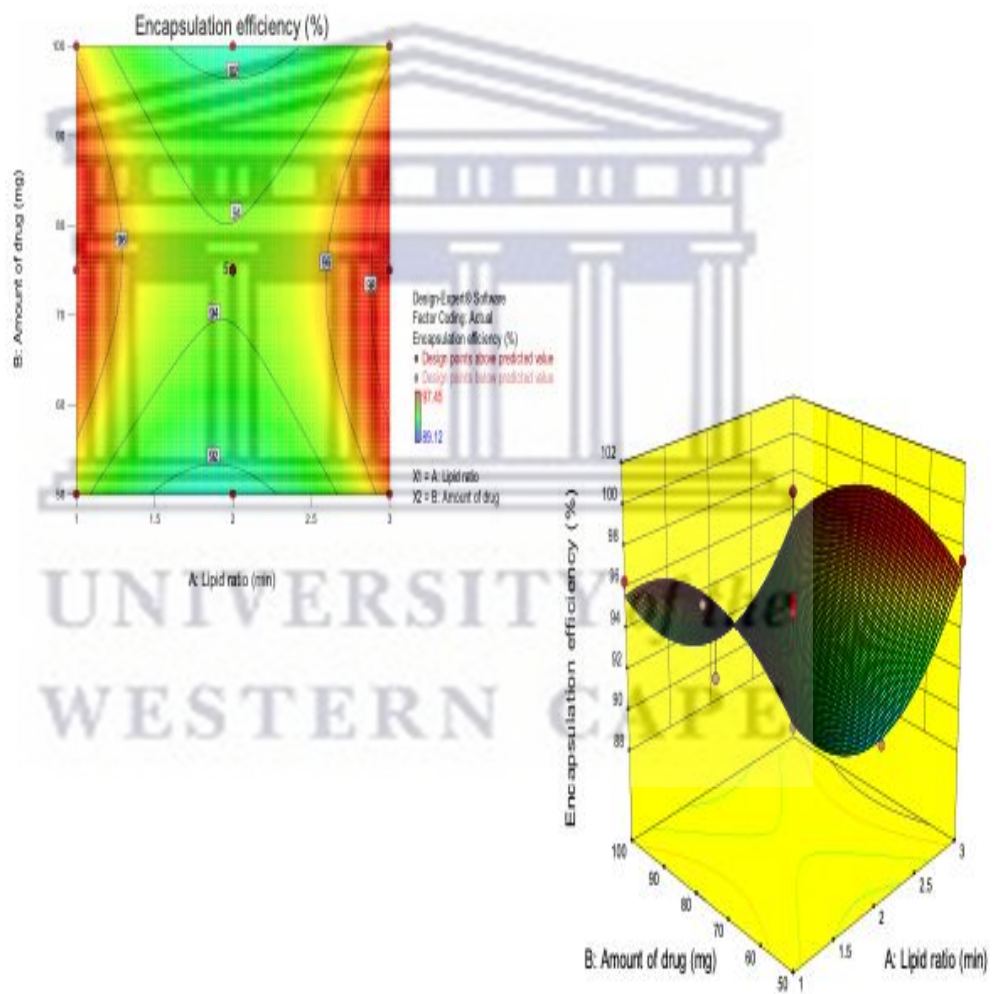


Figure 6.5. Surface plots showing the effect of lipid ratio and amount of drug variables on %EE of ABC in the liposomes formulations.

6.3.2 TEM analysis

The ABC-loaded liposomes structure was confirmed using TEM analysis. The TEM micrographs (Figure 6.6) were obtained at different magnifications. The result depicted the presence of liposomes vesicles with the appearance of the spherical shape of liposomes which is one of the major attributive properties of liposomes.

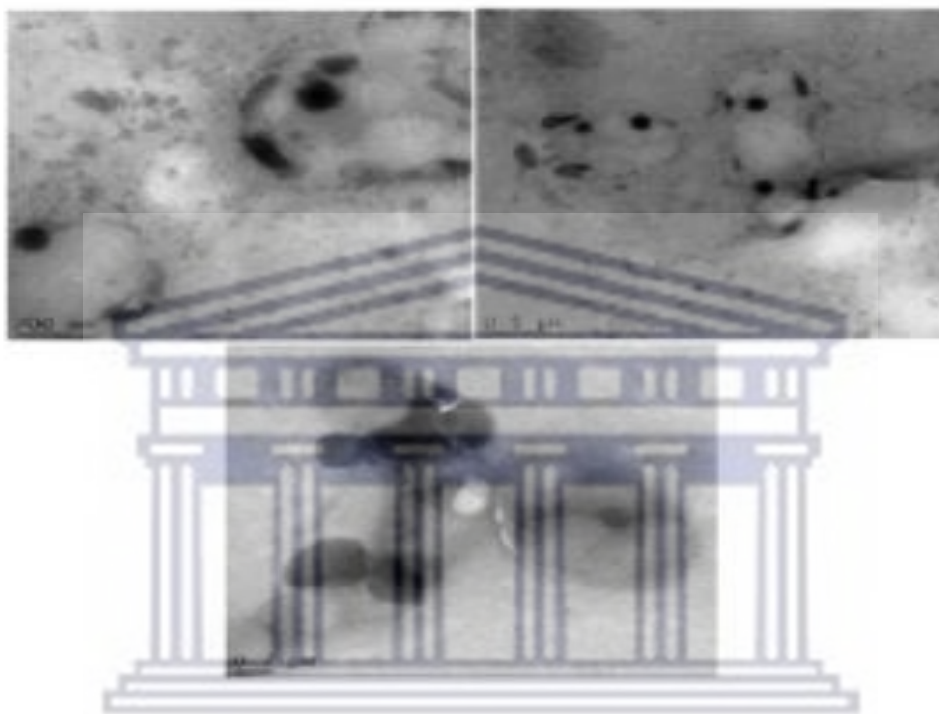


Figure 6.6. Unstained TEM micrographs of AL captured at different magnifications.

6.3.3. Thermal analyses

The DSC thermograms of the pure compounds (ABC, LEC, CHO), AL, and the control are shown in Figure 6.7. The DSC thermograms obtained with pure ABC and CHO showed single melting endotherms at 229.61 °C and 147.28 °C, respectively, confirming that both compounds exist in the crystalline state, correlating well with the melting behaviour previously reported for ABC and CHO in literature (Raffy and Teissié, 1999; Solaichamy and Karpagam, 2017). DSC analysis of LEC showed a glass transition temperature (T_g) at ≈ 187.17 °C, suggesting that LEC exists in the amorphous state. The control, which constituted a physical blend of the drug, LEC, and CHO in a 1: 1: 1 weight ratio, presented a small melting peak at 145.26 °C for CHO and an even smaller melting event at 223.43 °C for ABC. The almost undetectable melting points of these two compounds indicated the miscibility of the three compounds during melting. The DSC thermogram of AL depicted a broad and indistinct melting endotherm at 179.59 °C. This is ≈ 50 °C lower than that observed for pure ABC. This negative shift in the

melting temperature could be assigned to the melting of both CHO and ABC and may be attributed to a strong hydrophobic interaction between the drug and the lipid molecules, causing a change in the physical state of the drug-loaded carrier, as has been previously reported (Ramana *et al.*, 2010).

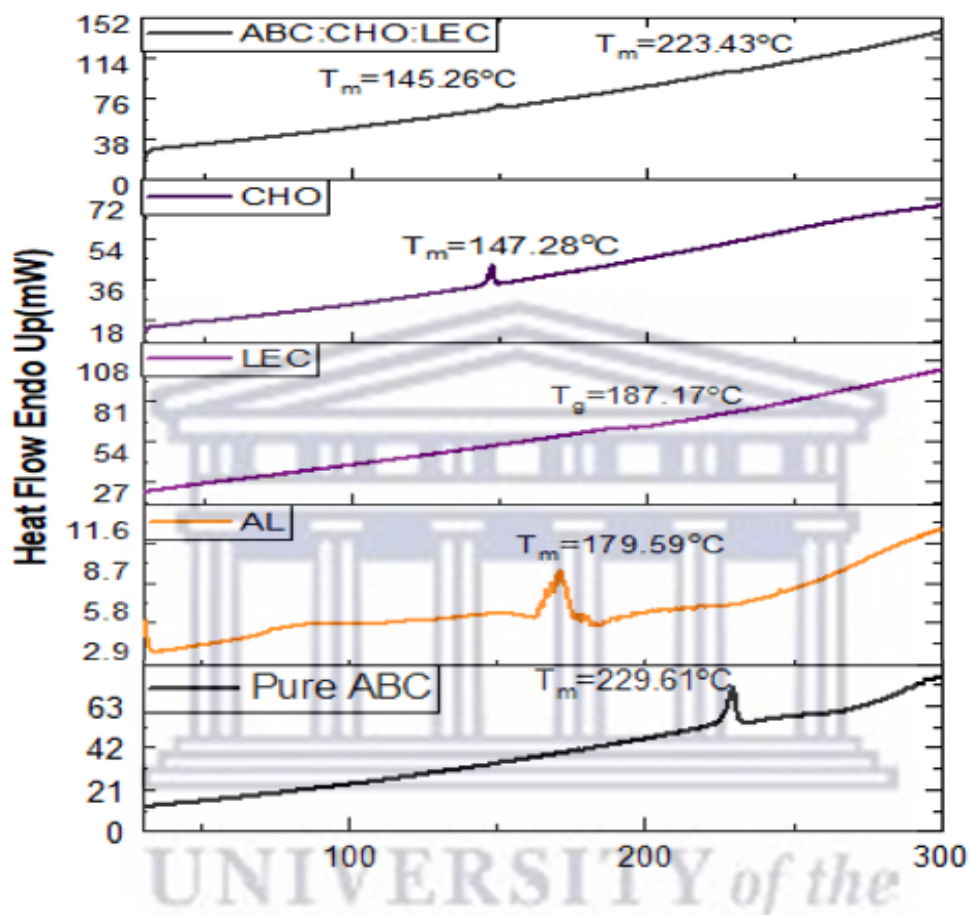


Figure 6.7. DSC thermograms obtained with ABC, AL, LEC, CHO, and the control.

The physical and chemical changes for the pure compounds (ABC, LEC, CHO), AL, and the control as a function of temperature were measured by TGA. An overlay of all thermogravimetric traces is presented in Figure 6.8. TGA of pure ABC showed an initial weight loss of 24.68% at 83.05 °C, assigned to the evaporation of water on the surface of the sample. Further weight loss was observed at 241.34 °C and 299.27 °C, resulting in a total of 65% weight loss. The TGA curve of LEC showed a total weight loss of 76.87% between the temperatures of 269.02 °C and 439.25 °C. The TGA curve of CHO depicted a one-step degradation signified by almost a 100% weight loss between the temperature of 279.45 °C and 358.43 °C. TGA of the control showed an onset of degradation at 229.66 °C and resulted in a total weight loss of 71.30%. Since the observed onset of degradation of the control was not lower than that observed with pure ABC, LEC, or CHO it can be deduced that the three

compounds are compatible with one another and that the mere physical mixture of the three compounds with one another did not result in any significant interaction which could lead to incompatibility. The TGA trace of AL showed loss in weight at 125.58 °C amounting to 17.28% and may be due to the evaporation of the surface water while showing a total loss in weight of 65.32% at 189.65 °C and 300.33 °C, respectively. The TGA curve of the control, a physical blend of the pure drug and the excipients presented a 71.30% weight loss between the temperature range of 229.66 °C to 411.28 °C.

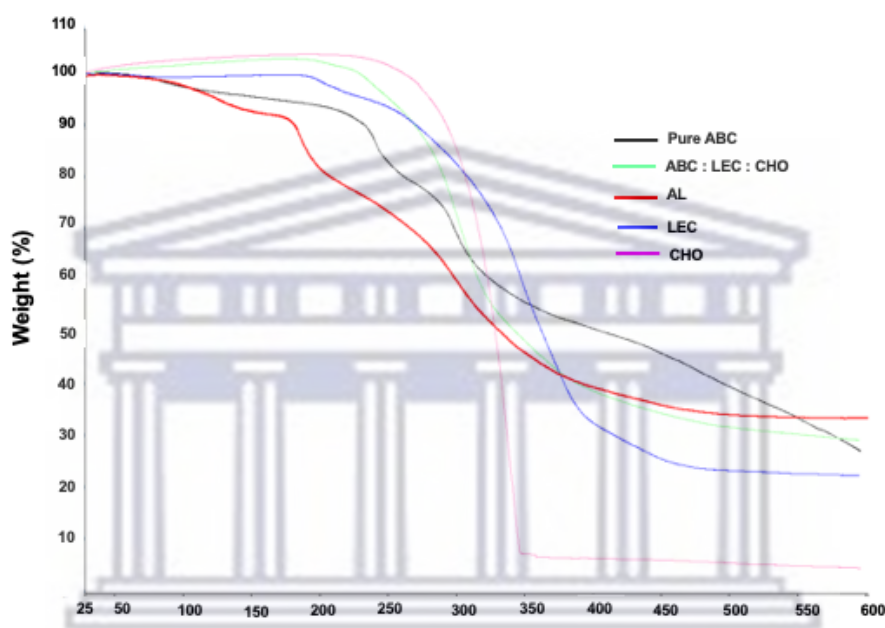


Figure 6.8. TGA curves for pure compounds (ABC, LEC, CHO), AL, and the control sample.

6.3.4. Spectroscopic and morphological analyses

FTIR results for the pure compounds (ABC, LEC, CHO), AL, and the control are presented in Figure 6.9. Pure ABC, LEC, and CHO depicted respective characteristic functional groups in the absorption regions as previously reported (Nzai and Proctor, 1999; Gupta *et al.*, 2014; Ghosal *et al.*, 2016). The FTIR spectrum for AL revealed the disappearance of most of the ABC characteristic functional groups, including the alcohol, alkene, and amine functional groups, while depicting a broad absorption peak of the lipids; hence this could be explained that the drug was dispersed molecularly within the liposome's formulation. The absence of new bands or functional groups suggests that no chemical interactions or new linkages were formed; hence efficient drug unloading at the anticipated site is expected. The control confirmed the presence of ABC while presenting the known functional groups attributed to ABC, although

associated with limited functional groups and could thus indicate the presence of the drug on the surface of the lipid, thereby signalling the non-encapsulation of the drug, unlike in the AL.

The powder X-ray diffraction patterns for the pure drug, LEC, CHO, AL, and the control are shown in Figure 6.10. The result displays intense characteristic peaks for ABC and CHO, thereby indicating their crystallinity with less intense and depleting diffraction peaks for the control therefore, supporting the miscibility of the compounds signified by the disappearance of the endothermic peak obtained during DSC analysis (Figure 6.7). LEC and AL are amorphous with no identification of any form of peaks as obtained from the diffraction patterns.

The morphology of the pure compounds (ABC, LEC, CHO), AL and the control were further assessed using SEM. The SEM images (Figure 6.11) exhibited irregular and block-like shapes for ABC with CHO and LEC showing smooth surface morphology and no typical particle shape which could be assigned to these two excipients. The SEM micrographs obtained for AL presented a smooth irregular morphology or shapes of rods and sphere for the drug loaded liposomes which are different from the morphology obtained for the pure drug indicating complete encapsulation of the drug in liposomes. The control further depicted irregular shapes on the surface morphology and a formation of clusters that signifies a spheroidal morphology suggesting the presence of the different excipients and the drug.



UNIVERSITY *of the*
WESTERN CAPE

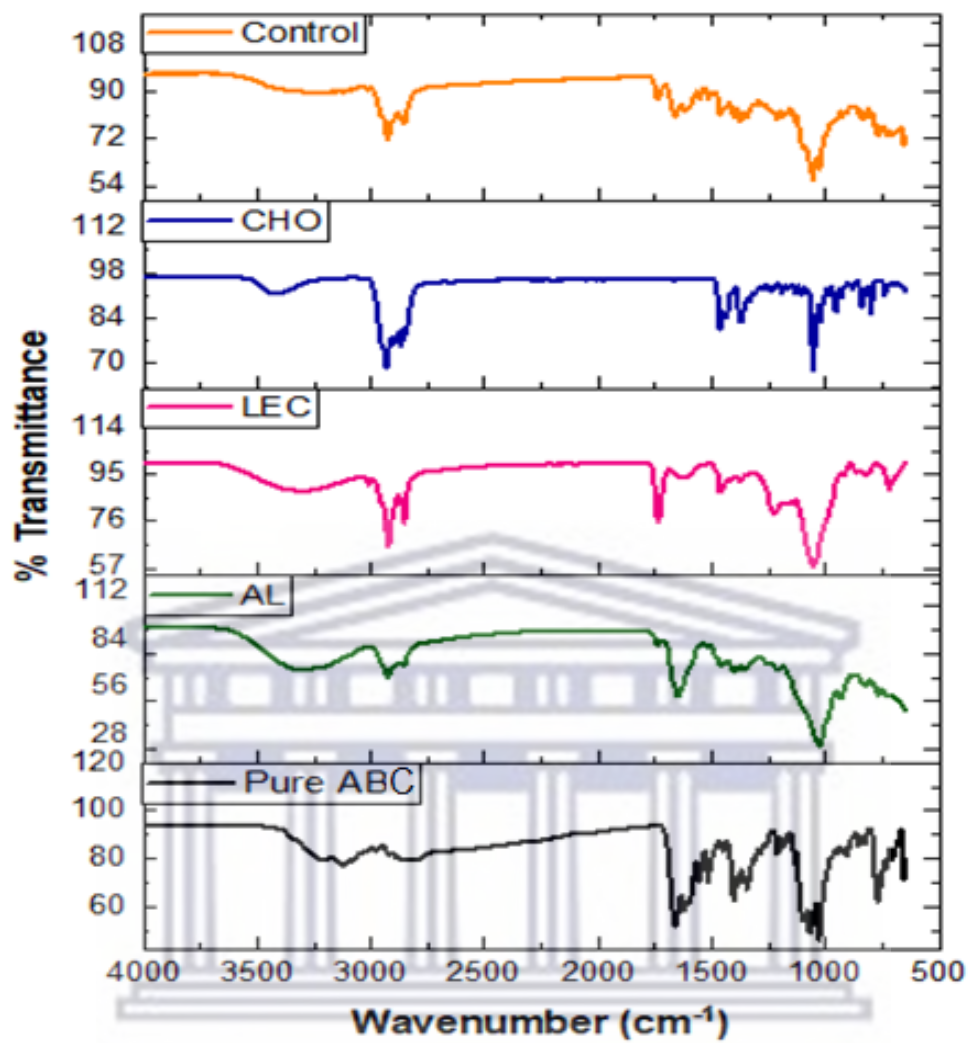


Figure 6.9. Overlay of the FTIR spectra obtained for pure ABC, AL, LEC, CHO, and the control.

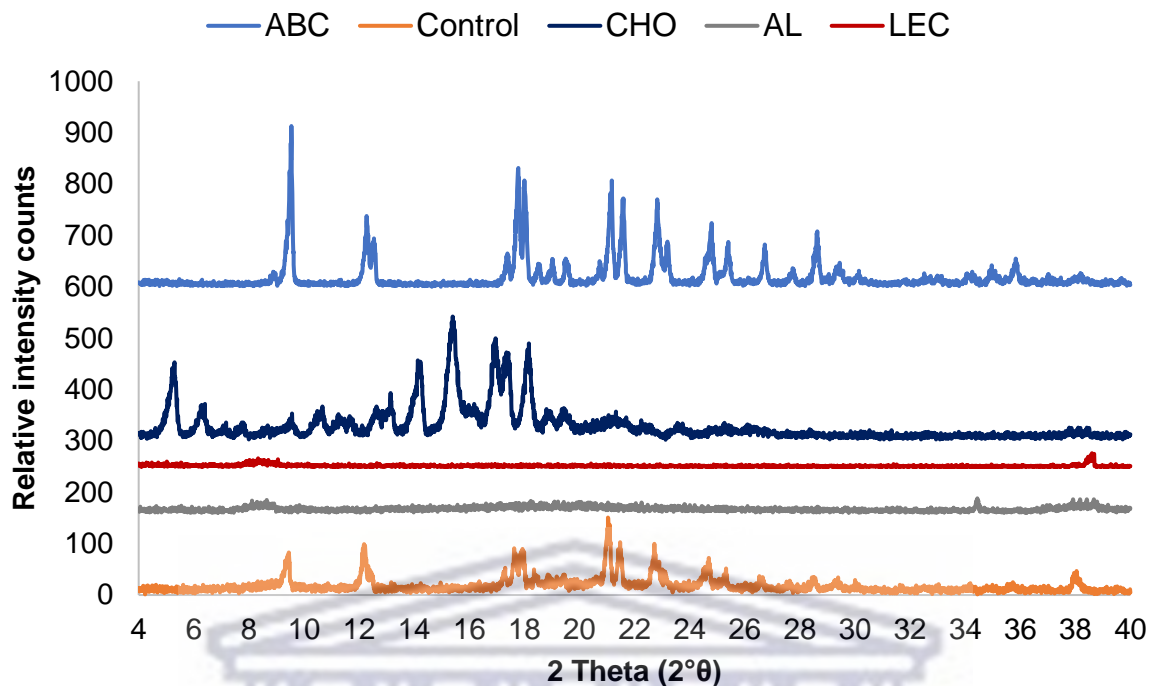


Figure 6.10. Overlay of the PXRD patterns obtained for ABC, AL, LEC, CHO, and the control.

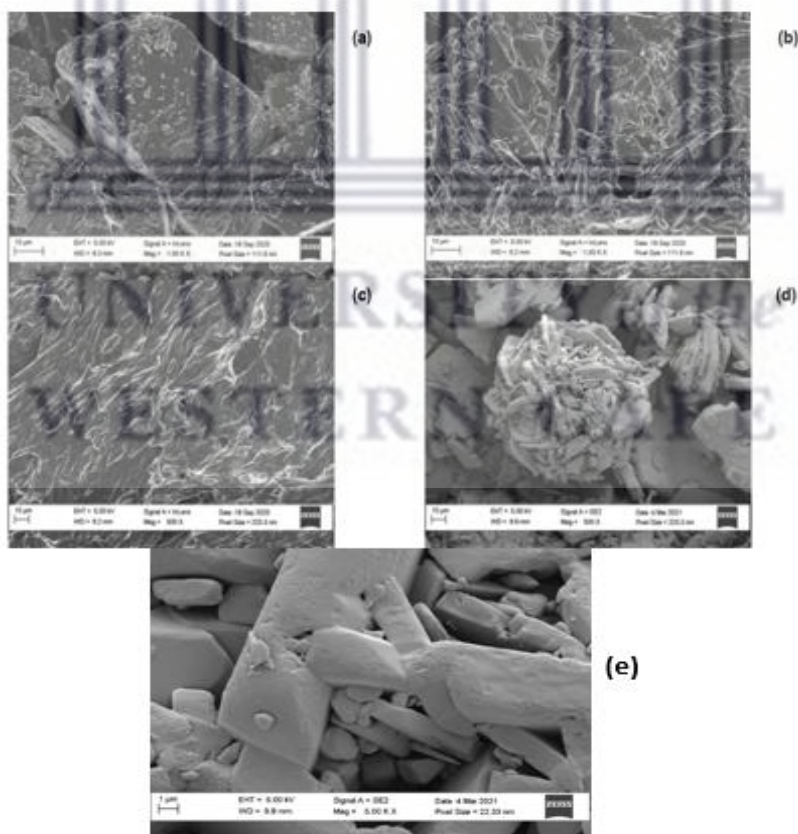


Figure 6.11. SEM micrographs obtained for (a) ABC, (b) CHO, (c) LEC, (d) control and (e) freeze-dried AL.

6.3.5. Equilibrium solubility

Equilibrium solubility evaluation of the pure drug (ABC), drug-loaded liposomes (AL), and the physical mixture of ABC: LEC: CHO is depicted in Figure 6.12. The results revealed a high solubility of ABC in all the different pH buffered media; however, the solubility of ABC was more pronounced in the ABC entrapped in liposomes in all the pH media, ranging from 289.17 – 317.17 mg/ml. ABC is a highly soluble ARV, the enhanced solubility of the drug in the formulated liposomes could be assigned to the solubilizing effect of the liposomes with the tendency of the liposomes delivery system to entrap both the hydrophilic and hydrophobic drugs, hence high amount of ABC is said to be entrapped in the aqueous core an indication of the formation of liposomes of smaller particle sizes.

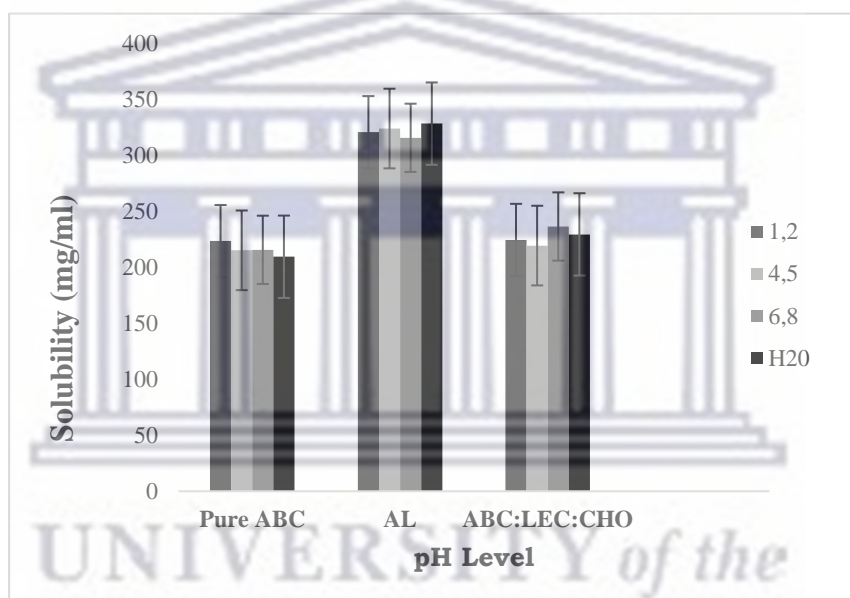


Figure 6.12. Equilibrium solubility of pure ABC, AL, and ABC physical mixture with excipients.

6.3.6. Drug release studies

The release data for pure ABC and AL conducted in different pH media over 30 minutes are depicted in Figure 6.13. ABC is a highly water-soluble ARV and therefore fast and almost complete dissolution thereof is expected. It was however pertinent to investigate how the encapsulation of ABC in a liposomes drug delivery system will affect the drug release. The drug release was investigated in pH 1.2 since the potential could exist to incorporate the Als into an oral solid dosage form. The drug release rate of AL was also investigated in pH 6.8 which is the typical pH of the mouth cavity, to provide more information on how fast ABC

would be released if incorporated into a sublingual or buccal dosage form. By plotting the drug released concentrations over time, focussing just on the data obtained within the first minute, it was observed that the liposomes system released ABC at a faster rate in pH 1.2 in comparison to the rate observed for pure ABC in the same dissolution medium. The rate of dissolution was very similar for pure ABC in pH 1.2 and pH 6.8, but the most noticeable difference was the slower dissolution rate of ABC from the liposomes system in pH 6.8. It was also noted that after 30 minutes the ABC-loaded liposomes did not release all the ABC, thus suggesting that this system could have a prolonged drug release ability.

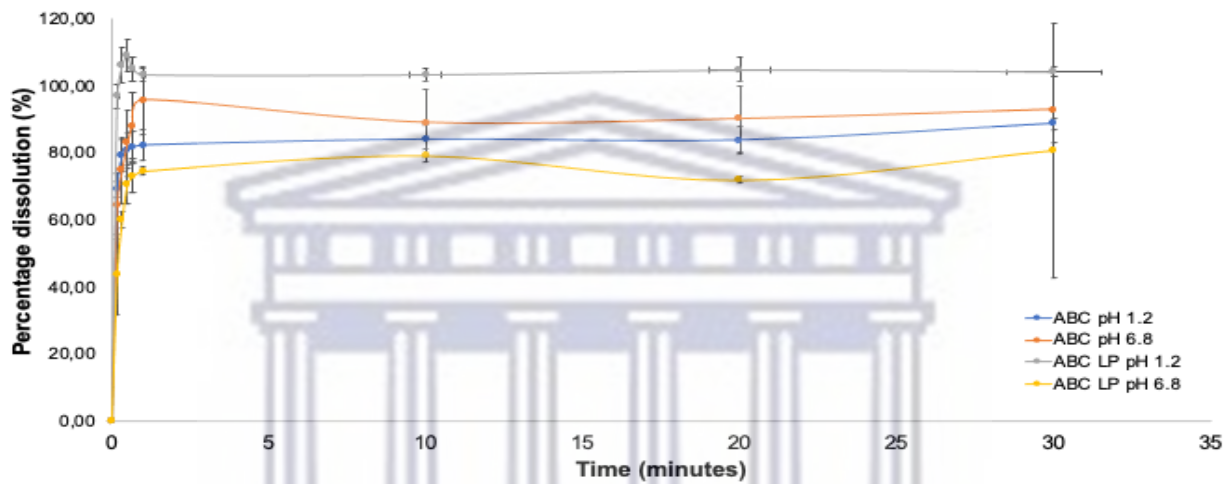


Figure 6.13. ABC release rate of pure ABC, in comparison with the release rate of ABC from the formulated liposomes in aqueous buffered pH 1.2 and 6.8 media

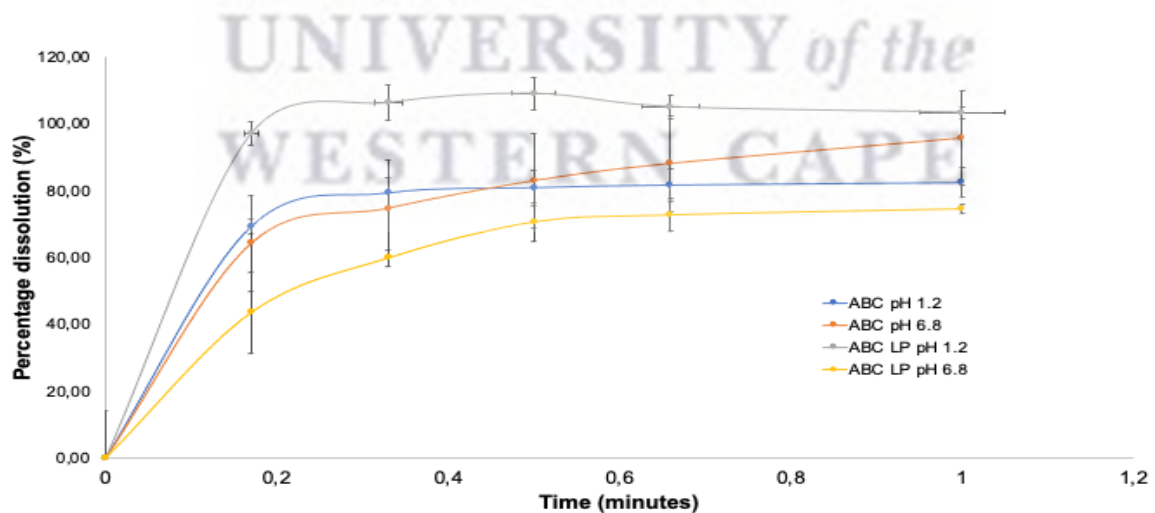


Figure 6.14. ABC release rate of pure ABC, in comparison with the release rate of ABC from the formulated liposomes in aqueous buffered pH 1.2 and 6.8 media in the dissolution time frame of 10 seconds to 1 minute.

6.3.7. Discussion on ABC-loaded liposomes

This part of the study investigated the encapsulation of ABC into a liposomal structure using the well-known thin-film hydration method. Physicochemical characterization of the liposomes indicated that liposomes were successfully formulated and that these structures exhibited particle sizes within the microparticles range, with overall uniform PS. The encapsulation process proved to be effective signified by a high %EE. The physicochemical characterization of AL showed that ABC exists in the amorphous state in the liposomal structure. This was deduced from DSC and PXRD results. The equilibrium solubility study (maximum solubility obtained over a 24-hour period) of AL carried out in different pH-buffered media exhibited an enhanced ABC solubility when entrapped in liposomes compared to the equilibrium solubility of the pure drug and the physical mixture of the drug with the excipients. This shows that the encapsulation of ABC in liposomes structure was highly effective with the liposomes containing a high drug load. Considering the significant increase in aqueous solubility of liposomes encapsulated ABC, it could be hypothesised that the oral drug dose could be reduced drastically. Such a reduction could lead to less of the AL needed in the dosage form formulation which could ultimately lead to the formulation of physically smaller tablets or a reduction in the dose volume of a liquid dosage form. Although this would be considered not essential for adult dosage forms such a dose reduction could potentially have a positive effect on the formulation of child-friendly dosage forms. To supplement this, the entrapment of ABC within the liposomes showed an improved drug release profile in pH 1.2 aqueous buffered medium, an aspect which could further strengthen the hypothesis of an ABC dose reduction. This hypothesis must however be supplemented with ABC permeability studies and pharmacokinetic studies.

6.4. Microencapsulation of ABC via spray drying

As already discussed in previous chapters, the spray drying technique is widely used in the pharmaceutical industry, especially in the research and development of novel drug delivery systems and improved drug delivery strategies (Stulzer *et al.*, 2009; M.N. *et al.*, 2010; Hoang Thi *et al.*, 2012; Tshweu *et al.*, 2014). Although evidence exists on the application of PPI and IN as wall forming agents in spray drying processes, most of these reports are in food sciences (Sun-Waterhouse, Wadhwa and Waterhouse, 2013; Bajaj, Tang and Sablani, 2015). At the time of writing this thesis, there are little or no literature reports that specifically studied the application of PPI and IN as wall formers or micro-encapsulants in the microencapsulation of

drugs using the method of spray drying. Therefore, this was found to be a novel approach that could provide interesting findings and broaden the current knowledge base.

For effective spray drying the most important aspect to consider is the feed preparation. To obtain effective particle formation and subsequently encapsulation it is important to either have all ingredients (drug and excipients) solubilised in a suitable solvent or to at least have a well homogenised suspension. ABC is a highly soluble ARV but for the sake of effective drug loading a solvent that would result in the highest solubility thereof was necessary. The decision to use distilled water buffered at pH 6.8 originated from equilibrium studies conducted using pure ABC and was reported in Figure 6.12. The spray drying process is clearly described in Chapter 4, paragraph 4.8.

After spray drying of ABC:IN: PPI (SD-ABC), the samples were collected, the percentage yield (62.4%), drug loading (73.4%) were calculated as shown in equation 4.9 and 4.10 followed by a thorough physicochemical characterization of the spray dried sample. To aid comparison ABC, PPI, IN and a control sample (physical mixture which consisted of ABC: PPI:IN) was included in the physicochemical characterization process.

6.4.1. Thermal analyses

The DSC thermogram of pure drug (ABC), PPI, IN, SD-ABC, and the control is depicted in Figure 6.15. The DSC result showed a sharp endothermic peak at 229.61 °C for pure ABC sulphate indicating the crystalline nature of the drug (Chadha *et al.*, 2011; Qwane, Mdluli and Madikizela, 2020). SD-ABC revealed no form of melting thereby suggesting an amorphous state of SD-ABC whilst showing a glass transition temperature (T_g) around 193.23 °C. Similarly, PPI and IN revealed no presence of a melting peak rather IN degraded around 237.34 °C. The control depicted melting of ABC in the physical mixture but with a decrease in the melting temperature which was witnessed around 187.57 °C, approximately 42 °C lower than that of pure ABC, hence indicating the drug interaction with the excipients and therefore potential miscibility of the drug and excipients.

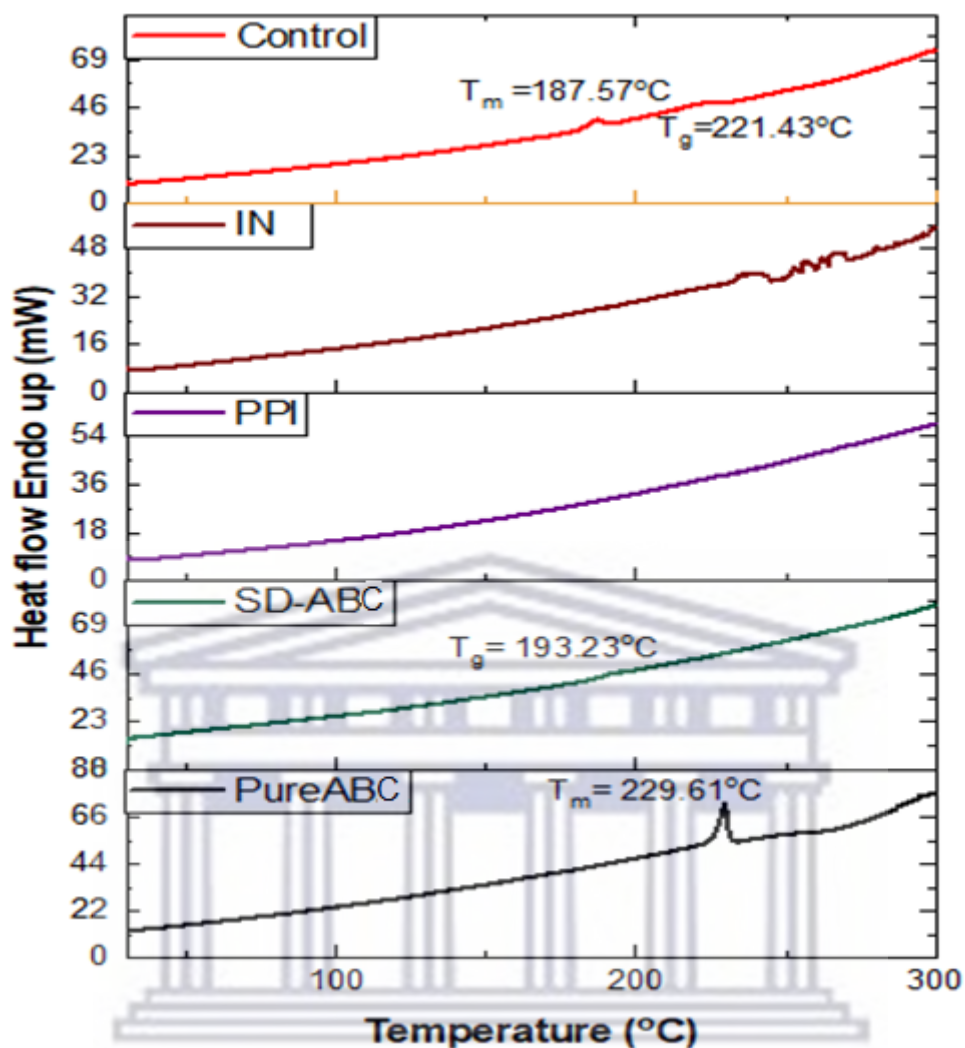


Figure 6.15. DSC thermogram of pure ABC, SD-ABC, PPI, IN, and control.

The result from TGA analysis of pure ABC, SD-ABC, PPI, IN and the control is presented in Figure 6.16. The TGA curve of ABC revealed an initial loss around 83.05 °C and could be attributed to evaporation of water on the surface with a total percentage loss of 65% calculated across the heating range of 25 – 600 °C. SD-ABC showed onset of decomposition at 192.56 °C revealing a total mass loss of 52.05%. The TGA trace obtained for pure PPI showed onset of decomposition at 240.91 °C with a total weight loss of 72.54%, within the tested temperature range. For IN, onset of thermal decomposition was observed at 250.50 °C with a total weight percentage loss of 83.01% across the tested temperature range. Analysis of control (ABC: PPI: IN), showed onset of degradation around 193.46 °C similar to that observed with ABC. This was a significant observation although the melting temperature of ABC was noted to be much lower in the control sample (Figure 6.15) the same degradation profile provided evidence that

the lower melting temperature was due to possible drug: excipient miscibility and not incompatibility which shifted the temperature towards the lower region.

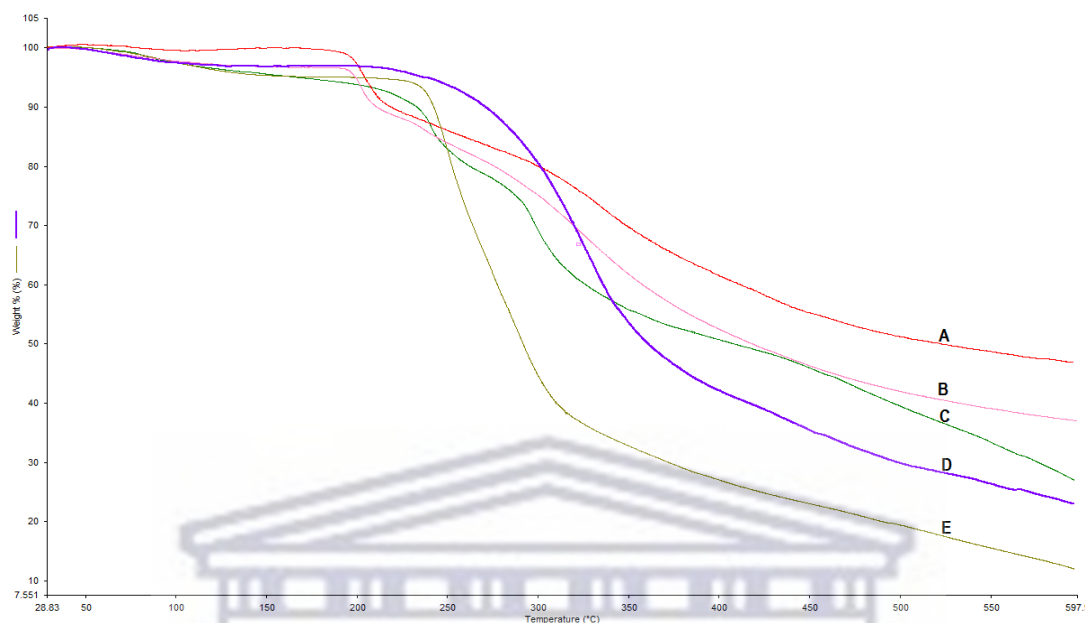


Figure 6.16. TGA curves for (A)SD-ABC, (B) control, (C) pure ABC, (D) PPI, I IN.

Data obtained from FTIR analysis and associated spectra of pure ABC, SD-ABC, PPI, IN and the control is depicted in Figure 6.17 and Table 6.8, respectively. ABC depicted all characteristic functional groups such as the hydroxyl and amine functional groups (Singh *et al.*, 2016; Terzopoulou *et al.*, 2016). SD-ABC showed a broadened peak with the disappearance of ABC associated peaks hence it could be deduced that ABC is dispersed within the spray dried particles thereby suggesting possible formation of an amorphous solid dispersions. PPI and IN revealed their respective characteristic functional groups especially the appearance of the amide and $\beta_2 \rightarrow 1$ glycosidic acid bonds respectively (Sun-Waterhouse, Wadhwa and Waterhouse, 2013; Bajaj, Tang and Sablani, 2015). The control depicted similar functional groups to the pure ABC therefore indicating no form of chemical interactions between the drug and excipients through mere physical mixing.

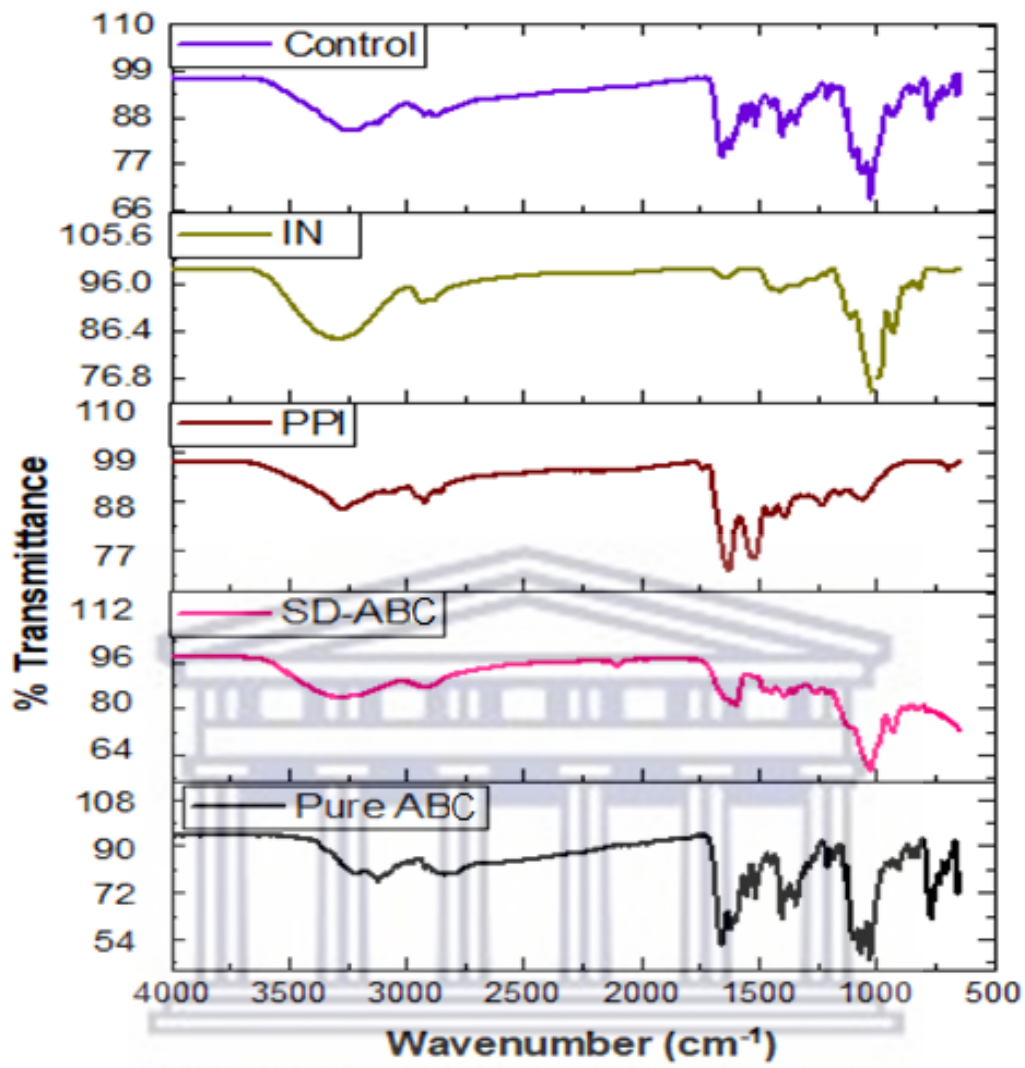


Figure 6.17. FTIR spectra of pure ABC, SD-ABC, PPI, IN and control.

UNIVERSITY of the
WESTERN CAPE

Table 6.8: FTIR spectra for pure ABC, SD-ABC, PPI, IN

Sample	Absorption band (cm ⁻¹)	Functional groups
Pure ABC	3123	O-H vibration
	2857	C-H
	1661	C=C
	1556	N-H
	1518, 1425	C-C
	1101, 1070, 1028	N-H
	825, 760	C-H
SD-ABC	3267	O-H
	2822	C-H
	1598	N-H, C-N amide II,
	1450	C-O-C
	1351, 1395	N-H, C-N amide III
	1027, 933, 822	N-H C-H
PPI	3274	O-H
	2925	C-H
	1630	C=O amide I
	1528	N-H, C-N amide II
	1393	N-H, C-N amide III
	1234	C-O-C symmetric
	1099	C-O
IN	3286	O-H
	2931	-CH ₂
	1641	C=C
	1417	O-H
	1018	C-O-C
	930	β ₂ →1 glycosidic acid

6.4.2. Morphology and habit of SD-ABC

Figure 6.18 exhibits the surface morphology of pure ABC, SD-ABC, PPI, IN and the control (physical mixture) observed using SEM analysis. The obtained micrographs for pure ABC clearly depicts an irregular shape with a fine flat, rod or block-like shaped morphology. The morphology of the SD-ABC showed spherical shape surface morphology with a smoother, more uniform surface and a sharp pinhole within the surface hence they are not coalesced. Such surface morphology was not observed with the pure drug thereby signalling a complete encapsulation and coating of the drug within the shell materials. PPI demonstrated a form of quatrefoil shape or a loose balloon surface morphology while IN showed a smooth spherical shape with a ready to burst surface morphology. The control revealed the presence of the drug identified from the rod- or block-like morphology on the surface hence confirming that the drug wasn't encapsulated unlike the SD-ABC where the drug was completely entrapped within

the sprayed powder whilst showing the presence of quatrefoil and smooth spherical shapes attributed to PPI and IN.

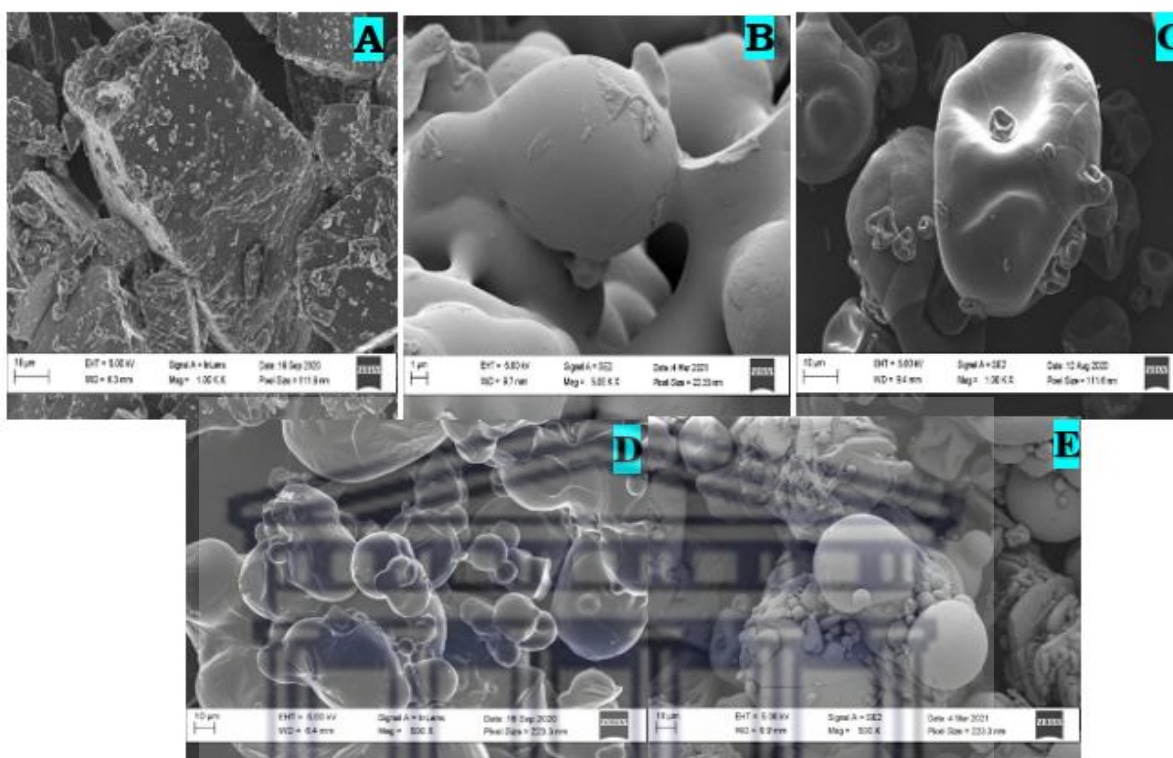


Figure 6.18. SEM images of (A) Pure ABC (B) SD-ABC (C) PPI, (D) IN, (E) control.

The PXRD data obtained for pure ABC, SD-ABC, PPI, IN, and the control to establish the crystalline or amorphous state of the drug and the excipients is presented in Figure 6.19. ABC demonstrated a crystalline form with the presence of the sharp peaks across the theta range. In the SD-ABC, PPI, and IN samples no traces of any peaks were found hence they are regarded as amorphous solids. The control also showed crystalline diffraction peaks which greatly corresponded with that obtained for ABC although with a decline in the intensity of the diffraction peaks which could be ascribed to less ABC being present in the physical mixture.

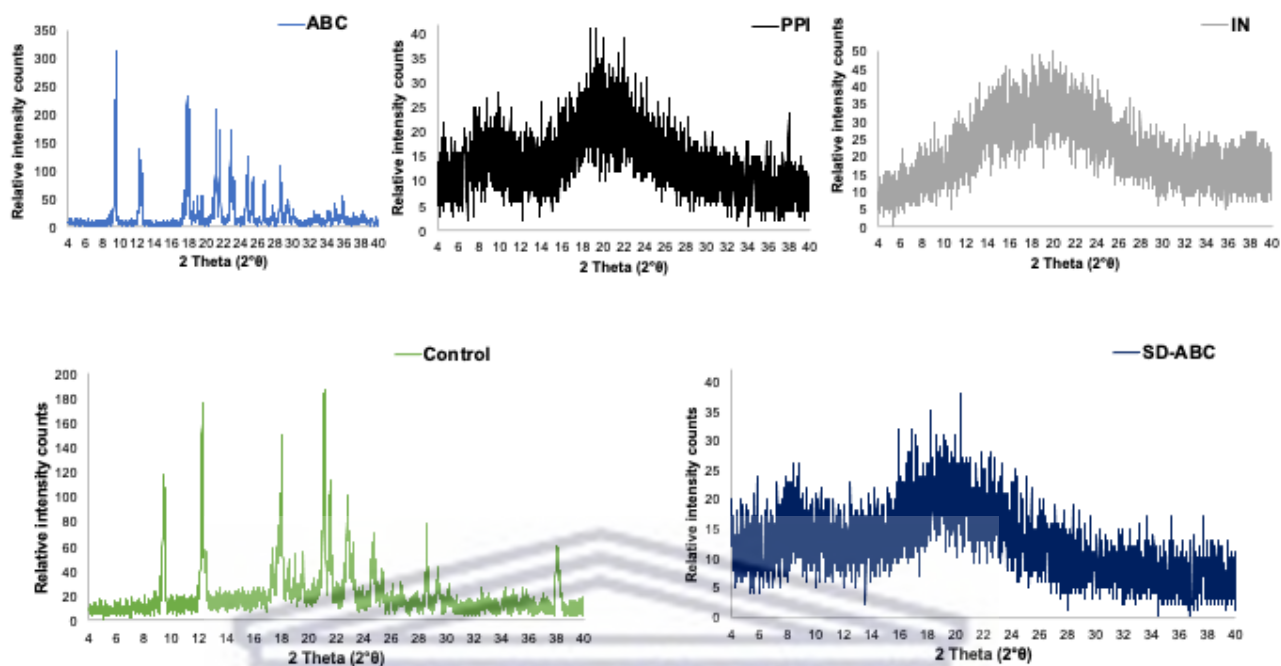


Figure 6.19. PXRD pattern of pure ABC, PPI, IN, SD-ABC, and control.

6.4.3. Equilibrium solubility studies

Equilibrium solubility of pure ABC, the physical mixture of ABC with PPI and IN and the SD-ABC is depicted in Figure 6.20. As mentioned, ABC is a highly water-soluble ARV. It is worthy to mention that SD-ABC and ABC physical mixture with PPI and IN showed increased solubility in all media used, with SD-ABC showing the highest solubility between 307.31 – 373.81 mg/ml. The high solubility of the SD-ABC could be assigned to the particle size reduction from the spray drying technique, but it is also apparent that the mere mixing of ABC with PPI and IN positively affected the aqueous solubility of the drug. Upon hydrolysis, proteins tend to unfold on the surface of water by exposing the hydrophilic or polar amino groups thereby causing an interaction with the aqueous medium which could possibly facilitate increased drug solubility.

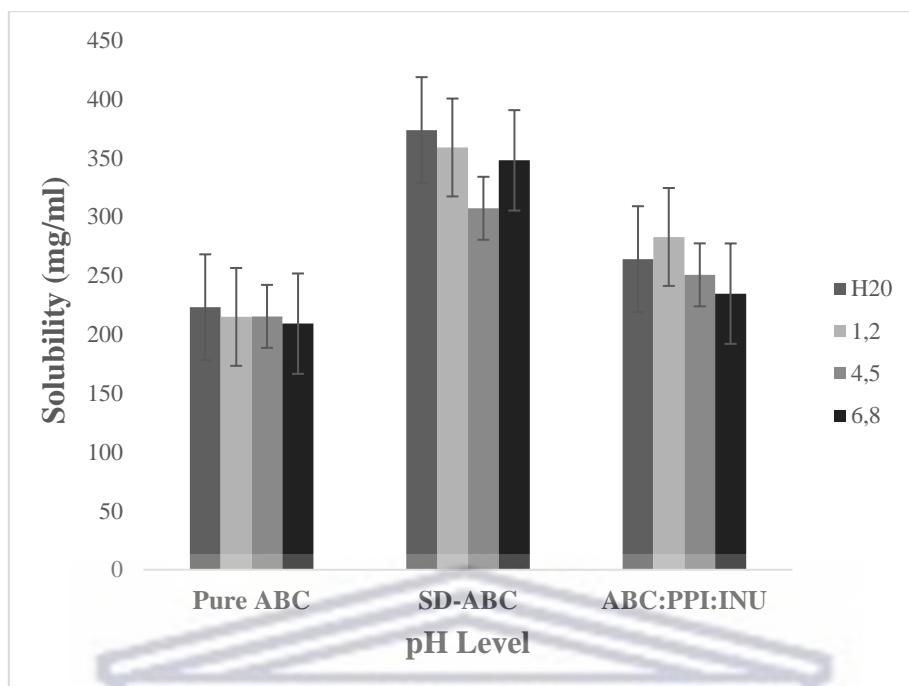


Figure 6.20. Equilibrium solubility profiles of Pure ABC, ABC physical mixture and SD-ABC.

6.4.4. Drug release studies

The release of ABC from the spray dried particles was investigated through dissolution studies conducted in pH 1.2 and 6.8 aqueous buffered media. From the dissolution studies the amorphous nature of ABC was confirmed from the very rapid dissolution rate (Figure 6.21). A significant advantage of the prepared amorphous solid dispersions is the fact that PPI and IN acts as stabilisers and thus allowing the supersaturated state to be maintained throughout a 30-minute dissolution test.

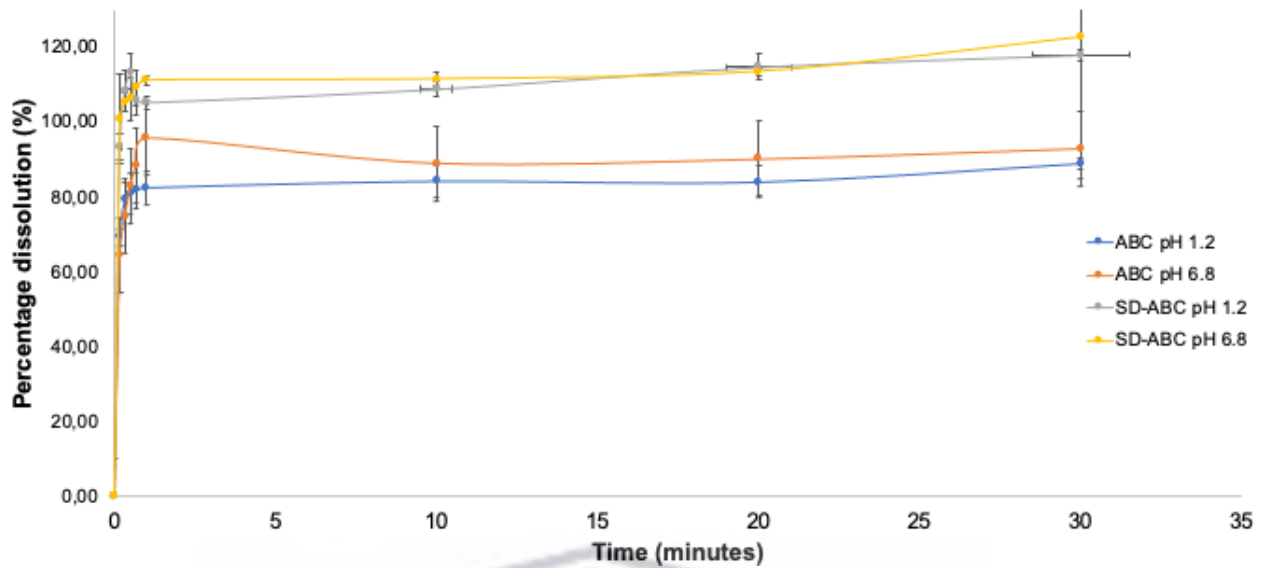


Figure 6.21. Drug release profiles of ABC encapsulated in PPI:IN in pH 1.2 and 6.8 buffered aqueous media at $37\text{ }^{\circ}\text{C} \pm 0.5\text{ }^{\circ}\text{C}$.

Figure 6.22 provides more insight on the ABC release during the first minute of the dissolution testing. The very rapid and complete drug release is evident from the graph and interestingly the dissolution profiles in pH 1.2 and 6.8 did not differ significantly from one another, being different from what was observed with AL (Figure 6.14).

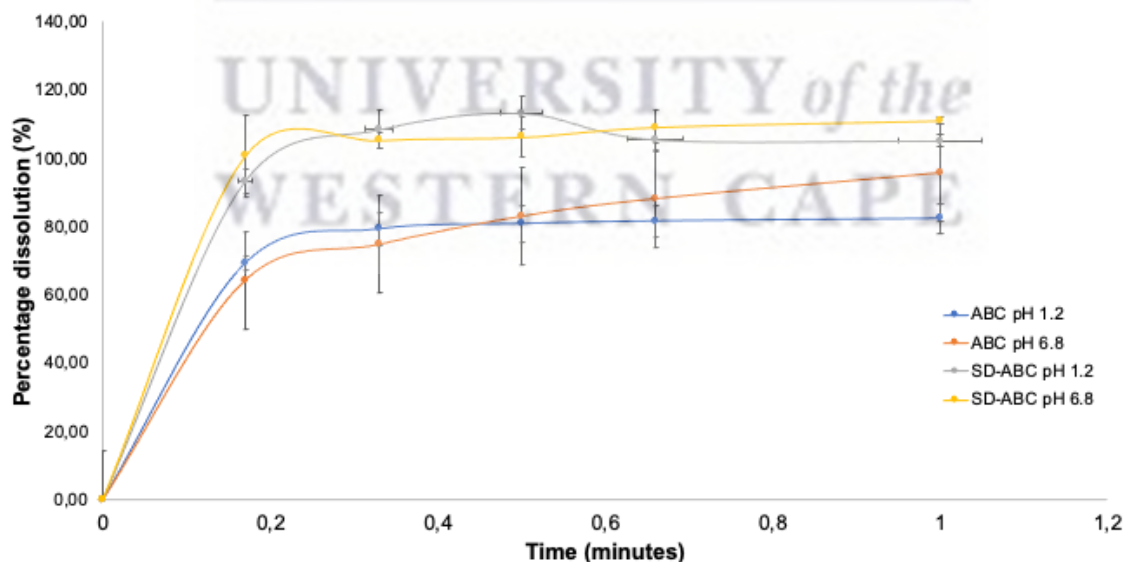
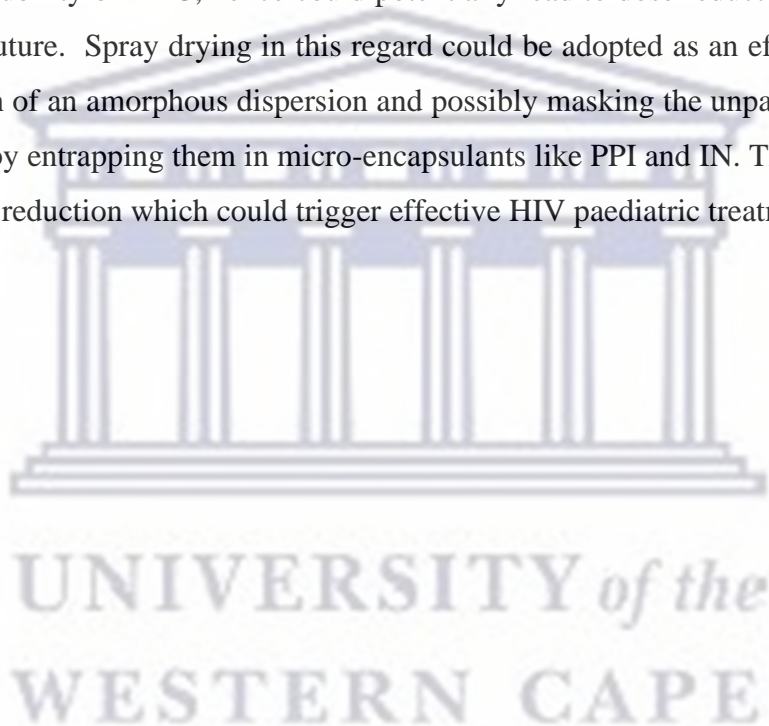


Figure 6.22. Drug release rate of ABC encapsulated in PPI:IN in pH 1.2 and 6.8 buffered aqueous media at $37\text{ }^{\circ}\text{C} \pm 0.5\text{ }^{\circ}\text{C}$, focussing only on the first minute of dissolution.

6.4.5. Discussion on the microencapsulation of ABC *via* spray drying

The physicochemical analyses of the spray dried microcapsule confirmed formation of an amorphous solid dispersions. Thermal analysis confirmed the thermal stability and miscibility of the combination of ABC with PPI and IN. SEM results revealed complete encapsulation of the drug within the microcapsule. This was confirmed through the different morphological structure or shapes obtained which showed the spray dried having complete different smooth and pinhole morphology from the pure drug. Although no particle size analysis was performed but was deduced from the scale of the SEM micrographs that the encapsulation processes resulted in particle size reduction. This in conjunction with the amorphous state significantly enhanced the solubility of ABC, hence could potentially lead to dose reduction amongst HIV children in the future. Spray drying in this regard could be adopted as an efficient technique for the formation of an amorphous dispersion and possibly masking the unpalatability taste of the ARV drugs by entrapping them in micro-encapsulants like PPI and IN. This would lead to potential dosage reduction which could trigger effective HIV paediatric treatment.



6.5. Conclusion

In conclusion, the aim to prepare an amorphous dispersion of ABC was successfully achieved through spray drying and liposomes encapsulation processes. Result indicated a huge increased percentage yield especially with spray dry technique and entrapment efficiency of the drug within the microparticles and liposomes respectively although liposomes depicted more than 90% EE when compared to over 70% drug loading obtained using spray drying. The physicochemical analyses of both the spray dried ABC microparticles and ABC-loaded liposomes, confirmed formation of an amorphous dispersion of ABC within the microparticles and liposomes respectively as deduced with DSC and PXRD followed by a complete encapsulation of the drug within the microcapsule and liposomes as confirmed by SEM with a spherical shape morphology when compared to block-like morphology of the pure drug. Entrapping of the drug in a liposomes and use of PPI and INU as micro-encapsulants and spray drying thereof resulted to a particle size reduction and was observed to significantly enhance the solubility and flowability of ABC. This could potentially lead to dose reduction amongst HIV children in the future. The release profile of the drug from liposomes and microparticles showed similar trend of release with a rapid and faster release rate in both pH 1.2 and pH 6.8 indicating an enhanced drug solubility and amorphous dispersion formation hence the release of the drug was not affected by the used coating materials. However, ABC-loaded liposomes did not release all the drug after 30 minutes, thus suggesting that this system could potentially have a prolonged drug release ability hence can further be modified for controlled for sustained and delayed release purpose in HIV paediatric treatment. Although these two encapsulation methods have depicted interesting results in the preparation of an ABC amorphous dispersion, however, spray drying technique has shown the potential to be adopted in the pharmaceutical industries due to its scalability as have been obtained from huge percentage yield in the preparation of the microparticles unlike the liposomes prepared using the thin film hydration method.

6.6. References

- Bajaj, P.R., Tang, J. and Sablani, S.S. (2015) 'Pea Protein Isolates : Novel Wall Materials for microencapsulating Flaxseed Oil', *Food and Bioprocess Technology*, 8(10).
- Bapolisi, A.M. (2020) 'Design, Formulation and Evaluation of Liposomes Co-loaded with Human Serum Albumin and Rifampicin', Rhodes University, South Africa, pp. 1–128.
- Bozzuto, G. and Molinari, A. (2015) 'Liposomes as nanomedical devices', *International Journal of Nanomedicine*, (10), pp. 975–999.
- Chadha, R. *et al.* (2011) 'Novel crystalline forms of abacavir sulfate: Preparation & characterization', *Journal of Pharmaceutical Education Research*, 2(2), pp. 1–8.
- Chiappetta, D.A. *et al.* (2010) 'Efavirenz - loaded polymeric micelles for pediatric anti-HIV pharmacotherapy with significant higher oral bioavailability', *Nanomedicine*, 5(1), pp. 11–23.
- Dirajlal-Fargo, S., Koay, W.L.A. and Rakhmanina, N. (2020) 'Pediatric antiretroviral therapy', in *Handbook of Experimental Pharmacology*, pp. 285–323.
- Ghosal, K. *et al.* (2016) 'Formulation Development, Physicochemical Characterization and *In Vitro-In Vivo* drug release of vaginal films', *Current HIV Research*, 14(4), pp. 295–306.
- Gupta, U. *et al.* (2014) 'Spectroscopic Studies of Cholesterol: Fourier Transform Infra-Red and Vibrational Frequency Analysis', *Materials Focus*, 3(3), pp. 211–217.
- Hoang Thi, T.H. *et al.* (2012) 'Development and evaluation of taste-masked drug for paediatric medicines - Application to acetaminophen', *International Journal of Pharmaceutics*, 434(2), pp. 235–242.
- Ivanovska, V. *et al.* (2014) 'Pediatric drug formulations: A review of challenges and progress', *Pediatrics*, 134(2), pp. 361–372.
- Kim, J. (2016) 'Liposomal drug delivery system', *Journal of Pharmaceutical Investigation*, 46(4), pp. 387–392.
- Ming Ong, S.G., Chiau Ming, I., Seng Lee, K., and Hay Yuen, K. (2016) 'Influence of the encapsulation efficiency and size of the liposomes on the oral bioavailability of Griseofulvin-loaded liposomes', *Pharmaceutics*, 5, 25; doi.3390/pharmaceutics8030025.
- Singh M.N. *et al.* (2010) 'Microencapsulation: A promising technique for controlled drug delivery', *Research in Pharmaceutical Sciences*, pp. 65–77.

- Nzai, J.M. and Proctor, A. (1999) 'Soy lecithin phospholipid determination by fourier transform infrared spectroscopy and the acid digest/arseno-molybdate method: A comparative study', *Journal of the American Oil Chemists' Society*, 76(1), pp. 61–66.
- Pattni, B.S., Chupin, V.V. and Torchilin, V.P. (2015) 'New Developments in Liposomal Drug Delivery', *Chemical Reviews*, 115(19), pp. 10938–10966.
- Penazzato, M. *et al.* (2019) 'Prioritising the most needed paediatric antiretroviral formulations: the PADO4 list', *The Lancet HIV*, 6(9), pp. 623–631.
- Pontali, E. *et al.* (2001) 'Adherence to combination antiretroviral treatment in children', *HIV Clinical Trials*, 2(6), pp. 466–473.
- Pontali, E. (2005) 'Facilitating adherence to highly active antiretroviral therapy in children with HIV infection: What are the issues and what can be done?', *Pediatric Drugs*, 7(3), pp. 137–149.
- Qwane, S.N., Mdluli, P.S. and Madikizela, L.M. (2020) 'Synthesis, Characterization and Application of a Molecularly Imprinted Polymer in Selective Adsorption of Abacavir from Polluted Water', *South African Journal of Chemistry*, (73), pp. 84–91.
- Raffy, S. and Teissié, J. (1999) 'Control of lipid membrane stability by cholesterol content', *Biophysical Journal*, 76(4), pp. 2072–2080.
- Ramana, L.N. *et al.* (2010) 'Development of a liposomal nanodelivery system for nevirapine', *Journal of Biomedical Science*, 17(1), pp. 1–9.
- Rushmi, Z.T. *et al.* (2017) 'The impact of formulation attributes and process parameters on black seed oil loaded liposomes and their performance in animal models of analgesia', *Saudi Pharmaceutical Journal*, 25(3), pp. 404–412.
- Ryan Phelps and Rakhmanina, N. (2011) 'Antiretroviral Drugs in Pediatric HIV-Infected Patients', *Pediatric Drugs*, 13(3), pp. 175–192.
- Schlatter, A.F., Deathe, A.R. and Vreeman, R.C. (2016) 'Review Article The Need for Pediatric Formulations to Treat Children with HIV', *AIDS Research and Treatment*, (16), pp. 1–8.
- Shah, C.A. (2007) 'Adherence to High Activity Antiretroviral Therapy (HAART) in pediatric patients infected with HIV: Issues and interventions', *Indian Journal of Pediatrics*, 74(1), pp. 55–60.

- Shashidhar, G.M. and Manohar, B. (2018) 'Nanocharacterization of liposomes for the encapsulation of water soluble compounds from *Cordyceps sinensis* CS1197 by a supercritical gas anti-solvent technique', *RSC Advances*, 8(60), pp. 34634–34649.
- Singh, D. *et al.* (2016) 'Development and characterization of a long-acting nanoformulated abacavir prodrug', *Nanomedicine*, 11(15), pp. 1913–1927.
- Solaichamy, R. and Karpagam, J. (2017) 'Molecular Structure, Vibrational Spectra and Docking Studies of Abacavir by Density Functional Theory', *International Letters of Chemistry, Physics and Astronomy*, (72), pp. 9–27.
- Sosnik, A., Chiappetta, D.A. and Carcaboso, Á.M. (2009) 'Drug delivery systems in HIV pharmacotherapy: What has been done and the challenges standing ahead', *Journal of Controlled Release*, 138(1), pp. 2–15.
- Stulzer, H.K. *et al.* (2009) 'Evaluation of cross-linked chitosan microparticles containing acyclovir obtained by spray-drying', *Materials Science and Engineering C*, 29(2), pp. 387–392.
- Sun-Waterhouse, D., Wadhwa, S.S. and Waterhouse, G.I.N. (2013) 'Spray-Drying Microencapsulation of Polyphenol Bioactives: A Comparative Study Using Different Natural Fibre Polymers as Encapsulants', *Food and Bioprocess Technology*, 6(9), pp. 2376–2388.
- Terzopoulou, Z. *et al.* (2016) 'Preparation of molecularly imprinted solid-phase microextraction fiber for the selective removal and extraction of the antiviral drug abacavir in environmental and biological matrices', *Analytica Chimica Acta*, 9(13), pp. 63–75.
- Tshweu, L. *et al.* (2014) 'Enhanced oral bioavailability of the antiretroviral efavirenz encapsulated in poly(epsilon-caprolactone) nanoparticles by a spray-drying method', *Nanomedicine*, 9(12), pp. 1821–1833.
- Walsh, J. *et al.* (2018) 'Patient acceptability, safety and access: A balancing act for selecting age-appropriate oral dosage forms for paediatric and geriatric populations', *International Journal of Pharmaceutics*, 536(2), pp. 547–562.
- Wang, Q. *et al.* (2019) 'Preparation and Pharmacokinetic Study of Daidzein Long-Circulating Liposomes', *Nanoscale Research Letters*, 14(14), pp. 321–348.

Chapter Seven

7. The encapsulation of AZT into liposomes and *via* spray drying

7.1 Introduction

Human immunodeficiency virus (HIV) is still one of the diseases rampaging the entire world with over 36.7 million people still currently affected with this virus while most of the people are located mainly in Sub-Saharan Africa. This includes more than 2 million children under the age of 15 years while showing the highest mortality rate hence they have become most risked, susceptible population which are heavily rampant in African region (Shah, 2007; Chiappetta *et al.*, 2010; Haberer and Mellins, 2010; AC, 2012; Reda and Biadgilign, 2012). Although the prevalence of HIV has reduced in recent years however, the number of new infections has been on serious rise (AIDs) deaths cases (Afe, Motunrayo and Ogungbade, 2018). The same therapeutic treatment given to adults which involves the highly antiretroviral therapy (HAART) is still the same treatment for HIV paediatric treatment. This treatment comprises of the combination of two or more antiretroviral drugs (ARVDs) hence they enhance HIV treatment by preventing viral replication while reducing virological and immunological loads (Afe, Motunrayo and Ogungbade, 2018). The treatment of children living with HIV involving the use of ARVDs has become irksome and highly complex. This is because almost all the ARV drugs are specifically designed for adults with fewer or no clinically approved paediatric ARV drugs or even liquid formulations thereby causing many children to receive unlicensed drugs globally every year (Davies *et al.*, 2008). This has promoted poor adherence among the children due to several factors such as the pill size and quantity which is the major cause of the difficulty in swallowing, constant and frequent administration of these multiple ARVDs. Many of these drug have shown poor solubility hence resulting in severe side effects among children, and poor drug palatability which is one of the criteria for paediatric formulations (Lin *et al.*, 2007; Shah, 2007; Davies *et al.*, 2008; Shahiwala, 2011; Schlatter, Deathe and Vreeman, 2016). An excellent adherence is achieved when the adherence level is 95% and more and have been witnessed majorly among HIV adults. However, this is not the case with the HIV paediatric patients where 50 to 70% adherence level have become impossible especially in the resource deprived nations (Laufs, Rettig-ewen and Bo, 2011; Lin *et al.*, 2011; Nichols, Steinmetz and Paintsil, 2017). This has become a major concern globally hence several nanotechnology approaches have been adopted in an attempt towards eradicating these factors associated with poor ARVD adherence in children. Nanotechnology approaches such

as use of polymer based matrixial nanostructure (Giaretta *et al.*, 2019), the design of paediatric novel granules in-situ self-assembly nanoparticles (Pham *et al.*, 2016), formation of improved sensory property nanostructure paediatric suspension (Prebianca *et al.*, 2020), formation of freeze-dried fast dissolving paediatric tablet (David Pittman 2018), taste masking of nanoparticles (Krieser *et al.*, 2020), development of monoolein based nanoparticles (Bianchin *et al.*, 2021), design of nanoparticle Oro-dispersible palatable paediatric formulation have all been studied. However, not many reports exist comparing the spray drying using PPI and INU as micro-encapsulants and liposomes encapsulation of AZT antiretroviral drug for HIV paediatric use. Therefore, this research has explored the spray drying and liposomes techniques in the microencapsulation of AZT with the aim of producing AZT microparticles as well as liposomes particles with the smallest particle size with improved solubility that could potentially result to reduced dose in HIV children in the future.

7.2. Formulation of AZT-loaded liposomes

7.2.1. Optimisation– Response Surface Methodology (RSM)

Design Expert 11 (State-Ease, Inc., Minneapolis, MN, USA) software was used for design of the experiment, regression and graphical analyses of the data obtained. With RSM, it is possible to evaluate the interactions of possible influencing parameters on treatment efficiency with a limited number of planned experiments. Lipid ratio and amount of drug are the variables used in the optimization of particle size (PS), polydispersity index (PDI), zeta potential (ZP) and encapsulation efficiency (%EE). Herein, the Box-Behnken design (BBD) was used to design the experiment and data obtained was modelled with it. The experimental design consisted of two variables with three levels i.e., low (-1), medium (0) and high (+1) giving 13 experimental runs. The levels and range of independent variables are shown in Table 7.1. During this optimisation phase, the data obtained from the 13 formulations was evaluated by multiple regression analysis and the second order polynomial equation fitted better between the responses (lipid ratio and amount of drug) and the input variables PS, PDI, ZP and %EE. The main effects and interactions between factors were determined as shown in the experimental design matrix by the BBD in Table 7.2.

Table 7.1: Levels and range of independent variables tested in 2³ Box 157Behnken design (BBD)

Factor	Low level (-1)	Medium level (0)	High level (+1)
Lipid ratio (LR)	1:1	1:2	1:3
Amount of drug (DA)	50 mg	75 mg	100 mg
Response	Unit		
Particle size	nm		
Polydispersity index			
Zeta potential	-Mv		
Encapsulation efficiency	%		

Table 7.2: Liposomes encapsulation of AZT using varying lipid ratios (LEC: CHO)

Formulation code	LEC: CHO mass ratio	Amount of drug (mg)
L1	1:1	75
L2	1:1	75
L3	1:2	100
L4	1:2	75
L5	1:1	75
L6	1:2	50
L7	1:1	75
L8	2:1	75
L9	1:1	50
L10	2:1	50
L11	1:1	100
L12	1:1	75
L13	2:1	100

7.2.2. Physicochemical characterization of AZT-loaded liposomes

7.2.2.1. PS, ZP, PDI and %EE

The PS, ZP and PDI results are shown in Table 7.3, Figure 7.1 and 7.2, respectively. The result demonstrated good PS within nano range (263.23 – 482.12 nm). It was observed that the mass of used LEC, CHO did not influence the PS significantly. Similar PS have been reported where they used egg phosphatidyl choline and dipalmitoyl phosphatidyl choline instead of crude soybean lecithin, although there was a slight increase in the PS we obtained using crude lecithin (Doijad *et al.*, 2009). The ZP was found to be very high and strongly negatively charged due to the electrostatic attraction or repulsion hence confirming a strong stability of the liposomes formulations that cannot be depleted by gastrointestinal or enzymatic attack. The PDI demonstrated values which are highly accepted for drug delivery with all showing less PDI values thereby confirming significant homogenized and well dispersed liposomes formulations with little, or no indication of aggregation expected.

Table 7.3: PS, ZP, PDI and %EE obtained during the RSM experiments.

Formulation	PS (nm)	PDI	ZP (-mV)	%EE
L1	263.23 ± 18.12	0.192 ± 0.04	-48.92 ± 1.29	95.28 ± 2.48
L2	470.16 ± 9.68	0.501 ± 0.02	-54.93 ± 1.06	98.05 ± 2.16
L3	475.14 ± 23.24	0.154 ± 0.03	-49.66 ± 1.36	93.71 ± 4.22
L4	482.12 ± 11.63	0.195 ± 0.01	-51.41 ± 1.14	92.86 ± 2.18
L5	404.74 ± 6.74	0.167 ± 0.09	-58.33 ± 1.04	97.07 ± 2.14
L6	243.47 ± 4.62	0.209 ± 0.06	-49.24 ± 1.18	94.92 ± 1.19
L7	326.16 ± 11.12	0.362 ± 0.05	-59.35 ± 2.04	96.57 ± 2.34
L8	323.26 ± 12.34	0.054 ± 0.05	-54.42 ± 1.07	90.23 ± 2.27
L9	302.67 ± 9.36	0.127 ± 0.04	-62.13 ± 1.16	96.91 ± 1.28
L10	804.21 ± 10.23	0.361 ± 0.04	-49.84 ± 1.21	96.61 ± 2.24
L11	662.72 ± 26.24	0.291 ± 0.03	-54.44 ± 1.06	96.14 ± 2.42
L12	584.24 ± 23.86	0.348 ± 0.02	-58.24 ± 1.17	92.62 ± 1.28
L13	516.72 ± 24.18	0.284 ± 0.01	-52.36 ± 1.04	95.04 ± 1.18

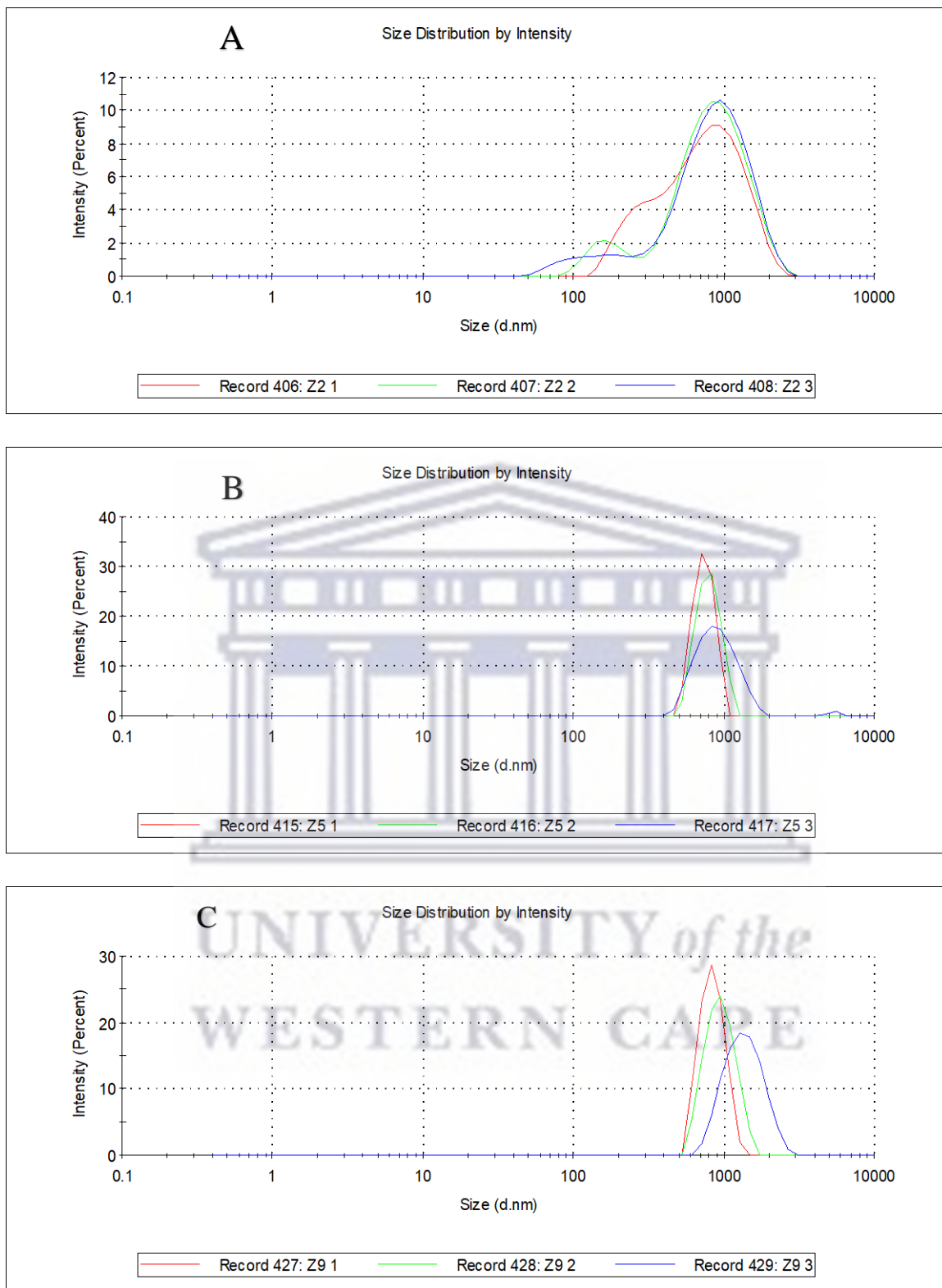


Figure 7.1. Different dispersed particle sizes of AZT-L.

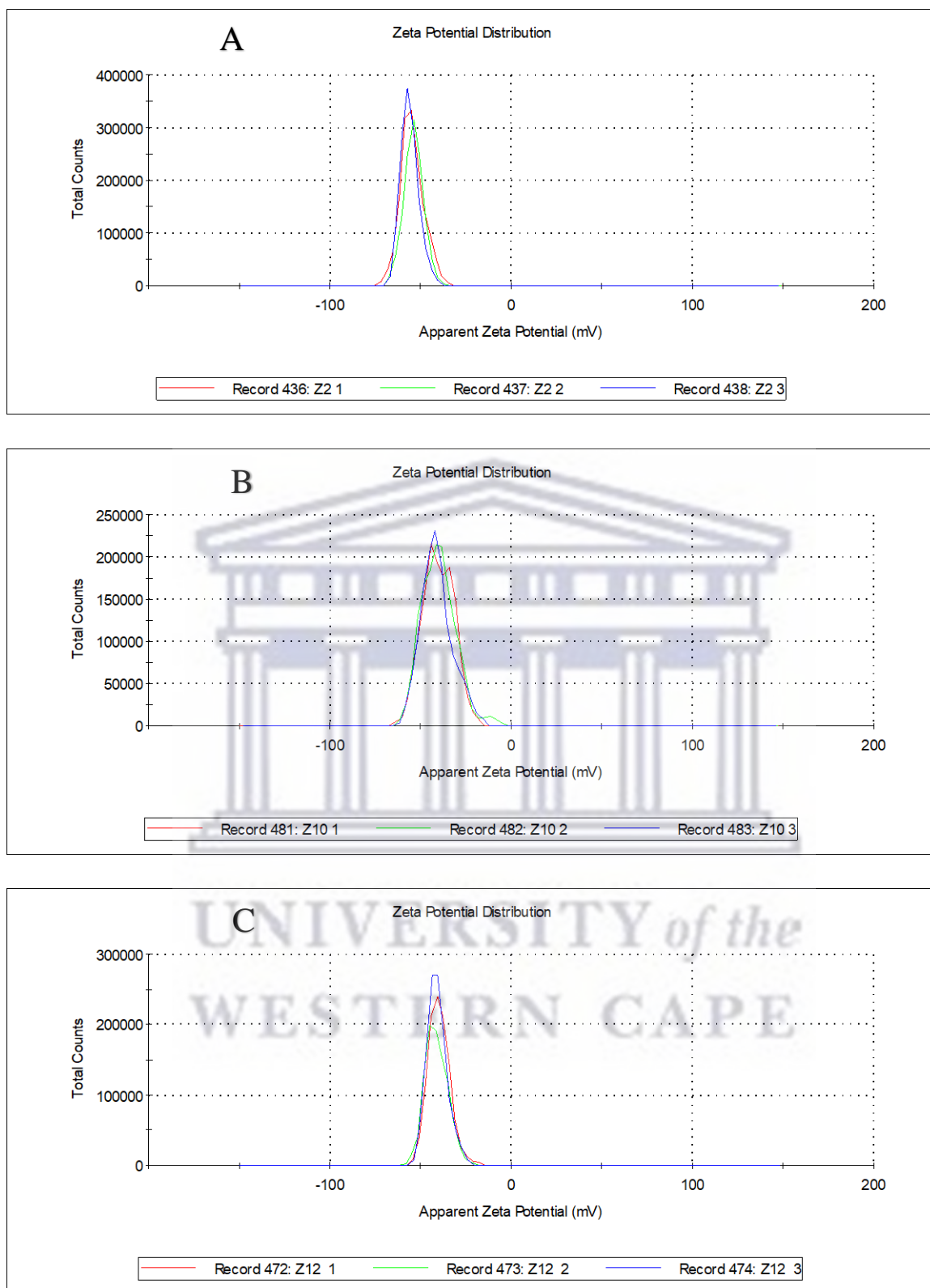


Figure 7.2. Obtained surface charges of AZT-L.

The percentage encapsulation efficiency (%EE) is presented in Table 7.3. The result showed high %EE of AZT in all the formulations but formulation (L2) consisting of 1:1 mass of LEC and CHO depicted the highest encapsulation efficiency of $98.05 \pm 1.37\%$. From here, this formulation (L2) was constantly reproduced and used for further analyses and was used in comparison with the pure drug and the blank. Higher %EE of this sort have been reported also for hydrophilic drugs such as cytarabine, ampicillin, fluorescein, and in some hydrophobic antiretroviral drugs like efavirenz, nevirapine thereby confirming the ability of liposomes to entrap both hydrophilic and hydrophobic drugs (Jaafar (Jaafar-maalej, Diab and Elaissari, 2010; Ramana *et al.*, 2010; Trucillo, Campardelli and Reverchon, 2018; Okafor *et al.*, 2019).

The statistical significance of the quadratic model was evaluated by the analysis of variance (ANOVA), as presented in Tables 7.4 – 7.7. The quadratic equation obtained from the ANOVA is given in equations 7.1 (PS), 7.2 (ZP), 7.3 (ZP) and 7.4 (%EE), respectively. Equation 7.2 does not have the A term because it is insignificant, that is, the effect of lipid ratio alone on PDI is insignificant.

$$Y = +474.85 - 8.41A + 134.04B + 29.80AB - 18.52A^2 - 45.02B^2 \quad (\text{Equation 7.1})$$

$$Y = +0.16 + 0.067B - 0.021AB + 0.011A^2 + 0.041B^2 \quad (\text{Equation 7.2})$$

$$Y = -44.35 - 20.74A + 17.75B - 27.40AB \quad (\text{Equation 7.3})$$

$$Y = +95.44 + 1.62A - 0.44B + 0.32AB - 3.71A^2 + 0.77B^2 \quad (\text{Equation 7.4})$$

The positive sign in front of these equations indicate synergistic effect of the factors, whereas negative sign indicates antagonistic factor effect. Tables 7.4 – 7.7 indicate significant F test-values for the optimization models and the models showed insignificant lack of fit. The predicted R^2 values of 0.9299, 0.6481 and 0.9034 respectively for PS, PDI and %EE responses are in reasonable agreement with the adjusted R^2 values of 0.9857, 0.8459 and 0.9708, respectively considering that their differences are less than 0.2. However for ZP, the predicted R^2 value is -0.4470 and the adjusted R^2 value 0.5840. A reliable model should also be able to predict response with a reasonable accuracy when compared with the experimental data. Figures 10a–d are the plots of Predicted versus Actual data for drug characteristics (PS, PDI and EE), showing experimentally obtained values compared with the predicted values from the models. Hence Figure 7.3, shows that the regression model can predict these liposomes

characteristics while Figure 7.4 shows the surface plot of the independent variables on PS, PDI, ZP and %EE.

Table 7.4: ANOVA of Quadratic model from BBD for PS

Source	Sum of Squares	df	Mean Square	F Value	p-value Prob > F	
Model	1.215E+005	5	24295.12	166.45	< 0.0001	significant
<i>A-Lipid ratio</i>	<i>424.03</i>	<i>1</i>	<i>424.03</i>	<i>2.91</i>	<i>0.1321</i>	
<i>B-Amount of drug</i>	<i>1.078E+005</i>	<i>1</i>	<i>1.078E+005</i>	<i>738.49</i>	<i>< 0.0001</i>	
<i>AB</i>	<i>3550.97</i>	<i>1</i>	<i>3550.97</i>	<i>24.33</i>	<i>0.0017</i>	
<i>A²</i>	<i>947.55</i>	<i>1</i>	<i>947.55</i>	<i>6.49</i>	<i>0.0382</i>	
<i>B²</i>	<i>5597.19</i>	<i>1</i>	<i>5597.19</i>	<i>38.35</i>	<i>0.0004</i>	
Residual	1021.74	7	145.96			
<i>Lack of Fit</i>	<i>831.76</i>	<i>3</i>	<i>277.25</i>	<i>5.84</i>	<i>0.0607</i>	<i>not significant</i>
<i>Pure Error</i>	<i>189.98</i>	<i>4</i>	<i>47.49</i>			
Cor Total	1.225E+005	12				

Table 7.5: ANOVA of Quadratic model from BBD for PDI

Source	Sum of Squares	df	Mean Square	F Value	p-value Prob > F	
Model	0.036	5	7.159E-003	14.18	0.0015	significant
<i>A-Lipid ratio</i>	5.227E-004	1	5.227E-004	1.04	0.3428	
<i>B-Amount of drug</i>	0.027	1	0.027	52.55	0.0002	
<i>AB</i>	1.806E-003	1	1.806E-003	3.58	0.1005	
<i>A²</i>	3.533E-004	1	3.533E-004	0.70	0.4305	
<i>B²</i>	4.600E-003	1	4.600E-003	9.11	0.0194	
Residual	3.535E-003	7	5.049E-004			
<i>Lack of Fit</i>	1.096E-003	3	3.652E-004	0.60	0.6487	not significant
<i>Pure Error</i>	2.439E-003	4	6.097E-004			
Cor Total	0.039	12				

T Table 7.6: ANOVA of Quadratic model from BBD for ZP

Source	Sum of Squares	df	Mean Square	F Value	p-value Prob > F	
Model	7473.09	3	2491.03	6.61	0.0118	significant
<i>A-Lipid ratio</i>	2579.64	1	2579.64	6.85	0.0279	
<i>B-Amount of drug</i>	1889.31	1	1889.31	5.02	0.0519	
<i>AB</i>	3004.14	1	3004.14	7.98	0.0199	
Residual	3389.34	9	376.59			
<i>Lack of Fit</i>	2993.49	5	598.70	6.05	0.0529	not significant
<i>Pure Error</i>	395.85	4	98.96			
Cor Total	10862.43	12				

Table 7.7: ANOVA of quadratic model from BBD for EE

Source	Sum of Squares	df	Mean Square	F Value	p-value Prob > F	
Model	56.66	5	11.33	80.73	< 0.0001	significant
<i>A-Lipid ratio</i>	<i>15.71</i>	<i>1</i>	<i>15.71</i>	<i>111.96</i>	<i>< 0.0001</i>	
<i>B-Amount of drug</i>	<i>1.17</i>	<i>1</i>	<i>1.17</i>	<i>8.34</i>	<i>0.0234</i>	
<i>AB</i>	<i>0.40</i>	<i>1</i>	<i>0.40</i>	<i>2.83</i>	<i>0.1365</i>	
<i>A²</i>	<i>38.03</i>	<i>1</i>	<i>38.03</i>	<i>270.97</i>	<i>< 0.0001</i>	
<i>B²</i>	<i>1.63</i>	<i>1</i>	<i>1.63</i>	<i>11.64</i>	<i>0.0113</i>	
Residual	0.98	7	0.14			
<i>Lack of Fit</i>	<i>0.69</i>	<i>3</i>	<i>0.23</i>	<i>3.19</i>	<i>0.1458</i>	<i>not significant</i>
<i>Pure Error</i>	<i>0.29</i>	<i>4</i>	<i>0.072</i>			
Cor Total	57.64	12				

UNIVERSITY of the
WESTERN CAPE

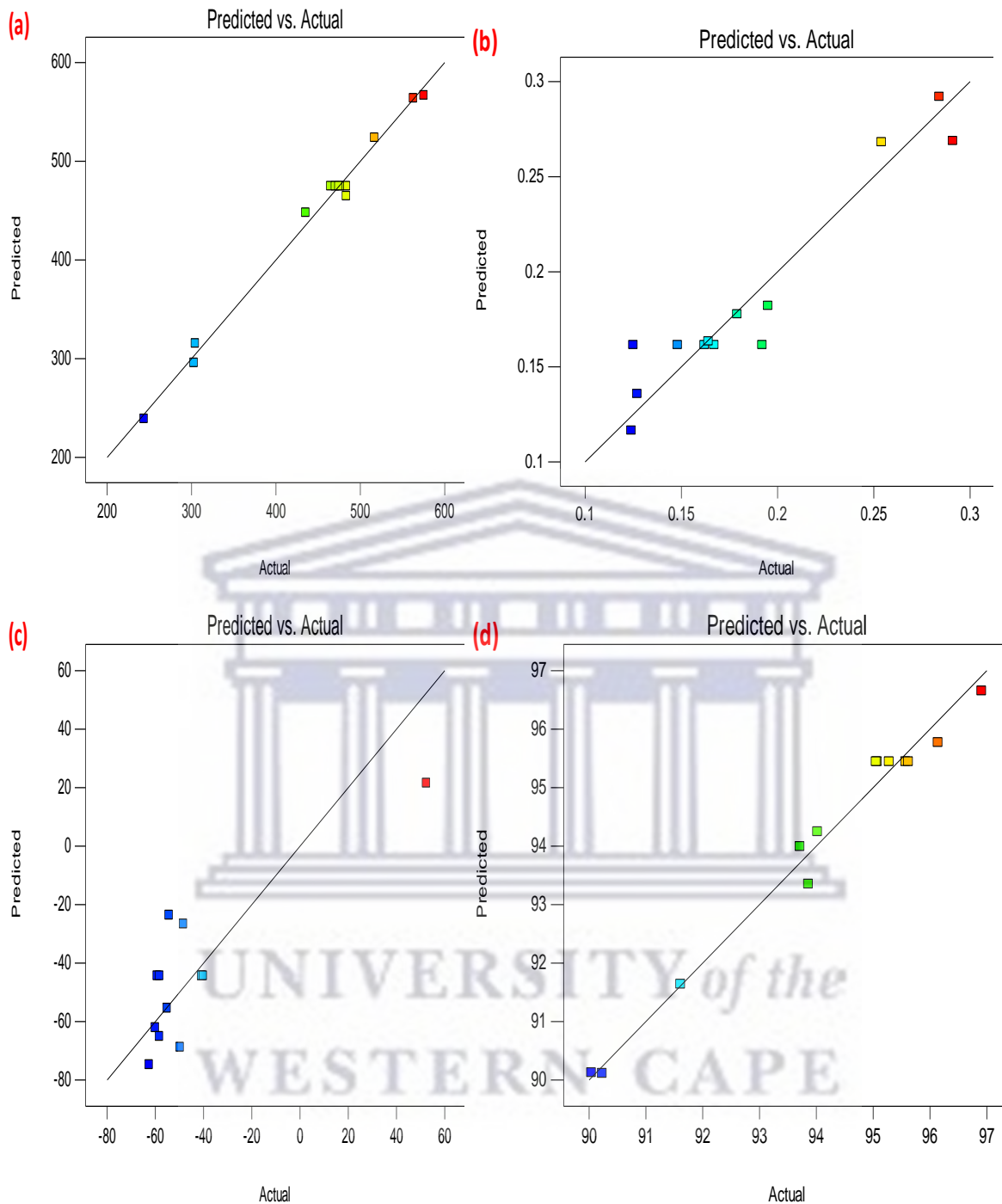
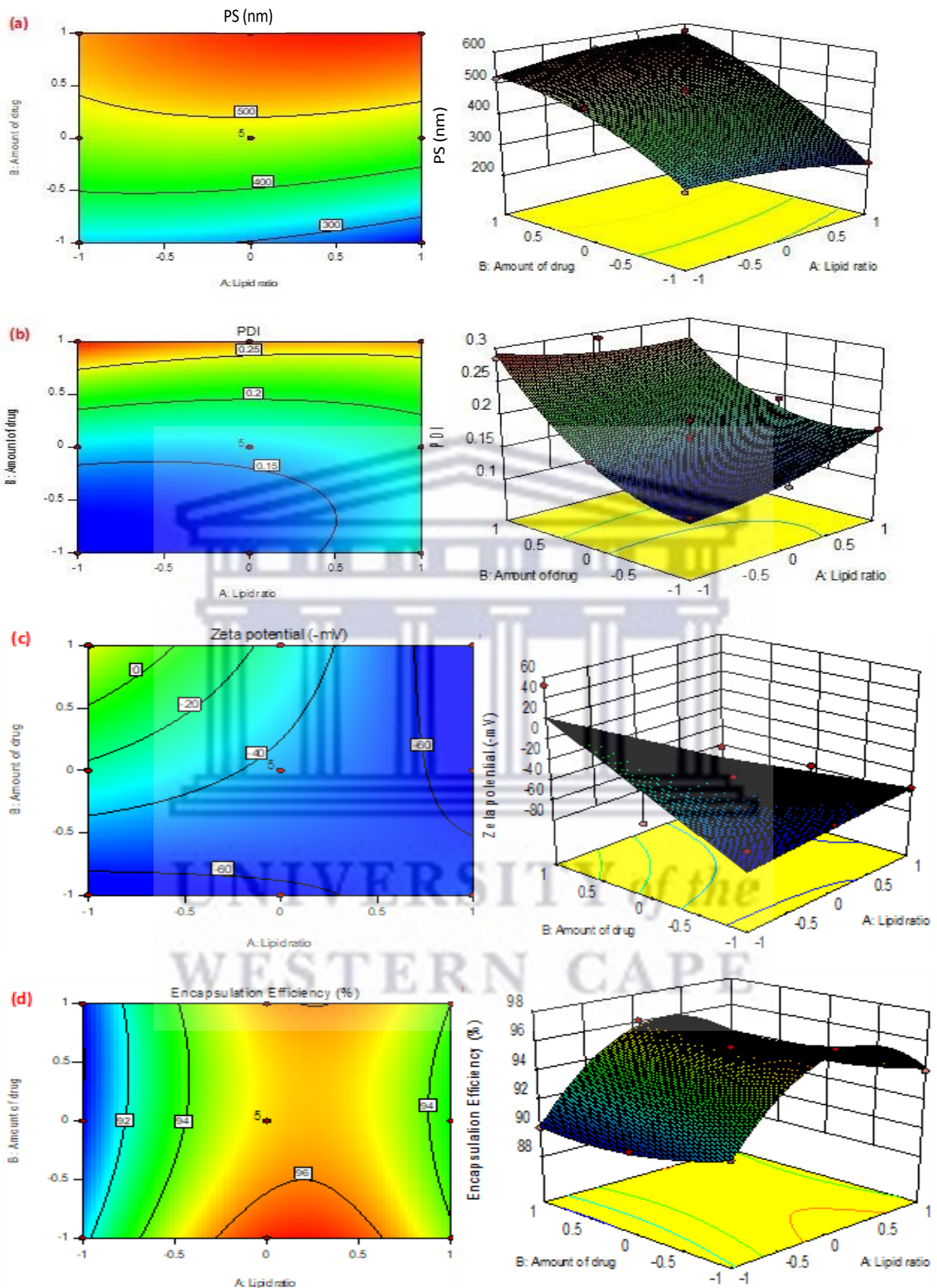


Figure 7.3. Plots of predicted versus actual data for (a) PS, (b) PDI, (c) ZP and (d) %EE.



Figures 7.4. Surface of interactive effects for (a) PS, (b) PDI, (c) ZP and (e) EE with. the left sideshowing the 2D (contour) plots while the 3D plots are on the right side.

7.2.2.2. Transmission electron microscopy (TEM)

The shape evaluation of the prepared liposomes was done using transmission electron microscopy (TEM) to confirm the presence of liposomes in the formulation. The shape examination result (Figure 7.5) confirmed the presence of a spherical shaped particles which is a strong characteristic of a liposomes hence this confirms the successful formation of AZT-loaded liposomes.

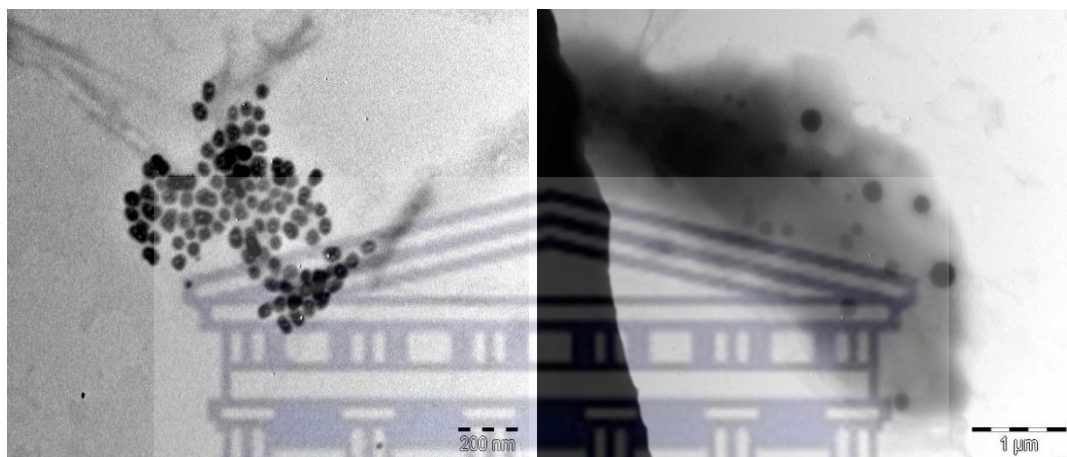


Figure 7.5. Unstained TEM images of AZT-L at different capturing magnifications.

7.2.2.3. Thermal analyses

DSC analysis was one of the thermal analyses carried out to investigate the thermal properties of the pure AZT, AZT-L, and the control (a physical mixture of AZT with CHO and LEC in the ratio it was used in liposomes preparation). The DSC curve (Figure 7.6) shows an endothermic peak at 124.16°C for pure AZT, with degradation occurring around 248°C. Similar melting temperature as well degradation have been previously established for pure AZT drug (Ravi, Kotreka and Saha, 2008; Shamsipur *et al.*, 2013; Porfirio *et al.*, 2015). CHO depicted a crystalline form with the presence of the endothermic peak at the temperature of 147.28°C while LEC was found to be amorphous but with the show of glass transition at 187.17°C. AZT-L was confirmed as amorphous with no form of melting peak although melting was confirmed on HSM technique. The control confirmed the presence of the AZT with the appearance of a decreasing endothermic peak at similar temperature while also confirming the presence of CHO at 138.32°C.

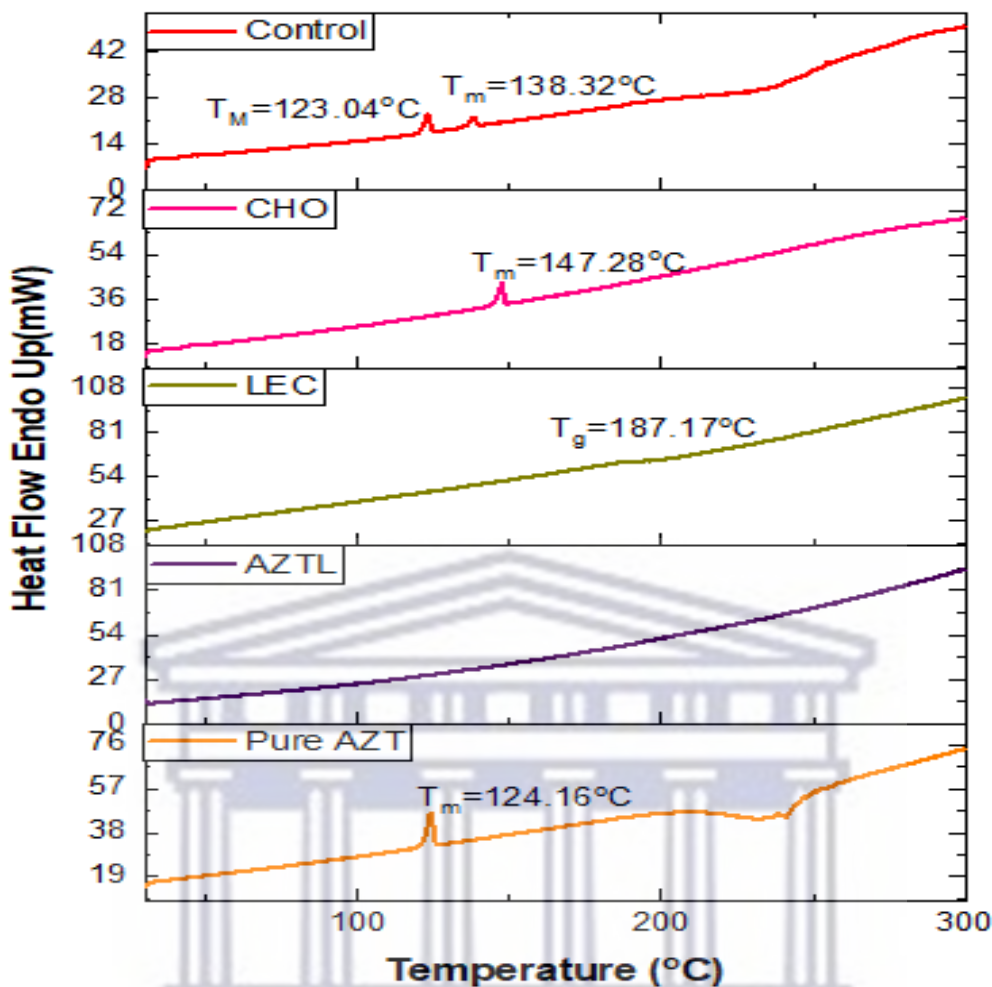


Figure 7.6. An overlay of DSC thermograms obtained with pure AZT, LEC, CHO, AZT-L, and the control.

The TGA result as depicted in Figure 7.7 showed that AZT had a mass loss of 84.91% while showing two steps of thermal events. LEC demonstrated a total loss in mass of 76.87% between temperatures of 269.02 °C and 439.25 °C with initial weight loss being witnessed around temperature of 62.62 °C. This first thermal event (weight loss) can be attributed to evaporation of the surface moisture. CHO depicted almost 100% loss in mass between the temperature of 279.45 °C and 358.43 °C. AZT-L demonstrated a weight loss of about 80% between 232.15 °C to 414.09 °C. For the control, there was a total loss in mass of 83.17 % between the temperature range of 232.15 °C and 414.09 °C. Based on the TGA and DSC results no incompatibility between AZT, LEC and CHO was identified.

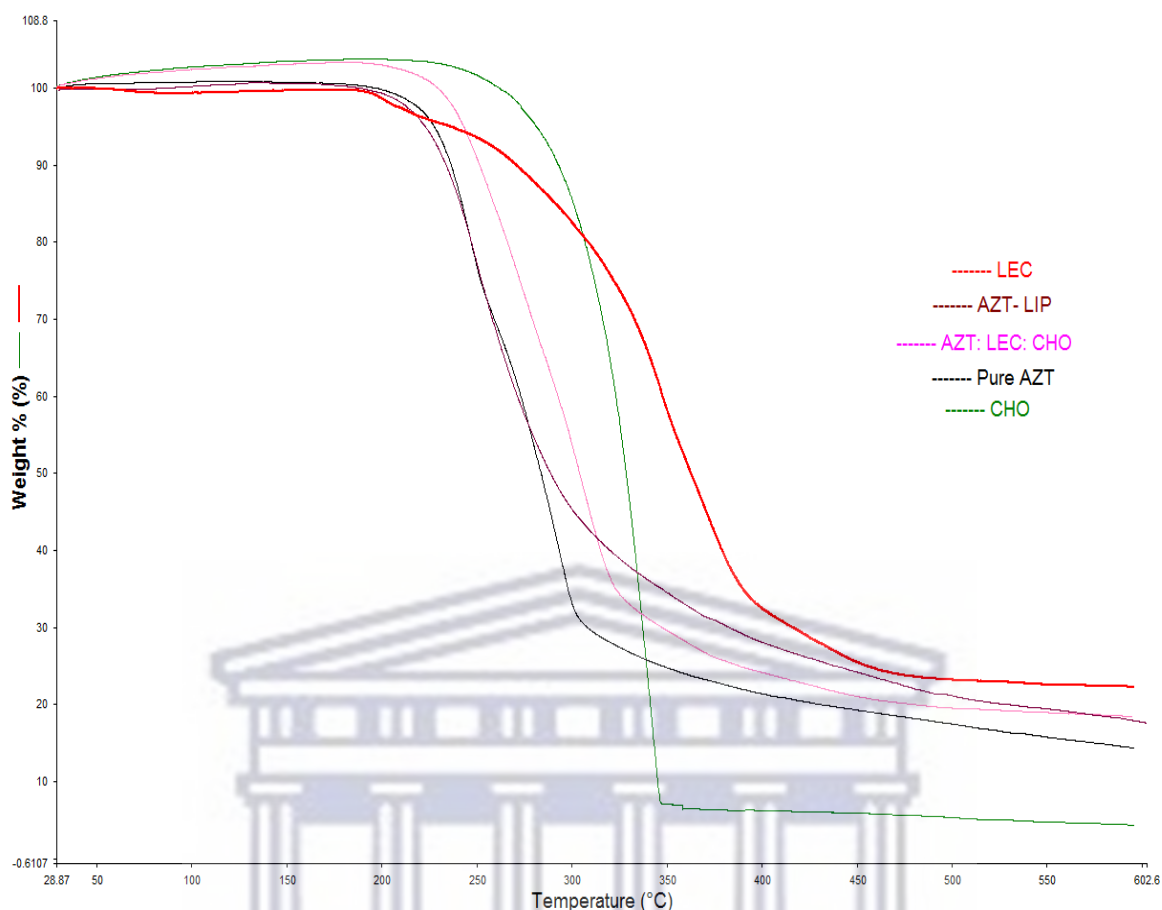


Figure 7.7. TGA curves of pure AZT, LEC, CHO, AZT-L, and the control.

7.2.2.4. Spectroscopic analysis

FTIR analysis for pure AZT, LEC, CHO, AZT-L and the control was investigated for any possible chemical interactions that could emanate from drug-excipient interactions. The FTIR spectra for pure AZT, LEC, CHO as shown in Figure 7.8 all demonstrated the respective characteristic functional groups as summarized in Table 7.8 which have been previously reported (Nzai and Proctor, 1999; Araújo *et al.*, 2003; Porfirio *et al.*, 2015; Ali *et al.*, 2018; Okafor *et al.*, 2019). AZT-L confirmed the presence of the drug in the formulation with the presence of the azide functional group assigned to the pure drug hence indicating molecular dispersion of the drug in the formulation while the control also confirmed presence of the drug as while depicting the presence of the lipid components too.

Table 7.8: FTIR data of pure AZT, LEC, CHO and AZT in liposomes

Sample	Absorption peak (cm ⁻¹)	Functional group
Pure AZT	3491 – 3923	O-H
	2391 – 2102	C=N=N=N azide
	1672	C=O
	1630 –1600	O-H
	1694	C=O
	1437 – 1465	C-H ₂
	1272 – 1292	C-O-C, C-O-H
LEC	3295	O-H
	3010, 2923, 2853	CH ₃ , CH ₂ , CH
	1737	C=O
	1465	CH ₂
	1055 – 1227	C-O-C of esters
	720	CH ₂
CHO	3428	OH
	2866 – 2930	CH ₂ , CH ₃
	1464, 1376	CH ₂ , CH ₃
	1055, 953, 799	CH
Control	3354	O-H
	2928 – 2104	C=N=N=N
	1686	C=O

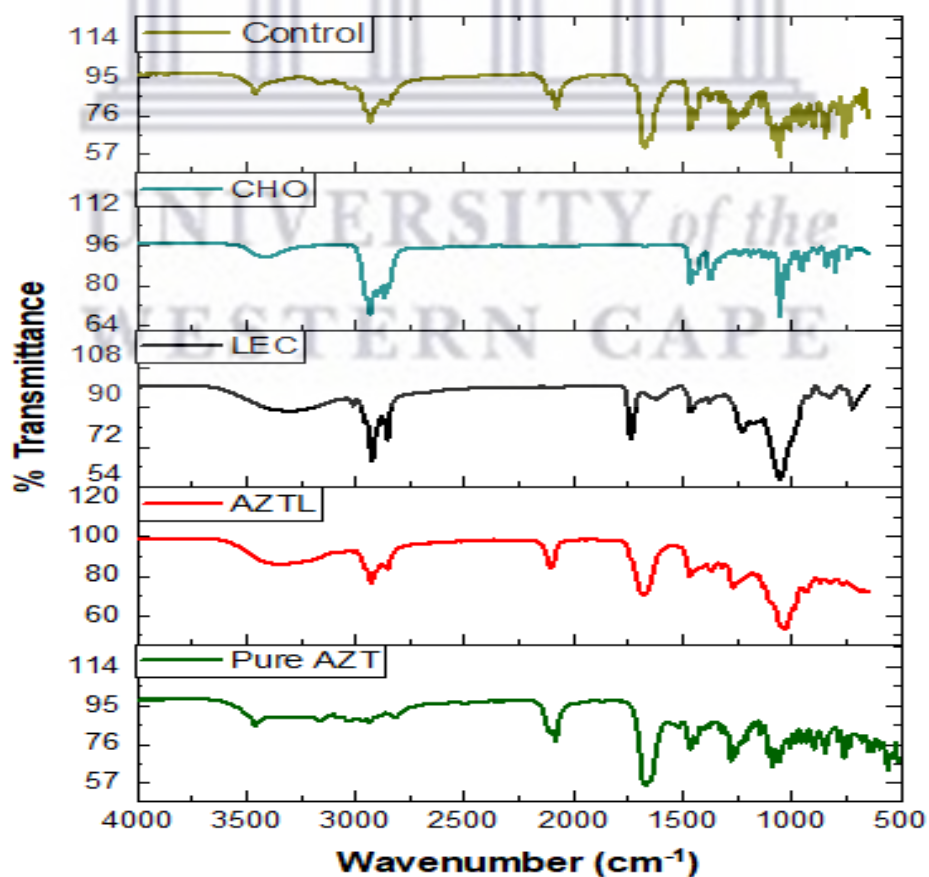


Figure 7.8. FTIR spectra of pure AZT, LEC, CHO, AZT-L, and the control.

7.2.2.5. Powder X-ray diffractometer (PXRD)

Figure 7.9 depicts the PXRD diffractograms obtained for AZT, LEC, CHO, AZT-L and, the control sample. The presence of sharp and intense peaks across the 2θ in the diffractogram of pure AZT indicated its crystalline nature while in case of AZT-L, the peaks were found to have depleted thereby confirming an amorphous state of AZT in the liposomes. Pure lecithin also showed amorphous halos due to its amorphous state as no melting peak was observed. Pure CHO and the control which comprises the physical mixture of drug resulted in a relatively less and semi-crystalline form with a less intense peaks at 2θ of approximately at 4, 6, 14, 16, 18 and 4, 8, 14, 16, 18, 22, respectively. The control showed the representation of the characteristics of an AZT molecular compound in the mixture with some crystallinity while the absence of the crystalline and intense peaks in the AZT-L suggest that the drug have been encapsulated within the liposomes hence the drug is molecularly dispersed or in amorphous form.

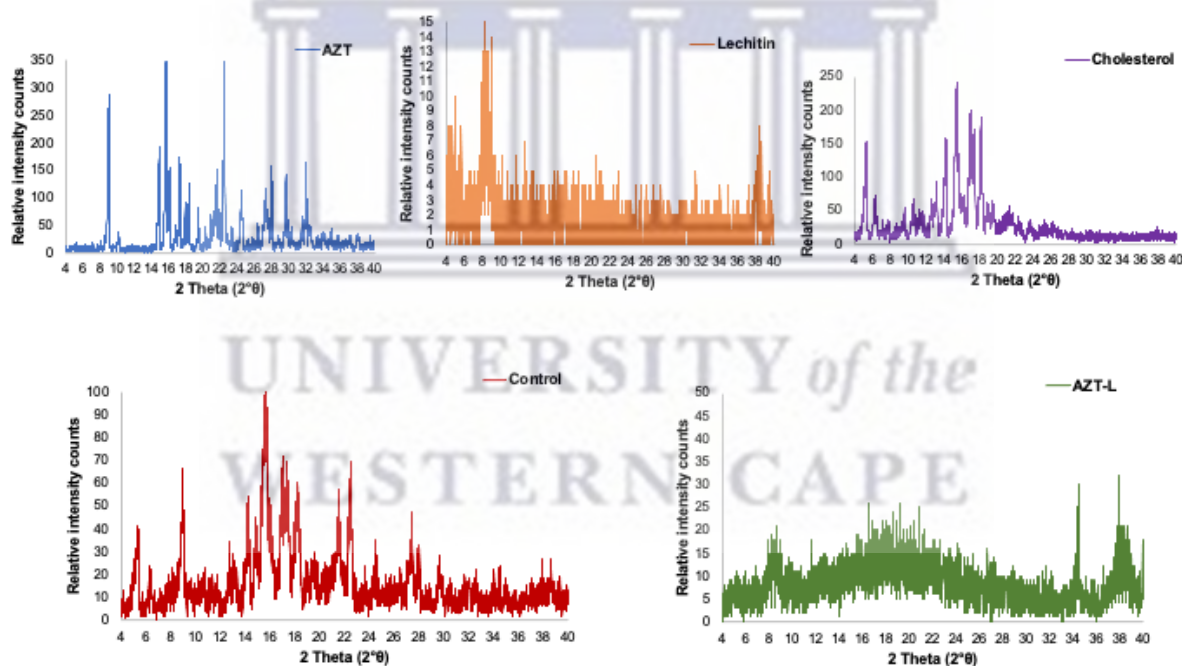


Figure 7.9. PXRD diffractograms obtained for AZT, LEC, CHO, Control and AZT-L.

7.2.2.6. Equilibrium solubility

Equilibrium solubility concentrations of pure AZT, the control and the AZT-L in various aqueous buffered media is depicted in Figure 7.10. Since AZT is a water-soluble ARV, the solubility in all the media was high but more pronounced in pH 6.8 and distilled water. The physical mixture of AZT with LEC and CHO depicted a decrease in the solubility of AZT

compared to the solubility of the AZT in liposomes. It could be suggested that the drug was more soluble in liposomes due to the fact that it was entrapped in an amorphous state rather in the physical mixture where the lipid components were not able to dissolve entirely within 24 hours. This agrees to the fact that liposomes delivery systems enhance the solubility of drugs hence it is regarded as a solubilising strategy in certain formulations. Therefore, it is germane to conclude that by entrapping AZT in the liposomes, the solubility of this drug was improved.

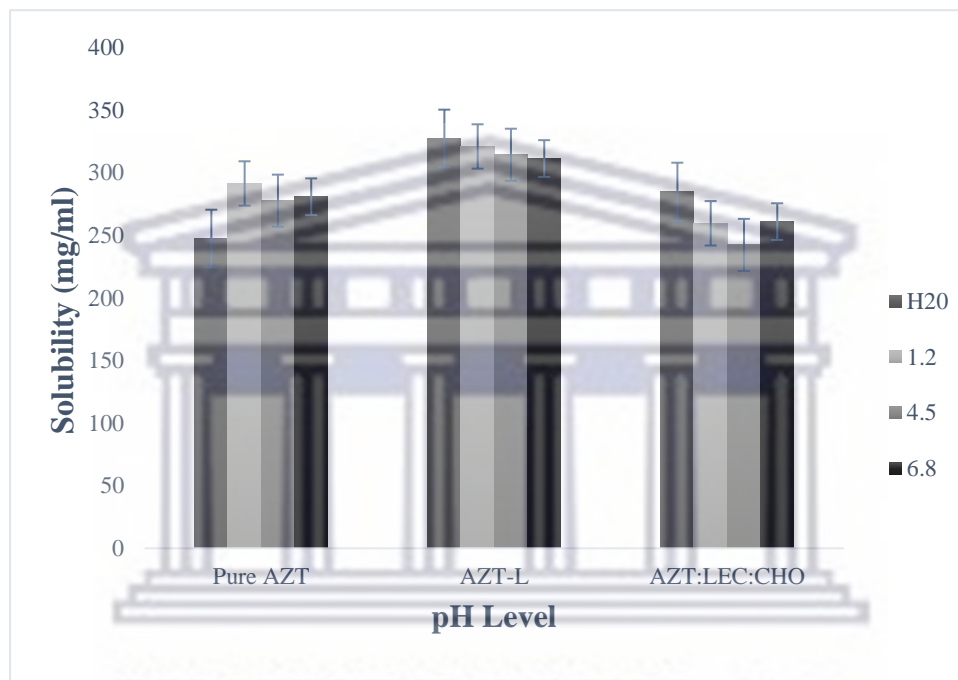


Figure 7.10. Solubility profiles of pure AZT, the physical mixture and AZT-L.

7.2.2.7. *In vitro* drug release studies

The dissolution of pure AZT and AZT-loaded liposomes was investigated in pH 1.2 for a period of 30 minutes. Only one dissolution medium was utilised based on the fact that AZT is a water-soluble ARV and therefore rapid and complete dissolution is expected within any dissolution medium. Therefore, based on the solubility data (Figure 7.10) as well as the fact that the liposomes are intended for oral administration only pH 1.2 was applied as dissolution medium.

Figure 7.11 depicts the *in vitro* dissolution profiles obtained for AZT and AZT-L in pH 1.2.

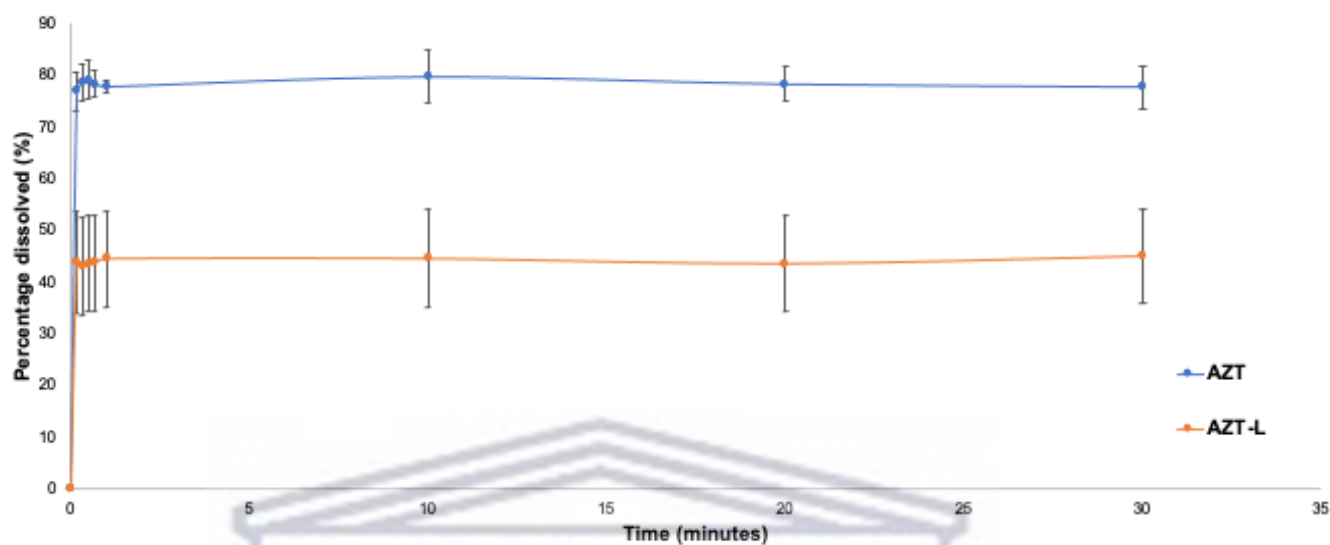


Figure 7.11. *In vitro* dissolution profiles of AZT in comparison with AZT-L.

Interestingly, the AZT-loaded liposomes showed reduced drug release over a 30-minute period. This was unexpected since AZT-L showed increased equilibrium solubility (Figure 7.10). However, it should be mentioned that equilibrium solubility was tested across a 24-hour period, thereby allowing a significantly longer time for AZT to solubilise, whilst the dissolution testing was only performed for a period of 30 minutes. Essentially, the lower dissolution rate of AZT upon encapsulation into a liposomes system could be utilised to formulate extended-release dosage forms, a strategy that could be beneficial for paediatric patients since it could allow the reduction in the dose frequency required.

7.3. The microencapsulation of AZT *via* spray drying using PPI and IN as wall formers

The primary objective of this work was to develop a novel drug delivery system in the form of AZT-containing microparticles by utilizing the spray drying process. Immediately after spray drying, the spray dried product (SD-AZT) was collected, and the moisture content was determined, and percentage yield calculated. The result showed that the moisture present in the SD-AZT was equivalent to 7.88% while the control was 8.96%. The percentage yield for SD-AZT, percentage drug loading was calculated to be 76.1% and 67.2% using the equations 4.9 and 4.10 respectively.

7.3.1. Physicochemical characterization of SD-AZT in comparison with the raw materials and a physical mixture

7.3.1.1. Thermal analyses

The DSC thermal analysis for pure AZT, PPI, IN, the SD-AZT, and the control was carried out using DSC analytical technique and the obtained DSC thermograms were analysed. The result (Figure 7.12) showed AZT in the sprayed dried formulation to have a slight reduction in the endothermic peak value similar melting point (121.25°C) hence amorphous formulation in comparison with pure crystalline AZT (124.16°C) (Araújo *et al.*, 2003; Magalhães *et al.*, 2018). The DSC thermogram of SD-AZT also compared very well with the thermogram obtained with the control, signifying that the drug was present in both SD-AZT in amorphous state with a depleted endothermic peak as well as in the control due to the clear identification of the melting point of AZT, no incompatibility between the drug and the excipients was identified.

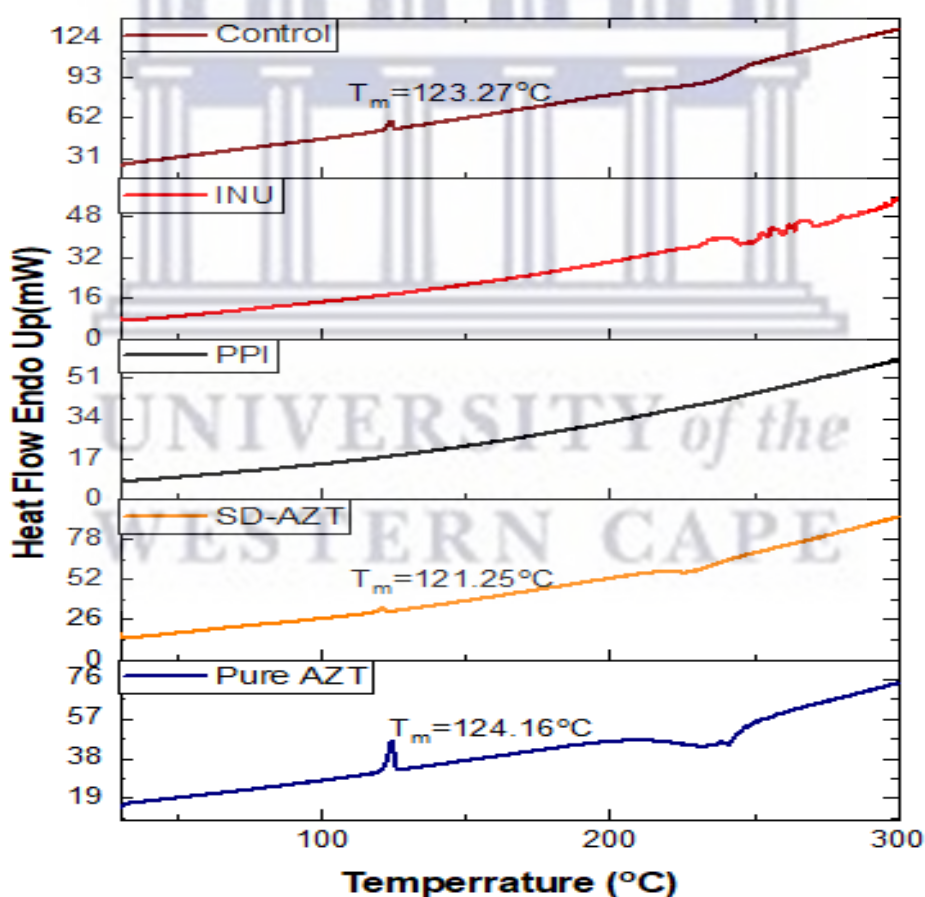


Figure 7.12. DSC thermograms of pure AZT, PPI, IN, SD-AZT, and the control.

TGA of the pure compounds (AZT, PPI, IN), the SD-AZT and the control was examined, and the result established, as shown in Figure 7.13 demonstrated that SD-AZT lost 65.31% weight at temperatures between 88.32°C to 336.97°C with an initial mass loss at 60.05°C due to loss

of the adsorbed surface moisture. For the control, an initial, insignificant weight loss was observed around 76.44 °C temperature while demonstrating decomposition at 222.95 °C with a total weight loss of 66.77%. The TGA thermograms obtained with PPI and IN showed these two compounds to remain stable to approximately 300 °C followed by significant degradation during further heating (Likhitha *et al.*, 2020). From the TGA results it was possible to conclude that no incompatibility between AZT, PPI and IN exist.

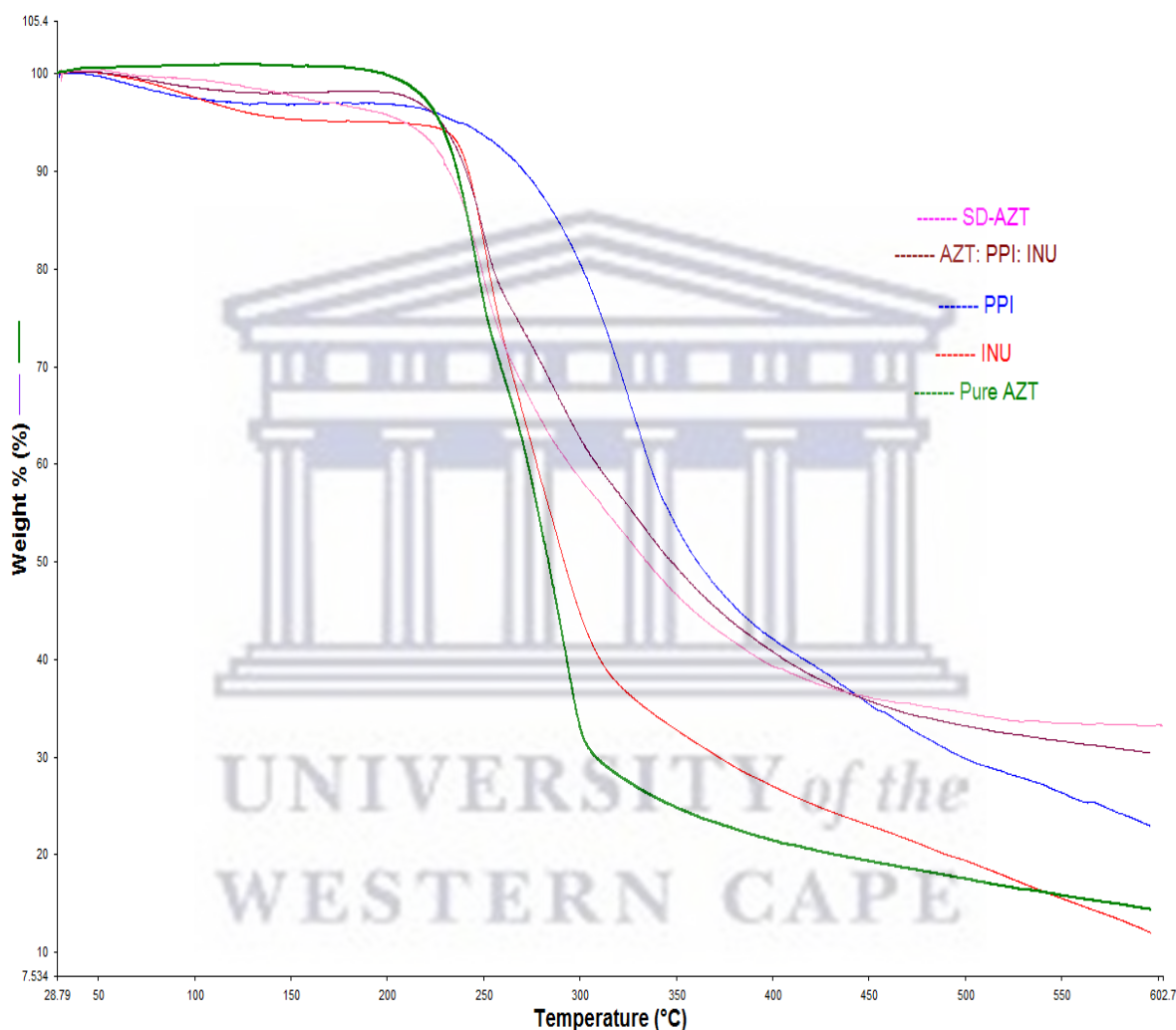


Figure 7.13. TGA curves for pure AZT, PPI, IN, SD-AZT, and the control.

7.3.1.2. Spectroscopic analysis of SD-AZT

FTIR results of pure AZT, PPI, IN, SD-AZT, and the control is summarised in Table 7.9 and spectra presented in Figure 7.14, respectively. PPI and IN demonstrated their known functional groups which includes the confirmation of the amide groups and the glycosidic acid respectively as have been previously established (Sun-Waterhouse, Wadhwa and Waterhouse, 2013; Bajaj, Tang and Sablani, 2015). In SD-AZT, the presence of AZT was confirmed with

the presence of the assigned functional groups of AZT which includes the alcohol group (OH) at 3491 cm⁻¹ and azide group (C=N=N=N) at 2391 cm⁻¹, respectively although the absorption peaks are not broad like in the pure drug, which could be suggestive of amorphization of AZT. The control which is made of the physical mixture of AZT and the excipients further revealed the presence of the functional groups of AZT like the azide group and that of the PPI and IN of amide groups and glycosidic acid respectively.

Table 7.9: FTIR absorption peaks and functional groups of pure AZT, PPI, IN, SD-AZT, and the control

Sample	Absorption peak (cm ⁻¹)	Functional group
AZT	3491 - 3923	O-H
	2391	C=N=N=N azide
	1672	C=O
	1630 - 1600	O-H
	2102	C=N=N=N
	1694	C=O
	1437, 1465	C-H ₂
	1272, 1292	C-O-C, C-O-H
PPI	3274	O-H
	2925	C-H
	1630	C=O amide I
	1528	N-H, C-N amide II
	1393	N-H, C-N amide III
	1234	C-O-C symmetric
	1099	C-O
IN	3286	O-H
	2931	-CH ₂
	1641	C=C
	1417	O-H
	1018	C-O-C
	930	β ₂ →1 glycosidic acid
SD-AZT	3316	O-H
	2381 - 2081	C=N=N=N
	1683	C=O
	1023	C-O-C
Control	3491 - 3923	O-H
	2391	C=N=N=N azide
	1672	C=O
	1630 - 1600	O-H
	2102	C=N=N=N
	1694	C=O
	1437, 1465	C-H ₂
	1272, 1292	C-O-C, C-O-H

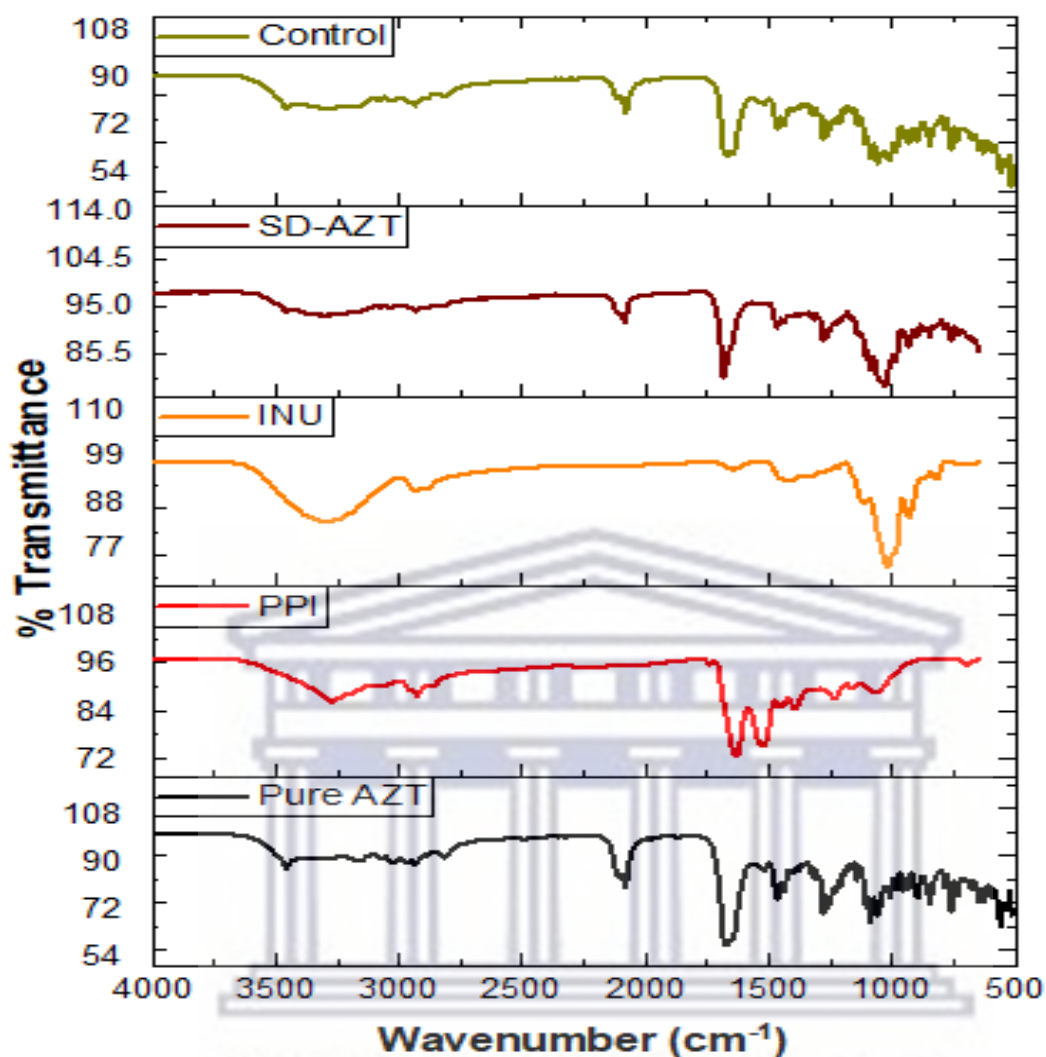


Figure 7.14. An overlay of the FTIR spectra of pure AZT, PPI, IN, SD-AZT, and the control

7.3.1.3. Powder X-ray diffraction of SD-AZT

Powder X-ray diffraction analysis to ascertain the crystalline or the amorphous state of AZT, PPI, IN, SD-AZT, and the control and the result have been illustrated in Figure 7.15. PXRD diffractograms depicted an intense and sharp peak along the 2θ thereby confirming the crystalline form of the pure drug. There was little or no sharp or intense peaks in the SD-AZT hence predicting a complete encapsulation, coating and dispersed molecularly drug in the microparticles hence regarded as an amorphous preparation. The control showed the presence of the characteristic crystalline peak in the 2θ region although not as intense and sharp like the pure drug while PPI and IN were confirmed amorphous due to the absence of the crystalline form and sharp peaks further lending credence the DSC result reported in the preceding section.

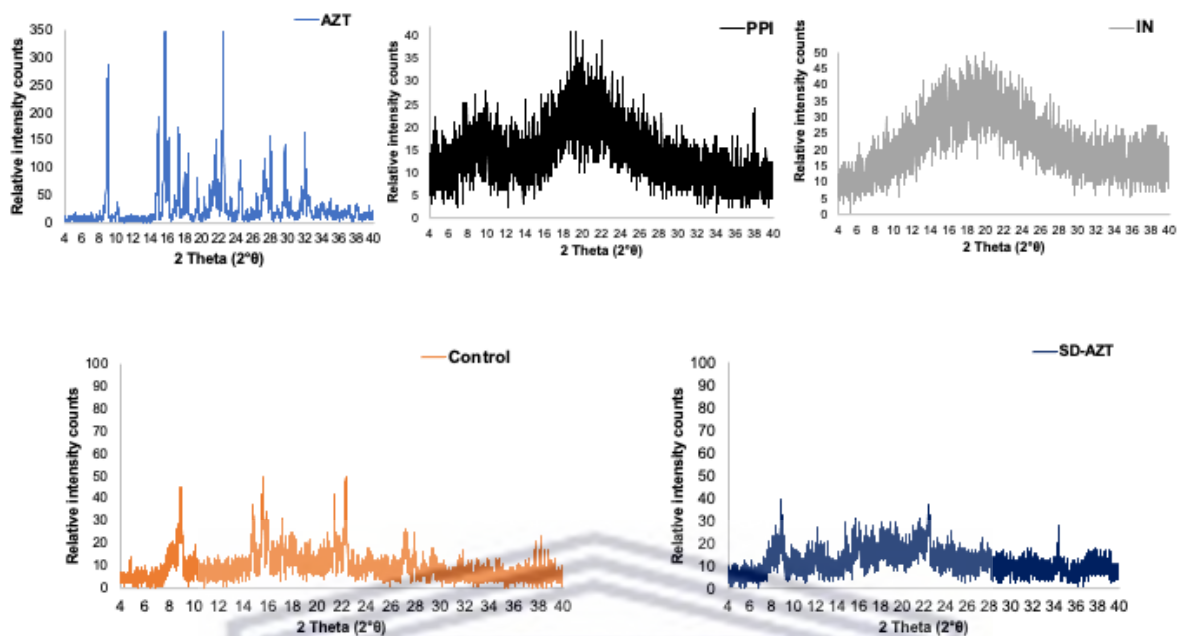


Figure 7.15. PXR D diffractograms obtained for AZT, PPI, IN and SD-AZT

7.3.1.4. Equilibrium solubility studies

Equilibrium solubility results involving pure AZT, the physical mixture of AZT with the excipients (PPI and IN), and SD-AZT using the shake-flask technique is depicted in Figure 7.16. The obtained solubility result showed that pure AZT demonstrated good solubility in all the pH media and in deionized water while showing its best solubility in pH 1.2. The solubility of AZT in the physical mixture with PPI and IN showed to be similar to pure AZT in all pH buffered media, except pH 4.5 which showed a decrease in the solubilised AZT concentration. SD-AZT exhibited the highest solubility in comparison with pure AZT and AZT in the physical mixture in all media. This improved solubility of AZT may be ascribed to the size reduction of the spray dried AZT microcapsules or to the fact that AZT exists in the amorphous state, as concluded from the PXR D analyses (Figure 7.15).

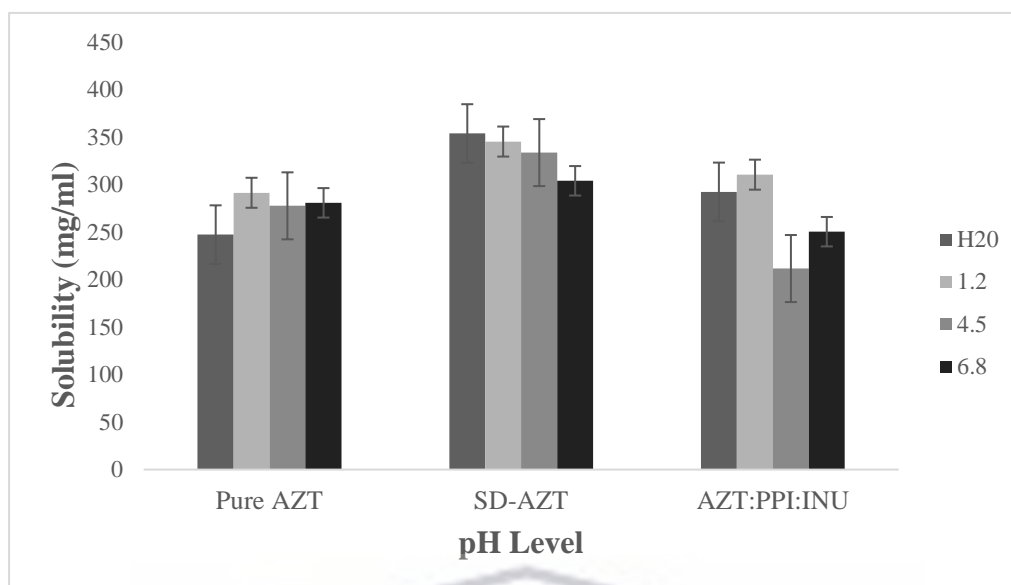


Figure 7.16. Equilibrium solubility of pure AZT, AZT: PPI: INU and SD-AZT

7.3.1.5. *In vitro* dissolution studies

For comparison purposes the *in vitro* dissolution testing of SD-AZT was also conducted only in pH 1.2. The obtained release profiles showed a burst release within the first 5 minutes signalling a biphasic release pattern (Okafor *et al.*, 2019). A higher dissolution rate for AZT from the spray dried preparation was noted (Figure 7.17), however it was also noted that the increase in dissolution rate was not significantly higher and therefore it was concluded that either AZT did not exist in a truly amorphous state or that the combination thereof with PPI:IN does not result in a rapid increase in dissolution, as would've been expected from the equilibrium solubility results (Figure 7.16).

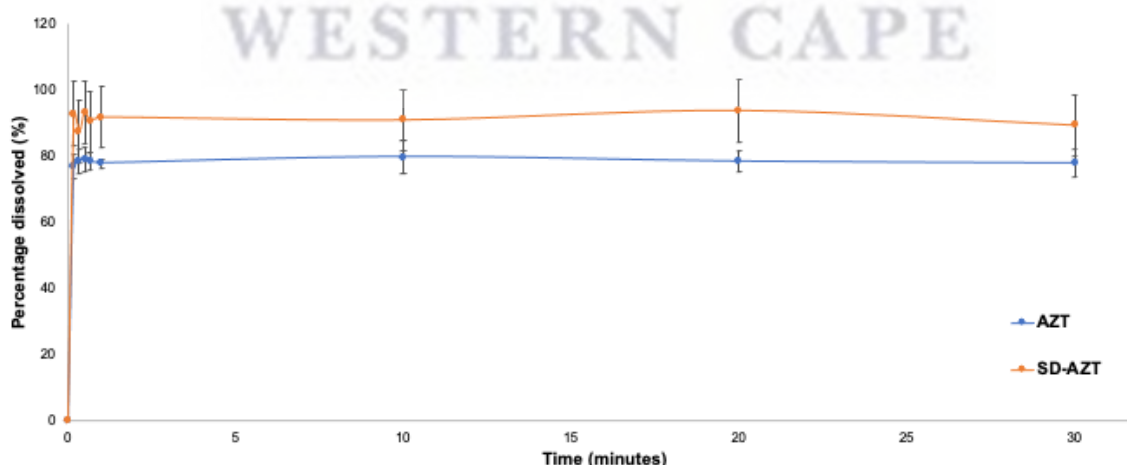
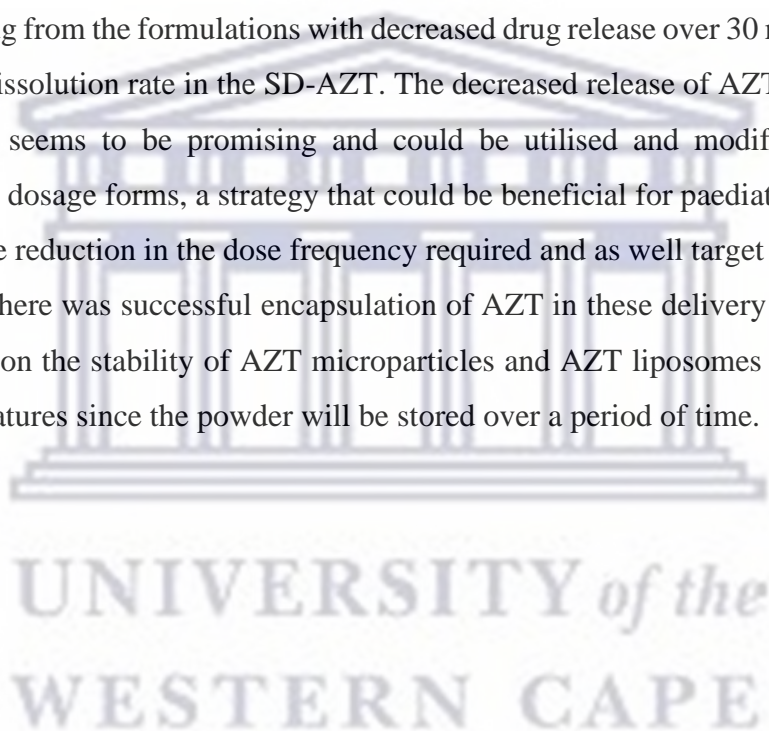


Figure 7.17. *In vitro* dissolution profiles obtained for AZT and SD-AZT over a 30-minute period in pH 1.2.

7.4. Conclusion

In the present study, the encapsulation of AZT using spray drying and liposomes of AZT was successfully carried out to produce an amorphous dispersion of AZT microparticles and AZT-L using the affordable natural excipients of PPI, INU, and CHO. The results illustrated a complete encapsulation of the drug within the delivery systems with high percentage yield, good loading and encapsulation efficiency and reduced particle sizes within nanometer capable of promoting dose reduction in futuristic HIV paediatric formulations and treatment. The physicochemical analyses of AZT microparticles and liposomes confirmed an amorphous preparation while showing an improved solubility. The release profiles of both the drug-loaded liposomes and the spray dried microparticles which was conducted only in pH 1.2 showed the release of the drug from the formulations with decreased drug release over 30 minutes for AZT-L and higher a dissolution rate in the SD-AZT. The decreased release of AZT from liposomes delivery system seems to be promising and could be utilised and modified to formulate extended-release dosage forms, a strategy that could be beneficial for paediatric patients since it could allow the reduction in the dose frequency required and as well target the infected cells only. Although there was successful encapsulation of AZT in these delivery systems, there is need for studies on the stability of AZT microparticles and AZT liposomes on storage under different temperatures since the powder will be stored over a period of time.



7.5. References

- Afe, A.J., Motunrayo, O. and Ogungbade, G. (2018) 'Factors Influencing Adherence to HAART among Patients Living with HIV Infection in Southwest Nigeria : A Cross-Sectional Analysis', *Journal of HIV and retro virus*, 1(1), pp. 2471–9676.
- Ali, M. *et al.* (2018) 'Engineered mixed oxide-based polymeric composites for enhanced antimicrobial activity and sustained release of antiretroviral drug', *International Journal of Biological Macromolecules*, (116), pp. 417–425.
- Araújo, A.S. *et al.* (2003) 'Thermal analysis of the antiretroviral zidovudine (AZT) and evaluation of the compatibility with excipients used in solid dosage forms', *International Journal of Pharmaceutics*, 260(2), pp. 303–314.
- Araújo, A.S. *et al.* (2010) 'Determination of the melting temperature, heat of fusion, and purity analysis of different samples of zidovudine (AZT) using DSC', *Brazilian Journal of Pharmaceutical Sciences*, 46(1), pp. 37–43.
- Bianchin, M.D. *et al.* (2021) 'Monoolein-based nanoparticles containing indinavir: a taste-masked drug delivery system', *Drug Development and Industrial Pharmacy*. Taylor & Francis, 47(1), pp. 83–91.
- Chiappetta, D.A. *et al.* (2010) 'Efavirenz-loaded polymeric micelles for paediatric anti-HIV pharmacotherapy with significantly higher oral bioavailability', *Nanomedicine*, 5(1), pp. 11–23.
- Davies, M. *et al.* (2008) 'Adherence to antiretroviral therapy in young children in Cape Town, South Africa, measured by medication return and caregiver self-report: a prospective cohort study', *BioMed Pediatrics*, 8(34), pp. 1–12.
- Deng, Y. *et al.* (2021) 'Development of nanoparticle-based orodispersible palatable pediatric formulations', *International Journal of Pharmaceutics*, 5(26), pp. 120–206.
- Dezani, A.B. *et al.* (2017) 'Solubility evaluation of didanosine: a comparison between the equilibrium method and intrinsic dissolution for biopharmaceutics classification purposes', *Brazilian Journal of Pharmaceutical Sciences*, 53(2), pp. 1–8.
- Dwivedi, C. *et al.* (2014) 'Role of liposomes in novel drug delivery system', *Journal of drug delivery and therapeutics*, 4(2), pp. 116–129.

- Dwivedi, C. and Verma, S. (2013) 'Review on Preparation and Characterization of Liposomes with Application', *Journal of Scientific & Innovative Research Review*, 2(2), pp. 2320–4818.
- Faria, M.J. *et al.* (2021) 'Lipid nanocarriers for anti-HIV therapeutics: A focus on physicochemical properties and biotechnological advances', *Pharmaceutics*, 14(1294) pp. 1–54.
- Giaretta, M. *et al.* (2019) 'Development of Innovative Polymer-Based Matricial Nanostructures for Ritonavir Oral Administration', *Journal of nanomaterials*.doi.org/1155/2019/8619819.
- Haberer, J. and Mellins, C. (2010) 'Pediatric Adherence to HIV Antiretroviral Therapy', *Current HIV/AIDS Rep*, 6(4), pp. 194–200.
- Jaafar-maalej, C., Diab, R. and Elaissari, A. (2010) 'Ethanol injection method for hydrophilic and lipophilic drug-loaded liposomes preparation', *Journal of Liposome Research*, 20(3), pp. 228–243.
- Kalepu, S. *et al.* (2013) 'Liposomal drug delivery system-A comprehensive review', *International Journal of Drug Development and Research*, 5(4).
- Karami, N., Moghimipour, E. and Salimi, A. (2018) 'Liposomes as a Novel Drug Delivery System: Fundamental and Pharmaceutical Application', *Asian Journal of Pharmaceutics*, 12(1), pp. 31–41.
- Kaur, C.D., Nahar, M. and Jain, N.K. (2008) 'Lymphatic targeting of zidovudine using surface-engineered liposomes', *Journal of Drug Targeting*, 16(10), pp. 798–805.
- Kim, J. (2016) 'Liposomal drug delivery system', *Journal of Pharmaceutical Investigation*. Springer Netherlands, 46(4), pp. 387–392.
- Krieser, K. *et al.* (2020) 'Taste-masked nanoparticles containing Saquinavir for pediatric oral administration', *Materials Science and Engineering C*, 117. doi: 10.1016/j.msec.2020.111315.
- Kuznetsova, D.A. *et al.* (2021) 'Novel biocompatible liposomal formulations for encapsulation of hydrophilic drugs – Chloramphenicol and cisplatin', *Colloids and Surfaces* 610, pp. 125673. doi: 10.1016/j.colsurfa.2020.125673.
- Laufs, U., Rettig-ewen, V. and Bo, M. (2011) 'Strategies to improve drug adherence', *European heart Journal*, (32), pp. 264–268.

- Likitha, U. *et al.* (2020) 'A study on interwoven hydrogen bonding interactions in new zidovudine-picric acid (1:1) cocrystal through single crystal XRD, spectral and computational methods', *Journal of Molecular Structure*, 12(11), pp. 18–52.
- Lin, D. *et al.* (2007) 'Palatability, adherence and prescribing patterns for children with human immunodeficiency virus infection in Canada', *Pharmacoepidemiology and drug safety*, (16), pp. 228–228.
- Lin, D. *et al.* (2011) 'Palatability, adherence and prescribing patterns of antiretroviral drugs for children with human immunodeficiency virus infection in Canada', *Pharmacoepidemiology and drug safety*, pp. 1246–1252.
- Lokhande, S.S. (2018) 'Liposomes drug delivery: An update review', *Pharma Science Monitor*, 9(1), pp. 188–202.
- Magalhães, M.C.R. S. *et al.* (2018) 'Permeability and in vivo distribution of poly(ϵ -caprolactone) nanoparticles loaded with zidovudine', *Journal of Nanoparticle Research*. *Journal of Nanoparticle Research*, 20(7). doi: 10.1007/s11051-018-4280-9.
- Maru, S. M. *et al.* (2011) 'Characterization of thermal and rheological properties of zidovudine, lamivudine and plasticizer blends with ethyl cellulose to assess their suitability for hot melt extrusion', *European Journal of Pharmaceutical Sciences*, 44(4), pp. 471–478.
- Mishra, H. *et al.* (2018) 'A comprehensive review on liposomes: a novel drug delivery system', *Journal of drug delivery and therapeutics*, 8(6), pp. 400–404.
- Mohima, T. *et al.* (2015) 'Encapsulation of Zidovudine in different cellulosic acrylic and methacrylic polymers loaded microspheres', *International Journal of Pharmacy and Pharmaceutical Sciences*, 7(1) 22–42.
- Mufamadi, M.S. *et al.* (2011) 'A Review on Composite Liposomal Technologies for Specialized Drug Delivery', *Journal of drug delivery system*. doi: 10.1155/2011/939851.
- Nichols, J., Steinmetz, A. and Paintsil, E. (2017) 'Impact of HIV-Status Disclosure on Adherence to Antiretroviral Therapy Among HIV-Infected Children in Resource-Limited Settings: A Systematic Review', *AIDS and Behavior*. Springer US, 21(1), pp. 59–69.
- Nzai, J.M. and Proctor, A. (1999) 'Soy lecithin phospholipid determination by fourier transform infrared spectroscopy and the acid digest/arseno-molybdate method: A comparative study', *Journal of the American Oil Chemists' Society*, 76(1), pp. 61–66.

- Okafor, N.I. *et al.* (2019) 'Encapsulation and physicochemical evaluation of efavirenz in liposomes', *Journal of Pharmaceutical Investigation*, (45), pp. 1–8.
- Panwar, P. *et al.* (2010) 'Study of Albendazole-Encapsulated Nanosize Liposomes', *International Journal of Nanomedicine*, (5), pp. 101–108.
- Patel, N. and Panda, S. (2012) 'Liposomes Drug delivery system : a Critic Review', *Journal of Pharmaceutical Science and Bioscientific Research*, 2(4), pp. 169–175.
- Pham, K. *et al.* (2016) 'Development and in vivo evaluation of child-friendly lopinavir/ritonavir pediatric granules utilizing novel in situ self-assembly nanoparticles', *Journal of Controlled Release*, (226), pp. 88–97.
- Porfirio, L. *et al.* (2015) 'Compatibility study of hydroxypropylmethylcellulose films containing zidovudine and lamivudine using thermal analysis and infrared spectroscopy', *Journal of thermal analytical calorim*, (120), pp. 817–828.
- Prebianca, G. *et al.* (2020) 'Improved sensory properties of a nanostructured ritonavir suspension with a pediatric administration perspective', *Pharmaceutical Development and Technology*. doi: 10.1080/10837450.2020.1805762.
- Rajendra, D. *et al.* (2009) 'Formulation and characterization of vesicular drug delivery system for anti-HIV drug', *Journal of global Pharma Technology*, 1(1), pp. 94–100.
- Ramana, L.N. *et al.* (2010) 'Development of a liposomal nanodelivery system for nevirapine', *Journal of Biomedical Science*, 17(1), pp. 1–9.
- Ramana, L.N. *et al.* (2012) 'Investigation on the stability of saquinavir loaded liposomes: Implication on stealth, release characteristics and cytotoxicity', *International Journal of Pharmaceutics*, 431(12), pp. 120–129.
- Ravi, P.R., Kotreka, U.K. and Saha, R.N. (2008) 'Controlled Release Matrix Tablets of Zidovudine : Effect of Formulation Variables on the In Vitro Drug Release Kinetics', *AAPS PharmSciTech*, 9(1), pp. 302–313.
- Reda, A.A. and Biadgilign, S. (2012) 'Review Article Determinants of Adherence to Antiretroviral Therapy among HIV-Infected Patients in Africa', *AIDS Research and Treatment*. doi: 10.1155/2012/574656.
- Schlatter, A.F., Deathe, A.R. and Vreeman, R.C. (2016) 'Review Article The Need for

- Pediatric Formulations to Treat Children with HIV', *AIDS Research and Treatment*, pp. 1–8.
- Shah, C.A. (2007) 'Adherence to High Activity Antiretroviral Therapy (HAART) in pediatric patients infected with HIV: Issues and interventions', *Indian Journal of Pediatrics*, 74(1), pp. 55–60.
- Shahiwala, A. (2011) 'Formulation approaches in enhancement of patient compliance to oral drug therapy', *Expert Opinion on Drug Delivery*, 8(11), pp. 1521–1529.
- Shailesh, S. *et al.* (2009) 'Liposomes: A review', *Journal of pharmacy research*, 2(7), pp. 1163–1167.
- Shamsipur, M. *et al.* (2013) 'Thermal Stability and Decomposition Kinetic Studies of Acyclovir and Zidovudine Drug Compounds', *AAPS PharmSciTech*, 14(1). doi: 10.1208/s12249-012-9916-y.
- Sopyan, I. *et al.* (2020) 'A Review : A Novel of Efforts to Enhance Liposomes Stability as Drug Delivery Approach', *Sys Review Pharm*, 11(6), pp. 555–563.
- Trucillo, P., Campardelli, R. and Reverchon, E. (2018) 'Encapsulation of Hydrophilic and Lipophilic Compounds in Nanosomes Produced with a Supercritical Based Process', in 2018, S.I.P.A. (ed.) *Advance in Bionanomaterials*. S.Piotto. Fisciano, Italy. doi: 10.1007/978-3-319-62027-5.
- Ubesie A.C. (2012) 'Pediatric HIV/AIDS in sub-Saharan Africa : emerging issues and way forward', *African Health Sciences*, 12(3), pp. 297–304.
- Witika, B.A., Smith, V.J. and Walker, R.B. (2021) 'Top-Down Synthesis of a Lamivudine-Zidovudine Nano Co-Crystal', *Crystals*, 11(33), pp. 1–18.

Chapter Eight

8. General conclusions and recommendations

8.1. Summary and conclusion

HIV/AIDS remains a global concern and worrisome burden due to a high number of people being affected by the viral infection, the number of HIV cases, challenges associated with the virus as well the mortality and morbidity cases of the HIV infection (Alebel *et al.*, 2020). The majority of the HIV cases are mainly discovered in the low-income countries mainly in the Sub-Saharan Africa where more than 71% of the global cases is found (Shahiwala and Amiji, 2007; Afe, Motunrayo and Ogungbade, 2018; UNAIDS, 2021). The discovery, adoption and establishment of the HAART, a combination of three or more ARVs in the treatment of HIV has shown to significantly improve the life span of HIV patients by suppressing the viral load of the infection hence improving the standard of living of the patients (Shahiwala and Amiji, 2007; Tewodros *et al.*, 2010). However, despite all the progress made in the treatment of this disease, children living with HIV are still suffering (Shahiwala, 2011; Galande, Khurana and Mutalik, 2020). This is because of the non-availability of child-friendly dosage forms hence children are forced to take the same ARV dosage forms specifically designed for adults. For children, adult dosage forms are typically difficult to swallow. This leads to adult dosage forms being manipulated by breaking and crushing it with subsequent mixing with water or juice. This leads to high variation in dose administration as well as children developing an aversion to taking the medication because of the bitter taste or poor palatability of the drugs. Consequently, the effective use of these drugs among HIV-infected children have been severely hampered thereby leading to therapeutic failure and poor adherence (Cram *et al.*, 2009; Chiappetta *et al.*, 2010; Lisziewicz and Toke, 2013; Owen and Rannard, 2016; Schlatter, Deathe and Vreeman, 2016; Dubrocq, Rakhmanina and Phelps, 2017; Adis Medical Writers, 2018; Chakravarty and Vora, 2021). These setbacks in the use of HAART have necessitated the pressing demand for child-friendly ARV formulations that could potentially solve most of these limitations.

This includes the adoption of several nanotechnology approaches and strategies including amorphous solid dispersions, encapsulation of the drugs in a nano-delivery system using spray drying and liposomes microencapsulation. These strategies have shown to pave the way in tackling most of the mentioned challenges because of the several advantages of these

approaches including enhancing the drug solubility, protecting of the active compounds from environmental conditions, production of fine microparticles with low water content and high stability, low toxicity of most of the excipients and the tendency to target a particular site of action (Sahoo and Labhassetwar, 2003; Ré, 2006; Poshadri and Kuna, 2010; Mansoori *et al.*, 2012; Akbarzadeh *et al.*, 2013; Arca *et al.*, 2017). In view of this, this study was aimed at developing ABC and AZT microcapsules using spray drying technique and as well as the formulation of ABC and AZT-L. These NRTIs drugs are frequently prescribed for paediatric HIV treatment hence they have become problematic in the treatment of these children with HIV (Maru *et al.*, 2011; Qwane, Mdluli and Madikizela, 2020). Due to these limitations, these drugs were entrapped in the natural excipients of PPI and IN and further spray drying the resultant drug solution to produce a potential amorphous dispersion of ABC and AZT microcapsules. More also, ABC and AZT-L were further formulated by encapsulating these drugs in liposomes. By adopting these strategies, a highly smaller particle size ARV microparticles and liposomes are expected with an enhanced solubility which could potentially solve the problem of frequent and high ARV dose in children with HIV. The use of the natural excipients such as PPI, IN and LEC in drug encapsulation is well documented. These excipients have heavily been studied in the encapsulation of different active compounds or core materials due to their low toxicity, biocompatibility, biodegradability, solubility improvement and taste masking property (Banerjee, 2001; Kaur and Gupta, 2002; Barac *et al.*, 2015; Mensink *et al.*, 2015; Chao, Aluko and Limited, 2018). Although before these excipients were used in enhancing the solubility, in spray drying and liposomes formulation of the ARV drugs, their functional properties as well their physicochemical properties were studied and established hence these excipients showed interesting functional properties including good foaming strength and stability, interesting emulsifying property and promising gelling ability.

The microencapsulated ABC and AZT microcapsules as well as the ARV loaded liposomes and their control were examined and characterized using various analytical techniques including HSM, DSC, TGA, FTIR, SEM, DLS, TEM, HPLC. The physicochemical properties of the spray dried drugs, and drug-loaded ARV liposomes were established and the aim of producing of ARV amorphous dispersion was achieved as confirmed with the characterization. The dissolution studies of the microencapsulated ARVs (SD-ABC, AL) along with the pure drugs were investigated in different pH media of 1.2 and 6.8. The release of the drugs from the respective delivery systems (microparticles and liposomes) were found to not have been affected by the nature or type of the coating materials or the excipients used as the release

profiles depicted a release of almost the entire drug within 30 minutes with a rapid and a faster release rate although the drug encapsulation in a liposomes showed the sign of a delayed release hence can be explored further. Based on the results obtained from using these two methods in the microencapsulation of the ARV drugs, the best method was predicted. Both methods highly enhanced the solubility of these selected drugs significantly, achieved high entrapment efficiency but this was much higher with liposome method than spray drying. More so, the spray drying technique produced a higher and better yield during the encapsulation compared to liposome method hence former could be more advantageous in the pharmaceutical industries in terms of high yield, the low moisture content and as well as the ease of the scalability. In conclusion, the spray drying technique was predicted to be an ideal and more efficient method in this work over conventional thin film liposomes method especially in the pharmaceutical industries mainly for future paediatric formulations with the novelty on the application of PPI and IN in the work using spray drying technique which has been barely reported.

8.2. Recommendations:

- I. Since only one drug was spray dried and encapsulated in liposomes at a time, it is important for co-encapsulation of two or more classes of the ARV drugs.
- II. The stability studies on storage for both the spray dried ARVs and ARV drug-loaded liposomes over period of time should be studied under varying temperatures.
- III. There is need for taste masking analysis for the spray dried microcapsules as well as the drugs in liposomes due to the use of IN natural sugar in the formulations.
- IV. Extended release of the drug from the microcapsules and liposomes delivery can be studied through combination and modification of different types of excipients.
- V. To reduce possible severe effects of the drugs on the normal or the non-infected cells when the drug is being released from liposomes, an investigation into functionalization of the surface of liposomes using different ligands should be explored to make liposomes specifically target the infected cells.
- VI. Potential use of spray drying technique in the formulation of the drug-loaded liposomes should be explored and compared with the conventional thin film hydration method of liposomes formulation.

8.3. References

- Afe, A.J., Motunrayo, O. and Ogungbade, G. (2018) 'Factors Influencing Adherence to HAART among Patients Living with HIV Infection in Southwest Nigeria : A Cross-Sectional Analysis', *Journal of HIV and retro-virus*, 1(1), pp. 2471–9676.
- Akbarzadeh, A. *et al.* (2013) 'Liposomes: Classification, preparation, and applications', *Nanoscale Research Letters*, 8(10), pp. 1–9.
- Alebel, A. *et al.* (2020) 'Mortality rate among HIV-positive children on ART in Northwest Ethiopia: A historical cohort study', *BMC Public Health*. BMC Public Health, 20(1), pp. 1–11.
- Arca, H.Ç. *et al.* (2017) 'Multidrug, Anti-HIV Amorphous Solid Dispersions: Nature and Mechanisms of Impacts of Drugs on Each Other's Solution Concentrations', *Molecular Pharmaceutics*, 14(11), pp. 3617–3627.
- Banerjee, R. (2001) 'Liposomes: Applications in medicine', *Journal of Biomaterials Applications*, 16(1), pp. 3–21.
- Barac, M.B. *et al.* (2015) 'Techno-functional properties of pea (*Pisum sativum*) Protein Isolates- A review', *Acta periodica technologica*, (46), pp. 1–18.
- Chakravarty, M. and Vora, A. (2021) 'Nanotechnology-based antiviral therapeutics', *Drug Delivery and Translational Research*. 11(3), pp. 748–787.
- Chao, D, and Aluko, R.E. (2018) 'Foaming properties of an isolated pea protein by thermal pretreatment', *CyTA - Journal of Food*. Taylor & Francis, 16(1), pp. 357–366.
- Chiappetta, D.A. *et al.* (2010) 'Efavirenz-loaded polymeric micelles for paediatric anti-HIV pharmacotherapy with significantly higher oral bioavailability', *Nanomedicine*, 5(1), pp. 11–23.
- Cram, A. *et al.* (2009) 'Challenges of developing palatable oral paediatric formulations', *International Journal of Pharmaceutics*, 365(12), pp. 1–3.
- Dubrocq, G., Rakhmanina, N. and Phelps, B. R. (2017) 'Challenges and Opportunities in the Development of HIV Medications in Pediatric Patients', *Pediatric Drugs*. Springer International Publishing, 19(2), pp. 91–98.
- Galande, A.D., Khurana, N.A. and Mutalik, S. (2020) 'Pediatric dosage forms-challenges and recent developments: A critical review', *Journal of Applied Pharmaceutical Science*, 10(7),

pp. 155–166.

Kaur, N. and Gupta, A.K. (2002) ‘Applications of inulin and oligofructose in health and nutrition’, *Journal of Biosciences*, 27(7), pp. 703–714.

Lisziewicz, J. and Toke, E.R. (2013) ‘Nanomedicine applications towards the cure of HIV’, *Nanomedicine: Nanotechnology, Biology, and Medicine*, 9(1), pp. 28–38.

Mansoori, M. *et al.* (2012) ‘A Review on Liposomes’, *International Journal of Advanced Research in Pharmaceutics and Bio Sciences*, 2(4), pp. 453–464.

Maru, S.M. *et al.* (2011) ‘Characterization of thermal and rheological properties of zidovudine, lamivudine and plasticizer blends with ethyl cellulose to assess their suitability for hot melt extrusion’, *European Journal of Pharmaceutical Sciences*, 44(4), pp. 471–478. .

Mensink, M.A. *et al.* (2015) ‘Carbohydrate Polymers Inulin, a flexible oligosaccharide. II: Review of its pharmaceutical applications’, *Carbohydrate Polymers*, (134), pp. 418–428.

Owen, A. and Rannard, S. (2016) ‘Strengths, weaknesses, opportunities and challenges for long acting injectable therapies: Insights for applications in HIV therapy’, *Advanced Drug Delivery Reviews*, (103), pp. 144–156.

Poshadri, A. and Kuna, A. (2010) ‘Microencapsulation technology: a review’, *Journal of Research Angraui*, 38(6), pp. 86–102.

Qwane, S.N., Mdluli, P.S. and Madikizela, L.M. (2020) ‘Synthesis, Characterization and Application of a Molecularly Imprinted Polymer in Selective Adsorption of Abacavir from Polluted Water’, *South African Journal of Chemistry*, (73), pp. 84–91.

Ré, M.I. (2006) ‘Formulating drug delivery systems by spray drying’, *Drying Technology*, 24(4), pp. 433–446.

Sahoo, S.K. and Labhasetwar, V. (2003) ‘Nanotech approaches to drug delivery and imaging’, *Drug Discovery Today*, 8(24), pp. 1112–1120.

Schlatter, A.F., Deathe, A.R. and Vreeman, R.C. (2016) ‘The need for pediatric formulations to treat children with HIV’, *AIDS Research and Treatment*, 2016. doi: 10.1155/2016/1654938.

Shahiwala, A. (2011) ‘Formulation approaches in enhancement of patient compliance to oral drug therapy’, *Expert Opinion on Drug Delivery*, 8(11), pp. 1521–1529. .

Shahiwala, A. and Amiji, M.M. (2007) ‘Nanotechnology-based delivery systems in HIV/AIDS

therapy', *Future HIV Therapy*, 1(1), pp. 49–59.

Tewodros, M. *et al.* (2010) 'Emerging nanotechnology approaches for HIV / AIDS treatment and prevention R eview', *Nanomedicine*, 5(2), pp. 269–285.

UNAIDS (2021) 'Global HIV Statistics; Fact Sheet 2021, Ending the AIDS epidemic'. (Accessed 7 March 2021).

Writers, A.M. (2018) 'Overcome the challenges of drug administration in children by developing age-appropriate formulations', *Drugs and Therapy Perspectives*, 34(11), pp. 518–521.

